

CHARACTERIZATION OF HEPATITIS C VIRUS INFECTION OF
HEPATOCYTES AND ASTROCYTES

Ziqing Liu

Submitted to the faculty of the University Graduate School
in partial fulfillment of the requirements
for the degree
Doctor of Philosophy
in the Department of Microbiology and Immunology,
Indiana University

February 2014

Accepted by the Graduate Faculty, of Indiana University, in partial fulfillment of the requirements for the degree of Doctor of Philosophy.

Doctoral Committee

Andy (Qigui) Yu, M.D., Ph.D., Co-Chair

Johnny J. He, Ph.D., Co-Chair

Randy R. Brutkiewicz, Ph.D.

Cheng C. Kao, Ph.D.

May 28, 2013

William J. Sullivan, Jr., Ph.D.

DEDICATION

I would like to dedicate this work to my loving mother, Ping, my Ph.D. advisor Dr. Johnny He, and my best friends Mr. Douglas Huntley and Dr. Ying Liu.

ACKNOWLEDGEMENTS

I would like to express my sincere gratitude to my advisor, Dr. Johnny He, for giving me the opportunity to develop my dissertation in his laboratory. His mentorship, guidance, and support have been invaluable throughout this process. Under his guidance, I have learned what science is and how to conduct scientific research. Most importantly, qualities like hard-work, honesty, persistence, patience, responsibility, warm-heartedness, and cooperativeness have been imprinted in me by his example, and they will surely accompany me and encourage me throughout my life.

I thank Dr. Andy Yu, Dr. Randy Brutkiewicz, Dr. Cheng Kao, and Dr. William Sullivan, who served on my research committee; they have offered much-appreciated advices in science and other related fields. I have learned a lot from their ideas, suggestions, and criticisms.

I would also like to thank all members of Dr. He's laboratory for their support and friendship. I especially would like to thank Dr. Park and previous lab members Dr. Fang Zhao and Dr. Jean Ndjomou for their contributions to the previous work on HCV in Dr. He's laboratory.

I would like to thank Dr. Kai-ming Chou and Dr. Christoph Naumann for allowing me to have a brief research rotation in their laboratories; the time was not long but both rotations were interesting experience for me.

To my fellow graduate students, I sincerely thank you for your friendship; there were so many joyful memories throughout these years.

I thank Jianyun Liu, Feifei Jiang, Jesie Lu, Yuanyuan Chen, and Hao Wen, for their friendship, companionship, suggestions and support.

I thank my entire family for their life-long love, understanding and encouragement. I especially thank my father Xingming Liu, my grandfather Demao Liu and grandmother Yueying Liao, for their unconditional love and support.

I would also like to thank Mr. Douglas Huntley, my best friend, for the countless inspiring conversations, for all the beautiful and sweet memories, and the eternal happiness and warmth he has brought into my life.

Last but not least, I would like to thank my lifelong teacher, friend, sister and “lover”, my loving mother Ping Liu. Every step in my life is filled with her love and encouragement; her thoughts help determine the way I approach life.

Characterization of Hepatitis C Virus Infection of Hepatocytes and Astrocytes

Approximately 2.8% of the world population is currently infected with hepatitis C virus (HCV). Neutralizing antibodies (nAbs) are often generated in chronic hepatitis C patients yet fail to control the infection. In the first two chapters of this study, we focused on two alternative routes of HCV transmission, which may contribute to HCV's immune evasion and establishment of chronic infection. HCV was transmitted via a cell-cell contact-mediated (CCCM) route and in the form of exosomes. Formation of HCV infection foci resulted from CCCM HCV transfer and was cell density-dependent. Moreover, CCCM HCV transfer occurred rapidly, involved all four known HCV receptors and intact actin cytoskeleton, and led to productive HCV infection. Furthermore, live cell imaging revealed the temporal and spatial details of the transfer process. Lastly, HCV from HCV-infected hepatocytes and patient plasma occurred in both exosome-free and exosome-associated forms and the exosome-associated HCV remained infectious, even though HCV infection did not significantly alter exosome secretion.

In the third chapter, we characterized HCV interaction with astrocytes, one of the putative HCV target cells in the brain. HCV infection causes the central nervous system (CNS) abnormalities in more than 50% of chronically infected subjects but the underlying mechanisms are largely unknown. We showed that primary human astrocytes (PHA) were very inefficiently infected by HCV, either in the free virus form or through cell-cell contact. PHA expressed all known HCV receptors but failed to support HCV entry. HCV IRES-mediated translation was functional in PHA and further enhanced by miR122 expression. Nevertheless, PHA did not support HCV replication regardless of miR122

expression. To our great surprise, HCV exposure induced robust IL-18 expression in PHA and exhibited direct neurotoxicity. In summary, we showed that CCCM HCV transfer and exosome-mediated HCV infection constituted important routes for HCV infection and dissemination and that astrocytes did not support productive HCV infection and replication, but HCV interactions with astrocytes and neurons alone might be sufficient to cause CNS dysfunction. These findings provide new insights into HCV infection of hepatocytes and astrocytes and shall aid in the development of new and effective strategies for preventing and treating HCV infection.

Andy (Qigui) Yu, M.D., Ph.D., Co-Chair

Johnny J. He, Ph.D., Co-Chair

TABLE OF CONTENTS

INTRODUCTION.....	1
1. HCV AND HEPATITIS C	1
1.1 Hepatitis C – global perspective, vaccines and therapeutics	1
1.2 HCV pathogenesis in the liver.....	2
1.3 HCV genome.....	3
1.4 HCV life cycle.....	7
1.4.1 HCV entry and its cellular receptors	7
1.4.2 HCV translation and replication and miR122.....	10
1.4.3 HCV assembly and release	11
1.5 HCVpp and HCVcc model systems	12
2. CELL-CELL CONTACT-MEDIATED VIRAL TRANSMISSION.....	16
2.1 Cell-cell contact-mediated transmission of viruses	16
2.2 Cell-free virus infection vs. CCCM viral transmission	17
2.3 Evidence for CCCM HCV transmission.....	19
3. EXOSOMES	20
3.1 Exosomes	20
3.1.1 Definition, cargo, biogenesis, and uptake.....	20
3.1.2 Physiological functions and therapeutic potentials	24
3.2 Exosomes and viruses	25
3.3 Exosome interactions with HCV	25
3.4 Exosome purification – current protocols	26
3.4.1 Precipitation with polymers	26
3.4.2 Ultracentrifugation.....	27
3.4.3 Immunocapture.....	27

4. HCV INTERACTION WITH THE BRAIN	28
4.1 CNS abnormalities in HCV patients	28
4.2 HCV infection of PBMC	28
4.3 HCV infection of the brain and pathological evidence.....	29
4.4 HCV entry into the CNS – the “trojan PBMC hypothesis”	30
4.5 HCV infection of the CNS in HIV-1/HCV co-infected individuals.....	31
5. SUMMARY OF THE BACKGROUND AND HYPOTHESES	32
MATERIALS AND METHODS	37
MATERIALS	37
Media and supplements	37
Plasmids and siRNAs.....	37
Antibodies	41
Reagents.....	41
Kits	42
METHODS.....	43
Cells and cell cultures	43
<i>Cell lines</i>	43
<i>Establishment of stable cell lines</i>	43
<i>Competent cells for cloning</i>	45
<i>Primary human hepatocyte cultures</i>	45
<i>Primary human brain cell cultures</i>	45
HCV patient plasma samples.....	46
Bacterial transformation	46
HCV RNA synthesis by <i>in vitro</i> transcription.....	46
Cell transfections.....	47
<i>Calcium phosphate precipitation</i>	47

<i>Lipofectamine transfection</i>	47
Reverse transcriptase activity assay.....	48
Preparation of pseudotyped viral particles and infection.....	49
Luciferase assay	49
HCVcc production, titration and infection	50
Co-culture assay and transwell assay.....	51
Flow cytometry.....	52
<i>CD81 surface expression</i>	52
<i>HCV CCCM transfer</i>	52
Immunofluorescence staining and confocal imaging	53
ReAsH labeling and 3D live cell imaging	53
Western blotting	54
RNA isolation and qRT-PCR.....	55
<i>RNA isolation</i>	55
<i>One-step Taqman qRT-PCR for HCV RNA</i>	56
<i>Two-step Taqman qRT-PCR for miR122</i>	56
<i>Two-step SYBR Green qRT-PCR for cytokine expression</i>	57
Preparation of bovine exosome-depleted medium and bovine exosome-depleted HCV.....	58
Exosome and HCV purification by Optiprep gradient ultracentrifugation	58
Acetylcholinesterase assay.....	59
Data acquisition and statistical analysis.....	60
RESULTS.....	61
CHAPTER 1: CELL-CELL CONTACT-MEDIATED HEPATITIS C VIRUS TRANSFER, PRODUCTIVE INFECTION AND REPLICATION AND ITS REQUIREMENT FOR HCV RECEPTORS.....	61

1.1 Formation of HCV infection foci in cell culture	61
1.2 Spread of HCV in cell culture is dependent on cell density.....	61
1.3 CCCM HCV transfer to Huh7.5.1 and primary hepatocytes.....	69
1.3.1 Optimization of the labeling methods in co-culture assay.....	69
1.3.2 CCCM HCV transfer among Huh7.5.1.....	72
1.3.3 CCCM HCV transfer to primary hepatocytes.....	75
1.4 CCCM HCV transfer vs. cell-free HCV infection	75
1.5 Indispensable roles of CD81, SR-B1, CLDN1 and OCLN in CCCM HCV transfer	82
1.5.1 Inhibition of CCCM HCV transfer by knockdown of HCV receptor(s) in target cells	82
1.5.2 No CCCM HCV transfer from Huh7.5.1 to other hepatoma and non- hepatoma cell lines.....	92
1.6 Roles of actin and microtubule cytoskeletons in CCCM HCV transfer.....	106
1.7 Live cell imaging of the CCCM HCV transfer in Huh7.5.1 cells: from conjugate formation to transfer	110
1.7.1 Construction and characterization of recombinant JFH1-c177-GFP	110
1.7.2 Construction and characterization of recombinant JFH1-TCcore.....	116
1.7.3 Live cell imaging of CCCM HCV transfer.....	122
1.8 CCCM transfer and productive HCV infection.....	129
1.8.1 Strategy I: Extended co-culture assay with neutralizing antibodies.....	129
1.8.2 Strategy II: FACS sorting of newly CCCM transferred target cells and continued culturing.....	135
1.8.3 Strategy III: Selective elimination of donor cells and continued culturing of target cells	137
CHAPTER 2: Exosome-Associated Hepatitis C Virus and Its Infectivity.....	140

2.1 HCV infection did not alter exosome secretion in hepatocytes	140
2.2 Association of HCV with exosomes	140
2.2.1 Optimization of iodixanol concentration for fractionation of HCV.....	140
2.2.2 Detection of HCVcc/patient plasma-derived HCV in exosome-containing fractions	145
2.3 Exosome-associated HCV was infectious.....	150
CHAPTER 3: Hepatitis C Virus (HCV) Interaction with Astrocytes:	
Non-productive Infection and Induction of IL-18	159
3.1 Establishment of human fetal brain primary cell cultures	159
3.2 Few astrocytes are infected by cell-free or CCCM HCV infection.....	159
3.3 HCV receptors expression on primary astrocytes.....	167
3.4 Insignificant HCV entry into astrocytes	167
3.4.1 HCVpp infection and spinoculation of brain cells.....	167
3.4.2 Unsuccessful VSV-G pseudotyping of HCVcc.....	175
3.5 HCV RNA translation in astrocytes and its enhancement by miR122.....	175
3.6 HCV replication in astrocytes and the effect of miR122.....	178
3.7 Effect of cytokines/chemokines/LPS on HCV replication in astrocytes	184
3.8 HCV-induced IL-18 expression in astrocytes	187
3.9 HCV direct neurotoxicity.....	192
DISCUSSION	195
Summary of the results	195
CCCM HCV infection <i>in vivo</i>	198
Roles of HCV receptors in the CCCM HCV infection.....	199
Difficulties of CCCM HCV infection of cells other than Huh7.5.1 cells and primary hepatocytes.....	201
The role of actin cytoskeleton in CCCM HCV infection.....	202

Temporal and spatial details of CCCM HCV transmission by 3D live imaging	203
Potential mechanism(s) of CCCM HCV infection – the possible involvement of lamellipodium	205
“Trojan exosomes” for HCV	208
Cell-free, CCCM and exosome-mediated HCV infection	211
HCV entry into the CNS – the infection of BBB, Trojan PBMC, or Trojan exosomes?.....	212
HCV and astrocytes	213
Conclusions.....	218
PERSPECTIVE	220
Future directions	220
Towards a “cure” for chronic hepatitis C	223
HCV mouse models	224
HCV infection of PBMC and its contribution to the pathogenesis of HCV-related diseases	226
Extra-hepatic HCV tropism.....	227
Treatment of HCV in PBMC and the CNS	229
REFERENCES.....	231
CURRICULUM VITAE	

LIST OF TABLES

Table 1. Expression of HCV receptors in different cell lines and its relationship to cell-free HCV virus infection.....	97
---	----

LIST OF FIGURES

Figure 1. HCV virion and genome.....	6
Figure 2. The HCV life cycle	9
Figure 3. <i>In vitro</i> HCV culture systems.....	14
Figure 4. Exosome cargos and biogenesis	23
Figure 5. HCV infection of target cells and transmission routes: summary of hypotheses.....	36
Figure 6. Formation of HCV infection foci in cell culture.	63
Figure 7. Cell density's effects on HCV spread at a low MOI.....	66
Figure 8. Cell density's effects on HCV spread at a high MOI.	68
Figure 9. Optimization of the labeling methods for co-culture assay.....	71
Figure 10. CCCM HCV transfer among Huh7.5.1 cells.....	74
Figure 11. CCCM HCV transfer between Huh7.5.1 and primary human hepatocytes...	77
Figure 12. CCCM HCV transfer versus cell-free HCV infection.	81
Figure 13. Effects of the Donor: Target ratio on CCCM HCV transfer.	84
Figure 14. Individual knockdown of CD81, SR-B1, CLDN1 and OCLN on Huh7.5.1 by siRNA and their effects on CCCM HCV transfer	88
Figure 15. Simultaneous knockdown of CD81, SR-B1, CLDN1 and OCLN on Huh7.5.1 by siRNA and its effect on CCCM HCV transfer.....	91
Figure 16. Expression of HCV receptors in different cells.....	94
Figure 17. Cell-free and CCCM HCV infection of HepG2, NKNT3 and CYNK10 cells.....	96
Figure 18. No CCCM HCV transfer from Huh7.5.1 to HepG2-CD81.	99
Figure 19. No CCCM HCV transfer from Huh7.5.1 to NKNT3-CLDN1.	101

Figure 20. No CCCM HCV transfer from Huh7.5.1 to CYNK10-CLDN1.	103
Figure 21. No CCCM HCV transfer from Huh7.5.1 to 293T-SR-B1-CLDN1.	105
Figure 22. Actin and microtubule cytoskeletons and CCCM HCV transfer.	109
Figure 23. Expression of C177-GFP fusion protein.	113
Figure 24. No incorporation of C177-GFP into JFH1 virions by <i>trans</i> -complementation	115
Figure 25. GFP and core expression in JFH1-c177-GFP RNA-transfected Huh7.5.1 cells.....	119
Figure 26. Characterization of recombinant JFH1-TCcore HCV.	121
Figure 27. Live cell imaging of CCCM HCV transfer (I)	124
Figure 28. Live cell imaging of CCCM HCV transfer (II)	126
Figure 29. Live cell imaging of CCCM HCV transfer (III).....	128
Figure 30. Neutralization of cell-free HCV infectivity with CBH-5 in the co-culture assay.....	132
Figure 31. CCCM HCV transfer leads to productive HCV infection (strategy I).	134
Figure 32. CCCM HCV transfer leads to productive HCV infection (strategy II).	137
Figure 33. CCCM HCV transfer leads to productive HCV infection (strategy III).	139
Figure 34. HCV infection does not affect exosome production.	142
Figure 35. HCV infection does not affect exosome size distribution.	144
Figure 36. Optimization of iodixanol concentration for HCV fractionation.	147
Figure 37. Detection of HCV in exosome-containing fractions.....	149
Figure 38. Detection of HCV in exosome-containing fractions with PEG exosome/HCV precipitation.	152
Figure 39. Detection of HCV in exosome-containing fractions using the NVT65 rotor for gradient centrifugation.....	154
Figure 40. Exosome-associated HCV in HCV-positive patient plasma.....	156

Figure 41. The infectivity of exosome-associated HCV.....	158
Figure 42. Human fetal brain primary cell cultures.....	161
Figure 43. HCVcc does not infect astrocytes by cell-free virus infection.....	164
Figure 44. Cell-cell contact does not lead to HCV infection of astrocytes.....	166
Figure 45. Expression of HCV receptors on astrocytes.	169
Figure 46. Insignificant HCVpp (Luc) entry into astrocytes.	172
Figure 47. Insignificant HCVpp (GFP) entry into astrocytes.....	174
Figure 48. VSV-G pseudotyping of HCVcc.	177
Figure 49. HCV RNA translation in astrocytes and its enhancement by miR122 expression.....	180
Figure 50. Effect of miR122 on HCV RNA stability, translation and replication in astrocytes.....	183
Figure 51. HCV replication in astrocytes with or without exogenous miR122 expression.....	186
Figure 52. Effect of cytokines/chemokines/LPS on HCV replication in astrocytes.....	189
Figure 53. Induction of IL-18 expression in astrocytes following HCV exposure.	191
Figure 54. Neurotoxicity induced by direct HCV exposure.....	194

LIST OF ABBREVIATIONS

aa	amino acid
AASLD	American Association for the Study of Liver Diseases
AchE	acetylcholine esterase
ATC	acetylthiocholine
ATCC	American Tissue Culture Collection
BBB	blood-brain barrier
BSA	bovine serum albumin
cDNA	complementary DNA
CD81	cluster of differentiation 81
CDS	coding DNA sequence
CFSE	carboxyfluorescein succinimidyl ester
CLDN1	claudin-1
CMFDA	5-chloromethylfluorescein diacetate
CNS	central nervous system
cpm	counts per minute
CSF	cerebrospinal fluid
DAA	direct-acting antiviral
DAPI	4', 6'-diamidino-2-phenylindole
DMEM	Dulbecco's Modified Eagle Medium
DMSO	dimethyl sulfoxide
ds	double stranded
DTBNBA	5,5-dithio-bis(2-nitrobenzoic acid)
DTT	dithiothreitol
E1	HCV envelope glycoprotein 1

E2	HCV envelope glycoprotein 2
EDTA	ethylene-diamine-tetra-acetic acid
Egr	early growth response protein 1
EGTA	ethylene-glycol-tetra-acetic acid
ELISA	enzyme-linked immunosorbent assay
EMCV	encephalomyocarditis virus
ER	endoplasmic reticulum
FACS	fluorescence-activated cell sorting
Fluc	firefly luciferase
FBS	fetal bovine serum
FDA	Food and Drug Administration
FITC	fluorescein isothiocyanate
GFAP	glial fibrillary acidic protein
GFP	green fluorescent protein
HAART	highly active antiretroviral therapy
HBSS	Hank's-buffered salt solution
HEPES	4-(2-hydroxyethyl)-1-piperazineethanesulfonic acid
HCV	hepatitis C virus
HIV-1	human immunodeficiency virus type 1
hr	hour
HSV	herpes simplex virus
HTLV-1	human T cell leukemia virus type 1
IL-1 β	interleukin 1 β
IL-4	interleukin 4
IL-6	interleukin 6
IL-10	interleukin 10

INF- γ	interferon gamma
IRES	internal ribosome entry site
kDa	Kilodaltons
LB	Luria Broth
LCM	laser capture microscopy
LPD	lymphoproliferative disorders
LPS	lipopolysaccharide
MAP-2	microtubule-associated protein 2
MC	mixed cryoglobulinemia
MCP-1	monocyte chemotactic protein 1
min	minute
ml	milliliter
MLV	murine leukemia virus
MP	movement protein(s)
nAbs	neutralizing antibodies
ng	nanogram
NHL	non-Hodgkin's lymphomas
NIH	National Institutes of Health
NP40	Nondiet P 40
NS	not significant/ HCV non-structural protein
nt	nucleotide
O/N	overnight
OCLN	occludin
ORF	open reading frame
PHA	human fetal primary astrocytes
PAGE	polyacrylamide gel electrophoresis

PBMC	peripheral blood mononuclear cells
PBS	phosphate-buffered saline
PCR	polymerase chain reaction
PD	plasmodesmata
PE	phycoerythrin
PEG	polyethylene glycol
PEG-IFN/RBV	pegylated interferon α plus ribavirin
PFA	paraformaldehyde
PI	propidium iodide
PMSF	phenylmethanesulphonylfluoride
Rluc	<i>renilla</i> luciferase
ROS	reactive oxygen species
RT	room temperature
RT-PCR	reverse transcription polymerase chain reaction
qRT-PCR	quantitative real time reverse transcription polymerase chain reaction
SDS	sodium dodecyl sulfate
siRNA	silencing RNA
SOC	standard of care
S.P.G.	streptomycin-penicillin-glutamine
SR-B1	scavenger receptor class B member 1
ss	single stranded
SVR	sustained virological response
TNF- α	tumor necrosis factor α
μ g	microgram
μ l	microliter
UTR	untranslated region

VRC	virus replication complexes
VSV	vesicular stomatitis virus
WB	Western blotting

INTRODUCTION

1. HCV AND HEPATITIS C

1.1 Hepatitis C – global perspective, vaccines and therapeutics

The latest global epidemiology studies indicate that more than 185 million people, which account for about 2.8% of the world population, are infected with hepatitis C virus (HCV) (1), among which 4.1 million are in the U.S (2). Although the incidence of new infections has become much lower since the development of blood screening tests in early 1990s, the morbidity and mortality due to HCV infections contracted in 1970s and 1980s are rising and are expected to continuously increase over the next ten years (3). HCV infection frequently leads to hepatitis (inflammation of the liver) and steatosis (fatty liver), and it is considered a leading cause for life-threatening chronic liver diseases such as liver fibrosis, cirrhosis and hepatocellular carcinoma (HCC) (4). It also presents the primary cause for liver transplantation in the U.S. and the Europe (5). Despite intensive research efforts during the last two decades, no HCV vaccines have become available (6, 7). The standard of care (SOC) for HCV infection used to be pegylated interferon α plus ribavirin (PEG-IFN/RBV) before May 2011. The treatment modality is not well tolerated and only has a less than 50% response rate for HCV genotype 1, the most prevalent HCV subtype (8, 9). The first two direct-acting antivirals (DAAs), the HCV protease NS3/NS4 inhibitors telaprevir and boceprevir, were approved by the FDA in 2011. The combinatorial treatment of these inhibitors with PEG-IFN/RBV has greatly improved the response rate from 50% to 70% in HCV genotype 1 patients (8, 9), although this response rate is not optimal. It is evident that a better understanding of HCV infection and pathogenesis is required to enable the development of new anti-HCV therapeutic and prophylactic strategies.

1.2 HCV pathogenesis in the liver

About 20% of HCV infections are spontaneously cleared within six months after the initial infection, which is termed as acute infection. The strong and specific cytotoxic T cells (CD8+) response observed in acute HCV infection is correlated with the control of viremia and is very likely the reason for acute liver damage (10). The remaining 80% of HCV infections are not cleared by the host immune system and these patients become chronically infected. In a timeframe of 10–40 years, these patients may progressively develop chronic hepatitis, steatosis and fibrosis, and 20% of them will progress to the end stage: liver cirrhosis. Each year, 5% of those with cirrhosis develop hepatocellular carcinoma (HCC) (11, 12). Chronic hepatitis is the inflammation of the liver characterized by the infiltration of immune cells into the liver after the host immune system fails to control viral replication during the acute phase. Steatosis is the production and accumulation of excessive fatty acids in liver cells, and it is observed in more than half of chronic HCV patients. Patients with chronic hepatitis and/or steatosis are at high risk of developing fibrosis, cirrhosis, and hepatocellular carcinoma (13). Many factors contribute to the stepwise development of liver diseases in chronic HCV patients. Besides risk factors like age, ethnicity, sex, co-infection with hepatitis B virus or human immunodeficiency virus type 1 (HIV-1) and host genetics, e.g., IL-28B gene variants, direct effects of HCV proteins and indirect impact of infiltrated immune cells are the two most important contributors to the disease progression. For example, HCV proteins exert direct impact by interacting with a variety of cellular processes. Several of the HCV proteins such as core, NS3, and NS5A target multiple cellular proteins in innate cellular antiviral pathways, so as to disarm the front line of antiviral defense and to hamper/delay the effective induction of adaptive immune response (14). Individual HCV proteins (core, NS3, and NS5A) are also reported to increase reactive oxygen species (ROS) production and induce oxidative stress in both cell culture and chronic HCV

patients. Cellular environment under oxidative stress favors the expression of profibrogenic genes/cytokines and induces cellular DNA mutations, both of which accelerate the development of fibrosis, cirrhosis, and HCC (15). In addition, the HCV core protein is known to interact with key regulators in lipid metabolism and induce steatosis (13). At last, core, NS3, NS5A and NS5B can interfere with the p53 and pRb pathways to exert their impacts on cell proliferation and apoptosis: a shortcut to oncogenesis (15). On the other hand, the infiltrated immune cells in liver still cannot effectively control viral infection, which leads to exhaustion of CD4+ and CD8+ effector T cells and continuous infiltration of immune cells. Although the HCV-specific immune response in chronic HCV patients is weak and ineffective in controlling virus infections, the repeated inflammation induces oxidative stress and causes destruction of liver tissue. The damaged liver tissue is then replaced through fibrogenesis, and the cycle of liver damage and re-building perpetuates until the development of fibrosis/cirrhosis (10, 16-18). All together, the potential host-related risk factors, the altered hepatocyte proliferation capacity by HCV proteins (15) and the “stressed” and growth-promoting microenvironment shaped by both HCV proteins and ineffective immune response in the liver (13, 15, 19) ultimately contribute to HCC development.

1.3 HCV genome

HCV is an enveloped, single-stranded (ss), and (+) sense RNA virus with a diameter of 55 – 65 nm. It belongs to the *Flaviviridae* family and has six subtypes, with HCV 1a, 1b and 2a to be the most prevalent (20). The HCV virion is composed of a RNA genome enclosed by capsid formed by core protein and an envelope embedded with HCV glycoprotein E1, E2 heterodimers (**Fig. 1A**). The HCV RNA genome is 9.6 kb in length and consists of 5' and 3' untranslated regions (UTR), and a single open reading frame (ORF) encoding all structural proteins and nonstructural proteins (**Fig. 1B**). The 5' UTR

and 3' UTR harbor several RNA secondary structures with essential functions in replication and translation. Among them is the internal ribosome entry site (IRES). It extends from 5' UTR into the core-encoding region and is responsible for 5' cap-independent translational initiation. Structural proteins include the envelope proteins E1, E2, the capsid protein core and a small 63 aa peptide p7 with putative ion channel function. During translation, these structural proteins are cleaved by two cellular proteases, the signal peptidase and the signal peptide peptidase (**Fig. 1B**, SP and SPP, blue and green arrow head). Non-structural (NS) proteins are NS2, NS3, NS4A, NS4B, NS5A, and NS5B. NS2 is a protease which, together with the N-terminal portion of NS3, cleaves the NS2-NS3 junction (**Fig. 1B**, black arrow head). NS3 has two distinct domains. Its N-terminal portion is a protease domain, which cleaves all the downstream junctions between NS proteins with the assistance of its cofactor NS4A (**Fig. 1B**, orange arrow head). Its C-terminal portion is a helicase which functions to unwind double-stranded RNA (dsRNA) substrate and secondary RNA structures during HCV replication. NS4A, as mentioned above, is a co-factor for NS3 protease. NS4B induces the formation of a specialized membrane structure, the "membranous web", where it serves as the scaffold protein for the HCV replication complex. NS5A is a hydrophilic phosphoprotein whose phosphorylation status is crucial to HCV replication. NS5B is a RNA-dependent RNA polymerase (RdRp) responsible for HCV genome replication (15, 21).

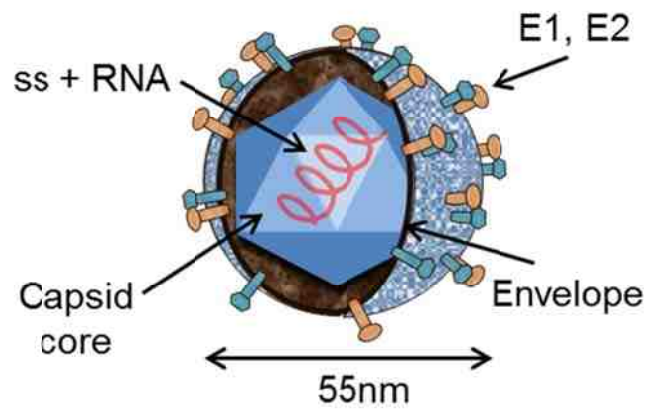
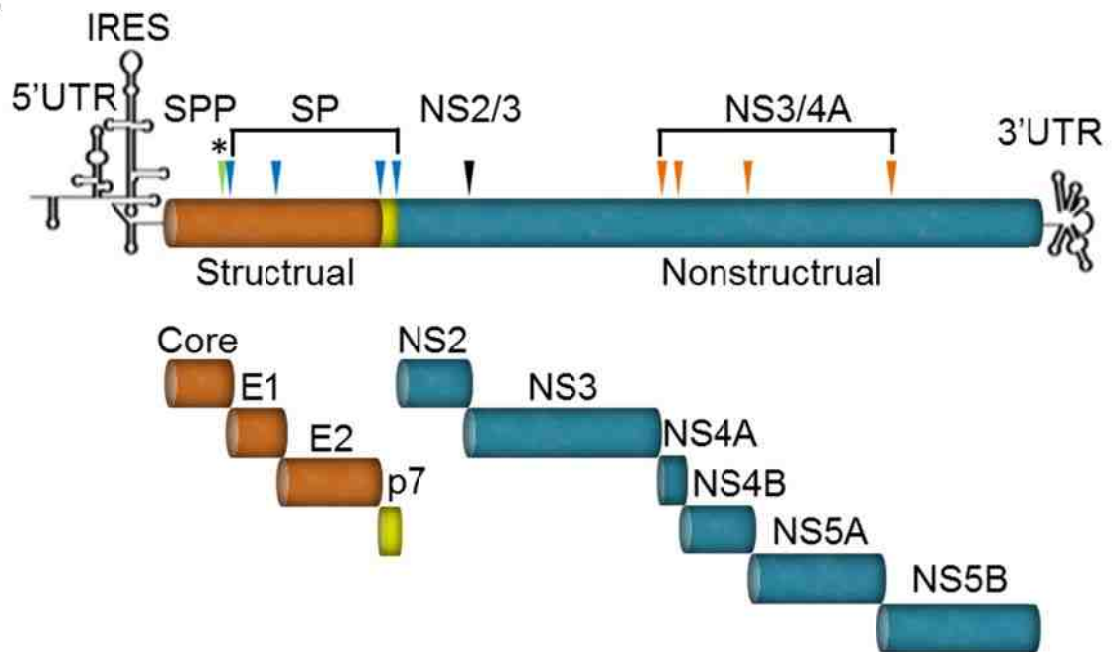
A**B**

Figure 1. HCV virion and genome. (A) HCV virion. (B) HCV genome. Cleavage sites of HCV polypeptide processing by different proteases are indicated in colored arrowheads: SP (signal peptidase, blue), viral proteases NS2/3 (black) and NS3/4A (orange). SPP (signal peptide peptidase) cleavage of SP-cleaved core (green arrowhead and *) generates mature core protein.

1.4 HCV life cycle

1.4.1 HCV entry and its cellular receptors

Generally, the HCV life cycle can be divided into the following stages: attachment, entry and fusion, translation and replication, assembly and secretion (15, 21). First, the attachment of virus to host cell is mediated by glycosaminoglycans (GAGs, e.g., heparin sulfate) (22) and the low density lipoprotein receptor (LDLR) (23, 24). Next, specific interactions between the viral glycoprotein E2 and cellular receptors induce receptor-mediated endocytosis (**Fig. 2**). This “entry” step has been intensively studied and four HCV entry receptors/ co-receptors have been discovered. The first one is a tetraspanin protein, CD81, which was discovered by screening for HCV E2-interacting proteins (25). The scavenger receptor class B type 1 (SR-B1) was subsequently found to also interact with HCV E2 and to play a role in HCV entry (26, 27). SR-B1 normally functions as a LDL/HDL receptor and is highly expressed in the liver and other steoidogenic tissues. Recently, two tight junction (TJ) proteins, claudin-1 (CLDN1) and occluding (OCLN) were discovered to confer susceptibility to HCV infection in human embryonic kidney cell line 293T (28) and mouse embryonic kidney fibroblast cell line NIH3T3 (29), respectively, even though they were not found to directly bind HCV envelope proteins. The current HCV cell entry model suggests roles of CD81 and SR-B1 in the early entry step and roles of CLDN1 and OCLN in the late entry steps. After attachment, HCV E2 interacts with cellular receptors CD81 and SR-B1, and their interaction triggers signaling cascades essential for entry and downstream events (30, 31). The virus is then transferred to CLDN1 and OCLN via CLDN1’s association with CD81 (32-34) and internalized by endocytosis, followed by pH-dependent fusion (35, 36). Interestingly, none of these four receptors are exclusively expressed in the liver, the primary target of

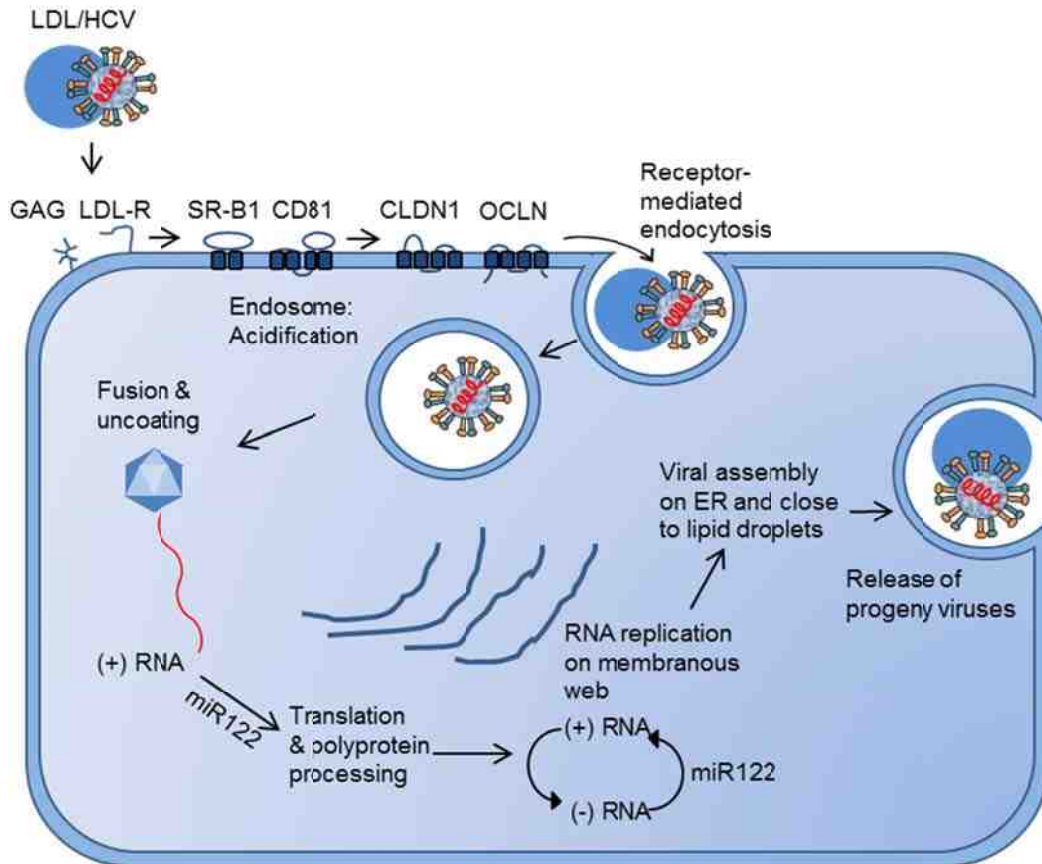


Figure 2. The HCV life cycle. First, virus attaches to the primary docking sites (GAGs or LDLR), interacts with cellular receptors SR-B1, CD81, CLDN1, and OCLN, and undergoes endocytosis and pH-dependent membrane fusion. Viral proteins are then translated and processed in the cytoplasm. The viral replication complex assembles on the membranous web to generate genomic viral RNA. Finally, HCV virions assemble on/close to lipid droplets and are released through unknown mechanisms.

HCV. Nevertheless, restrictions on steps other than entry can also shape the liver tropism of HCV, such as the requirement of liver-specific microRNA miR122 for HCV replication (37). Thus, it is possible that only human hepatocytes express all the cellular factors required for a complete HCV life cycle.

1.4.2 HCV translation and replication and miR122

Following fusion and release of HCV RNA into the cytoplasm, HCV translation is initiated on endoplasmic reticulum (ER) by binding of ribosomes to IRES. A single polypeptide of about 3,000 amino acids is synthesized and processed by both cellular proteases and viral proteases. The processed viral NS proteins, together with cellular co-factors, form a replication complex (RC) on the intracellular membranous web (38). The NS5B RdRp uses HCV (+)-strand genomic RNA as the template to produce (-)-strand intermediate RNA and then (+)-strand RNA can be produced in large quantity with (-)-strand RNA as the template. The ratio of (+)-strand RNA: (-)-strand RNA is always kept between 1000:1 and 100:1 in HCV infected cells and the presence of (-)-strand RNA is considered as the marker of active HCV replication (39-41).

Throughout HCV translation and replication, the role of miR122 is essential. In 2005, the liver-specific microRNA-122 was first discovered to be required for HCV replication (37). The mechanisms of action of miR122's role in HCV life cycle have been intensively studied since then. Generally, miR122 positively regulates HCV infection at three levels at least: stimulation of HCV translation (in both cell culture and *in vitro* translation systems) (42-44), enhancement of HCV RNA stability (45-47), and promotion of HCV replication and infectious virus production (37, 48-50). The current model stipulates that it mainly functions via binding to two target sequences in HCV 5'UTR. This binding relieves HCV IRES from an inhibitory long-distance RNA loop formed through base-

paring between 5'UTR and the core sequence, and hence stimulates HCV translation (44). This binding also recruits Argonaute 2 (Ago 2), the catalytic components of the RNA-induced silencing complex to HCV 5'UTR (47). But recruitment of Ago 2 does not lead to cleavage of HCV RNA, which is very common in RNA silencing of cellular mRNAs; instead, it stabilizes HCV RNA and slows its degradation by 5' exonuclease Xrn I (46). Nevertheless, how this binding promotes HCV RNA replication remains unclear. Besides the mechanistic studies, the clinical implications of miR122's involvement in HCV life cycle have also been widely explored. Serum miR122 level was recently suggested as potential biomarkers for chronic hepatitis C (51); treatment of HCV infection by targeting miR122 with antisense oligonucleotide was shown to lead to prolonged dose-dependent reductions in HCV RNA levels without evidence of viral resistance (52).

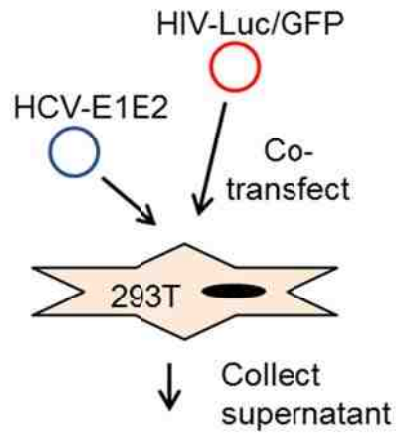
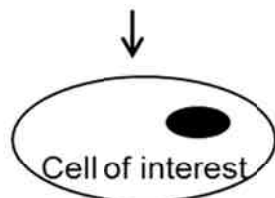
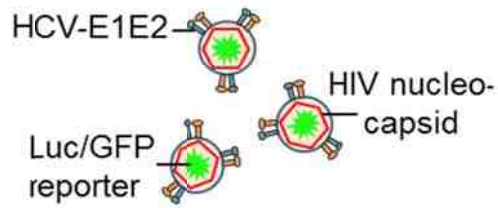
1.4.3 HCV assembly and release

After translation and processing, HCV proteins are targeted to lipid droplets (LD), a lipid storage organelle mainly consisting of triglycerols in preparation for viral assembly (53). Both HCV core and NS5A are targeted to LD after being processed. Their LD targeting changes LD distribution in the cells and is required for HCV infectivity (54-57). A recent study shows that disruption of microtubule network prevents HCV core-mediated LD redistribution and decreases viral titer in HCV-infected cells, indicating potential roles of microtubule network/transport in virus assembly (58). Additionally, the putative ion channel protein p7 and non-structural protein NS2 are not required for RNA replication, but are necessary for infectious virus production (59-63), suggesting their possible involvement in virus assembly or release. HCV assembly and release have also been stipulated to converge with the very-low density lipoprotein (VLDL) production pathway based on the findings that HCV virions are associated with LDL/VLDL *in vivo* and that

HCV proteins re-localize to LD after processing (53). Moreover, recent studies demonstrate that apolipoprotein E (ApoE) interacts with HCV NS5A and this interaction is important for HCV assembly and infectious virus production (64). Mouse hepatocyte cell lines can support HCV assembly upon ectopic expression of ApoE (65), suggesting that ApoE may present the last limiting factor for a complete HCV life cycle besides HCV receptors (limiting entry) and miR122 (limiting translation and replication). Taken together, the current model of HCV assembly is stipulated as follows. While HCV genome RNA is continuously produced from the replication complex in the membraneous web and HCV core are lined up on LD, the genome RNA and core are simultaneously recruited to the site of assembly (either on LD or on ER and close to LD) and nascent viral budding towards ER lumen, where HCV E1/E2 are already residing, takes place (66). During this process, viral proteins p7, NS2 and NS5 and cellular protein ApoE all play important roles. Nevertheless, the late steps in HCV life cycle are still not completely understood and await to be elucidated.

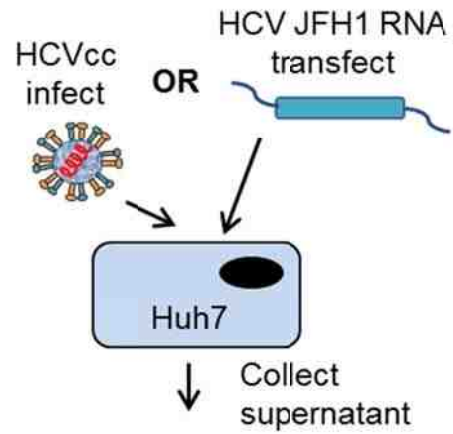
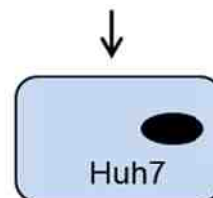
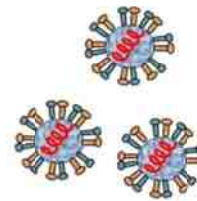
1.5 HCVpp and HCVcc model systems

HCV research has been long hampered by the lack of an *in vitro* reproducible HCV infectious system. To study HCV entry and other earlier steps in HCV life cycle, a pseudotyped HCV system (HCVpp) was created (**Fig. 3A**). It consists of an envelope-defective HIV core and HCV envelopes or other viral envelopes (67). This system has contributed in a great deal to the identification of HCV receptors and defining of HCV tropism. It leads to successful identification of the HCV co-receptors CLDN-1 (28) and OCLN (29) and better understanding of other earlier steps of HCV infection (34, 68, 69). The HCVpp system has several advantages. First, the HIV reporter virus is defective in HIV envelope gene, thereby only capable of single round infection (replication-defective),

A**HCVpp****HCV pseudoparticles**

Reporter expression

Single-round assay
Cell entry-only

B**HCVcc****HCV virions**

HCV RNA/ protein expression

Complete
HCV life cycle

Figure 3. In vitro HCV culture systems. (A) The HCV pseudoparticle (HCVpp) system. HCVpp contains an envelope (replication)-defective HIV core and a functional HCV envelope and has been used to study HCV glycoproteins-mediated cell entry. The HIV genomes have been engineered to express a reporter gene, such as luciferase or GFP, allowing for quantitative measurements of the virus entry. To make the HCVpp, 293T cells are co-transfected with HCV envelope expression plasmid HCV-E1E2 and envelope-defective HIV-luciferase (HIV-Luc) or HIV-GFP (HIV-GFP) reporter proviral DNA. Culture supernatants are collected at 48 hr post-transfection, cleared of cell debris, and saved as the HCVpp stock. Similarly, pseudotyped particles containing no envelope protein or vesicular stomatitis virus glycoprotein protein (VSV-G) are also prepared and used as negative and positive controls, respectively. The titer of the virus can be determined by HIV reverse transcriptase assay. **(B)** The HCV cell culture (HCVcc) system. HCVcc represents the only available *in vitro* cell culture system that recapitulates the complete life cycle of HCV. It requires a special JFH1 strain and the Huh7 or Huh7-derived hepatoma cell lines (Huh7.5 and Huh7.5.1 cells) to achieve efficient viral replication. HCVcc is produced by inoculation of Huh7/Huh7-derived cells with viral stock or by transfection of these cells with *in vitro* synthesized JFH1 RNA. Culture supernatants containing high titers of HCVcc are used to infect naïve Huh7.5.1 cells, and productive infections are monitored by qRT-PCR for HCV RNA or immunostaining of HCV antigens such as HCV core. Viral titers can be determined using the foci formation assay.

which allows accurate determination of HCV envelope protein-mediated virus entry. Second, the titers of the viruses can be easily determined by HIV reverse transcriptase activity assay. Third, because of insertion of the green fluorescent protein (GFP) or luciferase (Luc) reporter gene into the HIV genome, cell entry of pseudotyped viruses can be readily monitored on the basis of a single cell or a population of cells by simple reporter gene assays.

Another breakthrough in HCV research occurred in 2005, i.e., establishment of the first productive *in vitro* HCV culture system by three independent research groups (HCVcc, **Fig. 3B**) (70-72). Since then, as the only system that was capable of recapitulating the complete HCV life cycle *in vitro*, the HCVcc system and other derived systems have been widely used in HCV research. The HCVcc system involves the use of a unique HCV JFH1 strain (HCV subtype 2a) and a unique human hepatoma cell line Huh7 that is defective in the innate anti-viral cellular response. The JFH1 strain is able to replicate efficiently in Huh7 hepatoma cells and produce high titers of HCV. Based on the original HCVcc system, modifications were made to achieve even higher levels of viral replication and infectious virus production. Those modifications include the use of chimera HCV strains (e.g., J6/JFH1 chimera, H77/JFH1 chimera) and/or highly permissive cell clones derived from Huh7, such as Huh7.5, a subclone of Huh7 that was cured of a subgenomic HCV replicon by IFN- α treatment (73) and Huh7.5.1, a Huh7.5-derived highly permissive cell clone. Both the HCVpp and the JFH1 HCVcc systems have been established in our laboratory and have been extensively used throughout this study.

2. CELL-CELL CONTACT-MEDIATED VIRAL TRANSMISSION

2.1 Cell-cell contact-mediated transmission of viruses

Cell-cell contact-mediated (CCCM) viral infection and transmission has been demonstrated in many plant and animal viruses (74-76). Different animal viruses adopt different strategies for CCCM transmission. Herpesviruses, paramyxo-viruses and retroviruses can induce plasma membrane fusion between infected and uninfected cells followed by transfer of infectious viral materials into the uninfected target cell; this type of CCCM transmission frequently leads to syncytium formation (77-79). Herpes simplex virus (HSV) can bud on the basolateral membrane of an infected epithelial cell, then fuse with and penetrate a neighboring uninfected cell by binding to the viral entry receptors located at the tight junctions between the two cells (80). Some neurotropic viruses like rhabdoviruses, herpesviruses and paramyxoviruses can transfer across neural synapses (81-83). Poxviruses such as vaccinia virus (VV) can induce the formation of actin tails to project progeny viruses or viruses adhered to the surface of infected cells to uninfected cells, in proximity or distance (84). Retroviruses such as murine leukaemia virus (MLV) induce stable anchoring of filopodial bridges between infected and uninfected cells, allowing virions to travel from an infected cell to an uninfected cell in an actin-myosin-dependent fashion; viral receptors are required for such transfer, indicating virus–cell membrane fusion (85). HIV-1 can travel for up to 300 μm to infect a distant cell along nanotubes, a new form of intercellular communication and exchange of materials like protein and organelles by actin-motored movement (86, 87). This type of CCCM transmission is also receptor - dependent, indicating virus–cell membrane fusion. Additionally, retroviruses such as HIV-1 and human T cell leukemia virus type 1 (HTLV-1)

can induce the formation of virological synapses (VS) between infected and uninfected cells that subsequently facilitate CCCM viral infection and transmission (88, 89).

Viruses that utilize CCCM transfer often capitalize on one or more cellular processes to accomplish the transfer and in most cases the type of infected cell/tissue dictates the processes that become appropriated. In immune cells, HIV-1 and HTLV-1 subvert the immunological synapse machinery in the infected cells and induce cytoskeleton reorganization and polarized viral budding towards an uninfected receptor-expressing cell in a structure named virological synapse (90, 91). HIV-1 also “hijacks” the nanotube structures for intercellular communication in macrophages and T cells for CCCM virus transfer (86, 87), while HSV exploits the tight junctions among epithelial cells for viral spread (80). Most of the cellular machineries/physiological processes capitalized by viruses for their CCCM transmission involve actin and/or microtubule cytoskeleton, so that virus budding could be polarized towards uninfected targets, or the subcellular structure for CCCM transfer could be supported, or the virus could be delivered from infected cells to uninfected cells by actin/tubulin-motored transport.

2.2 Cell-free virus infection vs. CCCM viral transmission

Both cell-free virus infection and CCCM viral transmission have advantages and disadvantages. Cell-free virus infection enables host-to-host transmission of virus [except HTLV-1 which requires infected T cells to transmit between host (92)] and rapid transit of virus in biofluid circulation once inside a new host to spread to distant tissue/organ. However, cell-free virus infection usually encounters various biophysical and immunological barriers. Biophysical barriers include mucous membranes and a progressive loss of viral infectivity over time. In addition, in cell-free virus infection

involving random fluid-phase diffusion of the virus, the “searching” process for a target cell and viral attachment and binding to receptors on the target cell is probably the most rate-limiting step during the complete viral life cycle. Particularly, for viruses with low binding affinity/avidity to their receptors and viruses binding to more than one receptor (e.g. HIV-1 and HCV) or binding to receptors expressed at low levels, cell-free virus infection is disadvantageous. Immunological barriers to cell-free virus infection include innate humoral and cellular defenses during acute infection and adaptive immune responses such as neutralizing antibodies (nAbs), antibodies that specifically recognize viral antigens and “neutralize” the virus by clearing them out from circulation and virus-specific cytotoxic T lymphocytes during subsequent rounds of infection.

To the contrary, CCCM viral transmission and spread has several advantages by avoiding many of the obstacles described above for cell-free virus infection. Virus transmission between hosts via infected cell-associated virus could be more efficient than cell-free virus because the infected cell could adhere to and cross biophysical barriers like the mucous membranes in the new host while cell-free virus could not. Once inside the target tissue/organ in the new host, the virus spread by CCCM transmission could also be more efficient than spread by cell-free virus infection. First, direct viral transfer from an infected cell to a neighboring cell can avoid the rate-limiting random fluid phase diffusion step to search for and bind to viral receptors. Second, if viral receptors are recruited to the site of cell-cell contacts, which is true under most circumstances, the virus-receptors binding and viral entry can be even more efficient. A final advantage of CCCM viral transmission is the protection that provides for the infection from immunological barriers such as above-mentioned neutralizing antibodies. The protection could be either spatial because of limited or abolished accessibilities of

immune effectors to the virus, or temporal due to shorter or no exposure time of the virus to immune effectors, or both.

Among various types of CCCM transmission observed in different viruses, HIV-1 CCCM transmission across virological synapse has been well-characterized and serves as a great example for summarizing the common features of CCCM viral transmission. First, HIV-1 transmission across VS between T cells is suggested to occur much more rapidly, i.e., within 1 hour, and 18,000 fold more efficiently than cell-free virus infection (93). In addition, both viral envelope proteins and viral entry receptor CD4 are required for HIV-1 transfer. Moreover, the formation of VS involves aggregation of talin (actin-binding protein mediating interaction of integrin with F-actin) and other cell adhesion molecules at the cell-cell contact site and polarization of the microtubule organizing center (MTOC); the integrity of actin and microtubule cytoskeleton is absolutely required in HIV-1 VS (90, 94). Finally, HIV-1 transmission across VS is demonstrated to be resistant to trypsin treatment and patient-derived neutralizing antisera; it is thereby proposed to be the predominant route of HIV-1 dissemination *in vivo* and to contribute to HIV-1 persistence (93). Taken together, HIV-1 transmission across VS is featured by a rapid kinetics, the dependence on viral envelope proteins, viral receptors and intact actin and microtubule cytoskeletons, and the resistance to neutralizing antibodies. All these features point to the fundamental roles of CCCM HIV-1 transfer in viral dissemination and establishment of chronic infection (immune evasion). It is expected that other types of CCCM viral transmission share at least some of these features.

2.3 Evidence for CCCM HCV transmission

HCV research has been focused on cell-free virus infection for the past two decades, whereas there is some indirect evidence for CCCM HCV infection. Since the infectious

HCV cell culture system HCVcc was developed in 2005, HCV researchers have observed the formation of infection focus in HCVcc-infected hepatocyte culture (70). Infection focus is a focal area of infected cells containing about 20-100 cells. Its formation is strongly suggestive of localized viral spread between adjacent cells. Additionally, staining for HCV viral antigen in HCV patient liver biopsy also exhibits the pattern of discrete, localized HCV infection focus; another study with HCV RNA *in situ* hybridization even shows a gradient dispersion of viral genome around the center of infectious focus in patient liver biopsies (95-97). Moreover, a recent study demonstrates that CCCM HCV infection is relatively less sensitive to nAbs and neutralizing patient sera than cell-free HCV infection (98). In fact, if the extremely high cell density [2-3.0x10⁵ hepatocytes/cm² (99)] and presence of nAbs and other immunological responses (100) in the liver of chronic hepatitis C patients are considered, it is not difficult to conceive the advantages of CCCM HCV spread within the liver over cell-free virus spread.

3. EXOSOMES

3.1 Exosomes

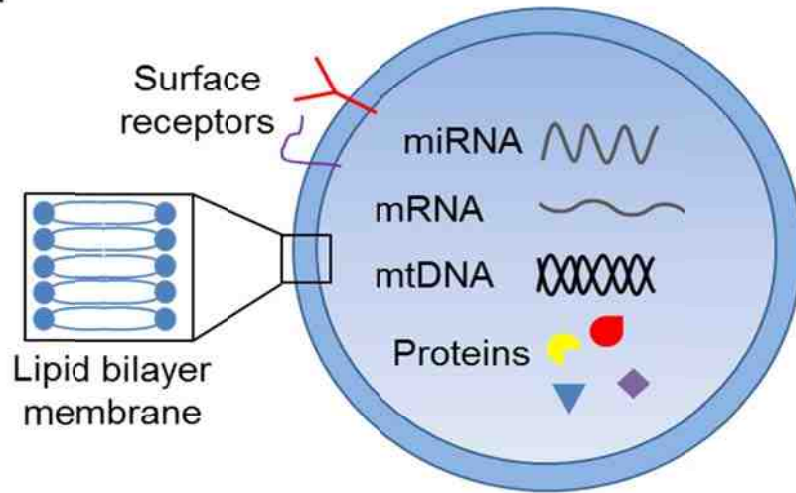
3.1.1 Definition, cargo, biogenesis, and uptake

In both cell culture supernatants and body fluids, there are abundant extracellular vesicles (EV) of different sizes, origins, and compositions (101). Among them, exosomes are, by definition, 30 nm – 120 nm small vesicles originated from endosome-derived MVB with a series of exosome markers (102). There are generally two types of exosome markers, cell-specific exosome markers and universal markers present in almost exosomes derived from any cell types. Cell-specific markers are usually

selectively enriched on exosomes derived from particular types of cells only (103, 104); exosomes with those markers are proposed to be used as biomarkers for disease diagnosis and prognosis. To the contrary, universal exosome markers are usually related to exosome biogenesis pathways and include endosome-associated proteins (e.g. Rab GTPase), tetraspanin membrane proteins (CD9, CD63, CD81, CD82), heat shock proteins (e.g., Hsp70), and acetylcholinesterase (AChE) (101, 105, 106). Besides exosome protein markers and protein cargos, other components of exosomes include lipids and nucleic acids (mRNA, miRNA, mtDNA) (**Fig. 4A**). Comparison of RNA profiles in exosomes and their originating cells reveals a selective enrichment of mRNAs and miRNAs in exosomes; these RNA can be functionally transferred to target cells for various effects, e.g. mRNA translation or target gene silencing following uptake of mRNA- or miRNA- contained exosomes (101).

Exosome biogenesis pathways are not completely understood. By definition, exosomes are formed by inward budding on the limiting membrane of endosome to form intraluminal vesicles (ILV) inside MVB (**Fig. 4B**). These MVBs either merge with lysosome and become degraded (lysosomal MVBs) or fuse with the plasma membrane and release the contained ILVs/exosomes (secretory MVBs) (**Fig. 4B**); these two distinct fates are suggested to result from distinct populations of coexisting MVBs in the same cell. Three pathways have been suggested to be involved in exosome biogenesis. RNAi knockdown of endosomal sorting complex responsible for transport (ESCRT) components or their accessory proteins leads to decreased ILVs in MVBs and/or decreased secretion of exosomes (101, 107), suggesting an ESCRT-dependent pathway for exosome biogenesis. However, ESCRT-independent pathways have also been suggested. Ceramide or tetraspanin are believed to play central roles in these alternative exosome biogenesis pathways (108-111).

A



B

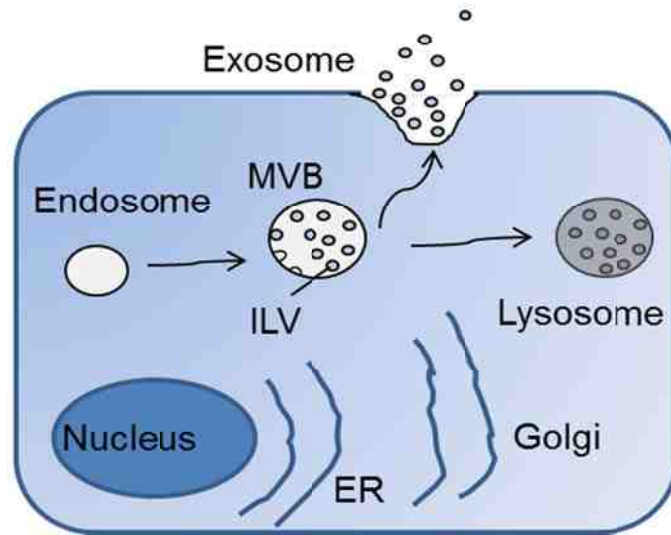


Figure 4. Exosome cargos and biogenesis. (A) Exosome cargos. Schematic diagram of exosomes showing lipid bilayer, typical protein markers and contents of exosomes. (B) Biogenesis of exosomes. The limiting membrane of endosome buds inwards to form multivesicular bodies (MVBs) and the contained vesicles are called intraluminal vesicles (ILVs). Distinct MVB populations predispose their distinct fates: lysosomal MVBs are targeted to lysosomes for degradation; secretory MVBs traffic to and fuse with the plasma membrane. The ILVs released upon the fusion are now called exosomes.

Functions of exosomes depend on their ability to interact with the recipient cells to either trigger signal transduction upon binding or to deliver their contents of proteins, lipids, and RNAs. However, exosome uptake by or effects on the recipient cells are still not clear, although it has been proposed that direct contact with target cell surface receptors and ensuing signal transduction, fusion with the cell membrane and release of cargos, and endocytosis followed by signal transduction or cargo release may all contribute to exosome entry into and effects on recipient cells (112, 113). The binding specificity of exosomes to the target cells has been documented (114, 115). It is likely mediated by cell surface adhesion molecules (116) and tetraspanin complexes (117), probably through their associated integrins (118). After binding to the target cells, stable association of exosomes with the plasma membrane is possible, especially on cells that display little endocytic activity (114). Alternatively, after binding to target cells, fusion of exosomes with the plasma membrane could take place, as detected by labeling exosomes with the lipophilic dye R18 (119); endocytosis of exosomes by the target cells could also take place, as demonstrated by accumulation of captured exosomes in endocytic or phagocytic compartments in various cells (120-122).

3.1.2 Physiological functions and therapeutic potentials

As an essential hallmark of multicellular organisms, intercellular communication had been believed to be mediated by direct cell–cell contact or transfer of secreted molecules. However, in the last two decades, exosome-mediated intercellular communication has emerged as a third mechanism. Since exosomes have a very broad range of producing cells and target cells, the physiological functions of exosomes almost extend to every discipline of biomedical science: immunology (123), cancer biology (124, 125), neurobiology (126-128) and prion diseases (129, 130). As mentioned earlier,

exosomes selectively incorporate cell-type specific proteins/nucleic acids. This is also true in cancer patients or individuals with Alzheimer's disease. Therefore, identification of disease-specific exosomal proteins or exosomal RNA/miRNA profiles as biomarkers has become a new area of exosome research (131-133). Lastly, because of the natural ability of exosomes to harbor proteins and nucleic acids of therapeutic potential and to reduce the susceptibility of those proteins/nucleic acids to degradation, both cell culture-produced exosomes and artificial exosome-resembling liposomes have been actively investigated for their potential as delivery vehicles for therapeutic proteins/nucleic acids (134).

3.2 Exosomes and viruses

Viruses, especially enveloped viruses, share many common characteristics with exosomes, including biophysical properties such as the size and density, biogenesis pathways, and uptake by cells. Therefore, exosomes and their biogenesis pathways are frequently usurped by viruses to transfer viral proteins (e.g., tegument of herpes simplex virus), viral RNA/miRNAs (e.g., Epstein-Barr virus), or even virions themselves (e.g., HIV-1) to uninfected cells (135-138), leading to viral spread, pathogenesis and immune evasion (139). Of particular note, "trans-infection" of T cells by HIV-1-loaded dendritic cells (DC) or macrophages to T cells has been found to be resistant to nAbs and contributing to immune evasion and viral dissemination in lymph nodes during early stages of the infection, while the above-mentioned HIV-1 transmission across virological synapse massively disseminates the virus within lymph nodes from T cells to T cells at later stages of the infection (138, 140-142).

3.3 Exosome interactions with HCV

A few studies suggest potential roles of exosomes and their biogenesis pathways in HCV infection. Using recombinant HCV envelope proteins, one study shows that CD81, one of the exosome markers and also one of the HCV entry receptors, could direct the secretion of HCV envelope proteins in the form of exosomes in CHO cells (143). Another study demonstrates the requirement of endosomal sorting complex responsible for transport (ESCRT)-0 components for HCV budding (144). Both studies suggest that HCV may usurp ESCRT-dependent exosome biogenesis pathway for its secretion. In addition, HCV RNA has been recently found to be secreted in exosomes and these exosomes, when taken up by plasmacytoid dendritic cells, could trigger innate immune response (145). Moreover, a recent study demonstrates by cryo-electron microscopy that 5.6% of cell culture-produced HCV particles are surrounded by an additional layer of “envelope”; but the biological nature of this extra “envelope” was not investigated (146). However, it is not clear whether infectious HCV virions can be secreted and transmitted to target cells in the form of exosomes.

3.4 Exosome purification – current protocols

Exosome research has been hampered by lack of a widely accepted “unifying” purification protocol. There are a few protocols that are currently used in the exosome research. Each has its pros and cons.

3.4.1 Precipitation with polymers

PEG polymers, e.g. PEG 8000, are widely used in precipitation of viral particles, including HCV (71). Some biotech companies provide “exosome isolation” kits which are based on water molecules’ exclusion effect of polymers. In our own hands, PEG 8000 successfully precipitates both HCV virions and exosomes from culture supernatant (see below). However, it is not certain whether polymer-based precipitation of

exosomes also co-precipitate macromolecules like protein complexes in the supernatants.

3.4.2 Ultracentrifugation

Ultracentrifugation was the first method used to isolate extracellular vesicles (147), it remains the “gold standard” of exosome isolation method and is often used as a reference for any newly developed methods. Following ultracentrifugation, further purification of exosomes can be performed by gradient density centrifugation. Sucrose density centrifugation was initially used to purify viruses in 1951 (148). It is probably the oldest and most widely used virus/particles/vesicles purification method. However, the recently developed iodixanol density gradient (the brand name is Opti-prep) has also been used in fractionation and purification of exosomes, viral particles and subcellular organelles; it could generate more consistent results compared to the conventional sucrose density gradient (149), probably due to the intrinsic properties of iodixanol such as neutral pH and physiological osmolarity.

3.4.3 Immunocapture

Immunocapture of exosomes using beads coated with antibodies against exosome surface marker is also used in exosome isolation (150). The advantage of this method compared to ultracentrifugation is its purity, as it is based on the specificity of the used antibody. However, the specificity also leads to the lack of diversity in this case. Exosomes are heterogeneous in nature. None of the known exosome markers have been confirmed to be expressed on every single exosome. Thus, immunocapture of exosomes with antibodies against any of these “markers” might result in selective isolation of only a fraction of the exosome population.

4. HCV INTERACTION WITH THE BRAIN

4.1 CNS abnormalities in HCV patients

HCV infection-related central nervous system (CNS) abnormalities including reduction of health-related quality of life (HRQL), chronic fatigue and cognitive impairments have been observed in about half of the chronically infected subjects and their daily lives are severely affected (151-155). Even in those who have been cleared of HCV infection in periphery spontaneously or after treatment, CNS abnormalities could still exist (156, 157), raising the possibility of extra-hepatic (CNS) HCV persistence/ latency. In addition, HCV-associated CNS abnormalities are observed less frequently in patients with other chronic liver diseases such as chronic hepatitis B and are independent of the severity of liver diseases (158-160), suggesting that hepatic encephalopathy commonly seen in severe liver diseases such as cirrhosis is not responsible for the HCV-related CNS abnormalities. Moreover, the correlation between HCV infection and CNS dysfunction is further confirmed with neuroimaging studies using cerebral proton magnetic resonance spectroscopy (160-162), suggesting that a cerebral biological/metabolic cause underlies the abnormalities. Taken together, the above psychometric and neuroimaging evidence implies that the HCV *per se* could cause CNS abnormalities.

4.2 HCV infection of PBMC

CNS abnormalities are not the only extra-hepatic manifestations of HCV infection. Since HCV's initial discovery as the etiologic agent responsible for non-A non-B hepatitis in 1989 (163), there are little doubts that human hepatocytes are the primary target cells for HCV infection. Nevertheless, clinically, HCV infection has been long associated with

immune dysfunction and lymphoproliferative disorders (LPD) such as mixed cryoglobulinemia (MC) and non-Hodgkin's lymphomas (NHL) (164-168). The prevalence of HCV in patients with NHL is reported to be 15%, much higher than that in healthy controls (1.5%) and also in patients with other hematologic malignancies (2.9%) (169). All these observations indicate a role of HCV in the etiology of the above-mentioned immune diseases. In addition, there is a growing body of evidence showing the detection of both (+)-strand HCV genomic RNA and (-)-strand HCV replication intermediate in all subsets of peripheral blood mononuclear cells (PBMC), macrophages, and monocyte-derived DCs from chronic HCV patients (156, 157, 165, 170-172), suggesting active viral replication in the immune cells of HCV-infected patients. Furthermore, several recent studies report successful infection of human primary T cells, monocyte-derived macrophages, and a few B-cell and T cell lines with HCV patient plasma and production of infectious progeny viruses (173-178); one study even identifies human CD5 as the entry receptor of HCV in human T lymphocytes (179). However, attempts to infect human PBMC or lymphoid cell lines with cell-culture produced HCV including the HCVpp and JFH1 HCVcc have proven to be difficult (180-182), even though efficient HCV IRES-dependent translation and polyprotein processing were shown in these cells (182), suggesting the lack or inadequacy of certain essential host factor(s) for HCV JFH-1 infection and replication in these cells.

4.3 HCV infection of the brain and pathological evidence

Pathological evidence for HCV infection of the brain has also been found. Positive strand HCV RNA in cerebrospinal fluid (CSF) and both (+)-strand and (-) -strand HCV RNA in various regions of brain have been found in post-mortem brain samples of HCV patients, suggesting HCV CNS invasion and active HCV replication in the brain (183-185). In addition, using the laser capture microscopy (LCM), a recent study successfully

identifies the HCV target cells in the brain to be astrocytes and microglia cells as both HCV RNA and viral proteins are detected in these cells but not in neurons or oligodendrocyte (186, 187). In the same study, HCV proteins-positive astrocytes are found to be only positive for the (+)-strand HCV RNA, while HCV proteins-positive microglia cells are found to be positive for both (+) and (-)-strand HCV RNA, indicating that active HCV replication is only occurring in microglia but not astrocytes. Moreover, microglia in HCV-infected subjects are shown to be highly activated and produce pro-inflammatory cytokines such as TNF- α , IL-1 β and IL-8 (188); *in vitro* infection of primary macrophages with HCV patient plasma also induces TNF- α and IL-8 production (178), suggesting the potential role of microglia in causing neuronal dysfunction in chronic HCV infection, likely via secretion of neuron-toxic cytokines. However, how astrocytes are infected and what roles do astrocytes play in HCV-induced CNS abnormalities remain to be addressed. Of particular note is that almost all studies on HCV infection of the CNS are based on examination of post-mortem brain samples. There are currently no studies on molecular mechanisms of HCV infection of the CNS and its role in HCV neuropathogenesis.

4.4 HCV entry into the CNS – the “trojan PBMC hypothesis”

Under normal physiological conditions, the human brain is believed to be protected by the blood-brain barrier (BBB) from bacterial or viral pathogen invasion. So a natural question arises about HCV CNS invasion: how does the virus enter the brain? To approach this question, sequence analysis of RNAs derived from serum, PBMC and CNS of HCV patients is performed. The results show that RNA sequences from CNS are closer to those from PBMC, rather than RNA sequences from serum (183, 185). A “trojan PBMC hypothesis” was then proposed (152) and could be summarized as follows. HCV can infect PBMC in the periphery, especially T cells or monocytes/ macrophages.

The infected immune cells can cross the BBB and bring the virus into the CNS. Thereafter, active replication of HCV in these cells could release more viruses and cause a secondary spread of HCV to target cells in the brain. Those target cells could be brain microglia cells, the resident macrophages of blood monocytic origin in the brain, or astrocytes, the cell type most abundant in the brain and most intimately linked to neuronal function. The infected microglia can also support active HCV replication and become another source of virus production in the CNS. HCV infection then starts to spread in the brain and the subsequent production of cytokines, viral proteins and other toxic factors from infected cells and bystander uninfected cells could lead to impairment of neuronal functions by direct impact on neurons or indirect impact on the neuron-supporting astrocytes. However, until today, the above hypothesis remains to be experimentally tested and substantiated. It also remains unclear at the molecular level whether and how HCV gains entry into these brain cells and whether the infection of these brain cells results in any demise in neurons.

4.5 HCV infection of the CNS in HIV-1/HCV co-infected individuals

HCV infection of the CNS is further complicated by the frequent occurrence of HIV-1/HCV co-infection. The prevalence of HCV in HIV-1-positive individuals is about 30% in the U.S. and Europe, likely due to shared transmission routes, both through blood product and injection drug use (189). In HIV-1/HCV co-infected patients, progression of the diseases caused by one virus is potentiated by the other. In HIV-1-infected patients, liver diseases are now the No.1 cause of death; in HIV-1/HCV co-infected patients, chronic HCV progresses into liver fibrosis or even HCC in a much faster pace (189, 190). Even if HCV infection alone does not cause severe dementia as seen in untreated HIV-1 patients, several studies have demonstrated that HIV-1/HCV co-infection causes further neurocognitive impairments compared to those with HIV-1/HCV mono-infection (191,

192). In addition, a recent study demonstrates that detection of HCV in the brain is unrelated to HCV viremia, but active HIV-1 disease and detectable CSF HIV-1 in HIV-1/HCV co-infected patients (193).

4.6 Astrocytes in CNS function

As the most abundant CNS cells, astrocytes play an essential role in maintaining homeostasis and normal function of the CNS (194). Among the well-recognized astrocytes functions are uptake and recycling of neurotransmitters, secretion of neurotrophic factors, antioxidant defense and being an integral part of the blood brain barrier (195). More importantly, astrocytes are also one of the major participants in CNS immune responses under various disease conditions including neurodegenerative diseases and pathogen invasions, when they produce key immune mediators such as cytokines, proteases, protease inhibitors, adhesion molecules, and extracellular matrix components (195, 196). Human astrocytes express toll-like receptors (TLR) 1-5, TLR9 and many other intracellular receptors for the recognition of viral antigens (197-199). During viral invasion of CNS, susceptible to the infection or not, astrocytes can usually recognize one or more viral antigens via TLRs and other receptors and mount an innate immune response, e.g. secretion of proinflammatory cytokines and other immune mediators (200). However, although the attempt of the response is to clear the infection, it can be a double-edged sword on neuron survival and functions, as many of the effectors in the response are also neurotoxic (200, 201). Nevertheless, it is not known yet whether HCV infection of the CNS changes cytokine expression profiles in astrocytes and if changes, how neurons are affected.

5. SUMMARY OF THE BACKGROUND AND HYPOTHESES

HCV is highly capable of evading the immune system, which leads to establishment of chronic infection in about 80% of infected people (202). Neutralizing antibodies are the main effectors of the humoral response against viral infections and one of the most important defense mechanisms in controlling viral spread within a host. However, although nAbs are generated in chronic HCV patients, they often fail to control the infection (203). Frequent alterations of HCV epitopes have been proposed to contribute to viral escape from recognition and elimination by the immune system (204, 205), yet it is highly conceivable that other immune evading mechanisms are involved. Since the isolation and identification of HCV in 1989 (163), a great deal of progresses have been made in our understanding of HCV virology and pathogenesis; examples include the discoveries of several HCV entry receptors/co-receptors: CD81, SR-BI, CLDN1, and OCLN (25, 27-29). However, HCV research has been mainly focused on cell-free virus infection. In contrast, CCCM viral transmission has been discovered and characterized in many other viruses and proposed to contribute to the immune evasion and establishment of chronic infection in many of those viruses (74). In addition, exosome-mediated viral protein/RNA/virion transfer has been observed in many other viruses and demonstrated to contribute to immune evasion and disease progression in virus-infected patients (139). Although HCV RNA was recently demonstrated to transfer intercellularly in the form of exosomes (145), interaction and relationship between infectious HCV virions and exosomes are not clear. Thus, our first two hypotheses are that CCCM viral transmission constitutes an important route for HCV dissemination among hepatocytes (**Fig. 5** and the Results section, CHAPTER 1), and that HCV can be secreted in the form of exosomes and that exosome-mediated HCV transmission constitutes an alternative route for the spread of HCV in hepatocytes (**Fig. 5** and the Results section, CHAPTER 2).

CNS abnormalities are observed in more than half of HCV-infected individuals regardless of the stage of liver diseases (152). Both HCV (+)-strand and (-)-strand RNA are found in the brain of HCV patients. The target cells of HCV in the CNS are suggested to be astrocytes and microglia cells because both of them are HCV RNA- and protein-positive (186, 187). Nevertheless, it is not known how HCV gains entry into these nonhepatic cells, whether HCV can productively infect these cells, whether HCV infection changes cytokine expression profiles in these cells and if changes, how neurons are affected. Considering the essential role of astrocytes, the most abundant cell type in the brain, in CNS function, our third hypothesis is that HCV infects astrocytes, leading to neuronal dysfunction (**Fig. 5** and the Results section, CHAPTER 3).

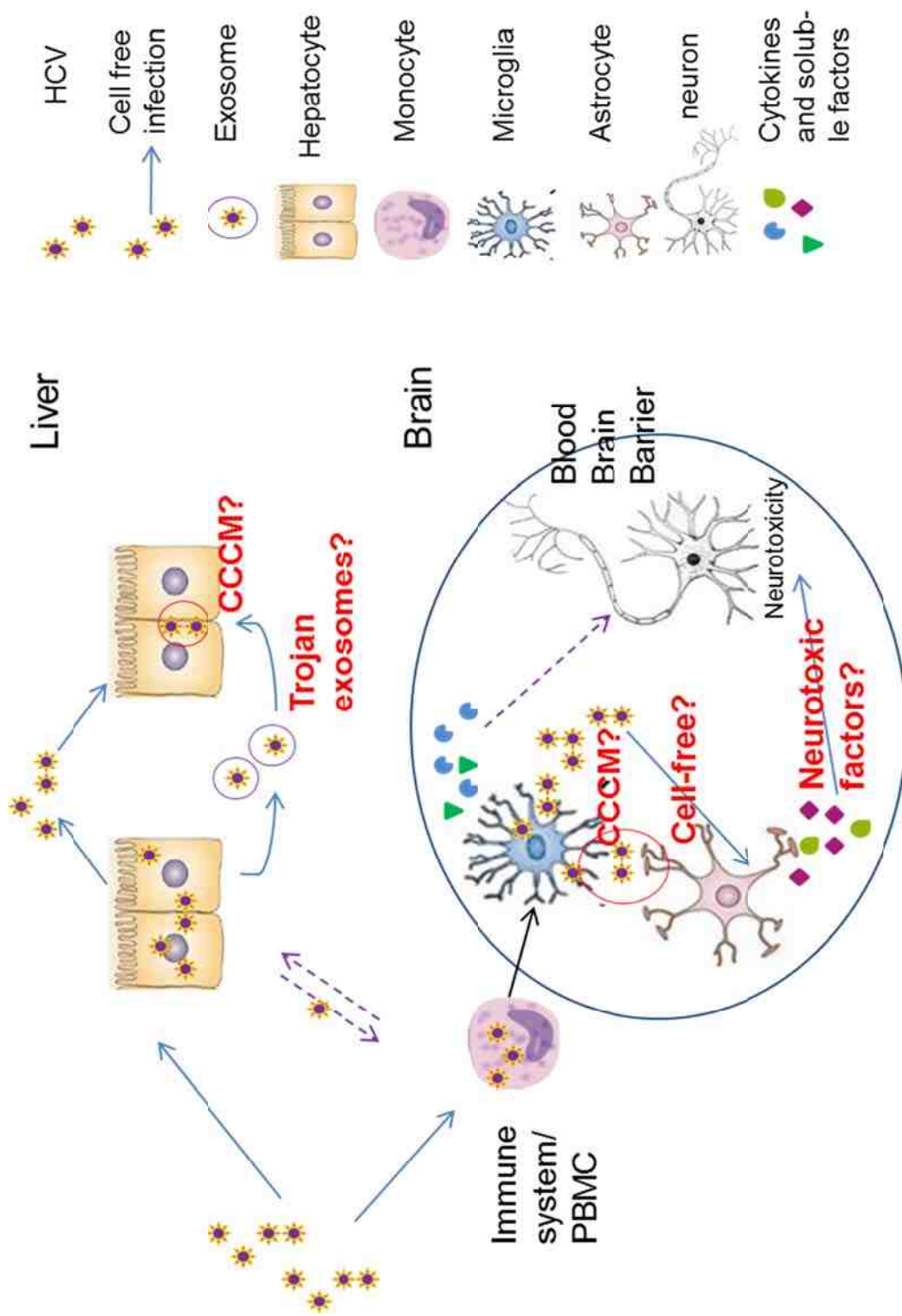


Figure 5. HCV infection of target cells and transmission routes: summary of hypotheses. HCV enters a host and infects hepatocytes and/or monocytes/PBMCs. HCV spreads in liver through cell-free virus infection, CCCM transmission (Results section CHAPTER 1) and exosome-mediated infection (Results section CHAPTER 2). On the other hand, the monocytes carrying HCV enter the CNS and differentiate into microglia. HCV virions produced by these actively replicating cells then infect astrocytes and resulting changes in cytokine production from astrocytes affect neuron survival (Results section CHAPTER 3). Crosstalks between hepatic and extra-hepatic HCV-targeted cells are possible but currently unknown.

MATERIALS AND METHODS

MATERIALS

Media and supplements

Dulbecco Modified Eagle Medium (DMEM), Roswell Park Memorial Institute 1640 (RPMI-1640) medium, Hank's balanced solution (HBSS), and hepatocyte culture media (PHH) were purchased from Lonza (Walkersville, MD). Neurobasal™ Medium, B27 Supplement, Ham's F-12 Nutrients Mixture (Ham's F-12), streptomycin-penicillin-glutamine (S. P. G., 100X), and 0.25% trypsin-EDTA (1X) were from GIBCO (Grand Island, NY). Fetal bovine serum (FBS) was from Hyclone (Logan, UT). F-12K Nutrient Mixture Kaighn's Mod. (F-12K) and 0.25% Trypsin were from Cellgro. Opti-MEM reduced serum media was from Invitrogen (Carlsbad, CA). Ampicillin sodium salt and kanamycin sulfate were from United States Biological (USB, Swampscott, MA). All the culture media described below were prepared in house. Luria Broth (LB) liquid medium contained 0.01 g/ml Bacto Tryptone, 0.005 g/ml Bacto yeast extract, 0.01 g/ml NaCl. LB agar plate was prepared with 7.5 g agar per liter of the liquid LB. Working concentrations of antibiotics for liquid and solid LB were 100 µg/ml for ampicillin and 50 µg/ml for kanamycin.

Plasmids and siRNAs

HCV receptors: pCMV-SPORT-Claudin1 and pCMV-SPORT-occludin expression plasmids were purchased from Open Biosystems (Lafayette, CO). pcDNA3-CD81 and pcDNA3-SR-B1 were constructed previously in our lab (206). Briefly, the coding DNA sequences (CDS) of CD81 and SR-B1 were amplified from pOTB7-CD81 and pOTB7-SR-B1 (Open Biosystems) by PCR and cloned into pcDNA3 with EcoRI and XhoI, Kpn

I and EcoR V, respectively. The sequences of the primers used are: 5'-CCC GAATTC ATG GAG CGA GCG CGC AAC GGC-3' and 5'-CCC CTCGAG CTA CTG AGG GAC TGC ACA GGC-3' for CD81; 5'-CCC GGTACC GAC ATG GGC TGC TCC GCC-3' and 5'-CCC GATATC CTA CAG TTT TGC TTC CTG-3' for SR-B1.

JFH1-core177-GFP and related plasmids: The full-length core and GFP fusion protein plasmid pJcore-GFP was previously constructed in our lab (unpublished data). Briefly, the full HCV core-encoding sequence was PCR amplified from pJFH1 (kindly provided by Dr. Takaji Wakita, Japan) with the primers 5'-CGC GG GAATTC ACC ATG AGC ACA AAT CCT AAA CC-3' and 5'-CGC GG GGATCC AGA GAC CGG AAC GGT GAT G-3', and then inserted into pEGFP-N3 plasmid at the N-terminus of GFP by EcoR I and BamH I. The other core-GFP fusion protein plasmid containing only the N-terminus 177 amino acids of core, the pCore177-GFP, was constructed in a similar fashion. Amino acids 1 to 177 of HCV core was PCR amplified using JFH1 as template, and with the forward primer 5'-CGCGG GAATTCA CCA TGA GCA CAA ATC CTA AAC C-3' and the reverse primer 5'-CGC GG GGATCC G AAG ATA GAA AAG GGG AAA CCG-3'. The PCR products and the pEGFP-N3 plasmid were digested with EcoR I and BamH I and ligated to obtain the pCore177-GFP plasmid. To insert GFP into JFH1 genome right after the 177 amino acid of core and obtain pJFH1-c177-GFP plasmid, a four-step strategy was adopted. First, the 3 kb sequence from the 5' untranslated region (5'UTR) to the nonstructural protein 2 (NS2) on pJFH1 was cloned into pBlueScript KSII (Stratagene, California) using EcoR I and Not I to obtain the much shorter intermediate cloning vector pBS-core-NS2 (6 kb). Secondly, Bgl II and Mlu I sites were introduced into both the two sides of GFP (based on pEGFP-N3) and the 177 position of core in pBS-core-NS2 vector by PCR with primers 5'-GA AGATCT G TGA GCA AGG GCG

AGG AGC-3' and 5'-ACC G ACGCGT CT TGT ACA GCT CGT CCA TGC-3' for GFP, and 5'-ACC G ACGCGT TT GCT GGC CCT GTT GTC CTG-3' and 5'-GA AGATCT G AAG ATA GAA AAG GGG AAA CCG-3' for pBS-core-NS2. Both PCR products were cloned directly to the pSC-A-Amp/Kan vector by TA cloning with the TOPO TA cloning kit. Thirdly, the pSC-A-MluI-GFP-Bgl II and pSC-A-Bgl II-pBS-core-NS2-Mlu I plasmids were digested with Bgl II and Mlu I and the two inserts GFP and pBS-core-NS2 were ligated to obtain pBS-core177-GFP-NS2. Lastly, the HCV sequence from 5'UTR to NS2 containing GFP at core 177 position was cut out from the pBS-core177-GFP-NS2 plasmid by EcoR I and Not I and inserted back into pJFH1 to obtain the pJFH1-c177-GFP.

JFH1-TCcore and intermediate plasmids: The JFH1-TCcore plasmid was constructed by mutagenesis using JFH1 as the template. A full-length (FLNCCPGCCMEP) tetracysteine (TC) tag (207) was inserted into the pBS-core-NS2 intermediate plasmid described above right after the third amino acid of the core (208) using the QuickChange mutagenesis kit XL II (Stratagene). The primers containing the inserted sequences are: forward primer 5'-GAC CGT GCA CCA TGA GCA CAT **TTC TCA ATT GTT GTC CTG GCT GTT GTA TGG AAC CTA** ATC CTA AAC CTC AAA GAA AAA CC-3' and reverse primer 5'- GGT TTT TCT TTG AGG TTT AGG ATT **AGG TTC CAT ACA ACA GCC AGG ACA ACA ATT GAG AAA** TGT GCT CAT GGT GCA CGG TC-3' (TC tag shown in bold). Afterwards, the region from the 5'UTR to NS2 containing the TCcore was cloned back into the pJFH1 plasmid using EcoR I and Not I to obtain pJFH1-TCcore.

pcDNA3-GFP-miR122 and intermediate plasmids: pcDNA3-GFP was constructed as follows. Briefly, GFP was digested from pEGFP-N1 (Clontech) by EcoR I and Xba I and inserted into pcDNA3. To obtain a miR122 expression plasmid, the coding sequence of human pri-miR122 was PCR amplified using pCSII-EF-RfA-pri-miR122 (a kind gift from Dr. Yoshiharu Matsuura, Osaka University, Japan) as the template with the forward primer 5'-AAG GAA AAA A GCGGCCGC CCT TAG CAG AGC TGT GGA-3' and reverse primer 5'-AAG GAA AAA A GCGGCCGC GCC TAG CAG TAG CTA TTT AG-3'. The amplified pri-miR122 PCR product was cloned into the pcDNA3-GFP plasmid at the Not I site right after the stop codon of GFP, which was named as pcDNA3-GFP-miR122.

Other plasmids: pcDNA3.1 was purchased from Invitrogen. pEGFP-N3 was purchased from Clontech (Mountain View, CA). HIV-Luc and HIV-GFP were previously constructed (209); both are pNL4-3-based HIV-1 reporter virus with a frameshift in the envelope gene and Luc/GFP expressed in place of nef. pCon1-E1E2 was generously offered by Dr. Charley Rice from Rockefeller University and encodes HCV envelope proteins E1 and E2 from the Con1 (HCV subtype 1b) strain. pHCMV-G was a kind gift from Dr. Joseph Sodroski of Harvard School of Medicine and encodes the glycoprotein from Vesicular Stomatitis Virus (VSV-G) downstream of the CMV promoter. HCV-Rluc subgenomic replicon (HCV 1b) was a generous gift from Dr. Seng-Lai Tan from EMD Serono Research & Development Institute (163). pEgr1-Fluc was constructed previously in our lab (210); it contains the firefly luciferase reporter gene downstream of Egr-1 promoter. All recombinant plasmids were verified by sequencing.

siRNAs: SiGENOME SMARTPool *siRNAs* against human CD81 (*siCD81*), SR-B1 (*siSR-B1*), CLDN1 (*siCLDN1*) and OCLN (*siOCLN*), and scrambled control *siRNA* (*siCtrl*) were purchased from Dharmacon (Lafayette, CO).

Antibodies

Mouse anti-HCV core (MA1-080, Affinity Bioreagents, Golden, CO), mouse anti-CD81 1.3.3.22 (sc-7637, Santa Cruz), mouse anti-CD81 (JS81, BD Bioscience), mouse anti-SR-B1 (610882, BD Bioscience), rabbit anti-CLDN1 (51-9000, Zymed/Invitrogen), mouse anti-OCLN (33-1500, Invitrogen, Carlsbad, CA), rabbit anti-OCLN (#42-2400, Invitrogen), mouse anti-MAP-2 (AP20, Santa Cruz), mouse anti-GFAP (Sigma), rabbit anti-GFAP (DAKO), goat anti-E2 (Meridian Life Science Inc, Memphis, TN), rabbit anti-CD63 (Systems Biosciences, Mountain View, CA), mouse anti- β actin (A1978, Sigma, St. Louis, MO), mouse anti-tubulin (Sigma), mouse anti-Hsp 70 (Santa Cruz), mouse normal IgG, rabbit normal IgG (Santa Cruz), monoclonal human anti-E2 clone CBH-5 and isotype-matched control human anti-cytomegalovirus monoclonal antibody R04 (both kindly provided by Dr. Steve Foug of Stanford University, California), goat anti-human IgG-phycoerythrin (PE) (Santa Cruz), goat anti-mouse IgG-Alexa488/Alexa555/Alexa647 (Invitrogen), goat anti-rabbit IgG-Alexa555 (Invitrogen), sheep anti-mouse IgG-HRP (Sigma), goat anti-rabbit IgG-HRP (Systems Biosciences), donkey anti-goat/rabbit IgG-HRP (Sigma), and mouse anti-CD81 (JS81) FITC conjugated (BD Bioscience).

Reagents

RNase A, phenylmethanesulphonylfluoride (PMSF), 4',6-diamidino-2-phenylindole (DAPI), acetylthiocholine (ATC), 5,5-dithio-bis(2-nitrobenzoic acid) (DTBNBA), Opti-prep density gradient medium, cytochalasin D (dissolved in DMSO), nocodazole, phalloidin-

TRITC, polyethylene glycol 8000 (PEG8000), poly-L-Lysine hydrobromide, polybrene, and the PKH26 cell labeling kit were purchased from Sigma. [Methyl-³H]-thymidine 5'triphosphate (³H dTTP) was from PerkinElmer (Boston, MA). Ficoll-PaqueTM was from Amersham Biosciences (Piscataway, NJ). Restriction endonucleases, heparinase I and exonuclease I were from New England Biolabs (Beverly, MA). Rat-tail type I collagen was from BD Bioscience (Bedford, MA). T4 DNA ligase was from USB (Cleveland, OH). The 5-chloromethylfluorescein diacetate (CMFDA) cell labeling dye, ReAsH TC tag labeling kit, TRIZOL, TRIZOL LS, and lipofectamine 2000 were from Invitrogen. Mounting solution fluoromount-G was from SouthernBiotech (Birmingham, AL). Bactotryptone, Bacto Yeast Extract, Bacto agar for LB bacteria culture were from Becton Dickinson (Sparks, MD). RNase inhibitor and deoxynucleotide triphosphates (dNTPs – dATP, dCTP, dTTP, and dGTP-) were from Promega Corporation (Madison, WI). Protease inhibitor cocktail set V was from Calbiochem (LaJolla, CA). Protein G agarose beads was from EMD Millipore (Billerica, MA). Recombinant human cytokines interleukin 1 β (IL-1 β), IL-4, IL-6, IL-10, tumor necrosis factor α (TNF- α), interferon γ (INF- γ), and the chemokine monocyte chemotactic protein 1 (MCP-1) were purchased from R&D Systems (Minneapolis, MN). G418 sulfate was from Santa Cruz Biotechnologies (Santa Cruz, CA). All other chemicals were from Fisher (LaGrange, KY).

Kits

The QIAamp Viral RNA Kit was from QIAGEN. The Annexin V Apoptosis Detection Kit APC was from eBioscience (San Diego, CA). The TaqMan One-Step RT-PCR Master Mix Reagents Kit, TaqMan MicroRNA Assays, TaqMan MicroRNA Reverse Transcription Kit, and the AmpliTaq Gold PCR system were from Applied Biosystems (Branchburg, NJ). The Quickchange II XL Site directed mutagenesis kit and Strataclone PCR cloning kit were from Stratagene (Cedar Creek, TX). The TOPO TA cloning kit and MEGAscript

T7 Kit were from Invitrogen. The plasmid DNA purification kits, the firefly and *renilla* luciferase assay systems, the Wizard SV Gel and PCR clean-up system for purification of DNA fragments from agarose gels, the GoTaq Flexi DNA Polymerase, and the ImProm II reverse transcriptase were from Promega Corporation. Bio-Rad DC Protein Assay and iQ SYBR Green Supermix was from Bio-Rad Laboratories.

METHODS

Cells and cell cultures

Cell lines

Huh7.5.1 hepatoma cell was obtained from Dr. Charles Rice's laboratory of Rockefeller University, New York; human embryonic kidney 293T cell, human hepatoma HepG2 cell, human neuroblastoma SH-SY5Y cell and human astrocytoma U373 cell were from American Type Culture Collection (ATCC, Manassas, VA); NKNT3 and CYNK10 human hepatoma cells were kindly provided by Dr. Ira Fox of the University of Pittsburgh School of Medicine, Pittsburgh, Pennsylvania. Huh7.5.1, 293T, HepG2, NKNT3, CYNK10 and U373 were maintained in DMEM supplemented with 10% heat-inactivated FBS and 1% S.P.G at 37°C with 10% CO₂. SH-SY5Y cell was maintained similarly in half Ham's F-12 and half DMEM.

Establishment of stable cell lines

A killing curve for Huh7.5.1 and U373 was performed to determine the G418 concentration to be used in the later selection process. Briefly, 1×10^4 Huh7.5.1/ U373 cells were plated in triplicate in a 96-well plate. After 24 hr incubation, the medium was replaced with fresh DMEM medium containing increasing concentrations of G418 (0 µg/ml, 100 µg/ml, 200 µg/ml, 300 µg/ml, 400 µg/ml, 500 µg/ml, 600 µg/ml, 700 µg/ml,

800 µg/ml, 900 µg/ml, 1000 µg/ml, 1200 µg/ml), and cell survival was determined during a period of 6 days. The medium was replaced every 72 hr. The appropriate concentration of G418 for selection of stable expressing cells was determined to be 400 µg/ml for Huh7.5.1 and 800 µg/ml for U373.

Huh7.5.1 cells (1×10^5 /well) were plated in a 12-well plate and transfected with 2 µg of pEGFP-N3 plasmid using Lipofectamine 2000 according to the manufacturer's instructions. The medium was replaced with fresh DMEM containing 400 µg/ml G418 at 24 hr post-transfection, and the cells were selected for two weeks with medium changed every 72 hr. At the end of the selection process, a single clone of GFP-positive cells were chosen and expanded. This clone was named Huh7.5.1-GFP and maintained in DMEM containing 200 µg/ml G418.

U373 cells stably expressing GFP or GFP-miR122 were established in a similar fashion. Briefly, U373 cells were transfected with pcDNA3-GFP or pcDNA3-GFP-miR122 and selected with 800 µg/ml G418 for two weeks. Two single clones of GFP-expressing U373 (named as U373-cDNA3-SC2/ SC4) and three single clones of GFP- and miR122-expressing U373 (named as U373-miR122-SC1/ SC2/ SC3) were selected and maintained in DMEM containing 200 µg/ml G418; the pooled clones of cells survived from the two week selection were also maintained similarly and named as U373-cDNA3-PC and U373-miR122-PC. The percentage of GFP-positive cells are >99% for all the single clones, 48% for U373-cDNA3-PC and 22% for U373-miR122-PC by flow cytometry.

Competent cells for cloning

GC5™ chemically competent *E. coli* for cloning was purchased from GeneChoice (Frederick, MD).

Primary human hepatocyte cultures

Cryopreserved human primary hepatocytes (Lonza) were plated on rat-tail type I collagen-coated plates and maintained in hepatocyte culture media (Lonza) as instructed by the supplier.

Primary human brain cell cultures

Human fetus cortex tissue (12-20 weeks) was obtained from Advanced Bioscience Resources (ABR, Alamada, CA). The tissue was first washed in ice-cold HBSS and removed of blood vessels and meninges with forceps, then dissociated by scissor dissection followed by repeated pipetting to obtain small pieces of tissue about 5 millimeters in size. The dissociated tissue pieces were digested with two volumes of 0.25% trypsin at 37°C for about 30 minutes. The digestion was stopped by adding DMEM medium containing 10% FBS and the tissue was washed for two more times with the medium. The digested tissue pieces were further dissociated into homogenous cell suspension by repeated pipetting with 25 ml, 10 ml, and then 5 ml pipettes. Lastly, the homogenous cell suspension was passed through 230 µm (60 mesh) and 94 µm (150 mesh) tissue sieves (Bellco Glass, Vineland, NJ) sequentially, to obtain single cell suspension. These cells were then extensively washed and seeded as below. To obtain pure astrocyte culture, cells were seeded at 1-1.5 million/ cm² in F-12K medium containing 10% FBS and 1% S.P.G. and replated with fresh medium for twice. To obtain pure primary neuron culture, cells were seeded into a 24-well plate at 1 x 10⁵ cells/ well in neurobasal medium supplemented with B27 and 1% S.P.G.; cells were never replated

and medium was change every three days. To obtain primary mixed brain cell culture, DMEM media containing 10%FBS and 1% S.P.G. was used.

HCV patient plasma samples

Plasma from chronic hepatitis C patients were kindly provided by Dr. Andy (Qigui) Yu from Indiana University School of Medicine, IN. They were collected in heparinized vials (15U heparin/ml) and frozen immediately in -70°C. HCV RNA titers in plasma 1, 3 and 5 were determined by quantitative RT-PCR (qRT-PCR) as described later and they were 6.8×10^5 , 2.1×10^7 , and 2.1×10^5 vge/ml (viral genome equivalent per ml), respectively. All plasma samples were treated with Heparinase I (6 U/ 140 μ l plasma) with the presence of RNase inhibitor (20 U/ 140 μ l plasma) at 30°C for 2-3 hr before any further processing or assays.

Bacterial transformation

Twenty-five microliters of GC5™ competent cells were mixed with 2 μ l DNA ligation product or 10 ng plasmid DNA, and incubated in ice for 30 min. The mixture was heat-shocked in a 42°C water bath for 45 sec and incubated on ice for 2 min. Five hundred microliters of 37°C pre-warmed LB medium was added to the mixture and they were incubated at 37°C for 1 hr with shaking at 150 rpm. Fifty to five hundred microliters of the culture were spread out evenly on an agar plate containing the appropriate selection antibiotic. The plate was incubated in a 37°C incubator upside down for 12-20 hr.

HCV RNA synthesis by in vitro transcription

pJFH1 and pJFH1-TCcore were linearized by Xba I; HCV-Rluc plasmid was linearized by Scal. These linearized DNA were purified by phenol/ chloroform extraction followed by ethanol precipitation and used as templates to transcribe viral RNAs *in vitro* using the

MEGAscript T7 Kit according to manufacturer's instructions. The synthesized viral RNA was purified by acidic phenol/chloroform extraction followed by isopropanol precipitation and frozen in ready-to-use aliquot in -70°C .

Cell transfections

Calcium phosphate precipitation

Plasmid DNA transfection into 293T cells and primary astrocytes were performed with the standard calcium phosphate precipitation method. For one 6 cm dish, 5×10^5 of 293T or primary astrocytes were seeded and cultured for 24 hr to achieve 40-50% confluency at the time of transfection. At this point, a 180 μl mixture of 8 μg total plasmid DNA and 0.22 M CaCl_2 was added dropwise to 180 μl of a 2XHBS (50 mM HEPES, 280 mM NaCl, 10 mM KCl, 1.5 mM Na_2HPO_4 , 12 mM Glucose, pH 7.1). The transfection mixture was incubated on ice for 20 min and then added dropwise into the cells. The culture medium was replaced after overnight (16 hr) incubation. Unless otherwise specified, the cells were cultured for another 48 hr before gene expression was examined. Transfection efficiencies were routinely monitored by adding a small amount of pEGFP-N3 (1/10 of the total plasmid DNA) into the transfection mixture and were usually 80-90% for 293T and 40-50% for primary astrocytes. When a different tissue culture plate was used, the number of cells and the amount of all solutions were scaled up or down based on the cultural surface area.

Lipofectamine transfection

Plasmid DNA transfections into cells other than 293T or primary astrocytes and RNA transfections (viral RNA, siRNA, or viral RNA and plasmid DNA) into all cells were performed with Lipofectamine 2000 according to the manufacturer's instructions. Briefly, in one 6 cm dish, $0.5\text{-}2 \times 10^6$ cells were plated and incubated for 24 hr to reach 80-90%

confluency at the time of transfection. Culture medium was replaced with the cell's culture medium without antibiotics right before transfection. Meanwhile, 8-20 μl lipofectamine was added into 500 μl Opti-MEM and the mixture was incubated at RT for 5 min. During this time, 8 μg viral RNA, or 3.2 μg plasmid DNA and 6 μg viral RNA, or 8 μg plasmid DNA were diluted in 500 μl Opti-MEM. The diluted nucleic acids and lipofectamine mixtures were combined and further incubated at RT for 20 min. Thereafter, the transfection mixture was added to the cells and medium was replaced after 6 hr of incubation. For RNA and RNA/DNA co-transfection, gene expression was examined starting from 6 hr post-transfection, while for DNA transfection, gene expression was not examined until 48 hr post-transfection. Transfection efficiencies were routinely monitored by adding a small amount of pEGFP-N3 (1/10 of the total plasmid DNA) into the transfection mixture or by simply utilizing the GFP-expressing plasmid already included in the transfection mixture. Transfection efficiencies vary with the cell type being transfected and the nature of the transfection (RNA, DNA, or co-transfection) and usually fall within a range of 40-80%. When a different tissue culture plate was used, the number of cells and the amount of all solutions were scaled up or down based on the cultural surface area.

Reverse transcriptase activity assay

Viruses in 1 ml cell culture supernatant was pelleted by spinning at 14,000 $\times g$ and 4°C for 90 min. The pellet was suspended in 10 μl dissociation buffer (0.25% Triton X-100, 1 mM DTT, 0.25 M KCl, 20% glycerol, and 50 mM Tris-HCl pH 7.5) followed by three times of freezing and thawing. A 40 μl mixture containing 34 μl RT assay buffer (0.083% Triton X-100, 8 mM DTT, 12.5 mM MgCl_2 and 0.083 M Tris-HCl pH 7.5), 1 μl ^3H dTTP, and 5 μl 5 units/ml of Poly (A)x(dT) was added to the 10 μl virus suspension mentioned above. The total 50 μl mixture was incubated at 37°C for 1 hr and then spotted onto

DE81 filter paper (Whatman, England). After three washes with 2XSSC (0.3 M NaCl, 0.03 M Sodium citrate, pH 7.0) and two washes with 95% ethanol, the filter paper was air-dried and determined of radioactivity in a Beckman LS6000IS scintillation counter. The virus titer was expressed as cpm/ml.

Preparation of pseudotyped viral particles and infection

All the pseudotyped viral particles were prepared in 293T cells as described below. Two million 293T cells were seed into a 10 cm dish and transfected with 21 µg HIV-Luc and 3 µg pcDNA3 (Env^{pp}), or 3 µg pCon1-E1E2 (HCVpp) or 3 µg pHCMV-G(VSVpp) by standard calcium phosphate transfection. At 72 hr post-transfection, culture supernatants were harvested, removed of cell debris by centrifugation at 1000 x g for 5 min, aliquoted and stored at -70°C. The viral titer was determined by reverse transcriptase assay as described in the previous section. For infection with these pseudotyped viruses, 5 x 10⁴ Huh7.5.1, SH-SY5Y, U373, or 1 x 10⁵ mixed primary brain cells were plated in a 24-well plate, or 2.5 x 10⁵ primary astrocytes were plated in a 6-well plate. After 24 hr incubation, 200,000 cpm Env^{pp} or HCVpp, or 2, 000 cpm VSVpp were added to the cells for infection at 37°C for 2 hr or spinoculation at RT and 1000 x g for 2 hr. The cells were removed of viruses, extensively washed with PBS, and cultured for 72 hr before harvest for the luciferase activity assay.

Luciferase assay

Firefly or *renilla* luciferase activities were measured with the luciferase assay systems from Promega according to the manufacturer's instructions. Briefly, cells were harvested by trypsinization, washed once with ice-cold PBS, frozen and thawed once (only required for *renilla* luciferase, not firefly luciferase), lysed with 25 µl 1X firefly or *renilla* luciferase lysis buffer at RT for 5 min, centrifuged at 12, 000 x g for 30 sec to remove cell

debris, and the supernatants were used as cell lysates. 5 μ l cell lysates were mixed with 20 μ l firefly or the *renilla* luciferase substrate and the luciferase activity was immediately measured using an Opticomp Luminometer (MGM Instruments, Hamden, CT). For pseudotyped virus infection or spinoculation, firefly luciferase activity was measured at 72 hr post-infection. For HCV-Rluc RNA co-transfection with pEgr1-Fluc plasmid in U373-cDNA3 or U373-miR122 stable cells, both *renilla* and firefly luciferase activities were measured at 72 hr post-transfection and Rluc reading was normalized to Fluc reading (transfection efficiency). For HCV-Rluc RNA co-transfection with pcDNA3-GFP or pcDNA3-GFP-miR122 in all other cells, *renilla* luciferase activity was measured at 6, 24, 48, 72, or 120 hr post-transfection and Rluc reading was normalized to % of GFP-positive cells (transfection efficiency) from flow cytometry analysis at 48 or 72 hr post-transfection.

HCVcc production, titration and infection

Huh7.5.1 cells were either transfected with viral RNAs (JFH1 or JFH1-TCcore) as described above, or inoculated with JFH1 viral stock (a generous gift from Dr. Wenzhe Ho of Temple University, Philadelphia, PA) at a multiplicity of infection (MOI) of 0.2 - 1. Supernatants containing HCV virions were collected 30 - 40 days post-transfection or 5 days post-infection, removed of cell debris by low speed centrifugation at 1000 x *g* and 4°C for 10 min, passed through a 0.22 μ m filter, and aliquoted and stored at -70°C and used as the virus stock. To obtain higher viral titer, the filtered culture supernatant was sometimes concentrated by the addition of 1/5 volume of 40% PEG8000 (final concentration of 8%) and precipitation at 4°C overnight, followed by centrifugation at 3500 *g* and 4°C for 30 min. The precipitated virus was suspended, stored at -70°C and used as the virus stock. The virus stock was titrated by the foci formation assay as previously described (211). Briefly, 10-fold serially diluted stock was added to Huh7.5.1

cells and medium was changed after two hours. Immunostaining against HCV core was performed at 72 hr post-infection and the number of foci formed at the highest dilution was used to calculate the virus titer, which was expressed as focus-forming units per milliliter (FFU/ml). The titers of our JFH1 viral stock were usually in a range of 10^4 to 10^6 FFU/ml. Unless stated otherwise, HCVcc infection was performed by incubation of HCVcc stock with target cells for 2 hr at 37°C at a multiplicity of infection of 0.1.

Co-culture assay and transwell assay

In the co-culture assay, Huh7.5.1 were infected with HCV for 3 days and used as the donor cells. The donor cells or the target cells were first labeled with PKH26 or CMFDA according to the manufacturer's instructions. Briefly, cells were trypsinized and labeled with 2 μ M PKH26 for 5 min at RT followed by incubation with 1% FBS/phosphate-buffered saline (PBS) to stop the labeling reaction and four extensive washes to remove any residual dye. Alternatively, media containing 1.25 μ M (for flow cytometry) or 5 μ M (for confocal imaging) CMFDA were directly added to cells growing in culture dishes. The cells were labeled at 37°C and 5% CO₂ for 30 min followed by a medium change to normal growth media and an extra 30 min incubation. The labeled donor/target cells were counted (or trypsinized and counted for CMFDA-labeled cells) and mixed with unlabeled target/donor cells and seeded to a 24- or 12-well plate at >90% confluence. Unless stated otherwise, the donor/target cells were allowed to co-incubate for approximately 20 hr, followed by collection for immunostaining and flow cytometry or confocal analysis. The transwell assay was carried out in a similar fashion except that neither donor nor target cells were labeled and the donor and target cells were seeded into the upper and lower chambers of the transwell (Corning, Lowell, MA), respectively.

Flow cytometry

CD81 surface expression

For detection of CD81 surface expression, cells were removed from culture dishes with 0.5 mM EDTA/PBS and directly labeled with mouse anti-CD81 (JS81) –FITC conjugated (1:100) for 30 min at 4°C, or labeled by incubation with mouse anti-CD81 (2 µg/ml) at 4°C for 30 min first and then with goat anti-mouse IgG-Alexa488 (1:500) at 4°C for 30 min. The labeled cells were suspended in PBS and analyzed by flow cytometry immediately. Between each step, the cells were extensively washed with PBS. Where appropriate, cell labeling with mouse normal IgG (2 µg/ml) or mouse normal IgG-FITC conjugated (1:100) was included as control.

HCV CCCM transfer

Cells from the co-culture assay, or the target cells from the transwell assay were trypsinized and fixed with 4% paraformaldehyde (PFA) for 10 min, followed by permeabilization with 50 µg/ml saponin for 15 min. Staining was performed with mouse anti-core primary antibody for 60 min followed by goat anti-mouse IgG-Alexa647 (for CMFDA-labeled or Huh7.5.1-GFP co-culture) or goat anti-mouse IgG-Alexa488 (2 µg/ml, for PKH26-labeled co-culture) secondary antibody for 60 min. All primary and secondary antibodies were diluted to 2 µg/ml in 1% FBS/PBS. All the steps for immunostaining of fixed cells were performed at room temperature. Between each step, the cells were extensively washed with PBS. Flow cytometry analysis was performed on a BD FACS Calibur or BD Accuri C6; only live cells were gated and cell debris were excluded from analysis.

Immunofluorescence staining and confocal imaging

Cells from the co-culture assay were fixed with 4% paraformaldehyde on coverslips, permeabilized with saponin and blocked in 1% FBS/PBS at RT for 30 min. Cells were stained with mouse anti-core primary antibody (2 µg/ml) at RT for 60 min followed by goat anti-mouse IgG-Alexa488 or Alexa555 (2 µg/ml) secondary antibody at RT for 60 min. The nuclei were stained with 0.25 µg/ml DAPI in PBS at RT for 15 min. The coverslips were mounted with Fluoromount G (Southern Biotech, Birmingham, Alabama) and microscopic images were taken using a Zeiss Axiovert 200 for epifluorescence or a Zeiss LSM510 for confocal images. For the detection of OCLN, siCtrl- or siOCLN-transfected Huh7.5.1 cells were fixed, permeabilized, and stained with mouse normal IgG (2.5 µg/ml) or mouse anti-OCLN (2.5 µg/ml) followed by goat anti-mouse IgG-Alexa555 secondary antibody (2 µg/ml). For F-actin staining, cells from the co-culture assay were fixed and permeabilized as above and then stained with 1 µg/ml phalloidin-TRITC in PBS at RT for 30 min. For the visualization of microtubules, cells from the co-culture assay were fixed with -20°C methanol for 3 min and then permeabilized and stained with mouse anti-tubulin (2 µg/ml) followed by Alexa555-conjugated secondary antibody (2 µg/ml). Cells were washed three times with PBS between each step.

ReAsH labeling and 3D live cell imaging

Culture supernatants were collected from JFH1-TCcore transfected Huh7.5.1 at day 42 post-transfection and concentrated 30-fold by using PEG8000 precipitation and titrated as described above. Huh7.5.1 cells were infected with the concentrated JFH1-TCcore virus (MOI=0.15) and labeled with ReAsH according to the instructions provided in the TC-tag detection kit (Invitrogen). These labeled cells were then used as donor cells. Specifically, at day 3 post-infection, cells were washed once with Opti-MEM (Invitrogen) and labeled with the ReAsH dye (1 µM final concentration) in Opti-MEM. Cells were

incubated at 37°C for 30 min, and then washed twice with 1X BAL (2,3-dimercapto-1-propanol) wash buffer (supplied in the kit, Invitrogen) in Opti-MEM for 5 min each. The wash buffer was removed, and the cells were washed once with PBS, trypsinized, and mixed at a 1:1 ratio with the Huh7.5.1-GFP target cells. The mixed cells were seeded onto poly-lysine-coated 35 mm glass bottom dishes to 90% confluence, and the media were replaced with DMEM media without phenol red at 2 hr post-seeding. Live cell imaging was set up after the media change. Images were taken starting at 9 hr post-seeding and continued for 18 hr. All images were acquired with a Zeiss LSM 510 confocal microscope fitted with a 20X air objective and a thermostatic stage incubator set at 37°C, 5% CO₂. ReAsH-labeled TCcore was visualized with the filter sets of excitation at 561 nm and emission at 620/80, and the GFP in target cells was detected using the filter sets of excitation at 488nm and emission at 528/45. A 13 slice X 0.9 μm Z stack was taken at each selected field every 18 min using the LSM 510 LUO software. Images were later processed and analyzed with Image J 1.45s. Unless otherwise specified, all red/green fluorescence images were Z projections (maximum intensity projection) from the original stack and all differential interference contrast (DIC) images were the most focused slice from the Z stack (the 7th slice).

Western blotting

At 48 hr post-transfection or 72 hr post-infection, cells were harvested by trypsinization, washed once with ice-cold PBS, pelleted at 4°C and 2000 x g for 5 min, and lysed on ice with a standard RIPA buffer (50 mM Tris-HCl pH 8.0, 0.5% NP40, 2 mM EDTA, 137 mM NaCl, and 10% glycerol) added with 1X protease inhibitor cocktail and 1X PMSF. After 30 min incubation, cell debris was removed by centrifugation at 4°C and 12,000 x g for 10 min and the supernatant (cell lysate) was determined of protein concentration with the Bio-Rad DC Protein Assay Kit. An equal amount of protein in the whole cell lysates

(25 µg for CLDN1, 50-100 µg for HCV core, 100 µg for SR-B1 and 100-200 µg for OCLN) was separated on a 8% (SR-B1 and OCLN) or 12% (all others) polyacrylamide-SDS gel, and then transferred onto nitrocellulose membranes (GE Healthcare). The membranes were blocked with 5% milk in TBST at RT for 30 min or at 4°C overnight, followed by probing with appropriate primary antibodies (1 µg/ml for mouse α-HCV core/Hsp70 and rabbit α-CLDN1/CD63, 2 µg/ml for mouse α-SR-B1 and rabbit α-OCLN, 0.5 µg/ml for β-actin and 1:500 for goat α-HCV E2) at RT for 2 hr or at 4°C overnight, and secondary antibodies (0.5 µg/ml) at RT for 1 hr. The protein bands were visualized by either adding homemade enhanced chemiluminescence reagents (for HRP-conjugated secondary antibodies) and imaging, or direct imaging for fluorescence intensity (for Alexa dyes-conjugated secondary antibodies) with a Bio-Rad ChemiDot MD system. For western blotting of exosome and/or virus fractions from Opti-prep gradient centrifugation, the fraction was diluted to 1.4 ml with PBS, centrifuged at 4°C and 20,000 x g for 90 min, suspended in 20 µl 4X SDS-PAGE sample buffer (8% SDS, 0.4 M DTT, 0.25 M Tris. HCl pH 6.8, 40% Glycerol and 0.1% bromophenol blue) and separated on a 12% SDS-PAGE gel. All the remaining steps were as same as cell lysates.

RNA isolation and qRT-PCR

RNA isolation

Total RNA was isolated from cells or 50-200 µl culture supernatants removed of cell debris by centrifugation at 1000 x g for 5 min using TRIZOL or TRIZOL LS (Invitrogen), respectively, according to the manufacturer's instructions. The isolated RNA was suspended in 10 µl nuclease-free ddH₂O and 200 ng cellular RNA or 2 µl supernatant RNA were used for downstream qRT-PCR detection. For the detection of patient plasma-derived HCV, if the sample was more than 140 µl, it was first concentrated to 140 µl with Amicon Ultracel-100K centrifugal filter device by centrifugation at 4000 x g

and 4°C for 25 min. Total RNA was then extracted from the samples with the QIAamp Viral RNA Mini Kit (QIAGEN) and eluted with 60 µl AVE buffer. Two microliters of the RNA were used for qRT-PCR.

One-step Taqman qRT-PCR for HCV RNA

HCV RNA in cells, culture supernatants, and patient plasma were detected using a TaqMan One-Step RT-PCR kit (Applied Biosystems) with HCV-specific primers and probe. The primers and probe for detection of JFH1 (HCV subtype 2a) were described previously (212) and their sequences were: forward primer KK3-0, 5'-CTG TCT TCA CGC AGA AAG CG-3'; reverse primer KM3-1, 5'-CAC TCG CAA GCG CCC TAT CA-3'; probe R6-84, 5'-CAT GGC GTT AGT ATG AGT GTC GTA CA-3'. The reverse primer was changed to KM3-1', 5'-CAC TCG CAA GCA CCC TAT CA-3', for the detection of patient plasma-derived HCV. The qRT-PCR reaction was set up in a 10 µl volume with 2 µl RNA template and a program as follows: 48°C for 30 min, 95°C for 10 min, and then 40 cycles at 95°C for 15 sec, and 60°C for 1min. Serially diluted *in vitro* transcribed JFH1 RNA was included as standards in parallel and used to calculate the absolute level of HCV RNA.

Two-step Taqman qRT-PCR for miR122

Cellular RNA (100 - 200 ng) was reverse transcribed to cDNA with the reverse transcription primer from Taqman MicroRNA Assay hsa-miR122-5p using the Taqman MicroRNA Reverse Transcription Kit (Applied Biosystems) according to the manufacturer's instructions. An aliquot of the reverse transcription products (0.667 µl out of 7.5 µl) were then mixed with 0.5 µl miR122-specific primers and probes from the Taqman MicroRNA Assay hsa-miR122-5p, 3.84 µl ddH₂O, and 5 µl 2X AmpliTaq Gold PCR Mastermix (Applied Biosystems). The total 10 µl qPCR reaction was performed

with a program as follows: 95°C for 10 min, and 40 cycles at 95°C for 15 sec, and 60°C for 1min. For endogenous expression level of miR122 in different cells, the small nuclear RNA U6 expression in these cells was also determined by two-step SYBR Green qRT-PCR using the ImProm II reverse transcriptase (Promega) and the iQ SYBR Green Supermix (Bio-Rad), and used for normalization of miR122 expression in these cells. The primers used were: 5'-TCC CCC GGG GTG CTC GCT TGG GCA GCA CA-3' and 5'-TCC CCC GGG AAA ATA TGG AAC GCT TCA CGA-3'. The qPCR program was: 95°C for 3 min, 40 cycles of 95°C for 15 s and 60°C for 1min.

Two-step SYBR Green qRT-PCR for cytokine expression

Cellular RNA (2.5 - 5 µg) was reverse transcribed to cDNA using the GoScript Reverse transcription system (Promega). qPCR was then performed in a 10 µl volume with an aliquot of the cDNA (0.5 - 0.8 µl out of 20 µl) using the SYBR Green JumpStart Taq Readymix (Sigma). The primers were described previously (213-217), and their sequences were: β-actin: 5'-GGC ATC CTC ACC CTG AAG TA-3' and 5'-AGG GCA TAC CCC TCG TAG AT-3'; IL-1α: 5'-CGC CAA TGA CTC AGA GGA AGA-3' and 5'-AGG GCG TCA TTC AGG ATG AA-3'; IL-1β: 5'-CCT GTC CTG CGT GTT GAA AGA-3' and 5'-GGG AAC TGG GCA GAC TCA AA-3'; IL-6: 5'-ACA ACA AAT TCG GTA GAT CCT CG-3' and 5'-AGC CAT CTT TGG AAG GTT CAG G-3'; IL-8: 5'-TGC CAA GGA GTG CTA AAG-3' and 5'-TCT CAG CCC TCT TCA AAA-3'; IL-18: 5'-GAC GCA TGC CCT CAA TCC-3' and 5'-CTA GAG CGC AAT GGT GCA ATC-3'; TNF-α: 5'-TCT TCT CGA ACC CCG AGT GA-3' and 5'-CCT CTG ATG GCA CCA CCA G-3'. The program used for qPCR was: 95°C for 3 min, 40 cycles of 95°C for 15 s, annealing (55°C for β-actin, 57.3°C for IL-1α, 59.8°C for IL-1β, 60.4°C for IL-6, 60.7°C for IL-8, 55.4°C for IL-18, and 58.6°C for TNF-α) for 15 s and 72°C for 45 s. The temperature of the annealing

step for each cytokine has been pre-optimized to ensure only one peak seen in the melting curve and only one PCR product with the correct size seen on an agarose gel. All the qPCR reactions were set up in a 10 μ l volume and performed on the C1000 Touch Thermal Cycler with the signal detected by CFX96 real time system (both from Bio-Rad, CA).

Preparation of bovine exosome-depleted medium and bovine exosome-depleted

HCV

Bovine exosomes were depleted from complete culture medium (DMEM supplemented with 10% FBS and 1% penicillin/streptomycin/L-glutamine) by ultracentrifugation overnight (~16 hr) at 4°C and 100,000 x g. The supernatants were then collected and if needed, sterilized by passing through 0.22 μ m filter and stored at 4°C as bovine exosome-depleted medium. For the production of bovine exosome-depleted HCV, Huh7.5.1 was inoculated with JFH1 viral stock and cultured for 3-4 days. Culture medium was then changed to bovine-exosome depleted medium; the cells were continued to culture for 24 hr and the culture supernatants were collected and saved as bovine exosome-depleted HCV.

Exosome and HCV purification by Optiprep gradient ultracentrifugation

Huh7.5.1 culture supernatants (30-400 ml) were removed of cell debris by centrifugation at 3000 x g for 10 min, passed through a 0.22 μ m filter, and concentrated by ultracentrifugation at 250,000 x g and 4°C for 90 min in a SW55Ti rotor or 130,000 x g and 4°C for 90 min in a SW28 rotor to obtain the exosome pellet. Meanwhile, a 5 ml 6-24% Opti-prep gradient was prepared with the Hoefer SG50 gradient maker. Specifically, 3 ml each of 2.4% and 24% iodixanol working solutions were prepared from the Opti-prep density gradient medium (60% w/v iodixanol in water) with the Opti-prep

diluent (235 mM KCl, 12 mM MgCl₂, 25 mM CaCl₂, 30 mM EGTA, 150 mM Hepes-NaOH pH 7.0). The two 3 ml working solutions were loaded into the two chambers of the gradient maker, respectively. A 5 ml 6-24% iodixanol continuous gradient was then generated with the gradient maker according to manufacturer's instructions. The exosome pellet was suspended in 500 µl PBS, loaded onto the Opti-prep gradient and centrifuged at 250,000 x *g* and 4°C for 2 hr in the SW55Ti rotor. Eleven fractions (500 µl each) were collected from top to bottom; an aliquot of each fraction was subjected to AchE assay, Western blotting, qRT-PCR, or foci formation assay.

Acetylcholinesterase assay

Acetylcholinesterase (AchE) activity was measured as described previously (218). Briefly, 5 µl culture supernatant or iodixanol fraction was mixed with 12.5 µl 10 mM ATC and 82.5 µl PBS, and then 100 µl 0.1 mM DTBNBA/PBS in a 96-well plate. The reaction was incubated at RT or 37°C for 5 to 30 min until yellow color appeared, at which point the absorbance of the reaction at 415 nm was measured with a plate reader spectrophotometer (Bio-Rad).

MTT assay

Human neuroblastoma SH-SY5Y cells were plated at a 96-well plate at a density of 1x 10⁴/ well and cultured for 24 hr (40-50% confluence). Then, the media was replaced with 80 µl supernatant being tested mixed with 40 µl serum-free SH-SY5Y-culturing media (half Nutrients Mixture Ham's F-12 and half DMEM). After 72 hr culturing, the cells were added with 30 µl 50 mg/ml MTT solution and incubated for additional 12-16 hr. Media was then removed and the violet crystals in the well were dissolved by adding 200 µl of acid-isopropanol (a 3: 22 ratio mixture of 0.2 N HCl and isopropanol) and shaking

for 20 min at room temperature. Absorbance at 655 nm and 595 nm was then taken and used to calculate the differences.

Data acquisition and statistical analysis

Where appropriate, values were expressed as mean \pm SD of triplicate experiments. All statistical analyses including one-way and two-way ANOVA followed by post hoc tests (bonferroni correction or Dunnett's test), and two-tailed unpaired student's t test were performed in Prism 5 (Graphpad Software, CA). A p value of < 0.05 was considered statistically significant (*), $p < 0.01$ highly significant (**) and $p < 0.001$ strongly significant (***). All data were representative of multiple repeated experiments.

RESULTS

CHAPTER 1: Cell-Cell Contact-Mediated Hepatitis C Virus Transfer, Productive Infection and Replication and Its Requirement for HCV Receptors

1.1 Formation of HCV infection foci in cell culture

A number of recent studies have demonstrated the linkage between cell-cell contact-mediated (CCCM) viral transmission and immune evasion (219); CCCM viral transmission has thereby attracted increasing attention and we are particularly interested in its potential usurpation by HCV as an alternative route of transmission. Consistent with several clinical reports showing a focal pattern of infected cells in HCV patient liver biopsy (95-97), we and others repeatedly noticed that in cell culture, clustered HCV-infected cells (the infection “foci”, usually with 10-50 cells) were observed at a very low MOI (**Fig. 6**, right column) and high cell density. To the contrary, higher MOI gave rise to approximately 80-90% HCV core-positive cells and less distinctive foci (**Fig. 6**, middle column). Formation of these infection foci at the lower MOI could result from division and proliferation of HCV-infected cells. Alternatively, it could be due to the close proximity of uninfected cells to HCV-infected cells and subsequent CCCM HCV transfer to the neighboring uninfected cells resulting in infection.

1.2 Spread of HCV in cell culture is dependent on cell density

To distinguish these two possibilities, we infected Huh7.5.1 cells with JFH1 virus of a lower MOI, removed the excessive virus, and then re-plated the cells at different cell densities. Following three days of continued culturing, the cells were processed for analysis of HCV core expression, a widely used marker for HCV infection. We reasoned that if infection focus formation resulted from proliferation of HCV-infected cells, these

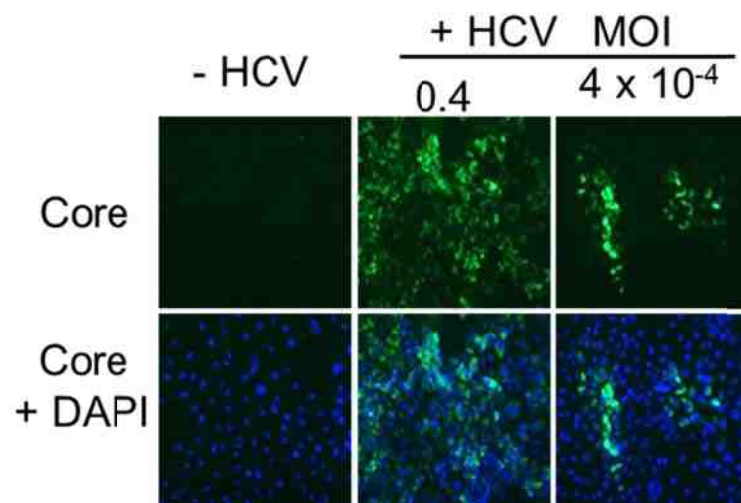


Figure 6. Formation of HCV infection foci in cell culture. Huh7.5.1 cells were inoculated with culture media (- HCV), or JFH1 virus at a high MOI of 0.4 (+ HCV), or JFH1 virus at a low MOI of 4×10^{-4} (+ HCV), cultured for 3 days and immunostained for HCV core (green) followed by DAPI counterstain (blue, for nuclei).

foci would be observed at any cell density and there would be no correlation between the number of infection foci and cell density; if infection focus formation resulted from CCCM HCV transfer, infectious focus would only be observed at high cell densities and there would be a positive correlation between the number of foci formed and cell density. To ensure the validity of the data, we assessed HCV core-positive cells by Western blotting for HCV core, immunofluorescence staining for HCV core followed by immunofluorescence microscopic imaging and manual counting of HCV core-positive cells under an immunofluorescence microscope, or flow cytometry analysis. Western blotting showed that the expression level of HCV core protein exhibited a gradual increase with higher cell density (**Fig. 7A**). Immunostaining of these cells for HCV core protein followed by immunofluorescence microscopic imaging showed an apparent increase in the number and intensity of core-positive cells with increased cell density (**Fig. 7B**). The formation of core-positive cell foci appeared to only occur at higher cell densities (**Fig. 7B**). Manual quantitation of core-positive cells showed a positive correlation between the number of core-positive cells and cell density (**Fig. 7C**). The positive correlation was further quantified by flow cytometry analysis of core-positive cells (**Fig. 7D**), and a two variable linear regression analysis gave rise to the correlation coefficient of 0.9883. In addition, we further show that this positive correlation between the percentage of infected cells and cell density is dependent on the MOI; when a higher MOI was employed for the initial infection, the overall much higher infection efficiency at all densities led to a decrease in the correlation between the percentage of infected cells and cell density (**Fig. 8**). Taken together, these results suggest that HCV is capable of infecting target cells via a cell-to-cell mechanism, i.e., CCCM HCV infection and transmission.

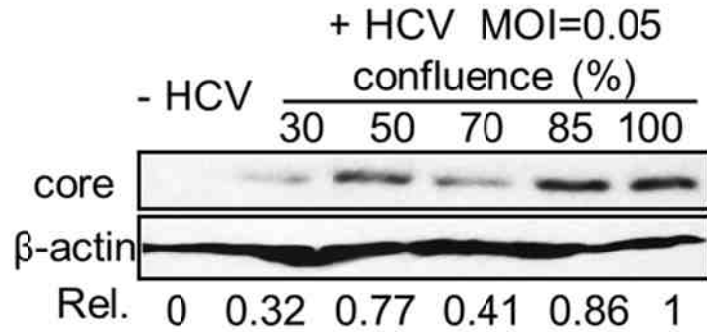
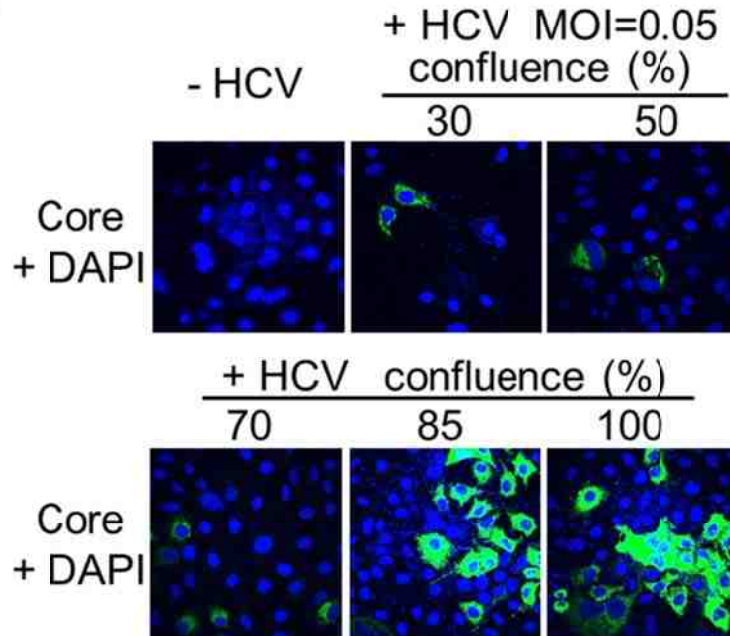
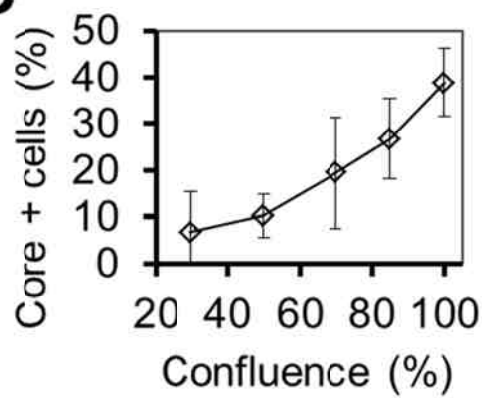
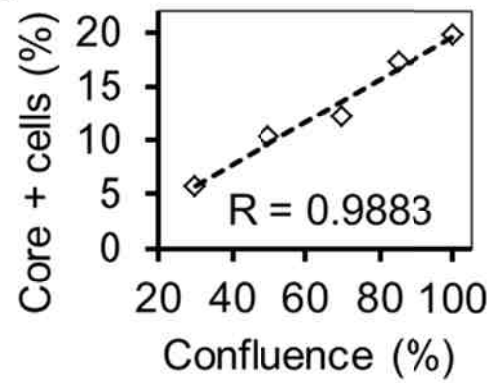
A**B****C****D**

Figure 7. Cell density's effects on HCV spread at a low MOI. Huh7.5.1 cells were inoculated with culture media (- HCV) or HCV JFH1 stock (+ HCV) at MOI = 0.05. At day 1 post-infection, the infected cells were replated at different densities which gave rise to 30%, 50%, 70%, 85%, and 100% confluence 3 days post-replating at which time the cells were harvested and analyzed by **(A)** Western blotting against HCV core, **(B)** immunostained for HCV core (green) and DAPI (blue) (representative images), **(C)** counted for core-positive cells under a fluorescence microscope, or **(D)** analyzed by flow cytometry for core-positive cells (correlation coefficient $R = 0.9883$, which was derived from a standard two variable mathematical regression analysis: cell confluence vs. percentage of core-positive cells).

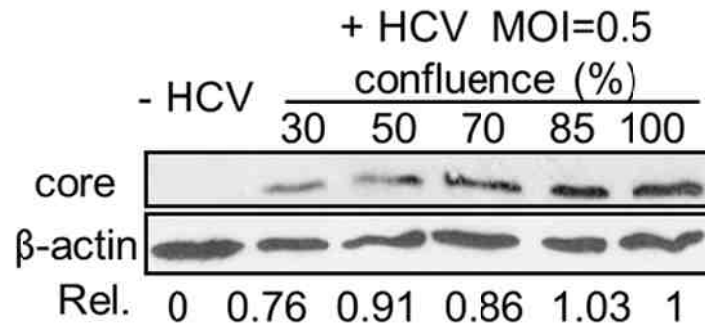
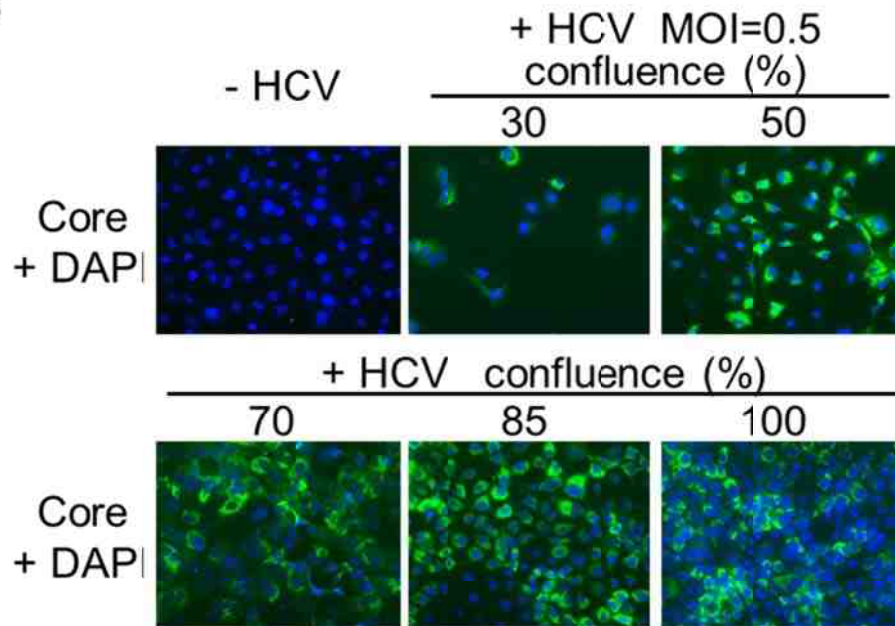
A**B****C**

Figure 8. Cell density's effects on HCV spread at a high MOI. The same with Fig. 7 A-C except that Huh7.5.1 cells were inoculated with JFH1 stock at MOI = 0.5.

1.3 CCCM HCV transfer to Huh7.5.1 and primary hepatocytes

1.3.1 Optimization of the labeling methods in co-culture assay

To characterize the CCCM HCV infection, we devised a co-culture assay that involved incubation of HCV-infected Huh7.5.1 donor cells with uninfected Huh7.5.1 target cells for a certain period of time and determination of the number of core-positive target cells from CCCM HCV transfer by immunostaining. One of the key elements in this co-culture assay was to identify an appropriate method to fluorescently label either the donor or target cells, so that they could be distinguished after immunostaining. In order to be used in the co-culture assay, this labeling dye has to be plasma membrane-permeable, retained stably in the cell for at least 24-48 hr after the labeling, and not extracted during fixation or permeabilization steps in the immunostaining. Among the various cell-labeling strategies being tested, DAPI DNA labeling was not appropriate due to very faint live cell labeling and free diffusion between cells resulting from its poor plasma membrane permeability and the reversible nature of its binding to DNA, respectively (microscopic observations); cell surface labeling of CD81 (expressed on more than 99% of Huh7.5.1 cells, **Fig. 45A**) with anti-CD81 primary antibody followed by Alexa488-conjugated secondary antibody was not suitable due to receptor recycling and thereby decreased fluorescence signal over time (difficult-to-separate peaks after 20 hr co-culture, **Fig. 9**); labeling with the cell-tracking dye CMPTX was not appropriate due to free diffusion of the dye between cells during co-culture (microscopic observations); labeling with the mitochondria tracker Rhodamine 123 was again not suitable because it was washed out of cells during the fixation step in immunostaining, when the mitochondria potential was lost (microscopic observations); labeling with the cell-tracking dye CFSE and subsequent co-culturing experiment was successful (**Fig. 9**) but its high sensitivity to

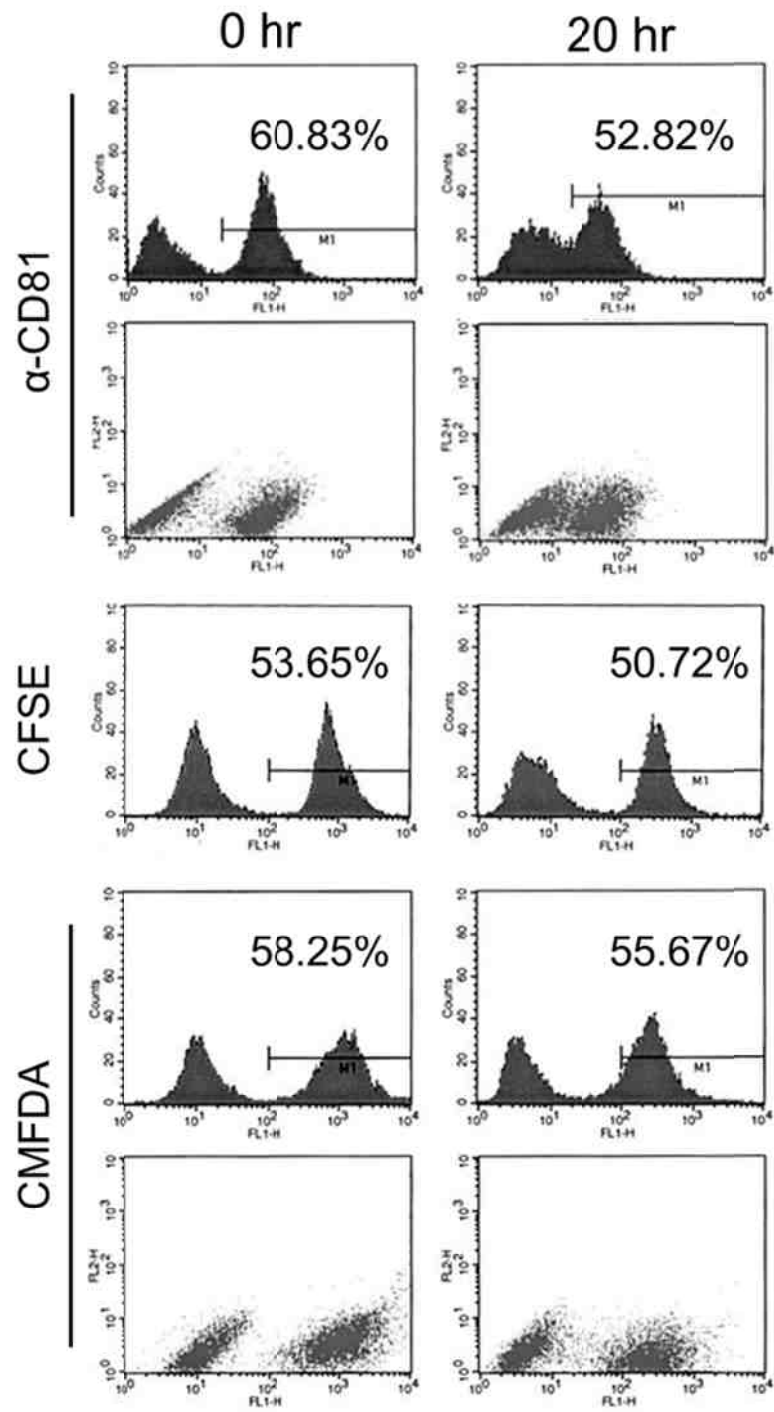


Figure 9. Optimization of the labeling methods for co-culture assay – test of CD81 surface labeling, CFSE labeling, and CMFDA labeling. Huh7.5.1 cells were labeled with α -CD81 primary antibody (2 μ g/ml, 4°C, 30 min) and then Alexa488-conjugated secondary antibody (2 μ g/ml, 4°C, 30 min), 2.5 μ M CFSE, or 1.25 μ M CMFDA. The labeled cells were mixed with unlabeled Huh7.5.1 cells at 1:1 ratio and fixed immediately (0 hr samples), or co-cultured at 37°C for 20 hr and then fixed (20 hr samples). The cells were analyzed with flow cytometry for the percentage of labeled cells. Both histogram and dot plots were shown for CD81 surface labeling and CMFDA labeling; only histogram was shown for CFSE labeling. The numbers on each histogram represent the percentage of labeled cells (M1-gated cells) in that plot, where the M1 gate was determined based on the 0 hr sample.

photobleaching (microscopic observations) led us to consider its derivative, the much more photostable CMFDA. At the end of the search, CMFDA and PKH26 labeling and stable GFP (**Fig. 9, 12A, 31A**) expression were found to be the most appropriate ways to label the donor/target cells, as they meet all the requirements to be used in the co-culture assay.

1.3.2 CCCM HCV transfer among Huh7.5.1

CCCM viral transmission requires different lengths of co-incubation times for different viruses and is often dependent on the ratio of donor cells (D) to target cells (T) (74, 93). Therefore, we started the co-culture assay with a D: T ratio of 1:1 and a co-incubation time of 20 hr for HCV. To distinguish target cells from donor cells, several cell-labeling strategies were exploited. First, we established a GFP-expressing Huh7.5.1 stable cell line with more than 95% GFP-positive cells as determined by flow cytometry (**Fig. 33A**, the “GFP only” bar), and used this cell line as the target cells in the co-culture assay. Incubation of these cells with HCV-infected Huh7.5.1 cells gave rise to core-positive and GFP-positive target cells (arrowhead, **Fig. 10A i, v, ix**). We also found two cell-tracking dyes, CMFDA (220) and PKH26, for labeling donor/ target cells to allow more flexibility in further experiments and to avoid the selection of stable GFP-positive cell lines for each cell to be tested. The thiol-reactive CMFDA dye universally and covalently labels proteins in the cell and the PKH26 dye labels cell membranes; both of them are well-retained, brightly fluorescent and relatively photostable. Incubation of CMFDA-labeled target cells with HCV-infected Huh7.5.1 cells showed core-positive and CMFDA-positive target cells (arrowhead, **Fig. 10A ii, vi, x**). Similar results were obtained using the PKH26 dye to label the target cells (arrowhead, **Fig. 10A iii, vii, xi**). We also labeled HCV-infected cells with CMFDA and used them as the donor cells and naïve Huh7.5.1

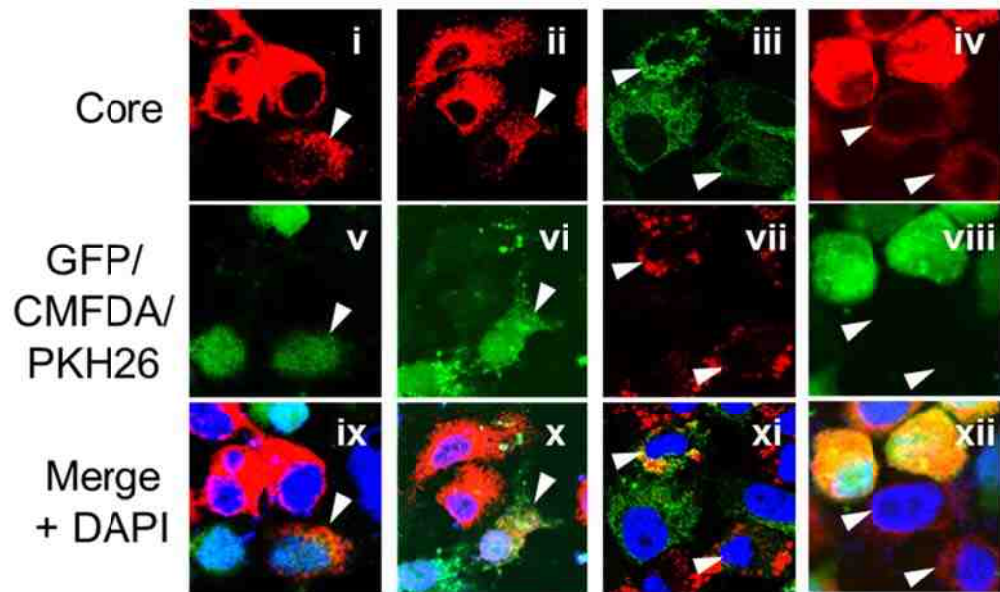
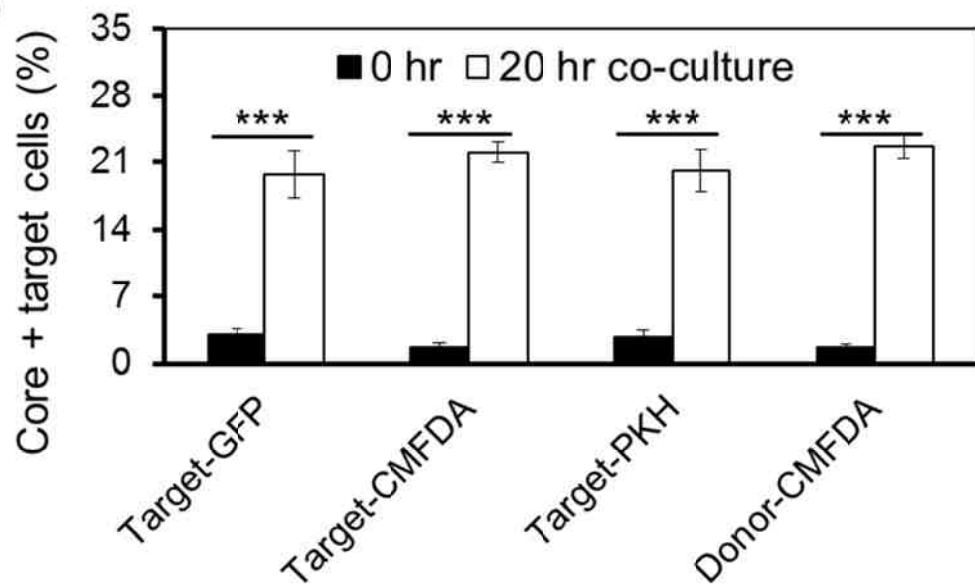
A**B**

Figure 10. CCCM HCV transfer among Huh7.5.1 cells. Huh7.5.1 cells were infected with JFH-1 virus at MOI = 0.1, cultured for 3 days, and co-cultured with GFP-expressing Huh7.5.1 (**A i, v, ix**), CMFDA-labeled Huh7.5.1 (**A ii, vi, x**) or PKH labeled Huh7.5.1 (**A iii, vii, xi**) target cells. Alternatively, the JFH-1-infected cells were labeled with CMFDA (**A iv, viii, xii**) and co-cultured with unlabeled Huh7.5.1 target cells. The donor:target cell ratio was 1. After 20 hr of co-culturing, the cell mixture was subjected to immunostaining against HCV core, followed by (**A**) confocal imaging (newly transferred target cells marked by arrowhead) or (**B**) flow cytometry analysis. Nuclei were counterstained with DAPI.

cells as the target cells for the co-culture assay. The results showed core-positive and CMFDA-negative target cells (arrowhead, **Fig. 10A iv, viii, xii**). Quantitation analysis by flow cytometry showed a comparable level of CCCM HCV transfer. i.e., about 20% of the target cells, among the different labeling strategies (**Fig. 10B**). Noticeably, in both GFP and CMFDA labeling strategies, the target cells exhibited less intense core staining when compared to the donor cells (**Fig. 10B**), potentially explained by the directionality of HCV transfer.

1.3.3 CCCM HCV transfer to primary hepatocytes

To ascertain that CCCM HCV transfer occurred in primary human hepatocytes (PHH), we performed the co-culture assay with CMFDA-labeled HCV-infected Huh7.5.1 as the donor cells and PHH as the target cells. The results showed core-positive and CMFDA-negative PHH target cells (arrowhead, **Fig. 11 A**), which were equivalent to approximately 20% of the total target cell population as determined by flow cytometry (**Fig. 11 B**). Taken together, these results confirmed CCCM HCV transfer in both human hepatoma cells and primary hepatocytes.

1.4 CCCM HCV transfer vs. cell-free HCV infection

The core-positive target cells that were detected following 20 hr of co-culturing (**Fig. 10 & 11**) could also result from infection of target cells with cell-free HCV virus from HCV-infected donor cells. To address this possibility, we determined the kinetics of CCCM HCV transfer and compared it to that of cell-free HCV infection. We labeled uninfected Huh7.5.1 target cells with PKH26 and performed the co-culture assay at a D: T ratio of 1:1 for 0, 3, 6, 9, and 20 hr. Flow cytometry analysis showed that core-positive and PKH-positive target cells began to emerge within 3 hr of co-incubation and gradually increased in number up to 20 hr (**Fig. 12A**). In parallel, we set up a transwell assay (**Fig.**

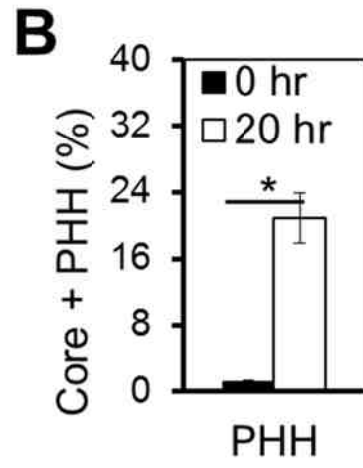
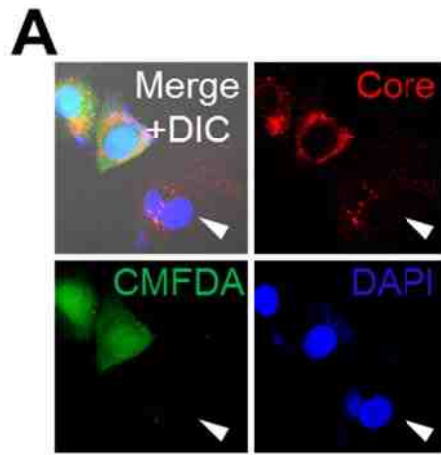
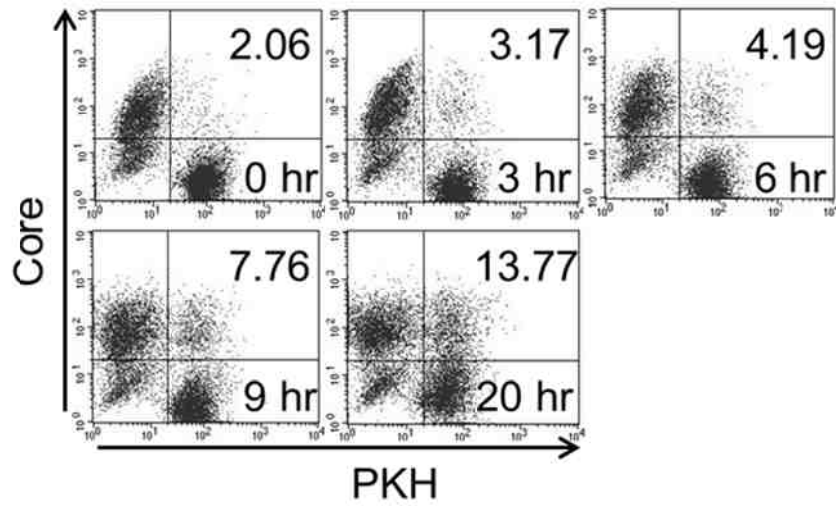
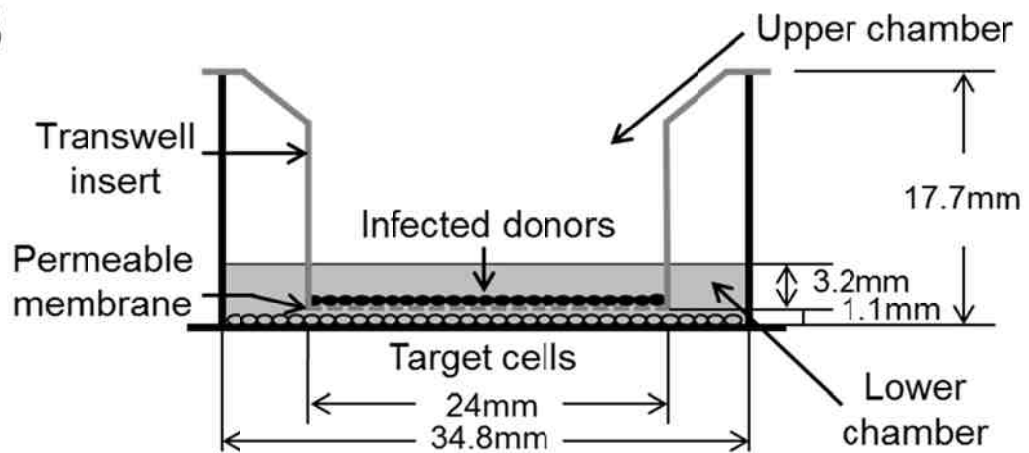
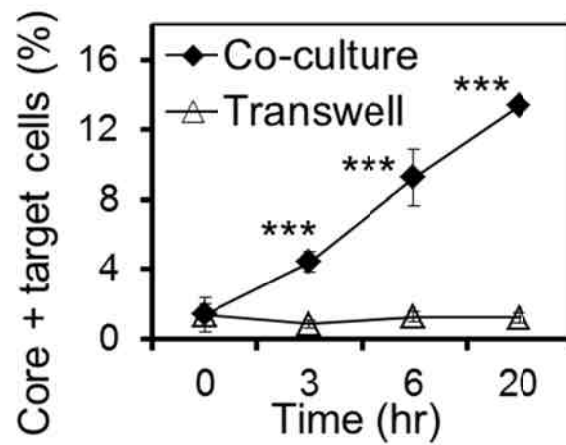


Figure 11. CCCM HCV transfer between Huh7.5.1 and primary human hepatocytes.

Human primary hepatocytes (PHH) were co-cultured with JFH-1-infected CMFDA-labeled Huh7.5.1 cells at a 1:1 ratio for 20 hr. The mixed culture was immunostained for HCV core and subjected to **(A)** confocal imaging or **(B)** flow cytometry. The human primary hepatocytes with CCCM HCV transfer were marked with an arrowhead in **(B)**.

12B), in which HCV-infected Huh7.5.1 donor cells were seeded on a 0.4 μm pore size permeable membrane on the transwell insert in the upper chamber and uninfected Huh7.5.1 cells were seeded in the lower chamber of the transwell. The permeable membrane with 0.4 μm pore size functions as a physical barrier to separate the donor cells from the target cells, and therefore only allows cell-free HCV to diffuse from the upper chamber of the transwell insert into the lower chamber of the transwell to infect cells, and at the same time excludes CCCM HCV infection. As the surface area of the insert is only half of that of the bottom of the lower chamber, a D: T ratio of 1:2 was used to achieve a comparable cell confluence between the upper and lower chambers. The cells in the lower chamber were harvested at the same time points as those in the co-culture assay, i.e., 0, 3, 6, and 20 hr, and stained for HCV core expression. Compared to the results of the co-culture assay, the transwell assay gave rise to very few core-positive target cells in the lower chamber of the transwell during the same time points (**Fig. 12C**). Therefore, the core-positive target cells detected within 20 hr of co-culturing (**Fig. 10 & 11**) likely resulted from CCCM HCV infection and not from cell-free virus infection. To ascertain that HCV virions can freely diffuse through the membrane on the insert, the transwell assay was extended to 48 and 72 hr. HCV-infected cells in the lower chamber were similarly determined using core immunostaining. Core-positive cells in the lower chamber only began to emerge at 24 hr and increased at 48 hr and 72 hr (line graph, **Fig. 12D**), the kinetics was very similar to that of the cell-free HCV virus infection of Huh7.5.1 cells by direct inoculation (**Fig. 12E**), which was routinely performed in the laboratory. These results not only support the notion that cell-free HCV infection takes a longer time than CCCM HCV infection but also confirm that cell-free HCV virus are capable of passing through the membrane and infecting target cells in the lower chamber. In addition, qRT-PCR was performed to compare the HCV RNA level

A**B****C**

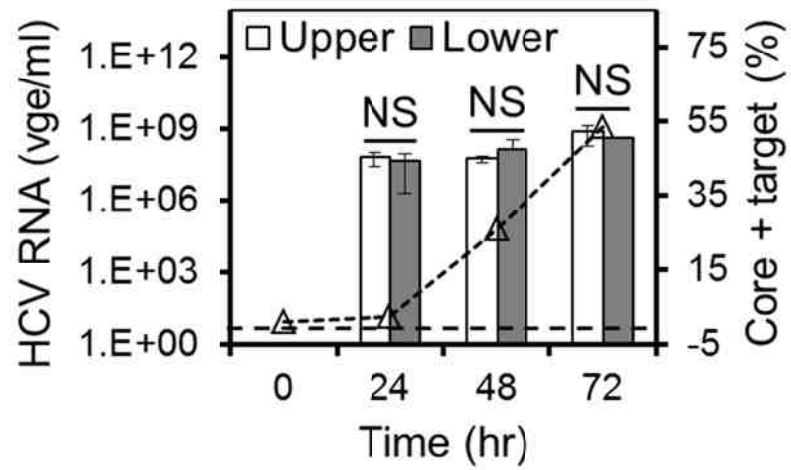
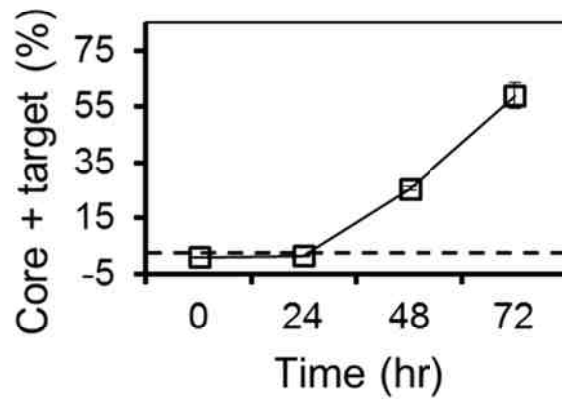
D**E**

Figure 12. CCCM HCV transfer versus cell-free HCV infection. **(A)** JFH1-infected Huh7.5.1 donor cells were co-cultured with PKH-labeled Huh7.5.1 target cells at 1:1 ratio for 0, 3, 6, 9 or 20 hr, followed by immunostaining for HCV core and flow cytometry analysis. The HCV core-positive and PKH-positive cells in the upper right quadrant represent cells with CCCM HCV transfer; they were expressed as the percentage of the total number of the cells and shown in the upper right quadrant in each dot plot. **(B)** Transwell assay. JFH1-infected Huh7.5.1 donor cells were seeded on top of a 0.4 μ m virus-permeable membrane in a transwell insert and Huh7.5.1 target cells were seeded in the lower chamber of the transwell. The cells were cultured for 20 hr with the same total number of cells as the co-culturing assay. The cells in the lower chambers were collected, immunostained for core protein and analyzed by flow cytometry. The transwell is drawn at a scale of 2:1 based on the real size. **(C)** CCCM HCV transfer kinetics in co-culturing and transwell assays at the same 1:2 ratio of D: T. **(D)** Similar transwell experiments were performed as described above in (B) except for extended culturing times. HCV RNA in the upper and lower chambers were determined by qRT-PCR (left Y axis, bar graph), whereas the percentage of core-positive cells in the lower chamber was determined by flow cytometry (right Y axis, dotted line). **(E)** Cell-free HCV infection kinetics. Huh7.5.1 cells were infected with HCV JFH1 (MOI = 1); cells were harvested at indicated times and stained for core-positive cells.

between the upper and lower chambers at 24, 48, and 72 hr. No differences of HCV RNA levels were found (bar graph, **Fig. 12D**), further confirming that HCV can diffuse through the 0.4 μm pore size permeable membrane on the insert and that CCCM infection, not cell-free HCV infection, is solely responsible for the newly infected target cells in 20 hr co-culture assay. Next, we determined whether CCCM HCV transfer was dependent on the D: T ratio. We performed the co-culture assay with the same co-incubation time (20 hr) and the same total number of donor and target cells but with different D: T ratios. The results showed that the percentage of core-positive target cells increased with increasing D: T ratios (**Fig. 13**), suggesting that a higher D: T ratio likely provided more opportunities for the target cells to be in contact with the HCV-infected donor cells. The increase in CCCM HCV transfer over the donor/target ratio appeared to be modest, likely due to an already higher number (density) of the starting cells in the co-culturing assay and thereby non-proportional increase in donor-target contacts over D: T ratio increase. In addition, our subsequent imaging data showed that CCCM HCV transfer did not necessarily occur between one donor cells and one target cell. Furthermore, in this co-culturing experiment, the same total number of cells was maintained when the donor to target (D: T) ratio was increased. Thus, increase of the D: T ratio does not necessarily translate to proportional increase of the contact between donor cells and target cells. In other words, there would be more cell-cell contact and its subsequent CCCM transfer among the donor cells themselves at a higher D: T ratio. But, the type of CCCM transfer was not accounted for in our experimental setting. Taken together, these results showed that CCCM HCV infection occurred more readily than cell-free HCV infection and was dependent on direct cell-cell contact.

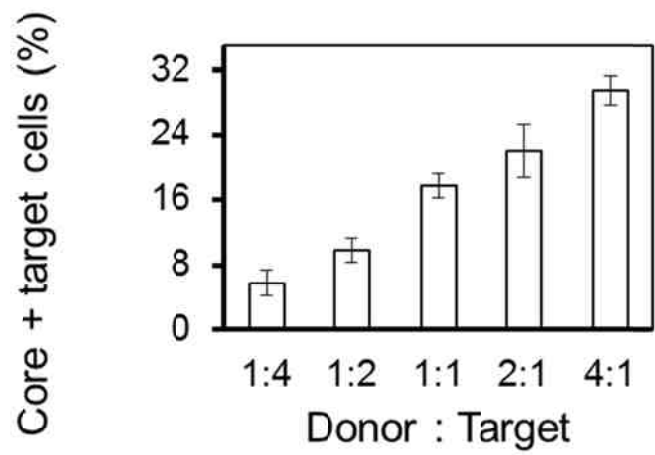
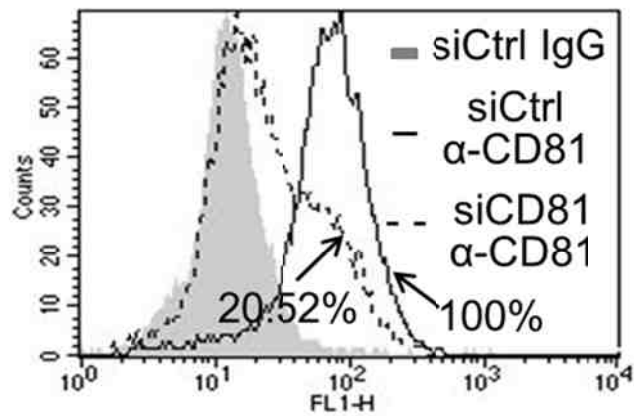
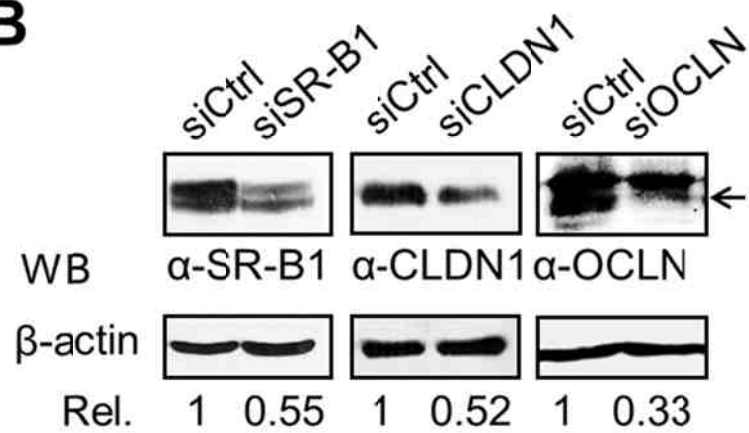


Figure 13. Effects of the Donor: Target ratio on CCCM HCV transfer. 20 hr co-culturing experiments were performed as described in Fig. 12 with different ratios of donor: target cells.

1.5 Indispensable roles of CD81, SR-B1, CLDN1 and OCLN in CCCM HCV transfer

1.5.1 Inhibition of CCCM HCV transfer by knockdown of HCV receptor(s) in target cells

CD81, SR-B1, CLDN1, and OCLN have been shown to be involved in cell-free HCV infection (25, 27-29). As an alternative route to cell-free virus infection, CCCM viral infection and transmission often require viral entry receptors that were originally defined for cell-free virus infection (93, 221, 222). Thus, we determined the roles of these four major HCV receptors in CCCM HCV transfer. First, we knocked down expression of each receptor individually with siRNA in Huh7.5.1 cells and used these cells as target cells in the co-culture assay. A maximal knockdown of each receptor by siRNA was pre-determined using different methods based on the availability of antibodies: 80% for CD81 by flow cytometry (**Fig. 14A**), 50% for SR-B1 and CLDN1 by Western blotting (**Fig. 14B**), and 70% for OCLN by both Western blotting and confocal imaging (**Fig. 14B** arrowhead, **14C**). We labeled these siRNA-transfected Huh7.5.1 cells and used them to perform a 20 hr co-culture assay with HCV-infected Huh7.5.1 donor cells. Compared to siRNA control, knockdown of CD81, SR-B1, CLDN1 and OCLN led to decreases in CCCM HCV transfer by 72%, 68%, 46% and 63%, respectively (**Fig. 14D**). In addition, we also used siRNA to knockdown all four receptors simultaneously in the target cells and performed the co-culture assay. Comparable knockdown efficiencies were achieved for each of these receptors as individual knockdown without apparent cyto- or genotoxicity (**Fig. 15A-C**). Interestingly, CCCM HCV transfer was almost completely abolished to target cells with decreased levels of all four receptors (**Fig. 15D**). Taken together, these data suggest that CD81, SR-B1, CLDN1 and OCLN are all indispensable for CCCM HCV transfer and provide evidence that they may function in a coordinated manner.

A**B**

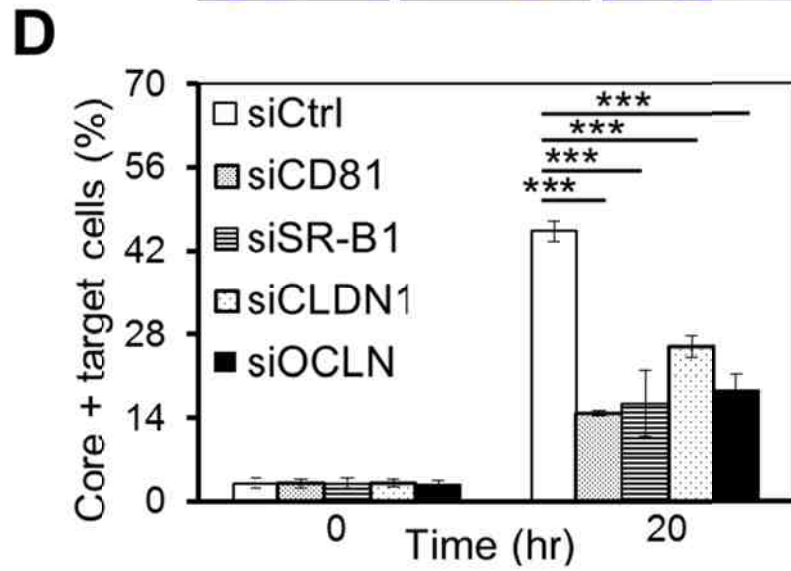
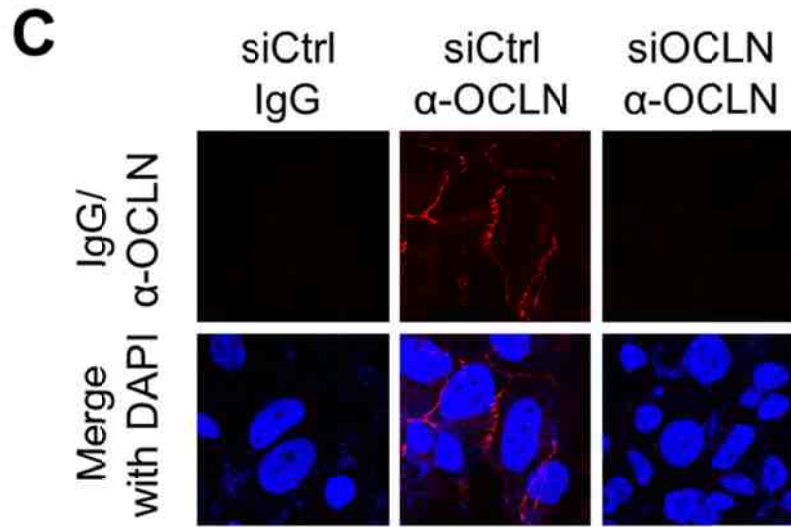
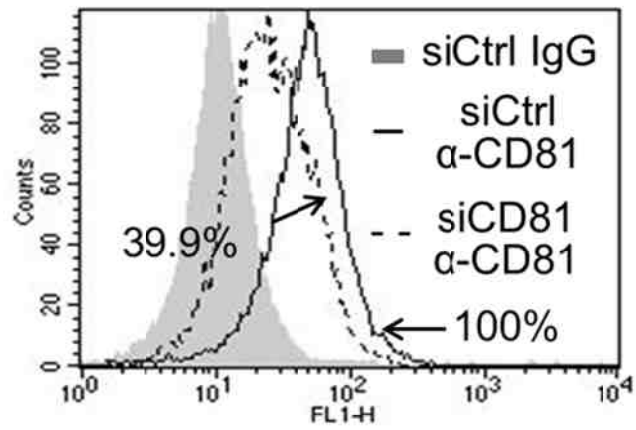
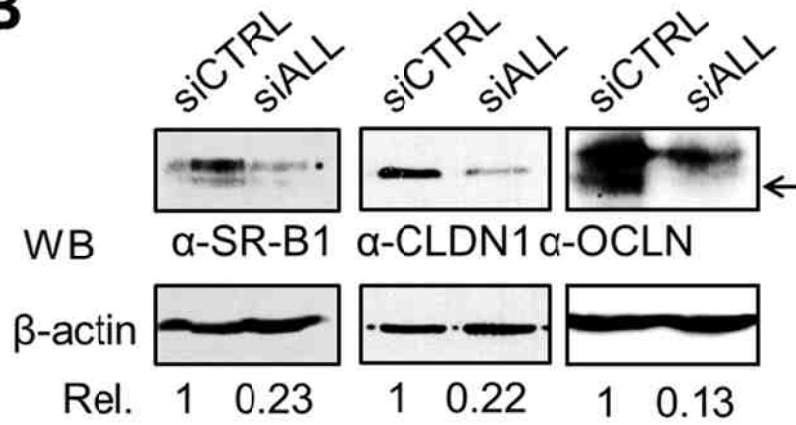


Figure 14. Individual knockdown of CD81, SR-B1, CLDN1 and OCLN on Huh7.5.1 by siRNA and their effects on CCCM HCV transfer. Huh7.5.1 cells were transfected with 100 nM siRNAs specific for CD81, SR-B1, CLDN1, or OCLN. Pre-experiments were performed to determine which siRNA concentration allowed maximal knockdown. At 48 hr post-transfection, cells were collected for analysis of **(A)** CD81 expression by flow cytometry, **(B)** SR-B1, CLDN1, and OCLN expression by Western blotting, and **(C)** OCLN expression by immunofluorescence staining and imaging. Scrambled siRNA control and isotype staining controls were included in each set of experiments as shown. **(D)** The siRNA transfected cells at 48 hr post-transfection were labeled with PKH and then co-cultured with JFH1-infected Huh7.5.1 cells at a 1:1 ratio for 20 hr. The mixed cells were then immunostained for HCV core and analyzed by flow cytometry for target cells with CCCM HCV transfer.

A**B**

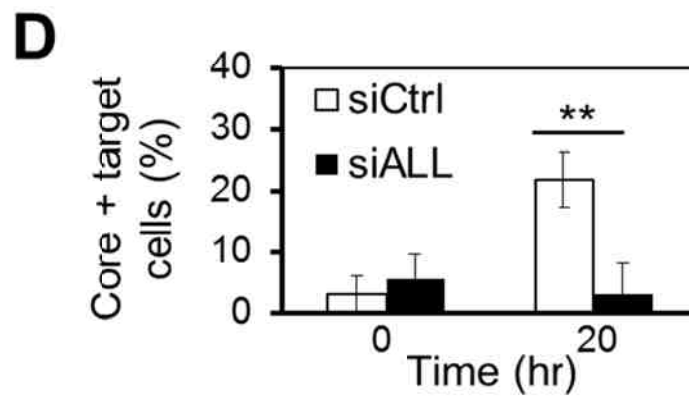
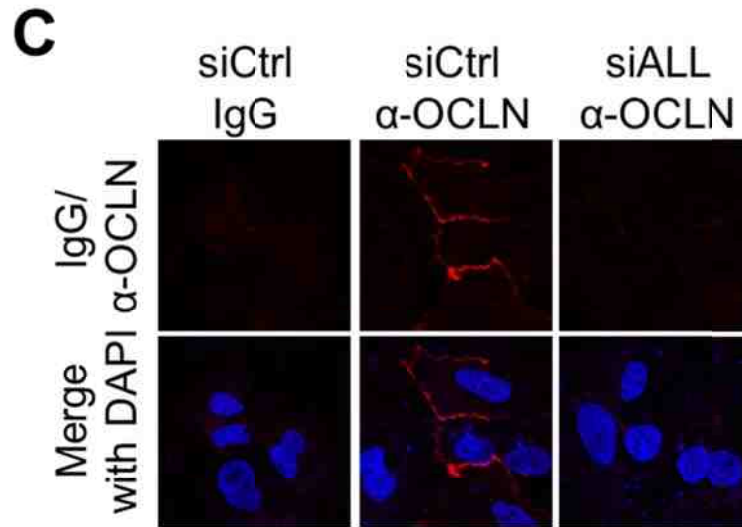


Figure 15. Simultaneous knockdown of CD81, SR-B1, CLDN1 and OCLN on Huh7.5.1 by siRNA and its effect on CCCM HCV transfer. Huh7.5.1 cells were transfected with all four siRNAs for CD81, SR-B1, CLDN1 and OCLN (50 nM each). At 48 hr post-transfection, cells were collected for analysis of **(A)** CD81 expression by flow cytometry, **(B)** SR-B1, CLDN1, and OCLN expression by Western blotting, and **(C)** OCLN expression by immunofluorescence staining and imaging. Scrambled siRNA control (200nM) and isotype staining controls were included in each set of experiments as shown. **(D)** The siRNA transfected cells at 48 hr post-transfection were labeled with PKH and then co-cultured with JFH1-infected Huh7.5.1 cells at a 1:1 ratio for 20 hr. The mixed cells were then immunostained for HCV core and analyzed by flow cytometry for target cells with CCCM HCV transfer.

1.5.2 No CCCM HCV transfer from Huh7.5.1 to other hepatoma and non-hepatoma cell lines

To further analyze the roles of these receptors in CCCM HCV transfer, we took advantage of a panel of human cell lines that constitutively express varied levels of HCV receptors and determined the relationships between HCV receptor expression and cell-free HCV infection or CCCM HCV transfer. The human hepatoma cell lines HepG2, NKNT3 and CYNK10 were used. HepG2 lacks CD81 expression but expresses medium to high levels of the other three major HCV receptors (35, 223-225). NKNT3 and CYNK10 both express very low levels of CLDN1, but have medium to high levels of the other HCV receptors (226, 227). We also included the HCV-susceptible Huh7.5.1 cell line and the non-hepatoma cell line 293T as controls. Huh7.5.1 expressed all four HCV receptors at a moderate to high level, while 293T expressed very high levels of CD81 and OCLN, but low level of SR-B1 and no CLDN1. Expression of all four receptors in these cells was confirmed (**Fig. 16 and Table 1**). Of all cell lines, only Huh7.5.1 was susceptible to cell-free HCV infection (**Fig. 17A and Table 1**). When each cell line was co-cultured with HCV-infected Huh7.5.1 cells, no CCCM HCV transfer was detected in cells other than Huh7.5.1 at 24 hr post co-culturing (**Fig. 17B**). These results confirmed the important roles of all four HCV receptors in both cell-free and CCCM HCV infection. We then introduced into the cells the receptor(s) that were not expressed and/or expressed at a lower level by ectopic expression and assessed the possibility of the CCCM HCV susceptibility in those cells. Ectopic expression of CD81 in HepG2 (**Fig. 18A**) gave rise to little CCCM HCV transfer from HCV-infected Huh7.5.1 (**Fig. 18B**). Similarly, ectopic expression of CLDN1 in NKNT3 (**Fig. 19A**) gave rise to little CCCM HCV transfer from HCV-infected Huh7.5.1 (**Fig. 19B**); ectopic expression of CLDN1 in CYNK10 (**Fig. 20A**) gave rise to little CCCM HCV transfer from HCV-infected Huh7.5.1

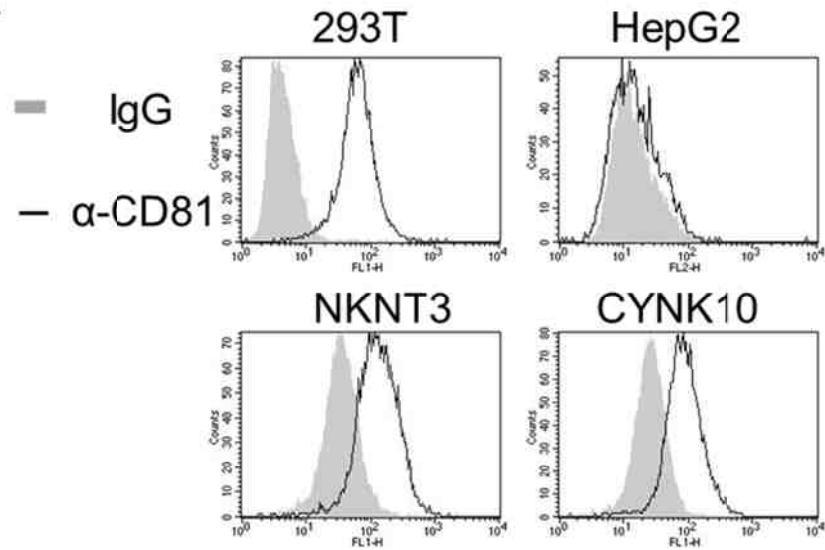
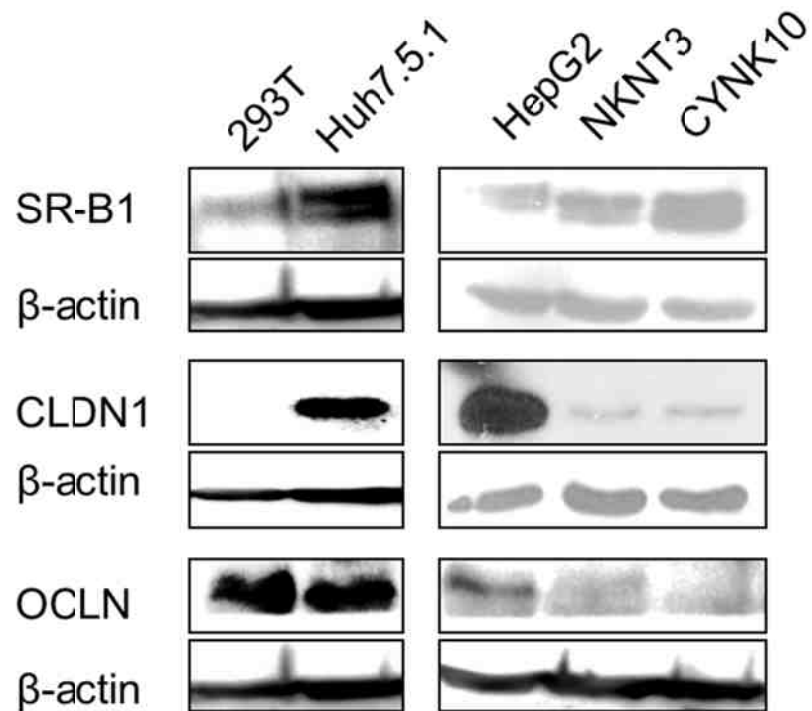
A**B**

Figure 16. Expression of HCV receptors in different cells. Expression of CD81 (**A**), SR-B1, CLDN1 and OCLN (**B**) in different cells were determined by flow cytometry (**A**) or Western blotting (**B**).

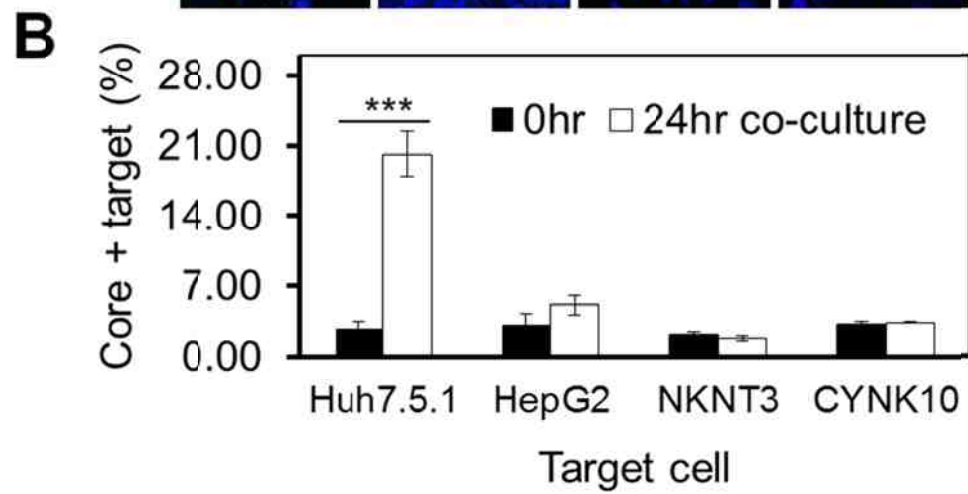
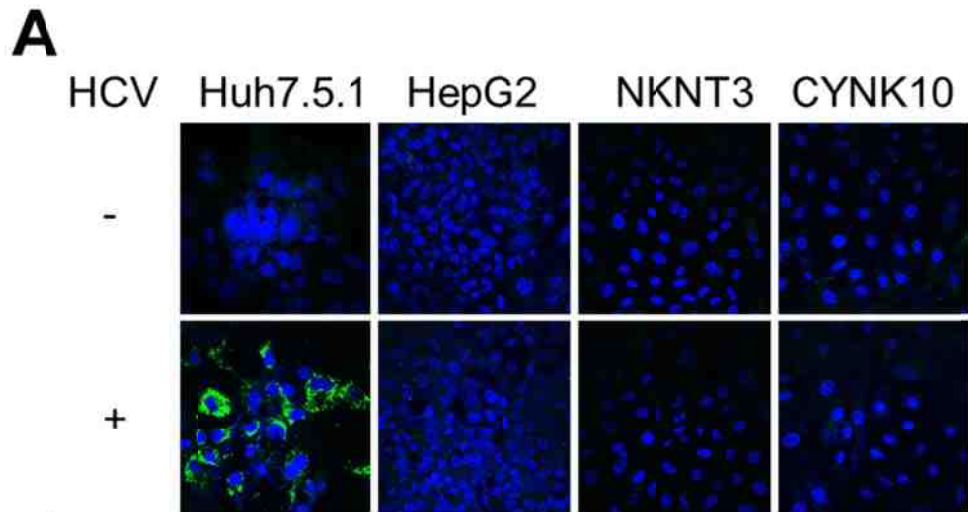


Figure 17. Cell-free and CCCM HCV infection of HepG2, NKNT3 and CYNK10 cells.

(A) Cell-free HCV infection. JFH1 (MOI = 1) were used to infect different cells. After 3 days of infection, cells were immunostained for HCV core and confocal images were taken. The nuclei were counterstained with DAPI. (B) CCCM HCV infection. JFH1-infected Huh7.5.1 donor cells were mixed with each of PKH-labeled target cells at 1:1 ratio and co-cultured for 24 hr. The co-cultured cells were immunostained for core and analyzed by FACS for core-positive target cells.

Table 1. Expression of HCV receptors in different cell lines and its relationship to cell-free HCV virus infection.

Cell line	CD81 ^a	SR-B1 ^b	CLDN1 ^b	OCLN ^b	Perm. to free HCV infection ^c
Huh7.5.1	++	+++	+++	+++	+++
293T	+++	+	-	+++	-
HepG2	-	++	+++	++	-
CYNK10	++	++	+	++	-
NKNT3	++	++	+	++	-

a: determined by immunostaining and flow cytometry

b: determined by western blotting

c: determined by inoculation of JFH1 viral stock and immunostaining for core after 3 days culturing

-: no expression or no infection

+: low expression

++: medium expression

+++: high expression

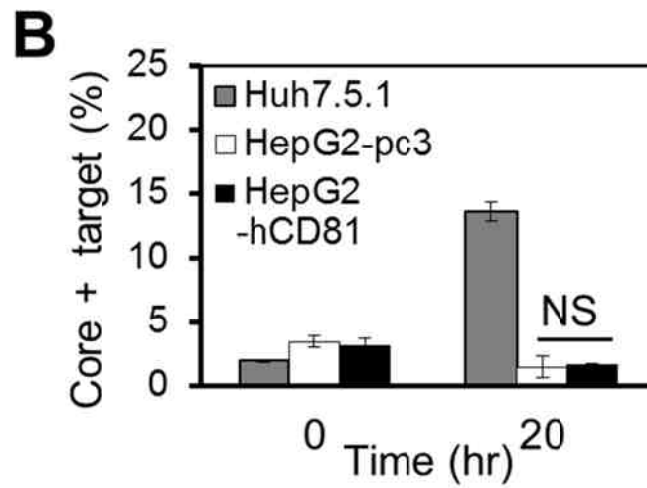
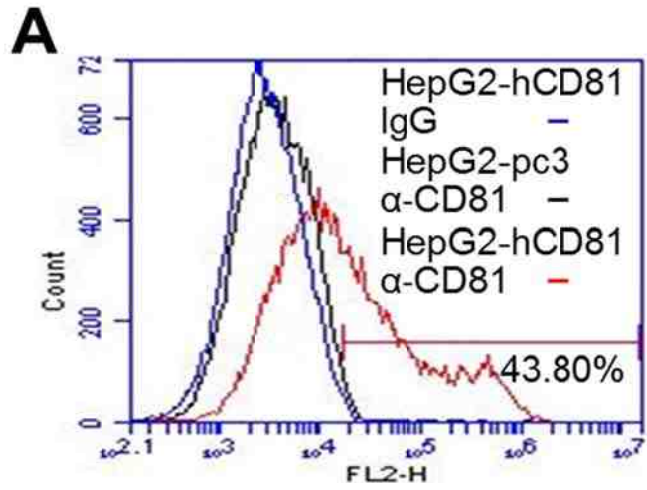


Figure 18. No CCCM HCV transfer from Huh7.5.1 to HepG2-CD81. HepG2 cells were transfected with pcDNA3-CD81. At 48 hr post-transfection, the transfected cells were collected for analysis of CD81 expression by flow cytometry (**A**). Simultaneously, these receptor-expressing HepG2 were labeled with CMFDA and co-cultured with JFH1-infected Huh7.5.1 cells at a 1:1 ratio for 20 hr. The mixed cultures were immunostained against HCV core and analyzed by flow cytometry for target cells with CCCM HCV transfer (**B**). Naïve Huh7.5.1 cells and pcDNA3-transfected HepG2 were included as controls in these experiments. NS: not significant.

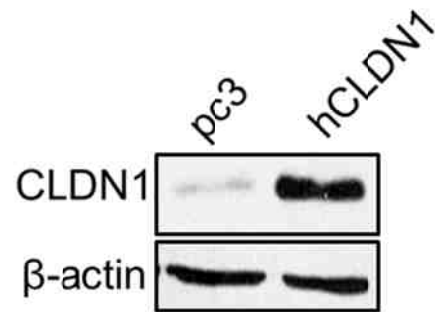
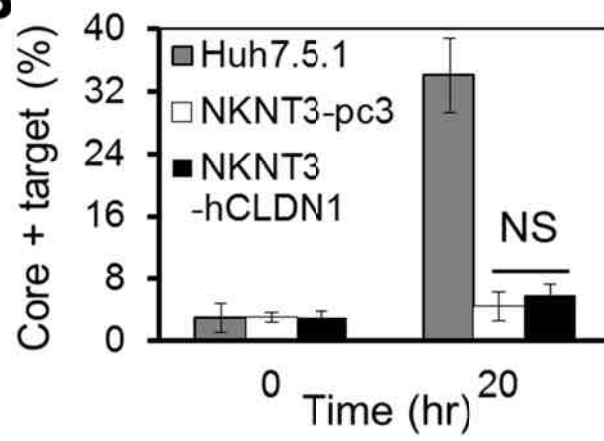
A**B**

Figure 19. No CCCM HCV transfer from Huh7.5.1 to NKNT3-CLDN1. NKNT3 cells were transfected with pCMV-CLDN1. At 48 hr post-transfection, the transfected cells were collected for analysis of CLDN1 expression by Western blotting (**A**). Simultaneously, these receptor-expressing NKNT3 cells were labeled with CMFDA and co-cultured with JFH1-infected Huh7.5.1 cells at a 1:1 ratio for 20 hr. The mixed cultures were immunostained against HCV core and analyzed by flow cytometry for target cells with CCCM HCV transfer (**B**). Naïve Huh7.5.1 cells and pcDNA3-transfected NKNT3 cells were included as controls in these experiments. NS: not significant.

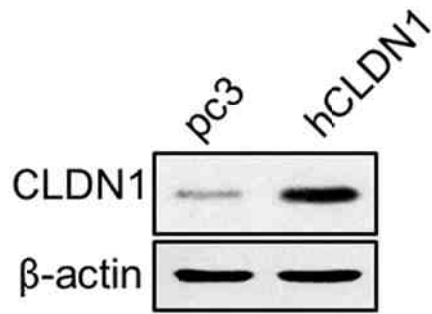
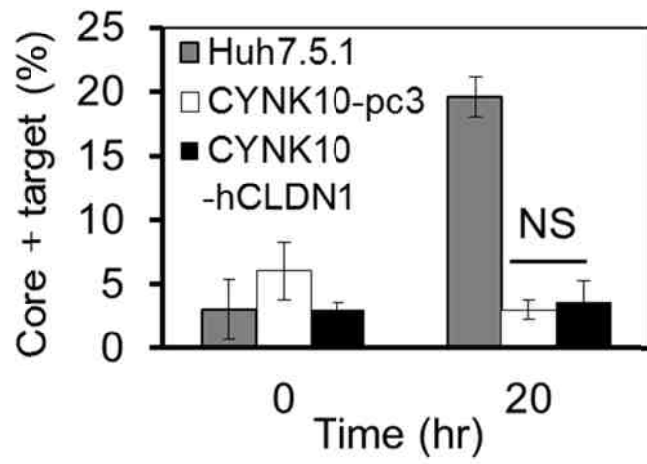
A**B**

Figure 20. No CCCM HCV transfer from Huh7.5.1 to CYNK10-CLDN1. CYNK10 cells were transfected with pCMV-CLDN1. At 48 hr post-transfection, the transfected cells were collected for analysis of CLDN1 expression by Western blotting (**A**). Simultaneously, these receptor-expressing NKNT3 cells were labeled with CMFDA and co-cultured with JFH1-infected Huh7.5.1 cells at a 1:1 ratio for 20 hr. The mixed cultures were immunostained against HCV core and analyzed by flow cytometry for target cells with CCCM HCV transfer (**B**). Naïve Huh7.5.1 cells and pcDNA3-transfected CYNK10 cells were included as controls in these experiments. NS: not significant.

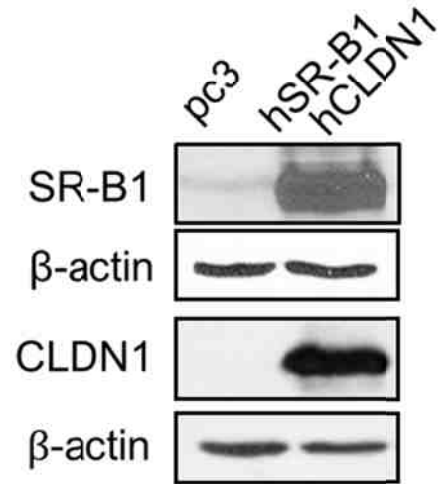
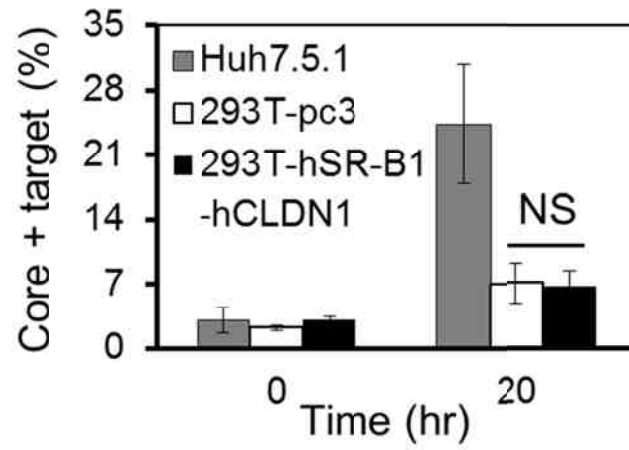
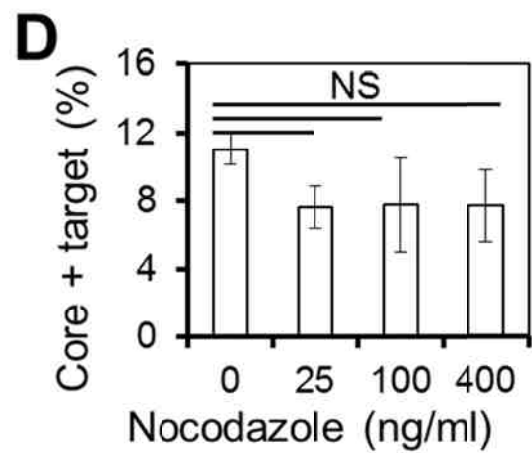
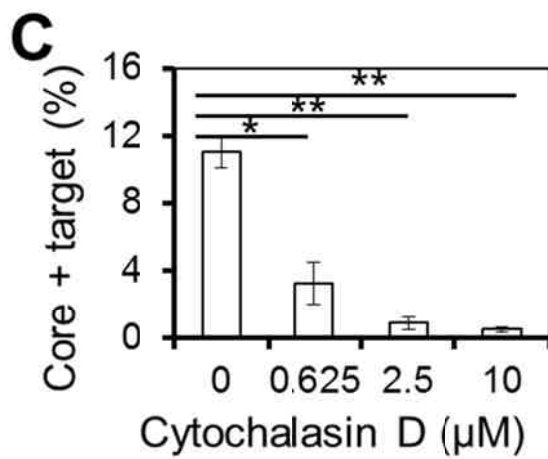
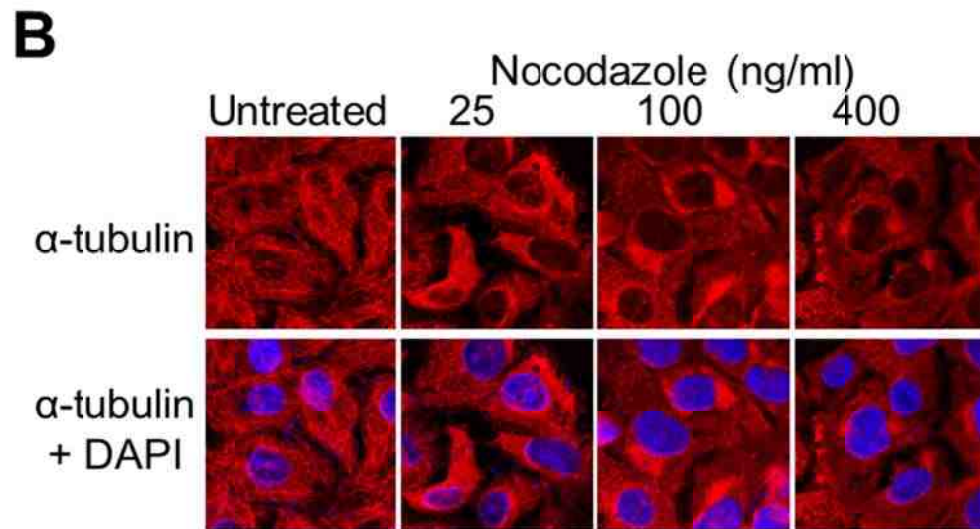
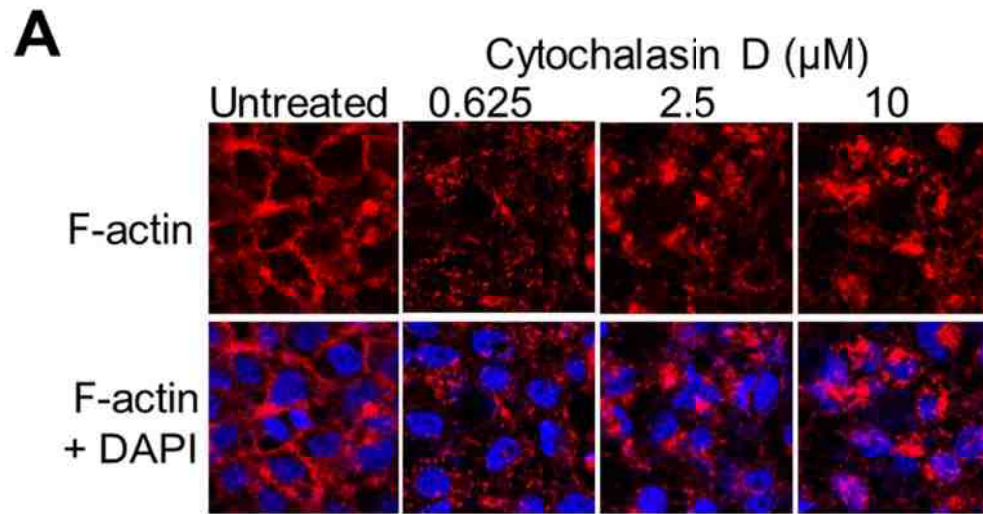
A**B**

Figure 21. No CCCM HCV transfer from Huh7.5.1 to 293T-SR-B1-CLDN1. 293T cells were transfected simultaneously with both pcDNA3-SR-B1 and pCMV-CLDN1. At 48 hr post-transfection, the transfected cells were collected for analysis of SR-B1 and CLDN1 expression by Western blotting (**A**). Simultaneously, these receptor-expressing 293T cells were labeled with CMFDA and co-cultured with JFH1-infected Huh7.5.1 cells at a 1:1 ratio for 20 hr. The mixed cultures were immunostained against HCV core and analyzed by flow cytometry for target cells with CCCM HCV transfer (**B**). Naïve Huh7.5.1 cells and pcDNA3-transfected 293T cells were included as controls in these experiments. NS: not significant.

(**Fig. 20B**); ectopic expression of both SR-B1 and CLDN1 in 293T (**Fig. 21A**) gave rise to little CCCM HCV transfer from HCV-infected Huh7.5.1 (**Fig. 21B**). Taken together, these results suggest that expression of all four major HCV receptors, CD81, SR-B1, CLDN1 and OCLN is essential but not sufficient for CCCM HCV infection.

1.6 Roles of actin and microtubule cytoskeletons in CCCM HCV transfer

To determine the roles of cytoskeleton in CCCM HCV transfer, we performed the co-culturing experiments in the presence of the actin polymerization inhibitor, cytochalasin D (228, 229). The effects of cytochalasin D on actin polymerization were confirmed by immunofluorescence staining of F-actin. As expected, in the absence of cytochalasin D treatment, all of the F-actin filaments were along the boundaries of adjacent cells where they made contact with each other (**Fig. 22A**). When the cells were treated with 0.625 μM cytochalasin D, F-actin filaments were polymerized on the tips of lamellipodia/filopodia instead of being expressed at cell-cell contacts. When the cytochalasin D concentration was further increased to 2.5 μM or 10 μM , F-actin filaments formed aggregates in the cytoplasm and lamellipodia/filopodia were not present. In parallel experiments, a significant decrease in CCCM HCV transfer occurred in co-culture treated with 0.625 μM cytochalasin D and a complete abrogation of CCCM HCV transfer was apparent in co-cultures treated with 2.5 μM and 10 μM cytochalasin D (**Fig. 22C**). We also performed similar experiments in the presence of the microtubule depolymerizing agent, nocodazole (230, 231), and determined its effects on CCCM HCV transfer. As expected, nocodazole treatment disrupted the microtubule cytoskeleton in a dose-dependent manner as determined by α -tubulin immunofluorescence staining, beginning with a gradual loss of the microtubule network, followed by more diffuse



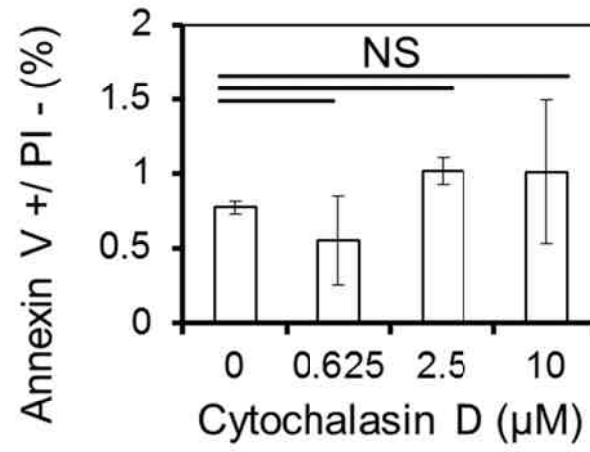
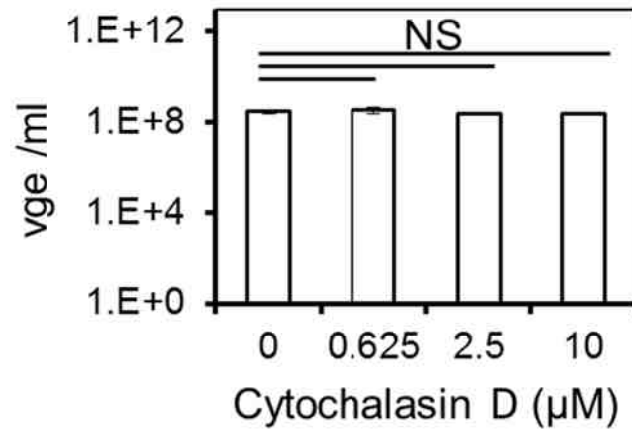
E**F**

Figure 22. Actin and microtubule cytoskeletons and CCCM HCV transfer. (A-E)

JFH1-infected Huh7.5.1 donor cells were mixed with CMFDA-labeled target Huh7.5.1 at a 1:1 ratio and seeded. Two hours post-seeding, cytochalasin D or nocodazole were added to the cultures at the indicated concentrations and the cells were cultured for an additional 18 hr. **(A)** Cytochalasin D-treated co-culture were stained with phalloidin-TRITC followed by DAPI, while **(B)** nocodazole-treated co-culture were immunostained with a mouse anti-tubulin antibody followed by goat anti-mouse IgG-Alexa555, and DAPI. **(C, D)** Both cytochalasin D- and nocodazole-treated co-culture were immunostained against HCV core and analyzed by flow cytometry for cells that underwent CCCM HCV transfer. The number of core-positive target cells within the initial 2 hr post-seeding period was also determined and subtracted from the 20 hr number. **(E)** Cytochalasin D-treated co-culture were labeled with APC-conjugated Annexin V followed by propidium iodide (PI) and analyzed by flow cytometry for cells that underwent apoptosis (Annexin V+/PI-). **(F)** Cytochalasin D's effect on HCV production. Huh7.5.1 cells were infected with JFH1 for three days and replated into 12-well plates at close to 100% confluency. At 2 hr post-seeding, culture media with indicated concentrations of cytochalasin D were changed and maintained for 18 hr. Supernatants were then collected and HCV RNA was quantified by qRT-PCR.

tubulin staining patterns in the cytoplasm (Fig. 22B). However, nocodazole treatment did not lead to significant changes in the level of CCCM HCV transfer in parallel experiments (Fig. 22D). The inhibition of CCCM HCV transfer by cytochalasin D treatment (Fig. 22C) was not due to cytotoxicity of cytochalasin D ((232) and Fig. 22E), or any adverse effects of cytochalasin D on HCV secretion from HCV-infected donor cells (Fig. 22F). Therefore, these results suggest that an intact actin network, but not the microtubule cytoskeleton may be required for CCCM HCV transfer.

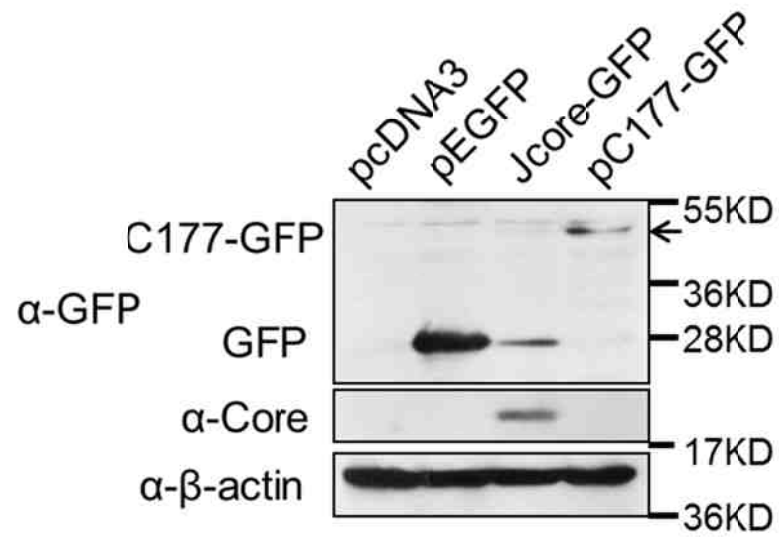
1.7 Live cell imaging of the CCCM HCV transfer in Huh7.5.1 cells: from conjugate formation to transfer

1.7.1 Construction and characterization of recombinant JFH1-c177-GFP

To directly dissect the spatial and temporal details of CCCM HCV transfer, we attempted to construct a fluorescently labeled HCV clone to characterize viral transfer in live cells. Among the three known HCV structural proteins E1, E2, and core, we decided to insert GFP to core in JFH1 right after the 177 aa. There were two reasons for the selection of the insertion site. (1). A part of the HCV 5'UTR extends into the N-terminus of core; considering the relatively large size of GFP (~700 nt), insertion of GFP to the N terminus could result in replication/ translation perturbation and would very likely affect virus production. Hence we decided to insert GFP to the C-terminus of core. (2). Translated core is processed by signal peptidase (SP) at 191 aa (the end of the C-terminus of core, also the junction of core and E1) and then by signal peptide peptidase (SPP) at 177 aa to generate the mature core protein. A recent study (233) showed that at least the first 177 amino acids were required to produce infectious HCV virions in J6/JFH1 strain. Therefore we decided to insert GFP at the 177 aa position of core to retain the infectivity of the recombinant virus and to avoid the cleavage of the fusion protein by SPP. Before

the insertion of GFP into JFH1, we first tested whether the c177-GFP fusion protein could be expressed and whether it could be packaged into virion through trans-complementation. We cloned the 1-177 aa of JFH1 core into the N-terminus of the EGFP gene in pEGFP-N3 and obtained the pC177-GFP plasmid. We transfected pC177-GFP and pJcore-GFP (a plasmid encoding full length core-GFP fusion protein that was constructed previously in our laboratory, unpublished data) into Huh7.5.1 and detected the expression of core-GFP fusion protein after two days by Western blotting. Cells transfected with pC177-GFP showed a clear band at 45 KD, which is the C177-GFP fusion protein, without any leaking expression of GFP or core (**Fig. 23A**, arrow). In contrast, the pJcore-GFP-transfected cells showed only distinctive GFP and core bands, but no GFP-core fusion protein (**Fig. 23A**), very likely due to the cleavage by SP or SPP. Microscopic examination showed that pC177-GFP-transfected Huh7.5.1 gave bright GFP fluorescence in both the nucleus and the cytoplasm (**Fig. 23B**) and that the pattern of cytoplasmic fluorescence (perinuclear “bubbles”) was very similar to HCV core immunostaining in infected cells (presumably core accumulation on the surface of lipid droplets, **Fig. 10A**). To test whether the fusion protein can be incorporated into HCV virions, we performed *trans*-complementation experiment by transfection of JFH1-infected Huh7.5.1 with pC177-GFP followed by detection of HCV core in both the cell lysate and culture supernatant with Western blotting. However, even though C177-GFP fusion protein was readily detected in cell lysate, no fusion protein could be detected in the culture supernatant (arrow, **Fig. 24 A**), suggesting that the C177-GFP fusion protein could not be packaged into HCV virions in infected cells. To ascertain this result, we also performed spinoculation (centrifugation of cells at 1000 x *g* and RT for 2 hr after addition of virus, refer to CHAPTER 3-3.4 of the Results section for details) of Huh7.5.1 with the above culture supernatant and measured GFP fluorescence in those cells by

A



B

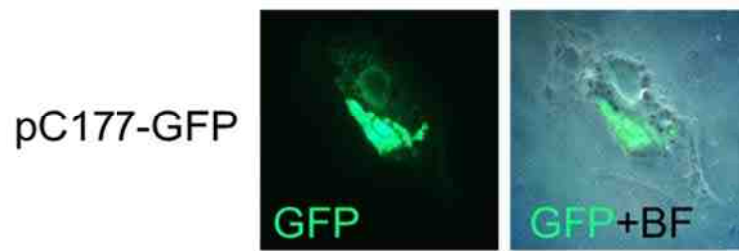


Figure 23. Expression of C177-GFP fusion protein. (A) Huh7.5.1 was transfected with pcDNA3, pEGFP-N3, pJcore-GFP, or pC177-GFP. At 48 hr post-transfection, cells were collected and immunoblotted with anti-GFP, anti-Core and anti- β -actin antibodies. (B) pC177-GFP-transfected Huh7.5.1 cells were examined by fluorescent microscope for GFP fluorescence at 48 hr post-transfection. BF: bright field.

A

		(1)	(2)	(3)	(4)	(5)
Infection	<i>JFH1</i>	+	+	-	+	+
Transfection (μ g)	<i>pcDNA3</i>	8	-	-	4	-
	<i>pEGFP</i>	-	8	-	-	-
	<i>pC177-GFP</i>	-	-	8	4	8

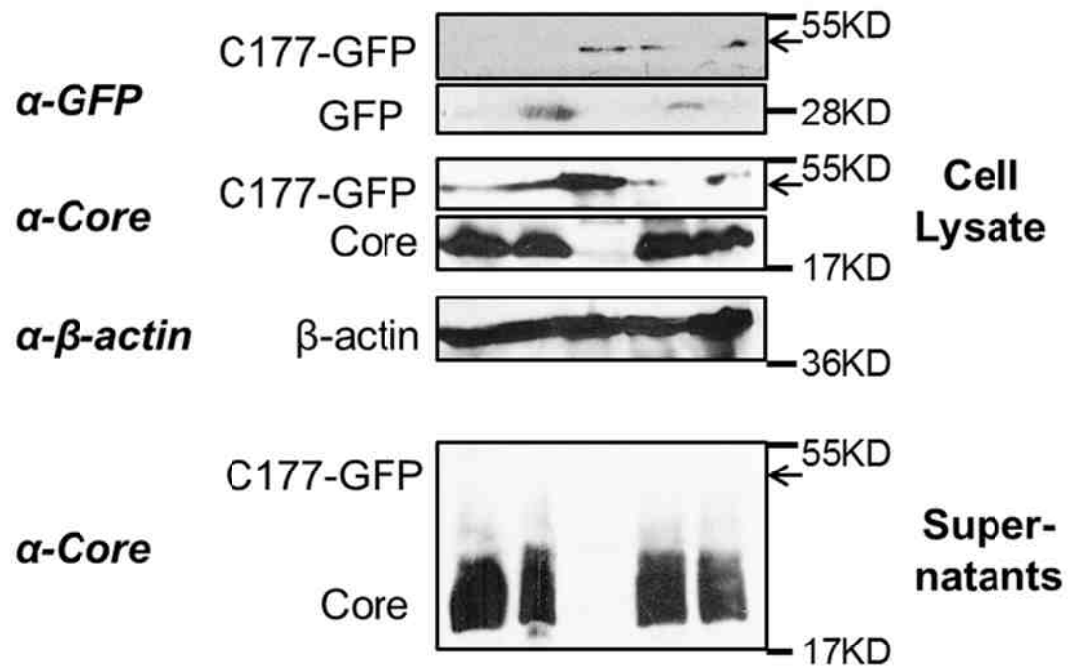
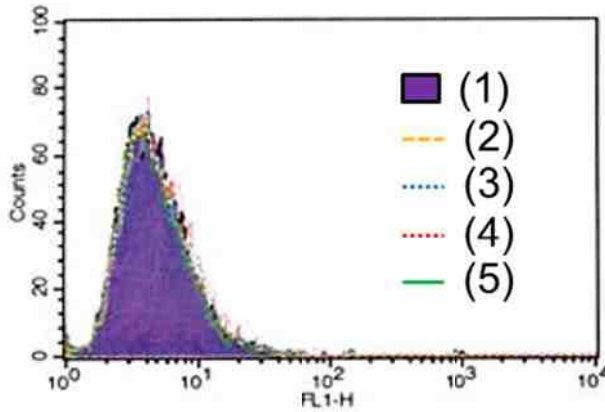
**B**

Figure 24. No incorporation of C177-GFP into JFH1 virions by *trans-complemetation*. Huh7.5.1 was infected with JFH1 virus at MOI = 0.2. At 48 hr post-infection, the cells were transfected with indicated amount of pcDNA3, pEGFP-N3 or pC177-GFP, and cultured for another 48 hr. Cells were collected and immunoblotted with anti-GFP, anti-Core and anti- β -actin antibodies (**A**, cell lysate). Culture supernatants were also collected, removed of cell debris by low speed centrifugation at 2000 x g for 10 min, passed through 0.22 μ m filter, and either ultracentrifuged at 250,000 x g and 4°C for 90 min and immunoblotted for core and c177-GFP fusion protein expression (**A**, supernatants), or added to Huh7.5.1 cells, spun at 1000 x g, RT for 2 hr (spinoculation), cultured at 37 °C for 3 hr and analyzed by flow cytometry (**B**). A histogram overlay of the GFP fluorescence intensity in Huh7.5.1 cells spinoculated with different supernatants was shown.

flow cytometry. But consistent with the Western blotting result, no peak shift of GFP fluorescence intensity was observed between the pCore177-GFP samples and the pEGFP control (**Fig. 24 B**).

The reason for the unsuccessful incorporation of C177-GFP into HCV virions by *trans*-complementation could be the competition from of large amounts of wide type core proteins expressed during the infection. Therefore, we constructed the JFH1-c177-GFP recombinant clone by inserting GFP into the JFH1 genome right after 177 aa of core. We transfected Huh7.5.1 cells with the wide type JFH1 RNA or the JFH1-c177-GFP RNA and determined HCV core and GFP expression by immunostaining followed by microscopic imaging. JFH1-c177-GFP-transfected cells demonstrated very faint HCV core staining and no GFP fluorescence (**Fig. 25**). Examination of HCV replication using strand-specific RT-PCR showed that JFH1-c177-GFP replicated at about the same level as wide type JFH1 in Huh7.5.1 (unpublished data from our laboratory). Briefly, the recombinant JFH1-c177-GFP replicated well, expressed viral proteins at a lower level than wide type JFH1, but didn't show any GFP fluorescence in transfected cells, likely due to the large size of the foreign GFP protein and subsequent perturbations in viral protein expression.

1.7.2 Construction and characterization of recombinant JFH1-TCcore

We therefore turned to the TC tag-biarsenical dye labeling system that has been successfully used to label and study several viruses in live cells [reviewed in (234)], including HCV (66, 208). Compared to the GFP-core fusion protein strategy, this system only requires insertion of a short nucleotide sequence encoding a peptide of 12 aa, including the tetracysteine (TC) tag (-CCxxCC-), into the viral genome without affecting virus translation, replication, assembly, production and infectivity (66, 208, 234). The

presence of the TC tag allows the tagged HCV core protein in the cells or in HCV to be detected live by microscopic imaging through its covalent binding to the cell membrane-permeable non-fluorescent biarsenical compound and its ensuing fluorophore. We constructed the HCV-TC clone in the context of JFH1, subsequently referred to as JFH1-TCcore (**Fig. 26A**). We transfected Huh7.5.1 cells with an equal amount of *in vitro* transcribed full-length JFH1 RNA or JFH1-TCcore RNA and monitored HCV replication and production using qRT-PCR. Compared to JFH1, JFH1-TCcore showed a slightly delayed viral replication (**Fig. 26B**) and virus production (**Fig. 26C**) and a 2-4 fold lower maximal level of virus production (**Fig. 26C**). Nevertheless, labeling of JFH1-TCcore-transfected and infected cells with the biarsenical compound did not alter the HCV-TCcore infectivity (66). We then determined the labeling specificity of the biarsenical compound (ReAsH) and the subcellular localization of the TC-tagged core protein. Huh7.5.1 cells were transfected with *in vitro* transcribed full-length JFH1 or JFH1-TCcore RNA and stained with ReAsH and then anti-HCV core antibody. ReAsH only labeled JFH1-TCcore-transfected cells and not JFH1-transfected cells (**Fig. 26D**). There appeared to be a complete overlap of ReAsH labeling with HCV core staining, confirming that ReAsH specifically bound to the TC tag and that the tag did not alter the subcellular localization of HCV core. Taken together, these results demonstrated the feasibility of using the JFH1-TCcore and ReAsH labeling system to track HCV core in live cells.

1.7.3 Live cell imaging of CCCM HCV transfer

We next performed live cell imaging to track CCCM HCV transfer with the JFH1-TCcore system. We infected Huh7.5.1 cells with JFH1-TCcore for 3 days and then labeled the cells with ReAsH. We used these ReAsH-labeled cells as donor cells and Huh7.5.1

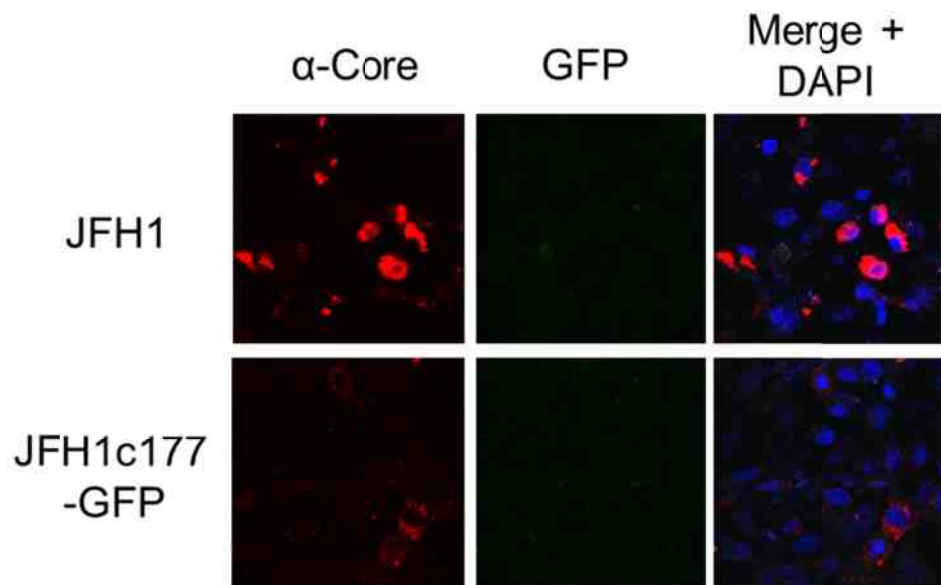


Figure 25. GFP and core expression in JFH1-c177-GFP RNA-transfected Huh7.5.1 cells. Huh7.5.1 cells were transfected with JFH1 or JFH1-c177-GFP RNA. At three days post-transfection, the cells were subjected to immunostaining for HCV core and DAPI nuclear staining.

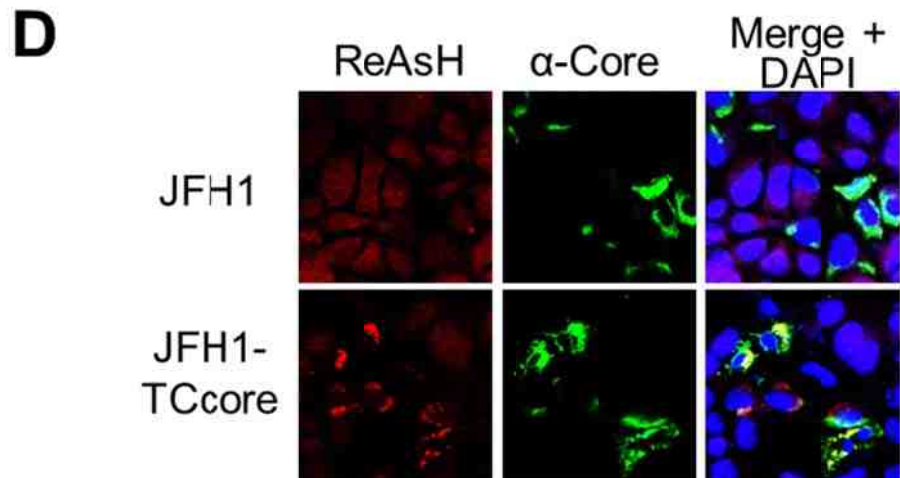
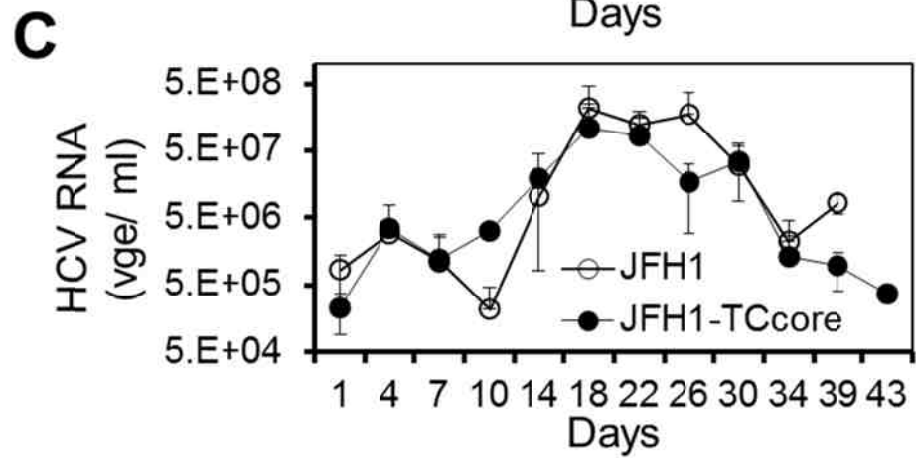
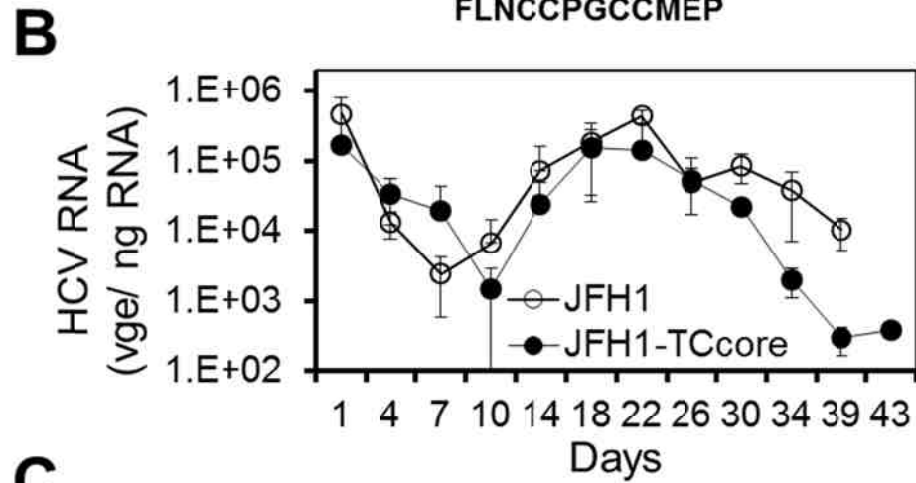
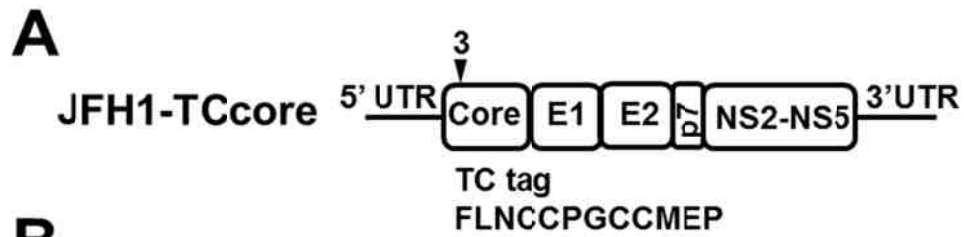


Figure 26. Characterization of recombinant JFH1-TCcore HCV. (A) JFH1-TCcore recombinant HCV clone. A TC tag-containing 12 aa peptide was inserted after the third amino acid of HCV JFH1 core. (B) & (C) Huh7.5.1 cells were transfected with an equal amount of *in vitro* transcribed full-length HCV JFH1 RNA or HCV JFH-TCcore RNA. Transfection medium was replaced with fresh culture medium and the cells were extensively washed 6 hr after transfection. RNA was isolated from the cells and the culture supernatants at indicated time points and was subjected to qRT-PCR to monitor HCV replication in the cells (B) and HCV production in the culture supernatants (C), respectively. (D) ReAsH labeling specificity of TCcore in JFH1-TCcore RNA-transfected Huh7.5.1 cells. Huh7.5.1 cells were transfected with JFH1 or JFH1-TCcore RNA. At three days post-transfection, the cells were first labeled with ReAsH, then immunostained for HCV core and DAPI nuclei staining.

cells stably expressing GFP (Huh7.5.1-GFP) as target cells and performed the co-culturing assay under live confocal imaging. Red (ReAsH)/ green (GFP) fluorescence and DIC images in the selected fields were taken every 18 min throughout the 18 hr co-culturing period. One single HCV-infected ReAsH-labeled Huh7.5.1 donor cell (labeled as D, **Fig. 27A**) had three recorded sequential transfer events (yellow arrowheads) to three contacted target Huh7.5.1-GFP cells (labeled as T1, T2 and T3, **Fig. 27A**) during this time period. For each transfer event, the donor cell either accumulated large numbers of viral puncta on the contact surface between the donor cell and the target cell (D and T1, **Fig. 27A i & ii**) or produced lamellipodium containing viral puncta at the contact sites (D and T2, D and T3, **Fig. 27A iii & iv**) prior to the transfer. Simultaneous transfer was also recorded (**Fig. 27B & C**). The orthogonal view (**Fig. 27B**) and 3D reconstruction of the transfer process (**Fig. 27C**) confirmed that the transferred viral puncta were located inside the target cell, as the viral puncta were visualized as yellow rather than red. 3D reconstruction of the donor-target contact sites for CCCM transfer in Fig. 27 further revealed that besides the obvious lamellipodium seen in some cases (Fig. 27 A iii and iv), small and unapparent lamellipodium-like structures full of viral puncta were also present at the donor-target contacts sites for the ongoing transfer (**Fig. 28**) in the other cases (Fig. 27A i, ii, B and C). The sizes of the pre-transfer viral puncta were estimated to be approximately 0.5 μm to 2 μm , suggesting that these puncta contain more than one single virus. The number of core puncta that were transferred from one donor cell to one target cell could reach up to 100 puncta during the 18 hr co-culturing period. Tracking the transfer of one single viral punctum revealed four distinct steps in the CCCM HCV transfer process: donor-target cell contact, viral punctum-target cell conjugate formation, transfer of viral punctum, and post-transfer (**Fig. 29A**). The transfer began with contact initiated between the donor and target cells (**Fig. 29A i**). Viral puncta

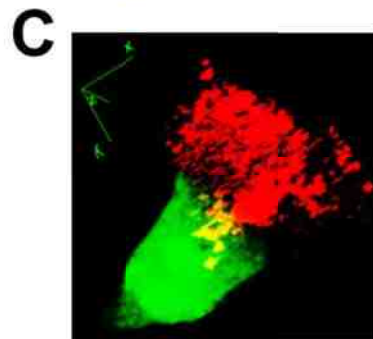
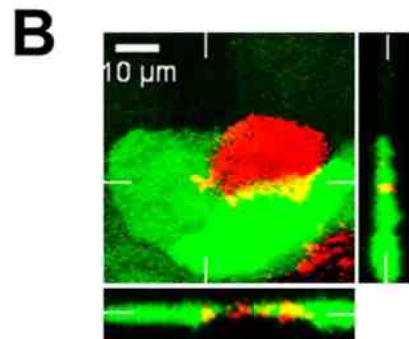
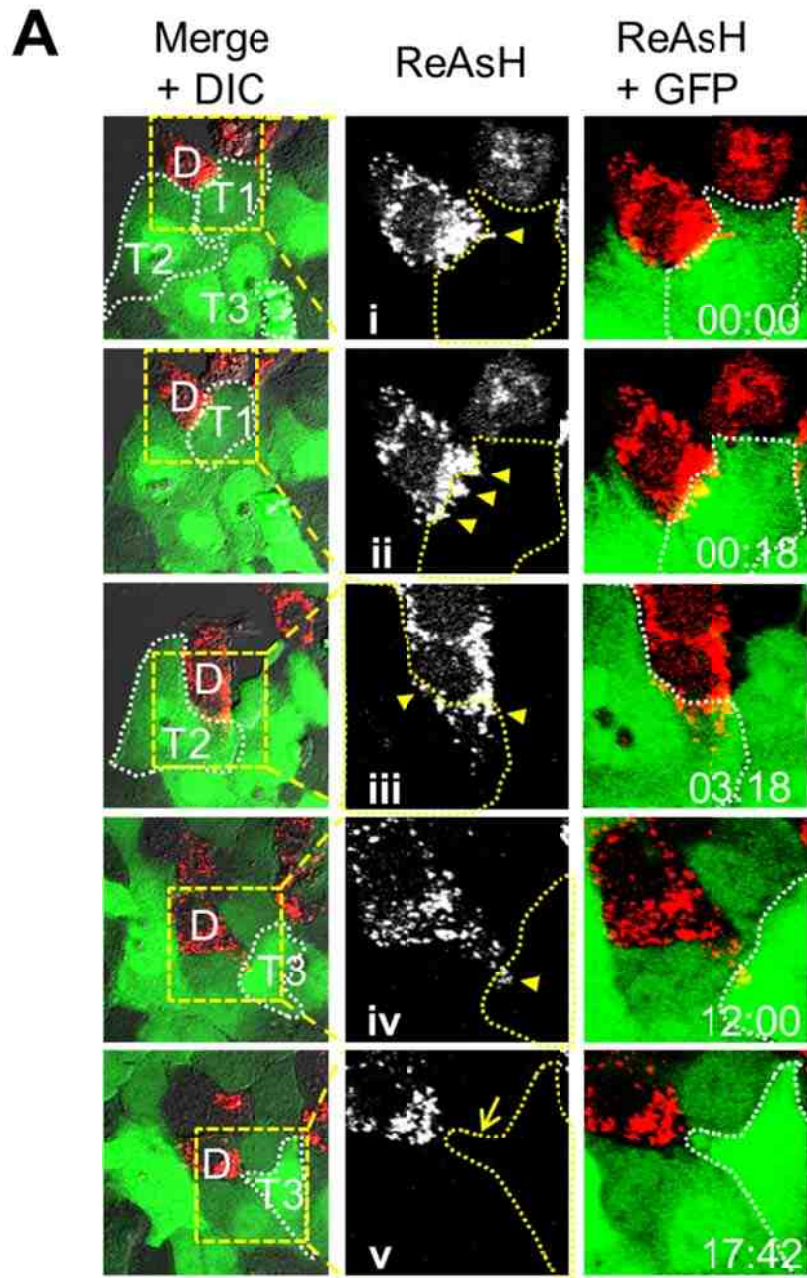


Figure 27. Live cell imaging of CCCM HCV transfer (I) – sequential viral transfer from one donor to 3 targets and concurrent viral transfer between one donor and two targets. JFH1-TCcore-infected ReAsH-labeled Huh7.5.1 donor cells (red) and Huh7.5.1-GFP target cells (green) were co-cultured and imaged live for 18 hr. **(A)** Sequential viral transfer from one donor to 3 targets. The ReAsH-positive TCcore-positive donor cell was labeled with “D” and the three GFP-positive target cells were labeled with T1, T2, T3 (outlined with white dotted lines). The ReAsH/GFP/DIC overlay was shown in the left panel, from which the boxed area was magnified and examined in the middle (ReAsH only) and the right (ReAsH/GFP overlay) panels. HCV transfer from the donor cell, D, to target cells T1 (**i & ii**), T2 (**iii**), and T3 (**iv**) was indicated by yellow arrowheads. The yellow arrow (**v**) indicated T3’s lamellipodium towards D after viral transfer. Time was shown in hr: min. **(B)** Concurrent HCV transfer from one donor cell to two target cells. Orthogonal views are shown and the positions of the perpendicular planes are indicated as notches. **(C)** 3D reconstruction of a transfer event between the donor cell and one target cell in **(B)**. This transfer event occurred at a later time than that shown in **(B)**.

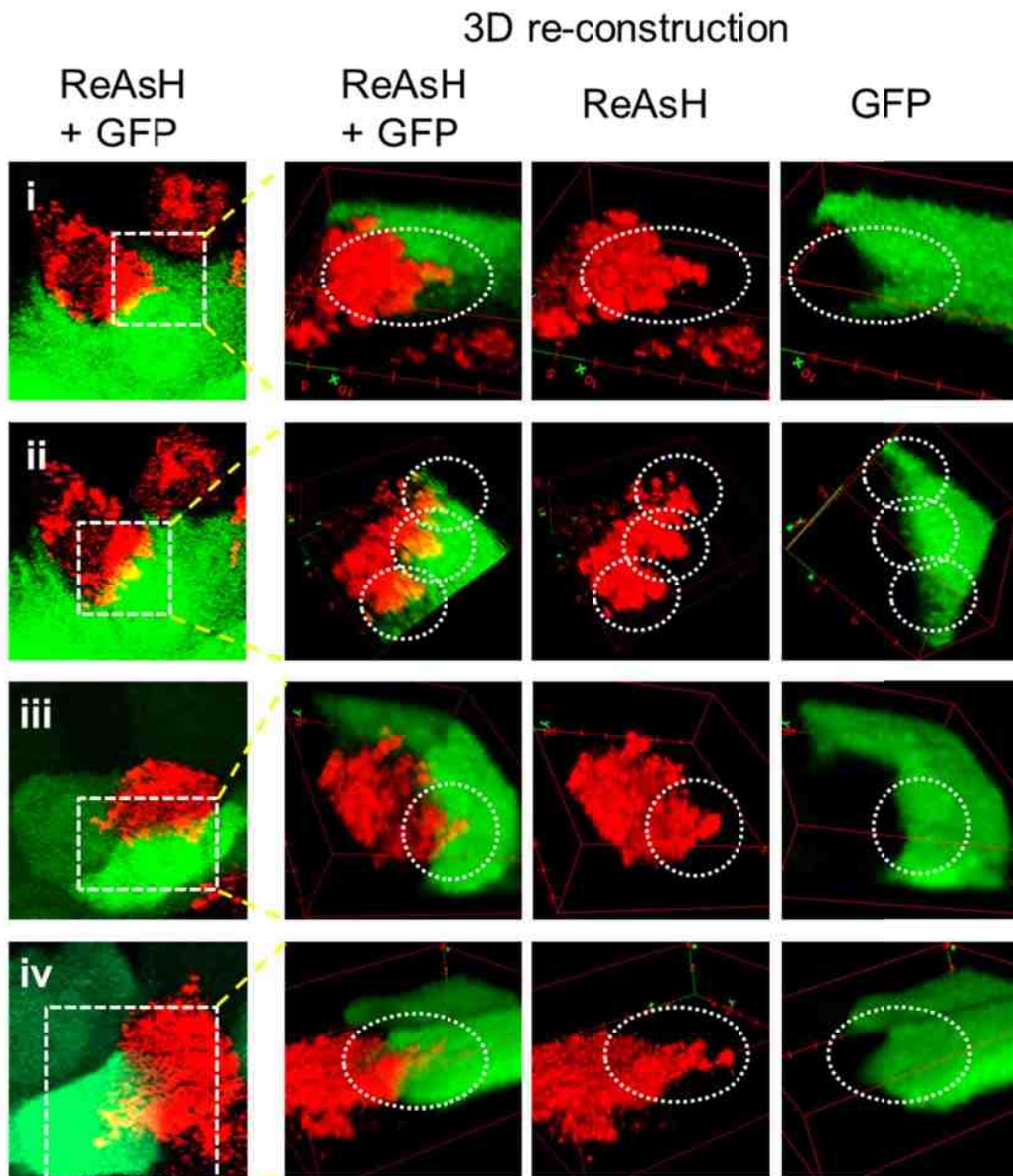


Figure 28. Live cell imaging of CCCM HCV transfer (II) – lamellipodium-like structures at the donor-target contact sites during CCCM transfer. The donor-target contact sites of CCCM transfer (boxed area in the left column) in Fig. 27A i **(i)**, ii **(ii)**, B **(iii)** and C **(iv)** were converted into 3D images (right three columns). Lamellipodium-like structures were circled with white dotted lines.

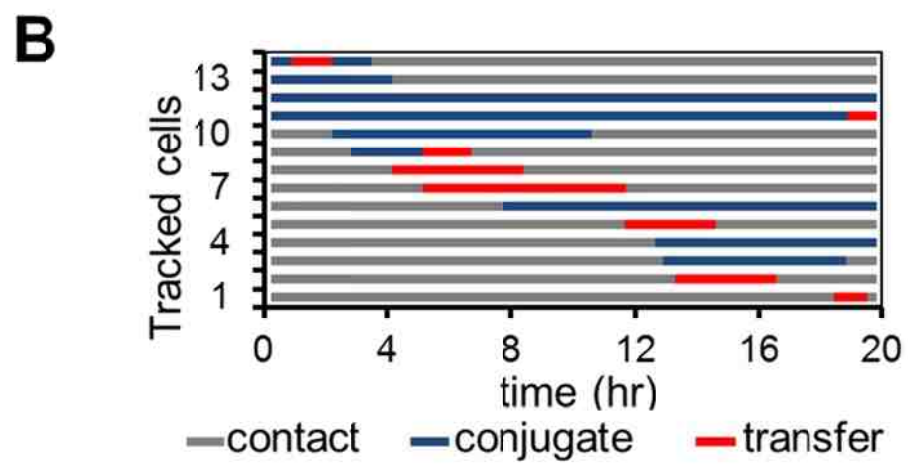
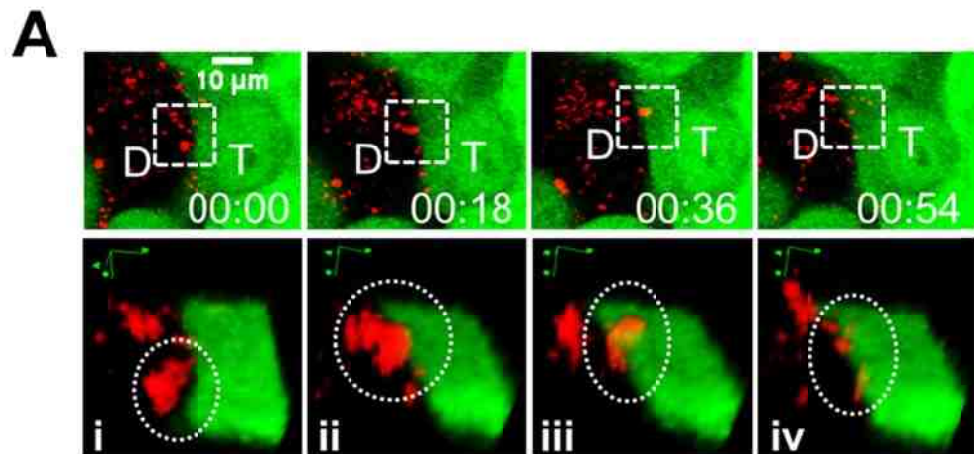


Figure 29. Live cell imaging of CCCM HCV transfer (III) – a four-step process. The same co-culturing experiment as in Fig. 27 and 28 was performed. **(A)** Transfer of a viral punctum (circled in the lower panel) into a target cell: **(i)** donor cell-target cell in contact before conjugate formation, **(ii)** formation of viral punctum-target cell conjugation, **(iii)** transfer of the viral punctum, and **(iv)** post-transfer. The lower panel is a 3D reconstruction of the boxed area in the corresponding upper panel. **(B)** Tracking of transfer events in 13 donor cells in one imaging field; each line represents one donor-target pair.

were formed within the donor cell and transitioned to the contact site between the donor and the target cells (**Fig. 29A i**). This was followed by the formation of viral punctum-target cell conjugate (**Fig. 29A ii**). The transfer took place when the viral punctum was localized in the target cell (**Fig. 29A iii**). The viral punctum likely dissipated into a few smaller puncta in the target cell (**Fig. 29A iv**), and presumably disappeared as viral uncoating took place. A single transfer event was estimated to take approximately 18 min to complete. To further understand the transfer process, we analyzed the transfer events in the entire tracked field (450 μm x 450 μm). There were a total of 33 ReAsH positive donor cells and 160 Huh7.5.1-GFP target cells in the field at the beginning of tracking ($t = 0$). During the 18 hr of tracking, 13 cells (13/33 = 39%) formed conjugates with target cells, 7 donor cells showed transfer (7/33 = 21%) and a total of 8 transfer events occurred (**Fig. 29B**). Each of these processes was confirmed with 3-dimensional reconstruction, as shown in **Fig. 27 B & C**. The average time duration of viral puncta-target cell conjugation between a donor cell and a target cell was calculated to be 408 min; and the average time for the actual transfer was calculated to be 171 min. The latter was much longer than the 18 min time for a single transfer event as estimated above; this is because there were more than one viral puncta transferred between one donor cell and one target cell. Taken together, these results provide the temporal and spatial details of CCCM HCV transfer and demonstrate the high efficiency of this transmission route.

1.8 CCCM transfer and productive HCV infection

1.8.1 Strategy I: Extended co-culture assay with neutralizing antibodies

To determine whether CCCM HCV transfer leads to productive HCV infection, we took advantage of a neutralizing HCV antibody CBH-5 that has been shown to be very

effective in blocking free HCV infection (235, 236). We first confirmed that CBH-5 neutralized free HCV infectivity in the supernatant from co-culture assay by over 99% at a concentration of 5 µg/ml while CCCM HCV transfer were not affected by it (**Fig. 30**). We then performed the above-mentioned co-culture HCV transfer assay in the presence of 5 µg/ml CBH-5 or a control isotope-matched R04 antibody (235, 236) and determined the percentage of HCV core-positive target cells at 24, 48 and 72 hr of co-culturing. The percentage of HCV core-positive target cells increased over time (**Fig. 31A & B**). Compared to the control R04, CBH-5 showed a slightly lower but still significant percentage of HCV core-positive cells and significant increases in the percentage of HCV core-positive cells over time. In addition, the mean fluorescence intensity of the core-positive cells exhibited increases over time in both R4 and CBH-5 treated co-cultures (**Fig. 31C**). Increases in the percentage and the mean fluorescence intensity of HCV core-positive target cells over an extended period of time in the presence of the neutralizing HCV antibody CBH-5 suggest that CCCM HCV transfer leads to productive HCV infection and replication. Culture supernatants were collected from co-cultures that were treated with each of the antibodies and tested for their infectivity. Very few HCV core-positive cells were detected with CBH-5-treated culture supernatants at each time point (**Fig. 31D**), confirming the HCV neutralizing capacity of the CBH-5 antibody.

1.8.2 Strategy II: FACS sorting of newly CCCM transferred target cells and continued culturing

To ascertain the productive nature of CCCM HCV transfer, we set up CCCM HCV transfer using stable GFP-expressing Huh7.5.1 as the target cells in the co-culture experiments. Following the initial 20 hr co-culturing in the presence of 5 µg/ml CBH-5 antibody, we used FACS to sort out the GFP-positive target cells and then monitored

□ CCCM transfer △ free virus infectivity

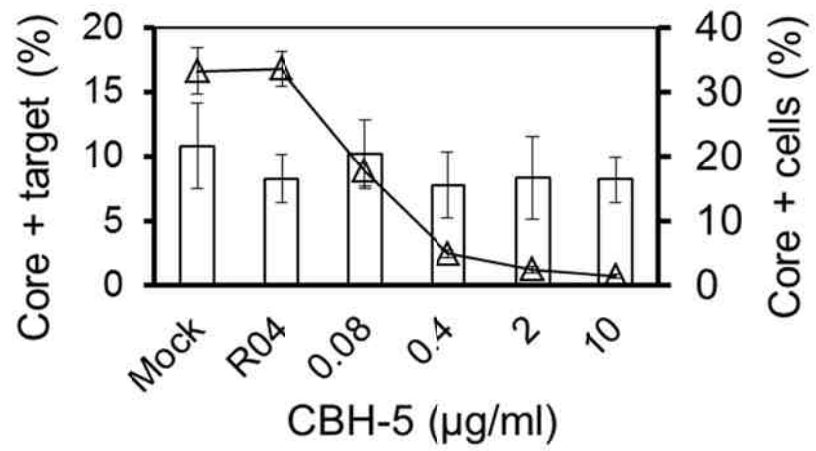


Figure 30. Neutralization of cell-free HCV infectivity with CBH-5 in the co-culture assay. Huh7.5.1 cells were infected with JFH1 virus at MOI = 1 and cultured for 3 days. Co-culture of the infected Huh7.5.1 donor cells and Huh7.5.1-GFP target cells were performed at 1:1 D: T ratio for 20 hr with the presence of culture media (Mock), 10 µg/ml R04 (isotype control antibody) or different concentrations of nAb CBH-5. Both the cells and supernatants were collected at the end of the co-culture. The cells were immunostained for HCV core and analyzed by flow cytometry for core-positive target cells (the amount of CCCM transfer, left Y axis, bar graph). The supernatants containing both nAbs and cell-free HCV viruses released from the infected cells during the co-culture were tested for cell-free virus infectivity by inoculating naïve Huh7.5.1 cells for three days and then core immunostaining followed by flow cytometry for core-positive cells (right Y axis, solid line).

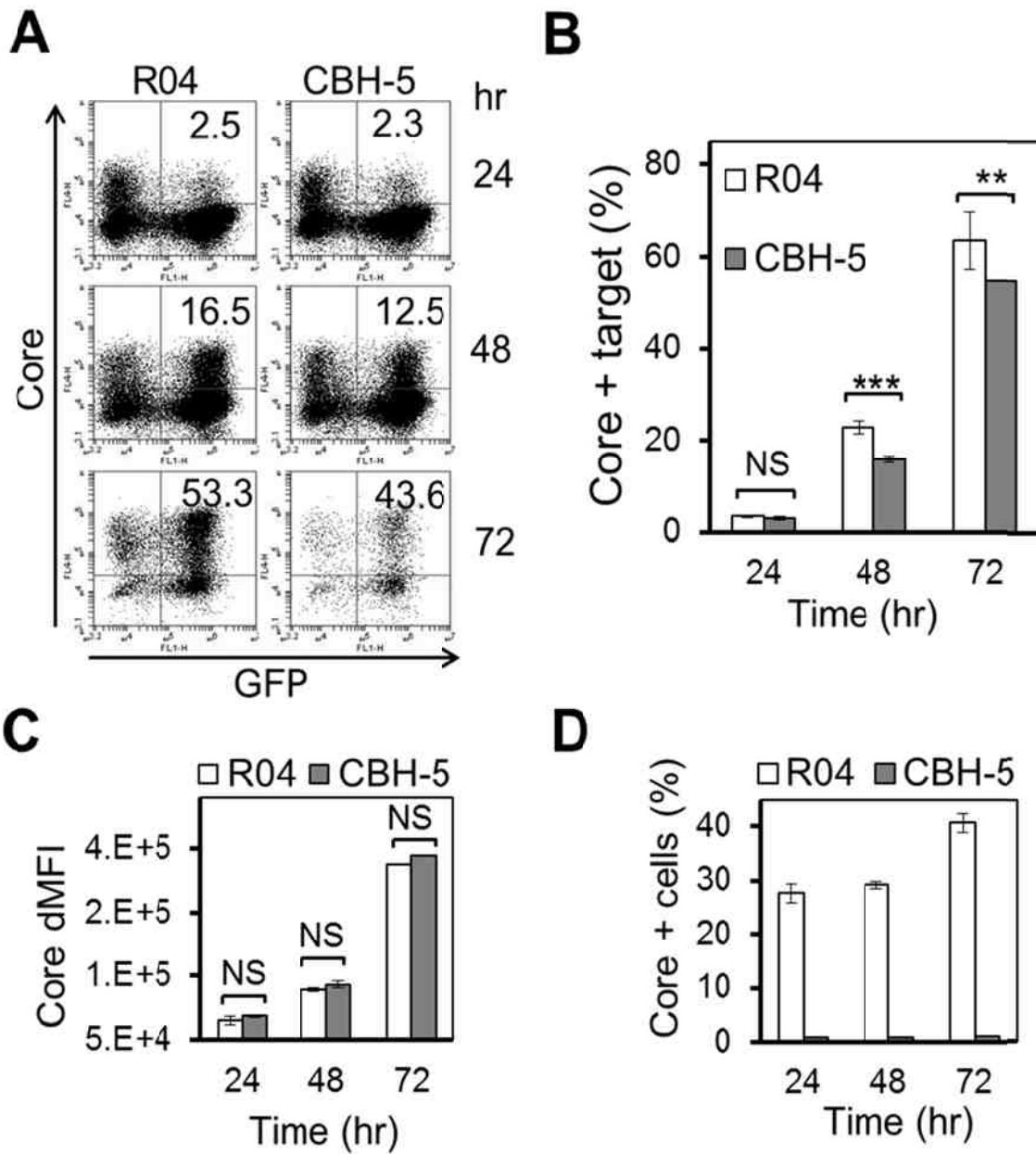


Figure 31. CCCM HCV transfer leads to productive HCV infection (strategy I). Infected Huh7.5.1 cells were co-cultured with GFP-expressing Huh7.5.1 cells at 1: 4 ratio in the presence of 5 µg/ml neutralizing antibody CBH-5 or a control antibody R04. The co-culture was replated every 24 hr and fresh antibodies were added. Meanwhile, aliquot of cells were collected for core staining followed by flow cytometry analysis for GFP+ and core-positive cells (**A-C**); the supernatants were collected and assayed for their infectivity by inoculating uninfected Huh7.5.1 and core immunostaining after three days for percentage of infected cells by flow cytometry. (**D**). (**A**) Representative kinetics of GFP+ and core+ cells; (**B**) data from multiple repeats; (**C**) the difference in mean fluorescence intensity (dMFI) of core staining in GFP+ cells from multiple repeats.

HCV replication in these sorted cells. The FACS yielded more than 97% GFP-positive cells, of which about 2% were HCV core-positive cells (**Fig. 32 A & B**). Similarly, the percentage of HCV core-positive and GFP-positive cells showed increases over an extended period of time up to 7 days. In parallel, there was a significant increase of HCV RNA in these cells between day 4 and day 7 (**Fig. 32C**) and the infectivity of the culture supernatants between day 4 and day 7 (**Fig. 32D**). These results confirmed HCV RNA replication in, and infectious virus production from the target cells following CCCM HCV transfer.

1.8.3 Strategy III: Selective elimination of donor cells and continued culturing of target cells

To further validate the productive HCV infection after CCCM transfer, we performed one day co-culturing of the infected Huh7.5.1 donor and the G418-resistant Huh7.5.1-GFP target cells followed by a six-day G418 killing of donor cells (total 7 days) to obtain pure target cell culture. Five microgram per milliliter CBH-5 was present throughout the co-culturing and the G418 killing to ensure that only CCCM, but not cell-free HCV infection took place. Complete killing of donor cells was confirmed by monitoring the percentage of GFP-positive cells in the culture (**Fig. 33A**), which reached 95% at D7, the same as that in Huh7.5.1-GFP cells (the “GFP only” bar). Similarly to the previous two strategies, continued culturing of the G418-selected target cells showed an increase of the percentage of HCV infected cells from D7 to D9 (**Fig. 33 B & C**). The percentage of infected target cells was still very high at D11 but slightly decreased compared to that at D9, likely due to high level of infection and ensuing cytopathic effects observed after D9. In parallel, large amounts of HCV virus production in the culture supernatants from D8 to D11 was confirmed (**Fig. 33D**). Taken together, results from all of the three strategies support the notion that CCCM HCV transfer leads to productive infection and replication.

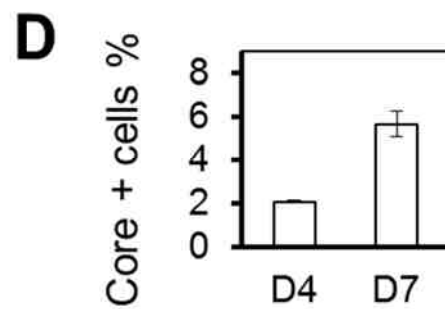
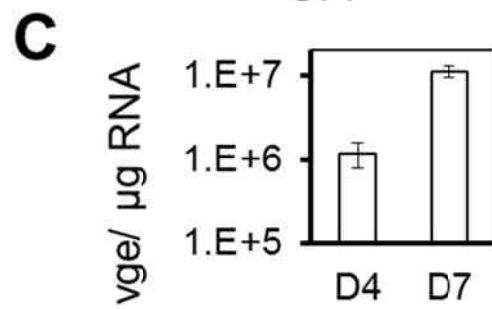
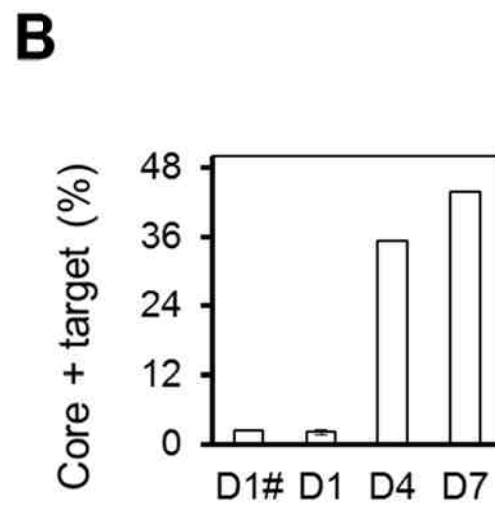
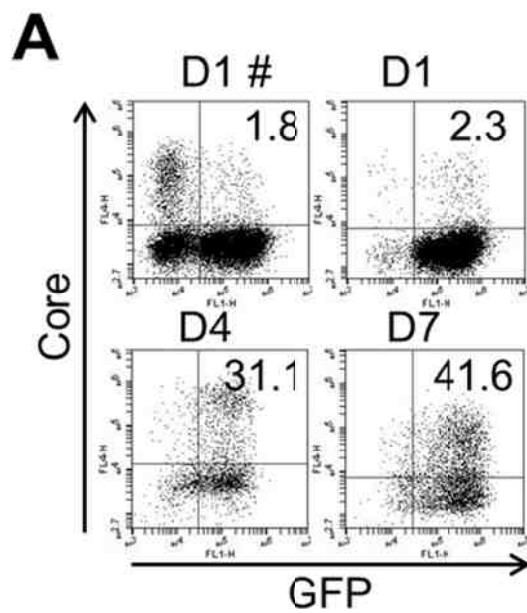


Figure 32. CCCM HCV transfer leads to productive HCV infection (strategy II).

Infected Huh7.5.1 cells were co-cultured with GFP-expressing Huh7.5.1 cells at 1: 4 ratio in the presence of 5 µg/ml neutralizing antibody CBH-5. GFP+ target cells were sorted out from day one (D1) of co-culturing and further cultivated for an extended period of time. Core+ cells in the purified GFP+ cell population were determined at day 4 (D4) and 7 (D7) by core immunostaining. **(A)** Representative kinetics of GFP+ and core+ cells; **(B)** data from multiple repeats. D1#: co-cultured cells prior to sorting. Cells and their culture supernatants were also collected at D4 and D7 and assayed for HCV RNA in the cell by qRT-PCR **(C)** or infectivity in the supernatant **(D)** as described in Fig. 29D, respectively.

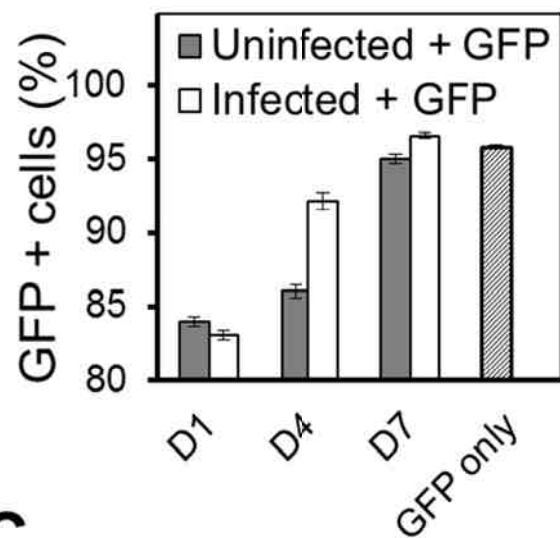
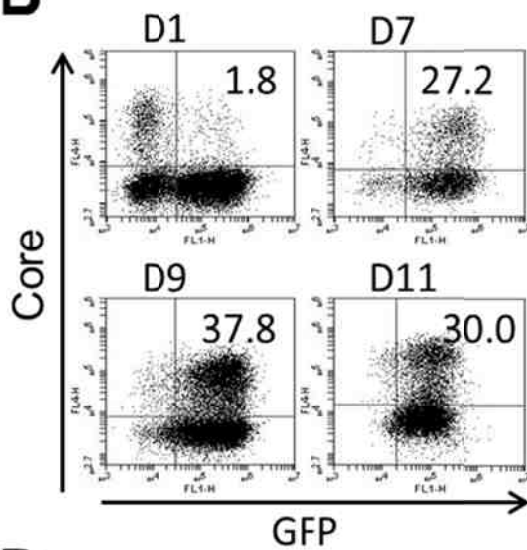
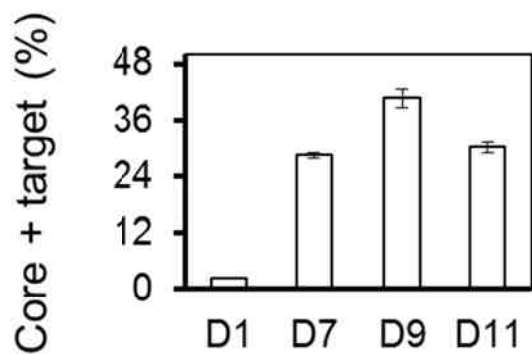
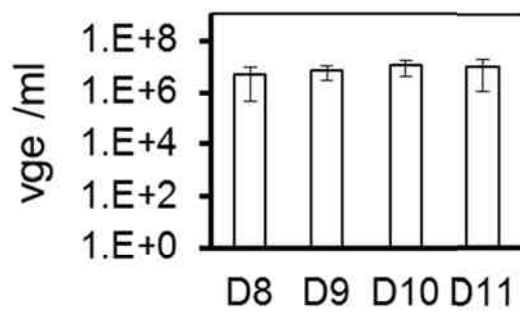
A**B****C****D**

Figure 33. CCCM HCV transfer leads to productive HCV infection (strategy III).

Co-culturing of infected Huh7.5.1 donor cells with G418-resistant Huh7.5.1-GFP target cells was performed at 1: 4 donor: target ratio for one day with the presence of 5 µg/ml of the neutralizing antibody CBH-5. The co-culture was then treated with 750 µg/ml G418 and 5 µg/ml CBH-5 for six days to selectively kill the donor cells and obtain pure culture of target cells. **(A)** G418 killing efficiency in the co-culture was monitored by percentage of GFP + cells with flow cytometry (white bar) and killing of a control mixed-culture consisting of uninfected cells and Huh7.5.1-GFP cells was also monitored (grey bar). **(B-D)** D7 culture consisting of pure target cells were further cultivated under 200 µg/ml G418 for four days. Cells were collected every other day and immunostained against core for percentage of newly infected target cells (representative dot plot in **B** and triplicated results in **C**, D1 co-culture before killing was also included). Supernatants were collected every day and HCV RNA was measured by qRT-PCR (**D**). Numbers in **B** represent the percentage of cells in the upper right quadrat (newly infected target) out of total cells.

CHAPTER 2: Exosome-Associated Hepatitis C Virus and Its Infectivity

2.1 HCV infection did not alter exosome secretion in hepatocytes

To understand the relationships between HCV and exosomes, we first determined whether HCV infection affected exosome secretion. Huh7.5.1 cells were infected with HCV JFH1 exosome secretion in the culture supernatants was monitored. HCV infection was confirmed by immunoblotting for HCV core expression in the cells (**Fig. 34A**). Exosome secretion was determined by measuring the activity of acetylcholinesterase (AChE), an exosome marker (106, 218). There was no difference of exosome secretion between HCV-infected cells and Mock-infected control cells within 60 hours post HCV infection (**Fig. 34B**). We next determined whether HCV infection affected the size distribution of exosomes using iodixanol (Optiprep) density gradient ultracentrifugation. Concentrated exosomes were prepared from the culture supernatants of Mock- or HCV-infected Huh7.5.1 cells and then fractionated through a 6-18% iodixanol density gradient by ultracentrifugation (218). The AChE activity assay of each fraction showed similar distribution patterns of exosomes from Mock- and HCV-infected cells, which peaks at fractions 2-4 (**Fig. 35**). Taken together, these results indicate that HCV infection does not result in significant changes in exosome secretion from hepatocytes.

2.2 Association of HCV with exosomes

2.2.1 Optimization of iodixanol concentration for fractionation of HCV

Considering the heterogeneous nature of the exosomes, the findings that HCV infection does not affect the overall exosome size distribution does not necessarily rule out the possibility that HCV is associated with exosomes. To address this possibility, we

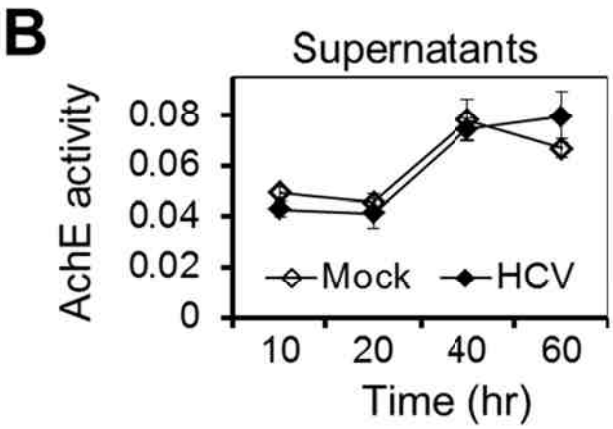
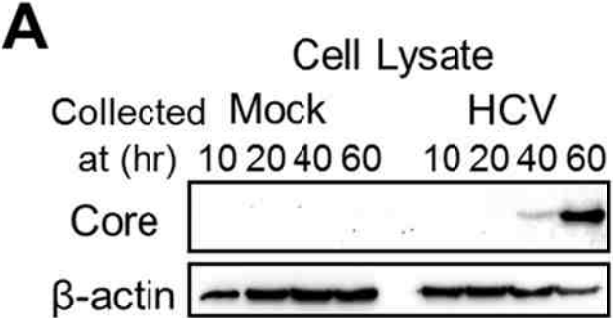


Figure 34. HCV infection does not affect exosome production. Huh7.5.1 cells were infected with HCV for 2 hr, removed of unbound viruses, extensively washed with PBS, and then added with complete culture medium. Conditioned medium (Mock) was used as a control. The complete culture medium was changed to bovine exosome-depleted medium at 2, 10, 20 and 40 hr post- infection and cells and supernatants were collected at 10, 20, 40 and 60 hr post- infection, respectively. The cells were lysed and immunoblotted for HCV core and β -actin (the loading control) (**A**). The supernatants were analyzed by AchE assay (**B**) for exosome production. AchE activities in culture supernatants (**B**) were normalized to the total cellular protein in panel **A**.

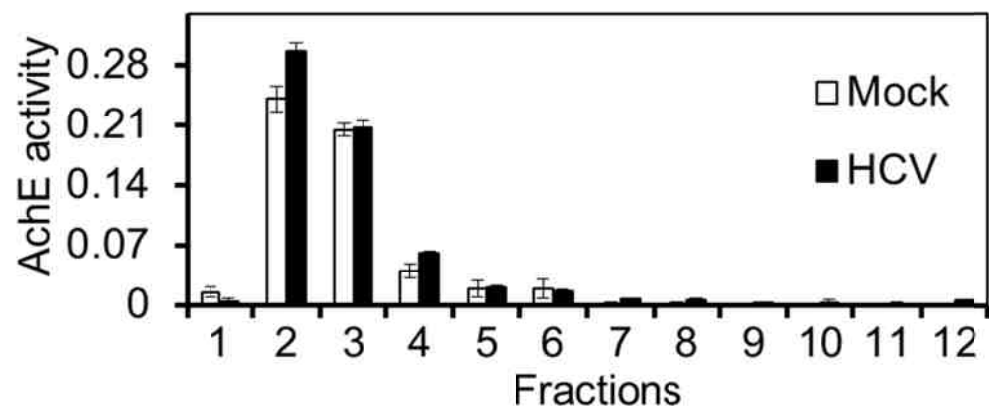


Figure 35. HCV infection does not affect exosome size distribution. Huh7.5.1 cells were infected with HCV or conditioned medium (Mock) for 72 hr and the culture medium was changed to bovine exosome-depleted medium and kept for another 24 hr. The culture supernatants were then collected, removed of cell debris by centrifugation at 3000 x *g* for 10 min, passed through a 0.22 μm filter, and concentrated by ultracentrifugation at 250,000 x *g* and 4°C for 90 min. The pellet was suspended in 500 μl PBS, loaded onto a 5 ml 6-18% iodixanol gradient and fractionated by ultracentrifugation at 250,000 x *g* and 4°C for 90 min in a SW55Ti rotor. Twelve 450 μl fractions were collected from top to bottom of the gradient; 15 μl of each fraction was used for AchE assay.

performed the similar ultracentrifugal fractionation as above but detected both exosome and HCV. However, the gradient centrifugation conditions above were originally designed for exosome detection only. Therefore, we first optimized the concentration of the iodixanol gradient to accommodate the density range of HCV in addition to that of exosome. Culture supernatants from HCV-infected Huh7.5.1 cells were concentrated and fractionated as above through a 6-18% iodixanol gradient and Western blotting against HCV core showed only the first half of a complete peak (**Fig. 36** upper panel). We then increased the concentration of iodixanol gradient to 6-20% and still found an incomplete peak of HCV core (**Fig. 36** middle panel). Lastly we found the iodixanol concentration of 6-24% able to accommodate HCV virions of all different sizes/densities (**Fig. 36** lower panel); a 6-24% iodixanol gradient was used for further experiments.

2.2.2 Detection of HCVcc/patient plasma-derived HCV in exosome-containing fractions

With the optimized protocol, we performed the fractionation of Huh7.5.1-derived exosomes and HCV, determined AchE activity in each fraction, isolated RNA from each fraction and determined HCV RNA level in each fraction using qRT-PCR. Similarly, the AchE activity assay showed exosomes in fraction 2-4 (open bars, **Fig. 37A**). In comparison, qRT-PCR analysis exhibited two peaks of HCV RNA (line graph, **Fig. 37A**): a major peak at fraction 7-10 and a minor one at fraction 2-4 that coincided with the exosome fractions. The exosome fractions were further confirmed by Western blotting using antibodies against two other exosome markers Hsp70 and CD63 (upper two panels, **Fig. 37B**). Consistent with the qRT-PCR results of HCV RNA, Western blotting using antibodies against HCV proteins E2 and core showed two peaks: one in fraction 2-4 and another in fraction 7-10 (lower panels, **Fig. 37B**). The size difference of E2 in exosome-associated HCV (fraction 2-4) and exosome-free HCV (fraction 7-10) could be

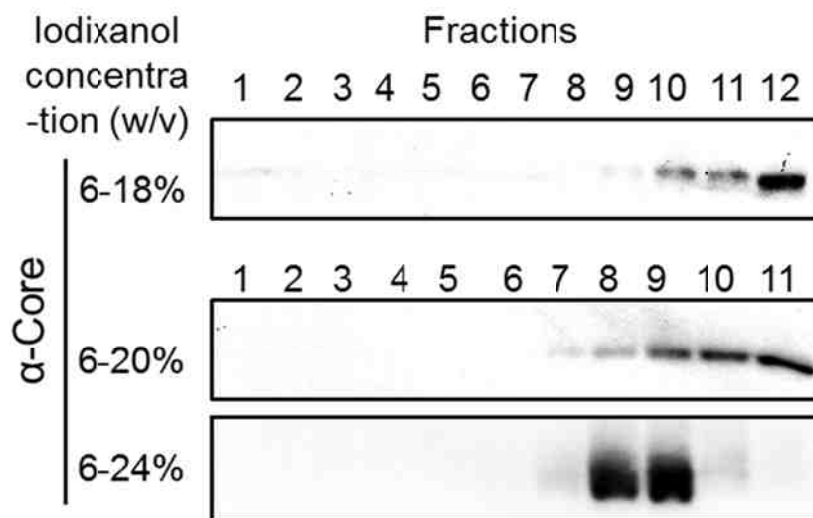


Figure 36. Optimization of iodixanol concentration for HCV fractionation. Huh7.5.1 cells were infected with HCV; the culture supernatants were collected, purified and concentrated as described in Fig. 35. The resulting pellet was suspended in 500 μ l PBS and fractionated on 5 ml 6-18% (the upper panel), 6-20% (the middle panel), or 6-24% (the lower panel) iodixanol gradient with the SW55Ti rotor. Twelve 450 μ l fractions (the upper panel) or eleven 500 μ l fractions (middle and lower panels) were collected from top to bottom of the gradient and each fraction was immunoblotted for HCV core.

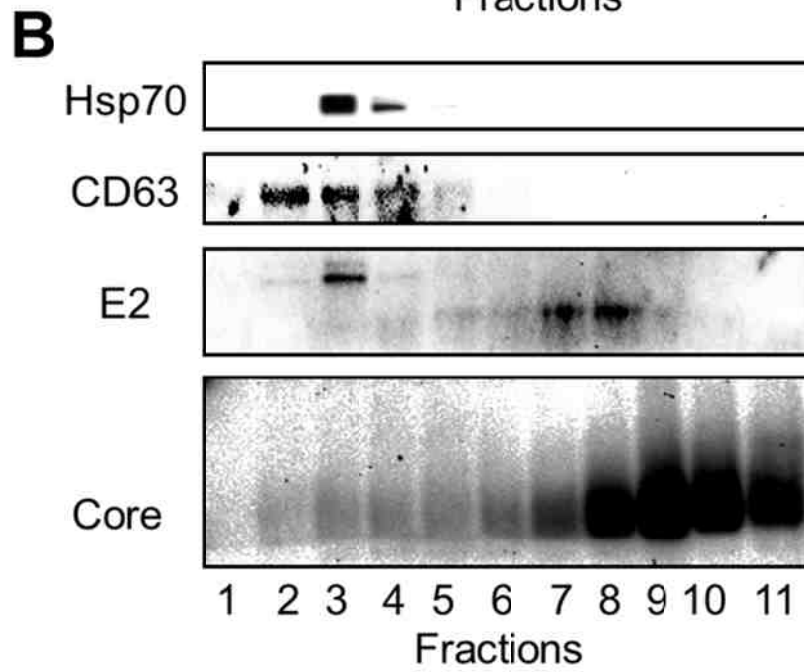
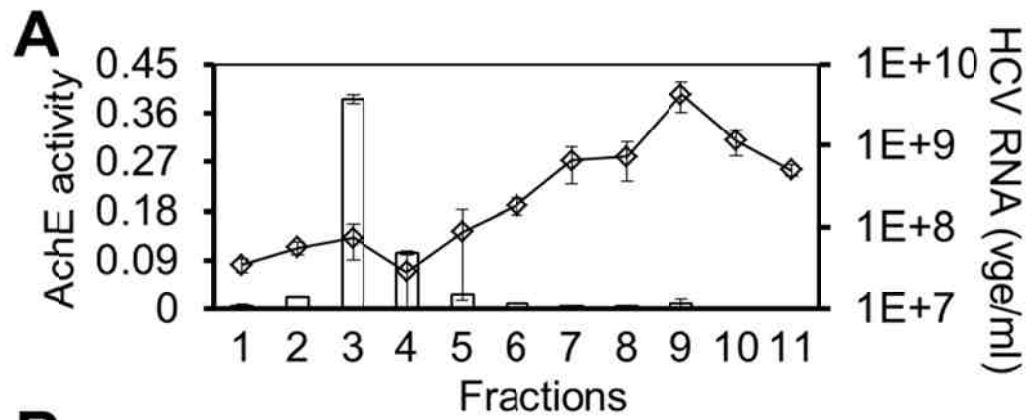


Figure 37. Detection of HCV in exosome-containing fractions. Huh7.5.1 cells were infected with HCV; the culture supernatants were produced and processed as described in Fig. 35 except that a 6-24% iodixanol gradient was used instead of 6-18% iodixanol and that the ultracentrifugation fractionation was performed for 2 hr instead of 90 min. Besides the AchE activity (**A**, open bar), RNA was extracted from each fraction and used for qRT-PCR for HCV RNA (**A**, line, vge: viral genome equivalent). Meanwhile, the fractions were subjected to Western blotting using anti-Hsp70, CD63, HCV E2, or core antibody (**B**). Please note that there were a total of 11 fractions collected with each 500 μ l, while there were 12 fraction collected with each 450 μ l in Fig. 35. The data were representative of multiple independent experiments.

due to several reasons (see Discussion below for details); the reason for two HCV peaks and only one HCV core peak in Fig. 36 is that the total volume of culture supernatant was increased from 30 ml to 120 ml. To confirm the co-fractionation of HCV and exosomes is not related to the method used for concentration or the rotor used for fractionation, we performed similar experiments but with PEG 8000 exosome/HCV precipitation (**Fig. 38**) or using the vertical rotor NVT65 for gradient ultracentrifuge (**Fig. 39**) and obtained similar results. Exosome-associated HCV was also detected in HCV-positive patient plasma (**Fig. 40**). It is interesting to point out that 3-20 fold more HCV RNA was detected in exosome-associated viruses than exosome-free viruses (**Fig. 40C**), suggesting that more HCV virions occur in the exosome-associated forms in patient plasma. Taken together, these results demonstrated that both HCV RNA and viral structural proteins core and E2 were detected in exosome fractions of cell culture produced HCV and suggest the presence of a subpopulation of exosome-associated HCV.

2.3 Exosome-associated HCV was infectious

To determine whether exosome-associated HCV was infectious, we performed the focus formation assay using each fraction obtained from gradient ultracentrifugation. Infection of Huh7.5.1 cells with both exosome-associated HCV fractions (fraction 2-4, **Fig. 41**) and exosome-free HCV fractions (fraction 7-10, **Fig. 41**) led to the formation of infection foci. The peak specific infectivity, expressed in foci formation units per viral genome equivalent (FFU/vge), of the former was estimated to be about 10 fold lower than that of the latter. These results showed that exosome-associated HCV was infectious but less effective than exosome-free HCV.

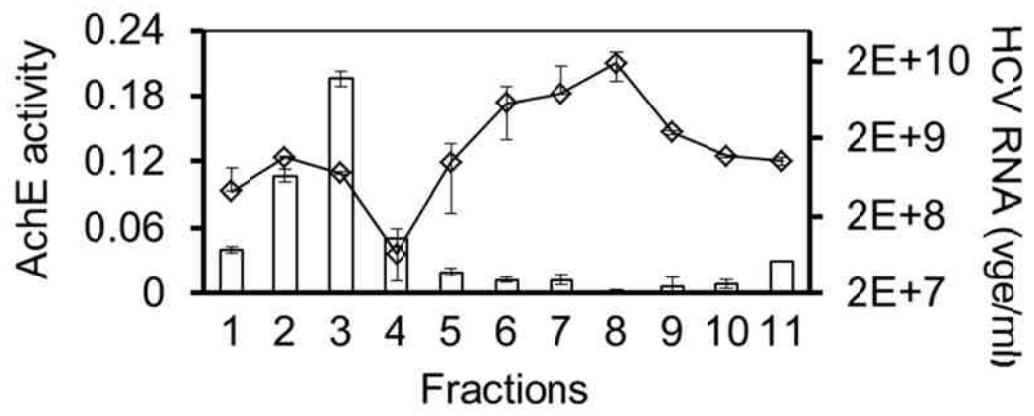


Figure 38. Detection of HCV in exosome-containing fractions with PEG exosome/HCV precipitation. Huh7.5.1-derived HCV and exosomes were produced, purified, concentrated, and fractionated as described in Fig. 37 except that HCV/exosomes were concentrated by PEG precipitation instead of ultracentrifugation, i.e. overnight incubation with 1/4 vol. of PEG 8000 at 4°C followed by centrifugation at 3500 x *g* and 4°C for 30 min. The collected fractions were assayed for AchE activity (open bars) or HCV RNA by qRT-PCR (line graph).

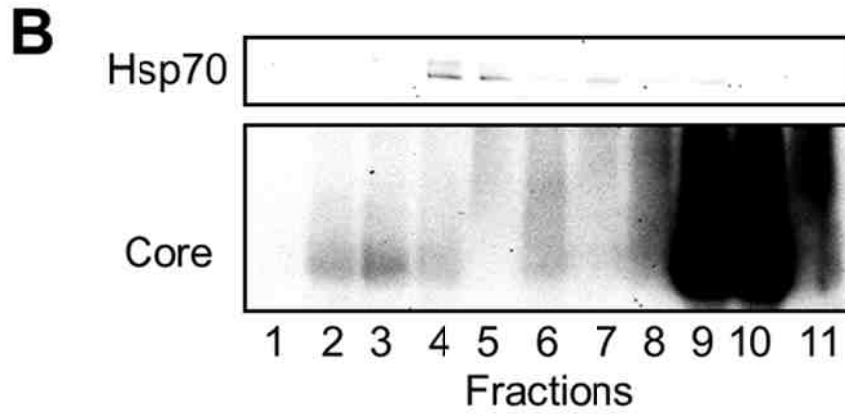
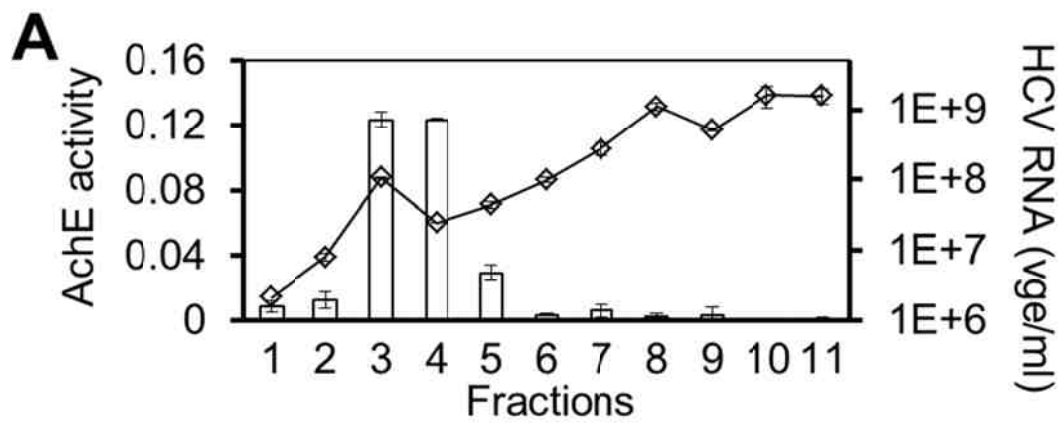


Figure 39. Detection of HCV in exosome-containing fractions using the NVT65 rotor for gradient centrifugation. Huh7.5.1-derived HCV and exosomes were produced, purified and concentrated as described in Fig. 37. The resulting HCV/exosomes pellet was suspended in 1 ml PBS and fractionated on a 10 ml 6-24% iodixanol gradient at 250,000 x *g* and 4°C for 60 min with the NVT65 rotor. Eleven 1 ml fractions were collected from top to the bottom of the gradient; each fraction was assayed for AchE activity (**A**, open bars), HCV RNA by qRT-PCR (**A**, line graph), or exosome marker Hsp70, and HCV core by Western blotting (**B**).

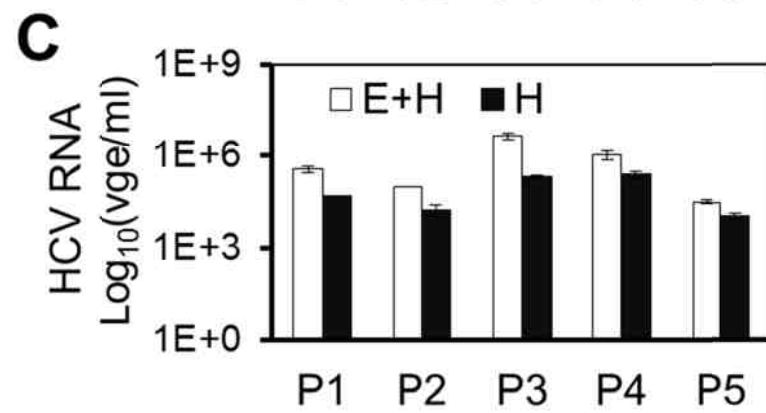
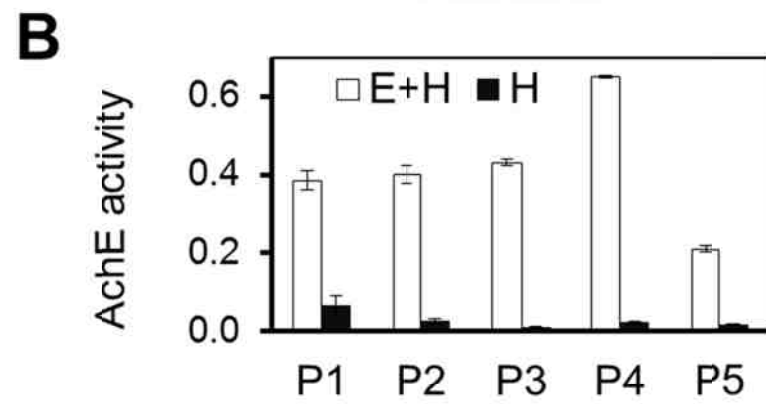
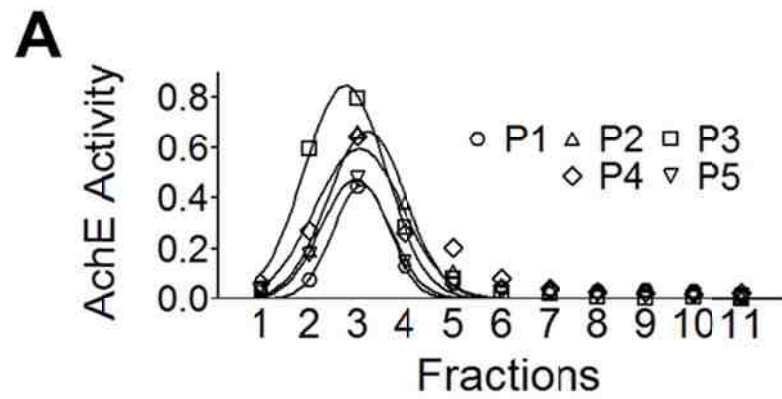


Figure 40. Exosome-associated HCV in HCV-positive patient plasma. Plasma from chronic hepatitis C patients (140 μ l each from five patients P1, P2, P3, P4, and P5) were diluted with PBS to 500 μ l and fractionated on a 6-24% iodixanol gradient as described above. An aliquot of each fraction was used for AchE assay (**A**, data were fit to Gaussian distribution). Then the fractions containing the exosomes (F1-F4) were pooled (exosome-associated HCV – E+H), while the fractions free of exosomes (F7-10) were pooled (exosome-free HCV – H). These pooled samples were used for AchE assay (**B**) or RNA isolation followed by qRT-PCR for HCV RNA (**C**).

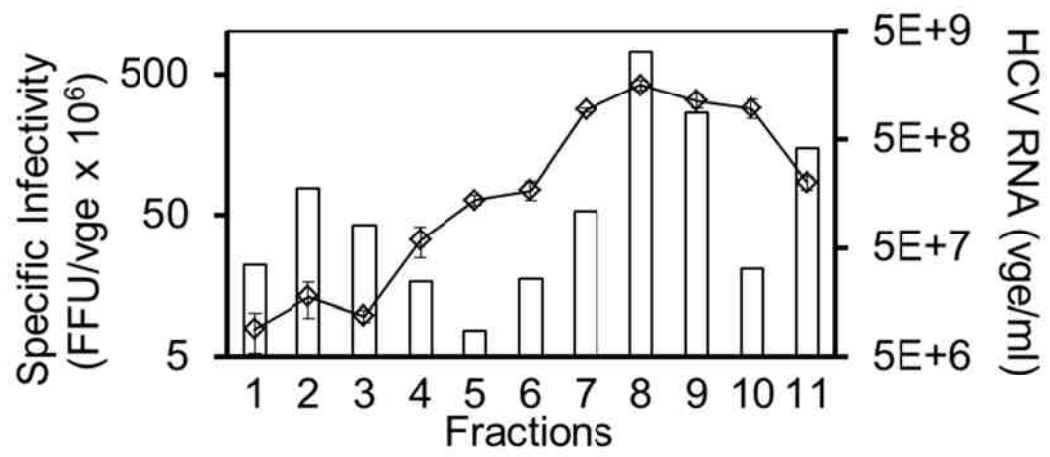


Figure 41. The infectivity of exosome-associated HCV. Huh7.5.1 were infected with HCV, the culture supernatants were produced, processed and fractionated as described above. An aliquot of each fraction was assayed for HCV infectivity by serial dilution followed by foci formation assay (open bars) and qRT-PCR for HCV RNA. The infectivity was expressed as the specific infectivity, i.e., foci-forming units (FFU) per viral genome equivalent (vge).

CHAPTER 3: Hepatitis C Virus (HCV) Interaction with Astrocytes: Non-productive Infection and Induction of IL-18

3.1 Establishment of human fetal brain primary cell cultures

Human fetal brain primary cells cultures have been widely used as a surrogate model system to study interaction of human brain cells with various pathogens and external insults (209, 237-239). Thus, we began by establishing these cultures in the laboratory. Briefly, aborted human fetus cortex of 12-20 weeks old was obtained from Advanced Bioscience Resources Inc (Alameda, CA) and used to prepare single cell suspension. Cells were then cultured in either primary neuron medium or DMEM, which gave rise to neuron only cultures or neuron/astrocyte mixed cultures, respectively. Immunofluorescence staining with neuron marker microtubule-associated protein 2 (MAP-2) and astrocyte marker glial fibrillary acidic protein (GFAP) showed that more than 99% cells in the primary neuron cultures were neurons (**Fig. 42**, the upper panel), and that the mixed cultures had both neurons and astrocytes with about 50% of each cells(**Fig. 42** the middle panel). Continuous passing of the mixed cultures gave rise to more astrocytes, e.g., 95% astrocytes at passage 4 (**Fig. 42** lower panels). Therefore these primary human astrocytes (PHA) between passage 4 and 10 were used throughout this study.

3.2 Few astrocytes are infected by cell-free or CCCM HCV infection

To determine whether astrocytes are susceptible to HCV infection, we infected PHA with newly established cell culture-produced infectious JFH1 (HCVcc) and monitored the level of intracellular HCV RNA over 72 hr. qRT-PCR showed that HCV RNA increased by about 1000 fold in HCV-susceptible Huh7.5.1 cells over 72 hr, while there was little

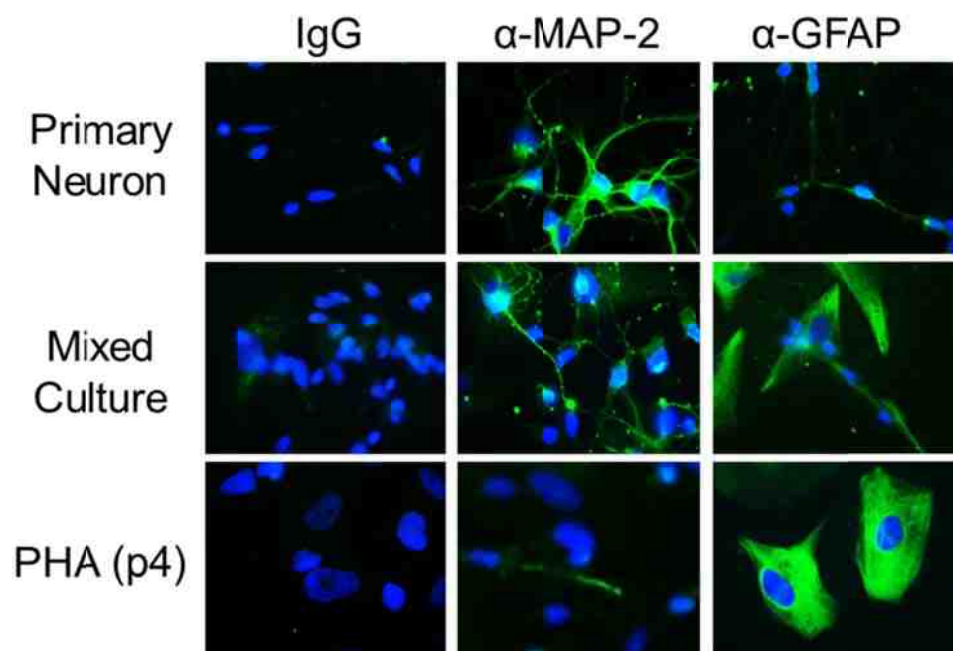


Figure 42. Human fetal brain primary cell cultures. Primary neurons (upper panels), mixed brain cell culture (middle panels), and primary human astrocytes (PHA, p4: passage 4, lower panels) were immunostained with normal IgG control, antibodies against the neuron marker MAP-2 (green), or the astrocyte marker GFAP (green). DAPI counterstaining (blue) was performed for nuclei; all images at 100X.

changes in HCV RNA in PHA (**Fig. 43A**). It is interesting to note that with the same amount of input virus inoculum, there was about 5 fold less HCV RNA detected in PHA than that in Huh7.5.1 at 2 hr post- infection (**Fig. 43A**). Consistent with the qRT-PCR results, immunostaining showed many HCV proteins core+/E2+ Huh7.5.1 cells but fewer HCV core+/HCV E2+ PHA at 72 hr post-infection (**Fig. 43B**). These results suggest that PHA are refractory to HCV infection, probably due to inefficient binding and/or entry into these cells.

Cell-cell contact-mediated HCV transfer has been shown to be an important route of HCV infection and transmission [CHAPTER 1 and (98, 211)]. Thus, we next examined whether cell-cell contact would lead to HCV infection of PHA. HCV-infected infiltrating T cells monocytes/macrophages have been stipulated to be the likely virus carriers into the CNS and the initial sources of HCV for astrocyte infection *in vivo*; these cells should be used in the cell-cell contact experiments. However, great difficulties have been experienced in establishing HCV infection in these cells using both HCVcc and HCV-positive patient sera [our own unpublished data and (181)]. As a proof-of-concept experiment, we used HCVcc-infected Huh7.5.1 that were labeled with the green CMFDA dye as donor cells and unlabeled PHA as target cells and performed cell-cell contact HCV transfer experiment as described in CHAPTER 1. Unlabeled Huh7.5.1 cells were included as the positive control for cell-cell contact-mediated HCV transfer. Immunostaining of HCV core of the mixed cells followed by flow cytometry analysis showed more than 45% core+/CMFDA- Huh7.5.1 cells, representative of both CCCM HCV transfer and cell-free HCV infection but only a background level of core+/CMFDA-PHA at 48 hr post co-culture (**Fig. 44**). These results suggest that PHA are not also susceptible to cell-cell contact-mediated HCV transfer and infection.

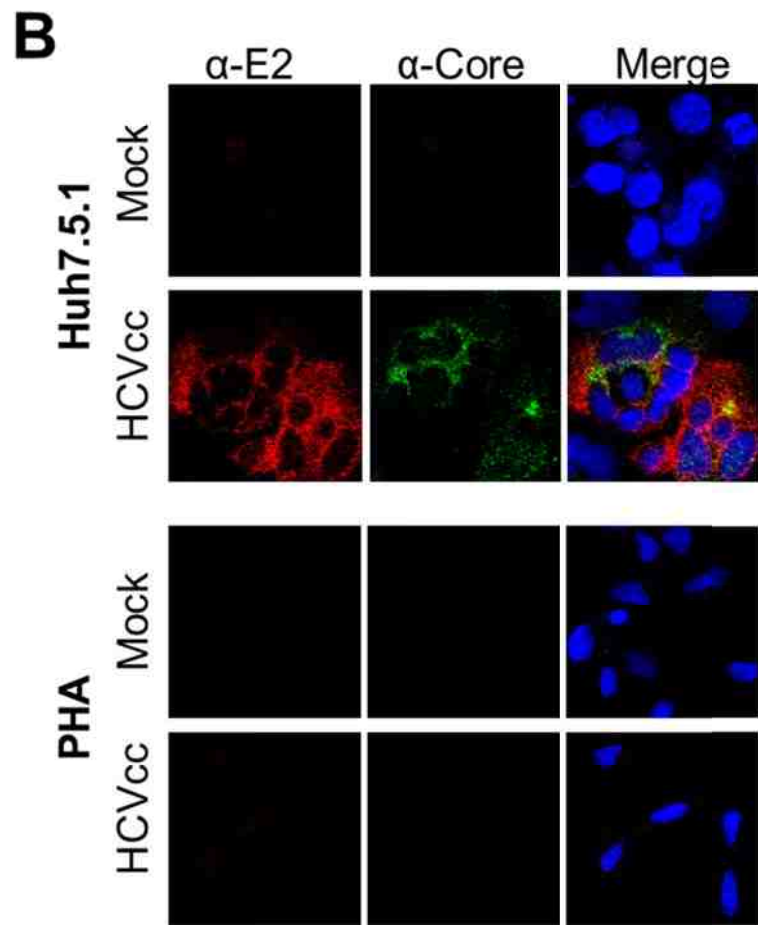
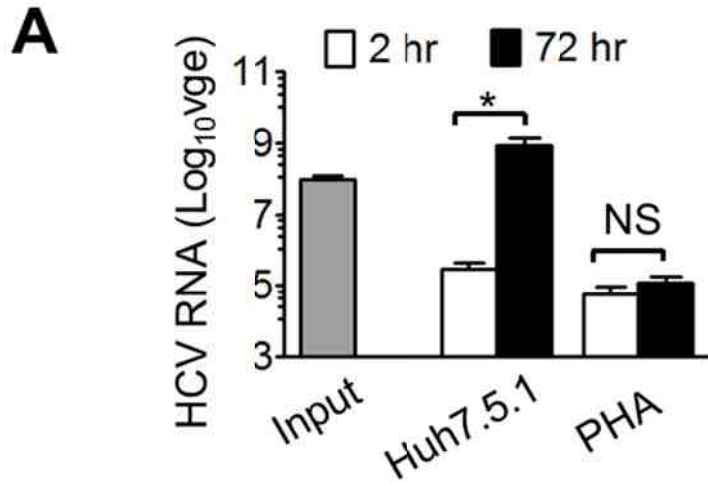


Figure 43. HCVcc does not infect astrocytes by cell-free virus infection. (A) PHA and Huh7.5.1 were infected with HCVcc (Input) for 2 hr, removed of unbound viruses, extensively washed with PBS, and then harvested, or allowed to culture for 72 hr and then harvested for total RNA isolation, followed by qRT-PCR for the HCV RNA level. vge: viral genome equivalents. (B) PHA and Huh7.5.1 were infected with HCVcc (HCVcc) as in panel A. Conditioned medium (Mock) was used as a control. Cells were fixed 72 hr post-infection and immunostained against HCV core (green) and E2 (red). DAPI counterstaining (blue) was performed for nuclei. Micrographs were taken at 100X.

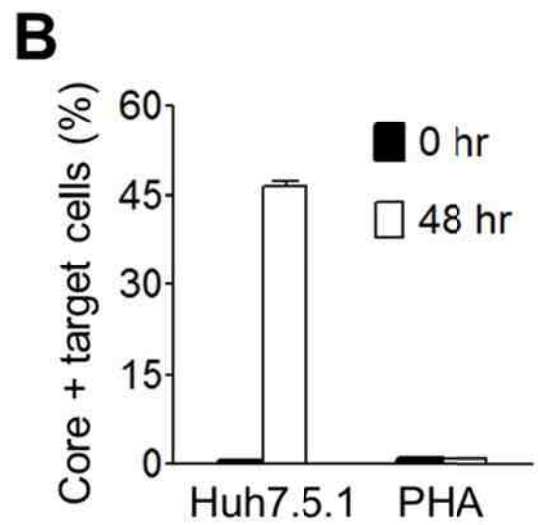
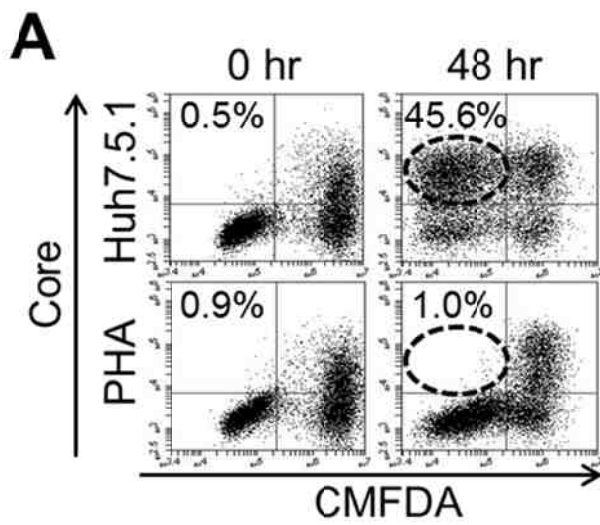


Figure 44. Cell-cell contact does not lead to HCV infection of astrocytes. HCV-infected Huh7.5.1 cells were labeled with 1.25 μ M CMFDA and then used as donor cells to incubate with target cells – uninfected Huh7.5.1 or PHA – at a 1:1 ratio for 48 hr. The mixed cells were then immunostained for HCV core and analyzed for the percentage of newly infected target cells in the mixed population, i.e., Core+CMFDA- cells (upper left quadrant) by flow cytometry. **A.** A representative dot plot; **B.** Aggregate data from three independent experiments.

3.3 HCV receptors expression on primary astrocytes

To assess the specific step(s) in HCV life cycle at which HCV infection of PHA is restricted, we began with HCV binding to cellular receptors (15). We determined the expression of all four known HCV receptors in PHA: CD81(25), scavenger receptor class B type I (SR-B1) (27), claudin-1 (CLDN1) (28) and occluding (OCLN) (29). Different detection methods were used based on the availability of specific antibodies. Surface labeling with α -CD81 antibody showed that CD81 was expressed on the surface of 50% PHA and at a very high level (**Fig. 45A & B**). Immunoblotting showed that SR-B1, CLDN1 and OCLN were all expressed in PHA but at a much lower level compared to Huh7.5.1 (**Fig. 45C**). Immunostaining followed by microscopic imaging showed that expression of SR-B1, CLDN1 and OCLN in PHA exhibited a diffused pattern in the cytoplasm, whereas expression of these receptors in Huh7.5.1 exhibited different subcellular localizations: mostly cytoplasmic for SR-B1, both cytoplasmic and on the plasma membrane for CLDN1, and mostly on the plasma membrane for OCLN (**Fig. 45D, 14C, 15C**).

3.4 Insignificant HCV entry into astrocytes

3.4.1 HCVpp infection and spinoculation of brain cells

To directly assess whether PHA are susceptible to HCV entry, we utilized the single-round pseudotyped HCVpp strategy (refer to the Introduction section, **Fig. 3A**, for details). Briefly, HCVpp is composed of an envelope (replication)-defective, reporter gene (Luc or GFP)-expressing HIV core and a functional HCV envelope; it allows single-round infection, so HCV glycoproteins-mediated cell entry can be accurately determined

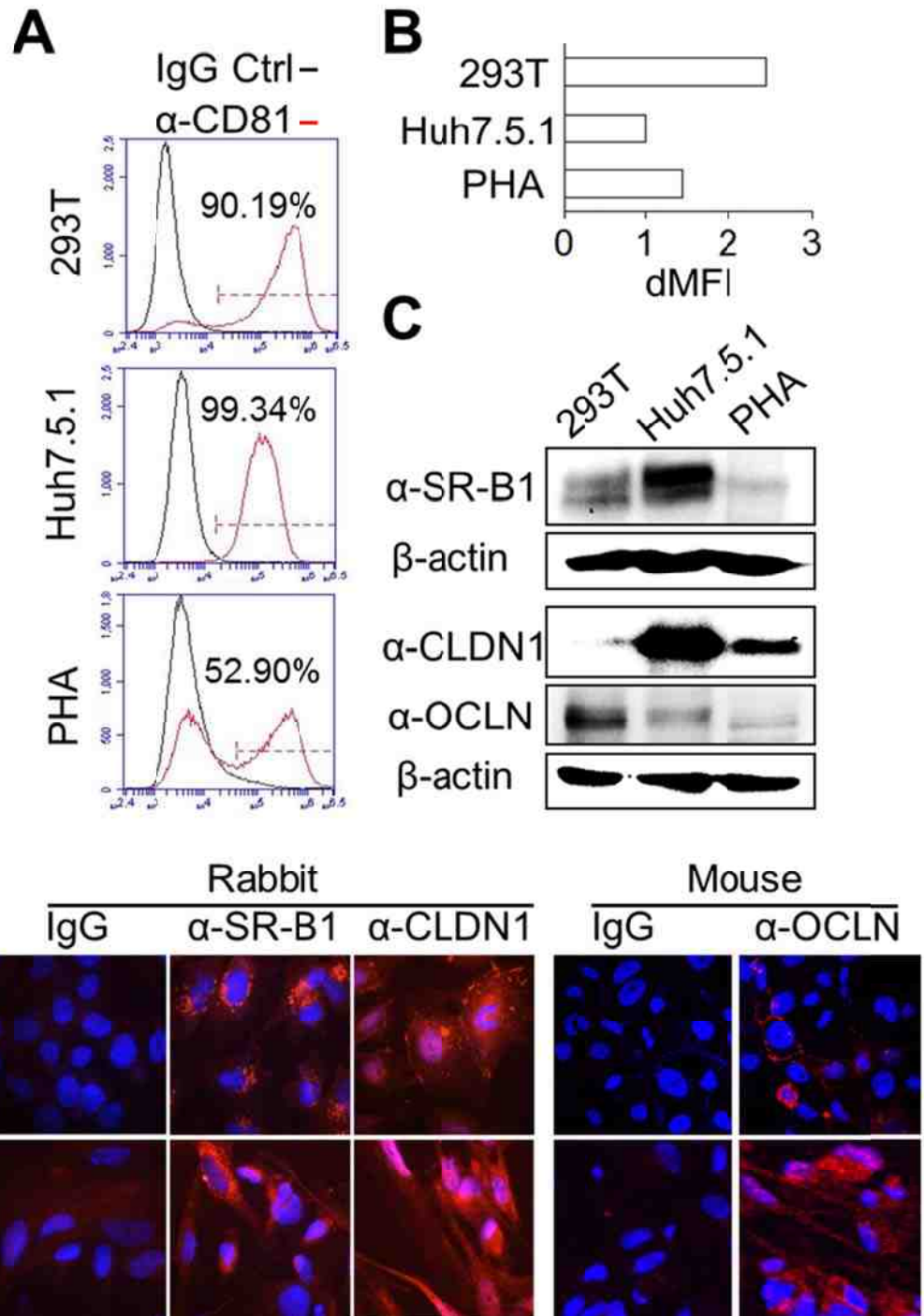


Figure 45. Expression of HCV receptors on astrocytes. CD81 expression in PHA was determined by cell surface labeling with α -CD81 antibody followed by flow cytometry analysis for the percentage of CD81-positive cells (red line, **A**) and the mean fluorescence intensity of CD81 staining (dMFI, **B**). An isotype-matched IgG was included as a control (black line, **A**). SR-B1, CLDN1, and OCLN expression were determined by Western blotting (**C**) and immunofluorescence staining followed by microscopic imaging (**D**). Huh7.5.1 and 293T cells were included as controls (**A-D**). β -actin loading control was included for Western blotting (**C**) and an isotype-matched staining control was included for flow cytometry (**A & B**) and immunofluorescence staining (**D**). Images were taken at 100X; DAPI staining was performed for nuclei (blue, **D**).

using the luciferase or GFP reporter gene assay. Env^{pp} containing no envelope protein and VSV^{pp} containing VSV-G envelope were included as the negative and positive control, respectively. HIV-Luc was first used to determine HCV entry into PHA. Compared to Env^{pp}, HCV^{pp} infection led to significantly higher luciferase activity in Huh7.5.1 cells, but little changes in PHA (**Fig. 46A**). It is interesting to note that unlike Huh7.5.1 cells, the luciferase activity in both Env^{pp}- and HCV^{pp}-infected PHA were 5 fold higher than Mock-infected PHA. This is likely a result of, envelope-independent uptake, e.g., nonspecific endocytosis of viral particles by PHA. To determine whether enhanced binding would lead to increase in the viral entry, we performed the infection using spinoculation, a well-established strategy to enhance the binding of virus particles to cellular receptors and thereby more viral entry (240). Similar patterns of data on viral entry were obtained except that a generally higher level of the luciferase reporter gene activity was detected in Env^{pp}- and HCV^{pp}-infected Huh7.5.1 and PHA (**Fig. 46B**). Human astrocytoma U373, human neuroblastoma SH-SY5Y, and the primary human fetal brain culture were also included in the spinoculation experiments, but none of these cells showed significant HCV^{pp} entry (**Fig. 46B**).

In addition, we also used the HIV-GFP reporter virus system to infect Huh7.5.1 and PHA and determined HCV entry by fluorescence microscopic imaging or flow cytometry for GFP expression. GFP expression was detected in both HCV^{pp} and VSV^{pp}-infected Huh7.5.1 cells (**Fig. 47A**). In contrast, GFP expression was only detected in VSV^{pp}-infected PHA through normal inoculation as well as through spinoculation (**Fig. 47B**). Use of flow cytometry for GFP expression in PHA was due to strong autofluorescence associated with PHA, which made it difficult to discern weak GFP-expressing PHA from autofluorescent PHA by fluorescence microscopic imaging. Taken together, HCV envelope-mediated HCV^{pp} entry into PHA appears to be minimal.

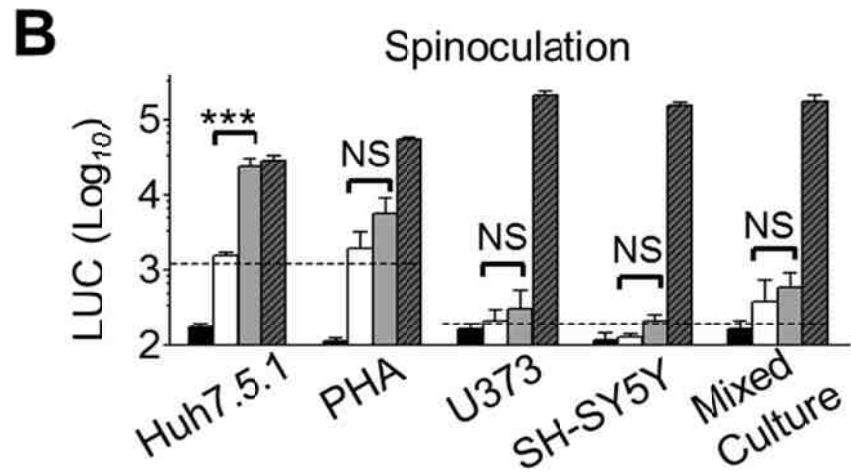
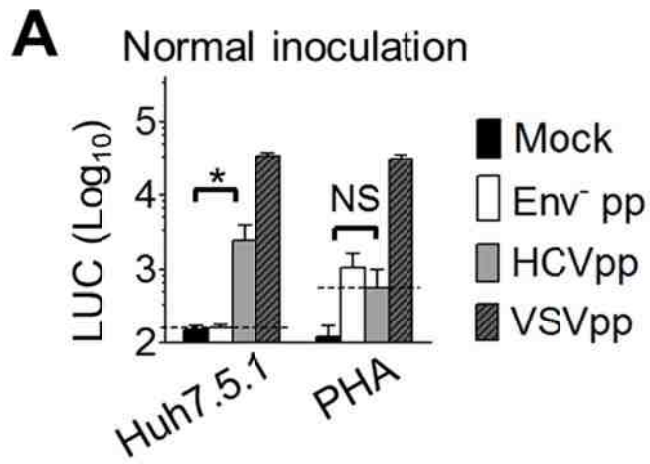


Figure 46. Insignificant HCVpp (Luc) entry into astrocytes. 293T cells were transfected with HIV-Luc reporter alone (Env^{pp}), or in combination with HCV Con1E1/E2 env (HCVpp), or VSV-G env (VSVpp). The supernatants were collected 48 hr post-transfection and used to infect target cells by incubation at 37° for 2 hr (Normal inoculation, **A**) or through centrifugation at 1000 g, room temperature for 2 hr (Spinoculation, **B**). The cells were allowed to culture for 72 hr before harvest for luciferase activity assay. Mixed culture: primary human mixed brain cell culture; LUC: the luciferase activity. Conditioned medium (Mock) was included as a negative control as well. All pseudotyped reporter viruses were quantitated by reverse transcriptase assay, and 200,000 cpm reverse transcriptase activity-equivalent Env^{pp} and HCVpp and 2000 cpm reverse transcriptase activity-equivalent VSVpp were used in all the infections.

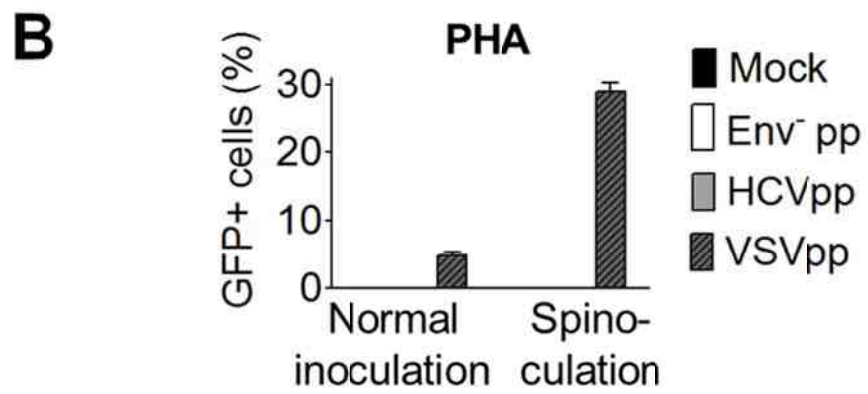
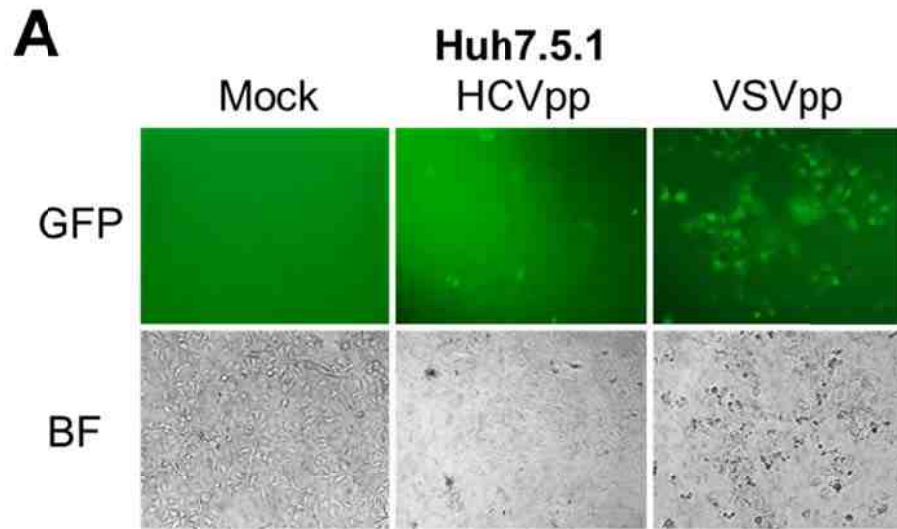


Figure 47. Insignificant HCVpp (GFP) entry into astrocytes. Huh7.5.1 and PHA were infected as described above in Fig. 46 except for that HIV-GFP reporter was used and that virus entry was assessed based on GFP expression by microscopic imaging (**A**, Huh7.5.1 spinoculation, images at 16X) or flow cytometry (**B**, PHA normal inoculation and spinoculation). Conditioned medium (Mock) was included as a negative control as well. All pseudotyped reporter viruses were quantitated by reverse transcriptase assay, and 200,000 cpm reverse transcriptase activity-equivalent Env^{pp} and HCVpp and 2000 cpm reverse transcriptase activity-equivalent VSVpp were used in all the infections.

3.4.2 Unsuccessful VSV-G pseudotyping of HCVcc

To bypass viral entry and study the downstream steps of HCV life cycle in astrocytes, we attempted to pseudotype the JFH1 HCVcc virus with VSV-G by trans-complementation. We first infected Huh7.5.1 with JFH1 virus and then transfected these cells with VSV-G; it was expected that the culture supernatants contain both wide type HCV virus and HCV virus coated with VSV-G protein (VSV-G-HCVpp). However, western blotting of HCV core and VSV-G demonstrated that albeit VSV-G expression in the transfected cells, no VSV-G pseudotyped HCV could be detected in the supernatant (**Fig. 48A**). To ensure that the undetectable VSV-G in the supernatant was not due to the relatively low sensitivity of western blotting, we also determined and compared the infectivity of supernatants collected from pcDNA3-transfected, HCV infected cells (containing only HCV) and that from different amount of VSV-G plasmid-transfected, HCV infected cells (containing HCV and presumably VSV-G-HCVpp). No difference in the infectivity of these supernatants was found by HCV core immunostaining of the infected cells (**Fig. 48B**) or quantification of HCV RNA in the infected cells (**Fig. 48C**). The unsuccessful pseudotyping of JFH1 with VSV-G could be due to competition from wide type HCV envelope proteins and/or lower incorporation efficiency of VSV-G (241).

3.5 HCV RNA translation in astrocytes and its enhancement by miR122

Immediately following virus entry and uncoating, HCV RNA translation takes place and virus proteins are synthesized (15). Therefore, we next examined whether PHA would support HCV RNA translation. We utilized a bicistronic HCV-Rluc subgenomic replicon that has been widely used in the study of HCV translation and replication (163). In HCV-Rluc, the HCV structural proteins downstream of HCV IRES are replaced with the *renilla* luciferase reporter gene, so the translation of Rluc is under the control of HCV IRES.

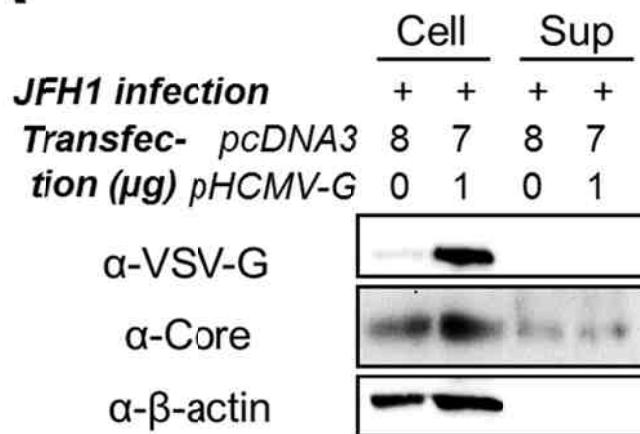
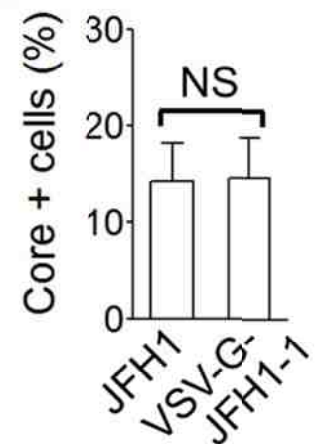
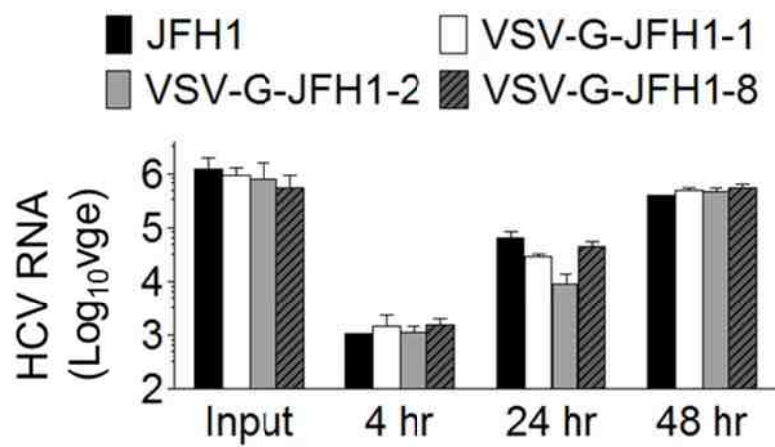
A**B****C**

Figure 48. VSV-G pseudotyping of HCVcc. Huh7.5.1 was infected with HCV JFH1 virus for 3 days and then transfected with 0 (JFH1), 1 (VSV-G-JFH1-1), 2 (VSV-G-JFH1-2), or 8 (VSV-G-JFH1-8) μg of the VSV-G-encoding pHCMV-G plasmid. At 72 hr post-transfection, cells were collected and lysed and cell lysates were immunoblotted for VSV-G, HCV Core and β -actin (**A**, cell); culture supernatants were also collected and subjected to centrifugation concentration followed by Western blotting (**A**, sup). Meanwhile, the culture supernatants were tested for infectivity by inoculating naïve Huh7.5.1 for 2 hr and collecting cells at 48 hr followed by HCV core immunostaining and flow cytometry analysis for the percentage of core + cells (**B**). Alternatively, the infectivity of the supernatants were determined by Huh7.5.1 inoculation and cell collection at 4, 24, and 48 hr post-inoculation, and RNA isolation followed by qRT-PCR analysis of HCV RNA (**C**). Only 0 and 1 μg pHCMV-G plasmid-transfected cells and supernatants were included in **A** and **B**. HCV RNA in the culture supernatants were also quantified and included as “input” in **C**.

Meanwhile, the encephalomyocarditis virus (EMCV) IRES is inserted upstream of HCV nonstructural proteins, translation of these proteins is under the control of ECMV IRES (**Fig. 49A**). We transfected the cells with the HCV-Rluc RNA and determined the luciferase activity of cells 6 hr post-transfection, which was used as an indicator of HCV IRES-mediated translation. A significant level of the luciferase activity was detected in all cells tested including PHA, although all cells had lower luciferase activities than Huh7.5.1 (**Fig. 49B**).

Several studies have recently shown that the expression of a liver-specific microRNA, miR122, is crucial for stimulation of HCV RNA translation in different non-hepatic cells (42-44). We compared constitutive miR122 expression in PHA with Huh7.5.1 and other cells. PHA, 293T and U373 all had extremely low miR122 expression, which were about 10^6 fold lower than that in Huh7.5.1 and 10^4 fold lower than that in HepG2 (**Fig. 49C**). We then determined whether increased miR122 expression would lead to further improvement in HCV IRES-mediated translation in PHA. Exogenous miR122 was introduced to PHA by transfection (**Fig. 49D**); its expression led to increases in the luciferase activity (**Fig. 49E**). Taken together, the results show that HCV IRES-mediated RNA translation is supported in PHA and can be further enhanced by exogenous miR122 expression.

3.6 HCV replication in astrocytes and the effect of miR122

In addition to HCV translation stimulation, miR122 is also suggested to positively regulate HCV infection by stabilizing HCV RNA (45-47) and promoting HCV replication (37, 48-50). Therefore we next determined the overall impact of miR122 on HCV translation, RNA stability, and replication in astrocytes by measuring luciferase activity at

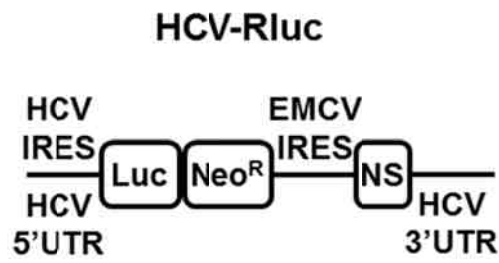
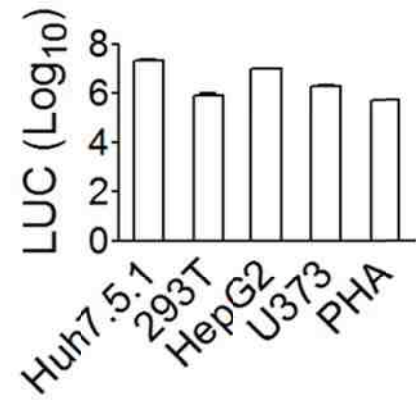
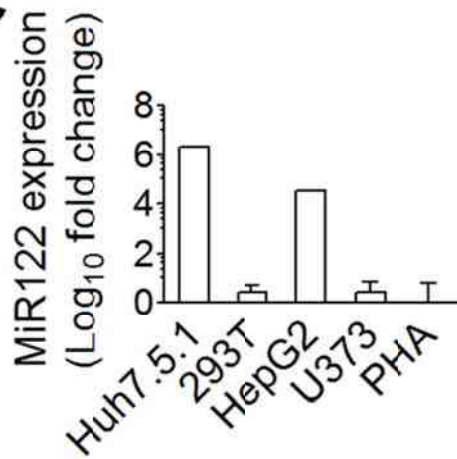
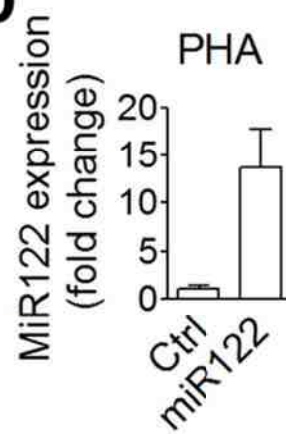
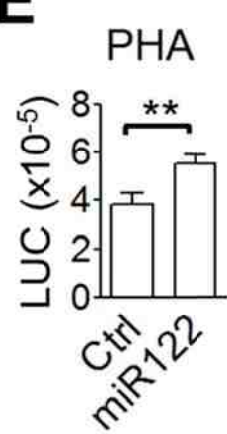
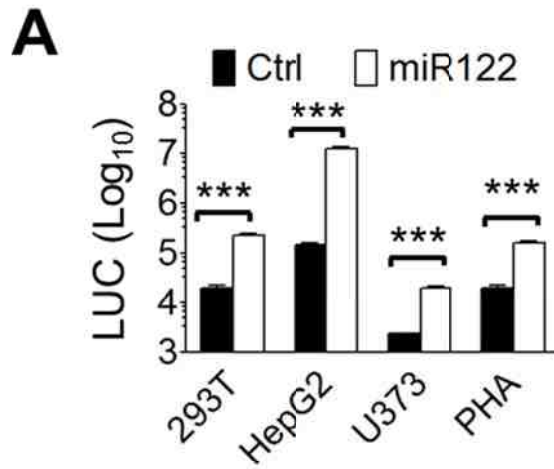
A**B****C****D****E**

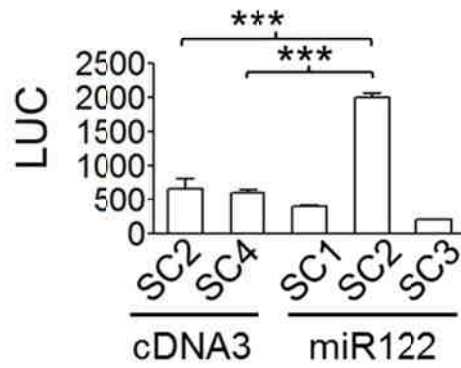
Figure 49. HCV RNA translation in astrocytes and its enhancement by miR122 expression. (A & B) A HCV genotype 1b subgenomic replicon HCV-RLuc DNA (A) was linearized and used as a template for *in vitro* transcription and RNA synthesis. The RNA was transfected into PHA together with pcDNA3-GFP plasmid (transfection efficiency control). The cells were cultured for 6 hr before harvest for the luciferase assay (B). Huh7.5.1, 293T, HepG2 and U373 were included for comparison in the experiments. For each cell, the luciferase activity was normalized to the transfection efficiency, which was determined by measuring the percentage of GFP-positive cells with flow cytometry at 72 hr post-transfection. (C) Endogenous miR122 expression in PHA. Total RNA was isolated from the cells for miR122 expression level by qRT-PCR. miR122 expression was normalized by U6 small nuclear RNA expression and expressed as fold change relative to PHA. (D & E) PHA were transfected with pcDNA3-GFP plasmid (Ctrl) or pcDNA3-GFP-miR122 plasmid (miR122) and cultured for 24 hr. The cells were then transfected with HCV-RLuc RNA and cultured for 6 hr before harvest for miR122 expression analysis by qRT-PCR (D) and the luciferase activity assay (E).

72 hr post HCV-Rluc RNA transfection. Significant increases of luciferase reading were found in all of U373, PHA, 293T and HepG2 cells with exogenous miR122 expression (**Fig. 50A**), suggesting an overall positive role of miR122 in all these cells. To confirm this enhancing effect, we also compared U373 stable clones selected from miR122- and empty vector- transfected cells. Among the selected three miR122-expressing single clones, only clone 2 (miR122-SC2) gave significantly higher (3 fold) luciferase readings than the negative controls (cDNA3-SC2/SC4) at 72 hr post HCV-Rluc RNA transfection (**Fig. 50B**). Quantification of miR122 in these clones with qRT-PCR revealed that clone 2 expressed 20 fold more miR122 than the controls, but this expression level was actually 10 fold lower than clone 1 and 3 (miR122-SC1/ SC3) (**Fig. 50C**). The apparent discrepancy between clone 2 and clone 1 and 3 could be a result from random insertion of miR122 into chromosomes during clone selection and possible subsequent disruption of important cellular pathway(s) involved in the miR122/microRNA metabolism or miR122's interaction with HCV RNA. Thus, to minimize the interference from random miR122 genome insertion, we compared the miR122-expressing U373 pooled clones (miR122-PC) with the control U373 pooled clones (cDNA3-PC). The results showed that 6 fold higher miR122 expression in miR122-PC (**Fig. 50E**) led to a 3 fold increase in luciferase signal (**Fig. 50D**), confirming that miR122 expression has an overall positive impact on HCV RNA stability, translation and replication in astrocytes.

A recent study reported that miR122 expression in non-hepatic cell lines was sufficient to facilitate efficient and continuous HCV replication (49). Therefore we next monitored HCV replication kinetics in astrocytes to determine whether or not the virus could self-replicate with or without the help of miR122 in astrocytes. We used the same bicistronic HCV-Rluc subgenomic replicon as above except for that the luciferase activity was



B U373 Single Clones



D U373 Pooled Clones

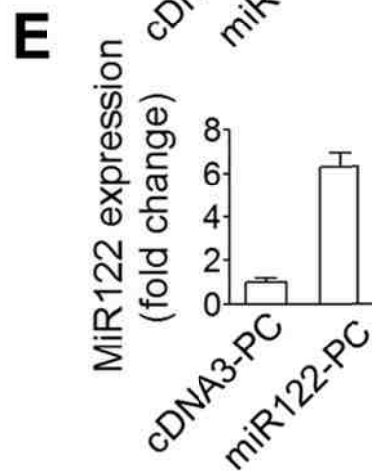
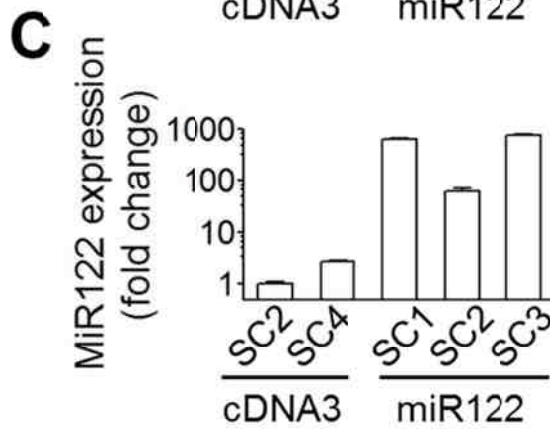
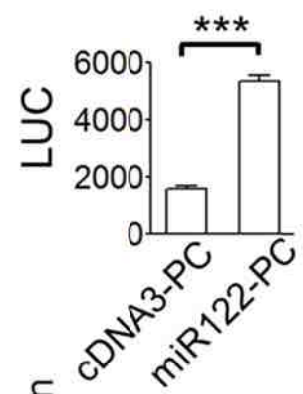


Figure 50. Effect of miR122 on HCV RNA stability, translation and replication in astrocytes. (A) PHA and other cells as indicated were transfected with HCV-Rluc RNA and pcDNA3-GFP plasmid (Ctrl) or pcDNA3-GFP-miR122 plasmid (miR122). Cells were cultured for 72 hr before harvest for the luciferase activity assay. For each cell, the luciferase activity was normalized to the transfection efficiency, i.e., the percentage of GFP-positive cells with flow cytometry. (B-E) U373 cells stably expressing miR122 (single clones U373-miR122-SC1/ SC2/ SC3 in B & C, pooled clones U373-miR122-PC in D & E) were generated and transfected with HCV-Rluc RNA and pEgr1-Fluc plasmid, cultured for 72 hr and assayed for Rluc and Fluc activities (B, D) and miR122 expression by qRT-PCR (C, E). U373 cells stably expressing the backbone vector pcDNA3-GFP (single clones U373-cDNA3-SC2/ SC4 in B & C, and pooled clones U373-cDNA3-PC in D & E) were included as control. Rluc activities were normalized to Fluc activities to ensure comparable transfection efficiency (B & D). miR122 expression was expressed as fold change relative to cDNA3-SC2 (C) or cDNA3-PC (E).

monitored for an extended period of 120 hr post-transfection. We first found that even without miR122 expression in Huh7.5.1 cells, the luciferase activity gradually increased and maintained at a relative stable level after a brief decline due to degradation of input transfected RNA, likely resulting from HCV RNA replication (open diamond, **Fig. 51A**). In contrast, the luciferase activity in all other cells including PHA showed a continued decline during 120 hr (open diamond, **Fig. 51B-E**), suggesting abortive HCV replication in these cells without exogenous miR122 expression. We next introduced miR122 into these cells and determined its effects on HCV replication in these cells. Compared to Huh7.5.1 without miR122 transfection, expression of miR122 in Huh7.5.1 gave rise to an overall higher level of luciferase activity but maintained the similar kinetics (closed diamond, **Fig. 51A**). As expected, miR122 expression in PHA and U373 showed generally enhanced luciferase activity until 72 hr post RNA transfection; however, it was not able to rescue the declining kinetics (closed diamond, **Fig. 51B & C**). Consistent with other studies (49, 242), miR122 expression in 293T and HepG2 led to increased luciferase activity from 48 hr post-transfection (closed diamond, **Fig. 51D & E**). These results showed that PHA did not support HCV replication regardless of miR122 expression and suggest that HCV replication is likely blocked in PHA.

3.7 Effect of cytokines/chemokines/LPS on HCV replication in astrocytes

Viral infection of the brain usually causes inflammation in the CNS (243). Priming of brain cells with proinflammatory cytokines in cell cultures, which mimics the inflammatory environment in virus-infected brain, could enhance virus infection of brain cells (244-247). Therefore, we decided to test whether exposure of PHA to various cytokines/chemokines/bacterial LPS could pre-dispose these cells to support HCV replication. Among those tested include bacterial LPS, chemokine MCP-1, and pro-

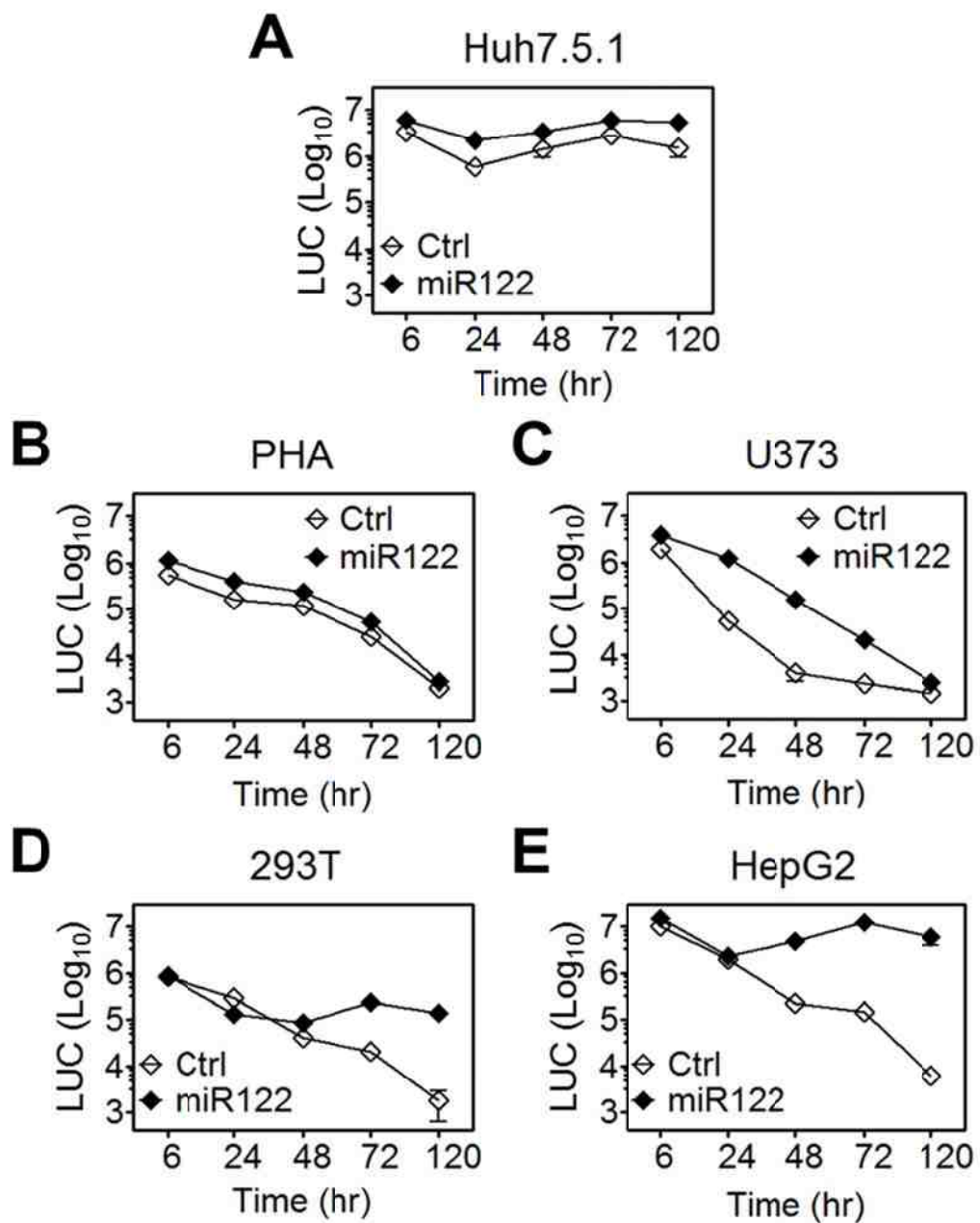


Figure 51. HCV replication in astrocytes with or without exogenous miR122 expression. Huh7.5.1 (A), PHA (B), U373 (C), 293T (D) and HepG2 (E) were transfected with HCV-Rluc RNA and pcDNA3-GFP control plasmid (Ctrl, open diamond) or pcDNA3-GFP-miR122 plasmid (miR122, closed diamond). Cells were harvested at 6, 24, 48, 72 and 120 hr post-transfection for the luciferase activity assay. For each cell type, the luciferase activity was normalized to the transfection efficiency, i.e., the percentage of GFP-positive cells at 72 hr post-transfection with flow cytometry.

inflammatory cytokines IL-1 β , IL-4, IL-6, IL-10, TNF- α and INF- γ . The concentrations of these agents were determined based on previous studies (244, 245) and they were all between 10-100 EC50 of these agents according to the manufacturer. Interestingly, none of these pre-treatments led to enhanced HCV-Rluc expression in U373 (**Fig. 52A**). Instead, IL-1 β , TNF- α , INF- γ and LPS pre-treatments led to significant inhibition of HCV-Rluc expression. Similarly, IL-1 β treatment inhibited HCV-Rluc expression in PHA, while IL-4 gave rise to no effects (**Fig. 52B**). These results are not unexpected, considering the antiviral nature of IFN- γ and INF- γ -like effects of IL-1 β , TNF- α , and LPS. It is possible that the interactions between HCV infection and the signaling pathways of cytokines being tested are different from those in other viral infections of cells that are able to be primed by cytokine pre-treatments.

3.8 HCV-induced IL-18 expression in astrocytes

Even though astrocytes do not support HCV entry and replication, the possibility cannot be excluded that HCV interaction with astrocytes leads to changes in astrocytes and eventual neuron demise. Astrocytes have been shown to be important in evoking inflammatory response in the CNS in response to invaded pathogens and physical injury (195, 196, 200). Thus, we performed HCV infection of PHA as described above, i.e., 2 hr incubation and removed the viruses and determined the expression levels of several selected pro-inflammatory cytokines 24 hr post-infection. Interestingly, among all the cytokines tested (IL-1 α , IL-1 β , IL-6, IL-8, IL-18 and TNF- α), only IL-18 expression was significantly induced, i.e., by about 2 fold, compared to the conditioned medium mock treatment (**Fig. 53A**). To further verify these findings, we included IFN- γ in these experiments, as IFN- γ is known to induce IL-18 expression (248, 249). Compared to the mock treatment or the treatment with fresh culture medium, like IFN- γ treatment,

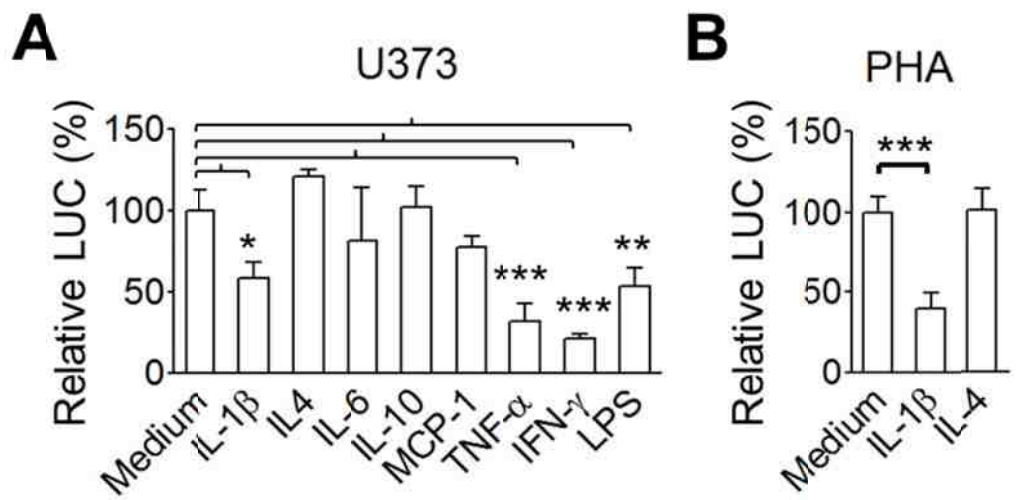


Figure 52. Effect of cytokines/chemokines/LPS on HCV replication in astrocytes.

(A) U373 cells were treated with culture medium (Medium), 5 ng/ml IL-1 β , 10 ng/ml IL-4, 10 ng/ml IL-6, 10 ng/ml IL-10, 100 ng/ml MCP-1, 10 ng/ml TNF- α , 10 ng/ml INF- γ or 100 ng/ml LPS for 24 hr, transfected with HCV-Rluc RNA and pcDNA3-GFP-miR122 plasmid, cultured for 72 hr, and harvested for the luciferase activity assay. (B) PHA were treated with culture medium, 5 ng/ml IL-1 β or 10 ng/ml IL-4 for 24 hr, and then transfected with HCV-Rluc RNA and pcDNA3-GFP-miR122 plasmid, cultured for 72 hr, and harvested for the luciferase activity assay. All cytokines/chemokines/LPS were diluted in the culture medium. The luciferase activity was expressed as the percentage of that of the Medium control.

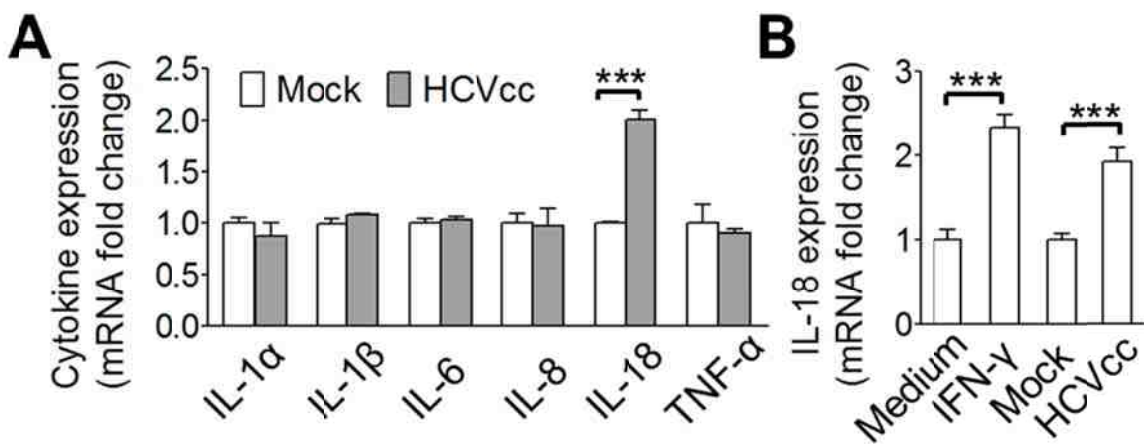


Figure 53. Induction of IL-18 expression in astrocytes following HCV exposure.

(A) PHA were cultured in a 6-well plate and then added 6 ml HCVcc (viral titer: 1.84×10^8 vge/ml by qRT-PCR) or conditioned medium (Mock) and incubated for 2 hr. HCV was removed and the cells were then extensively washed with PBS and cultured for 24 hr before harvest for total RNA isolation and qRT-PCR for cytokine expression. Expression of each cytokine was first normalized to that of β -actin and its relative level in the control (Mock) was set to 1. (B) PHA were treated with PHA culture medium (Medium), 50 ng/ml IFN- γ , conditioned medium (Mock) or HCV virus (HCVcc) for 24 hr. The expression level of IL-18 in these cells was determined by qRT-PCR and expressed as fold change relative to that of Medium treatment.

HCV exposure led to robust IL-18 expression in PHA (**Fig. 53B**). These results suggest that HCV could alter astrocyte function in the absence of productive HCV infection and replication.

3.9 HCV direct neurotoxicity

IL-18 is an important regulator in neuroinflammation and neurodegeneration (250). To determine whether HCV interaction with astrocytes such as IL-18 induction could have any detrimental effects on neurons, we performed the same HCV infection experiment as above, collected the culture supernatants, and determined their effects in neuron survival (+PHA). The MTT assay showed that none of the PHA supernatants including the one from HCV infection affected neuron viability (**Fig. 54A**). The negative results could be due to the lower level of IL-18 in the supernatants. The other possibility that HCV could affect the CNS is through its direct interaction with neurons. To address this possibility, HCV was directly exposed to neurons in the absence of PHA (-PHA). To our great surprise, compared to the conditioned medium mock treatment, the culture medium alone or IFN- γ treatment, HCV exposure led to a significant decrease of neuron survival, i.e., by about 35% (**Fig. 54B**). The neurotoxicity appeared to maintain up to 4-fold dilution of the input virus (**Fig. 54C**), which corresponded to a viral titer of 4.7×10^7 vge/ml.

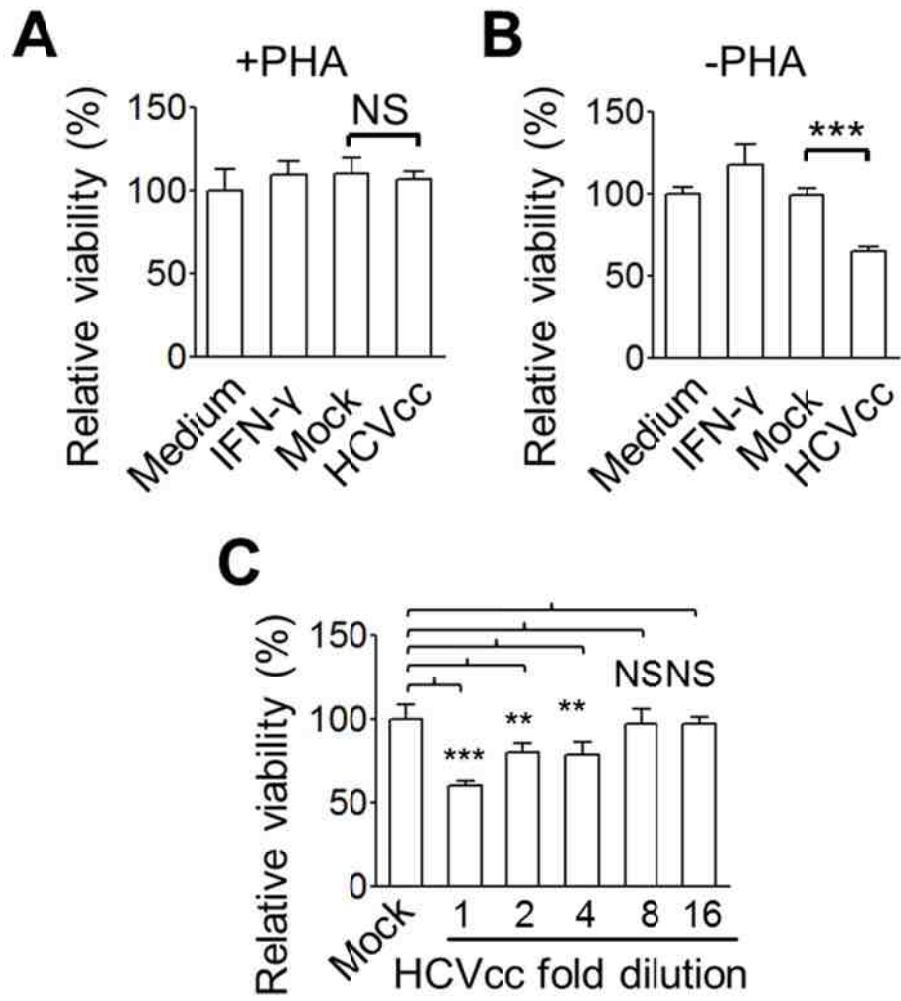


Figure 54. Neurotoxicity induced by direct HCV exposure. (A) PHA were treated with PHA culture medium (Medium), 1 µg/ml IFN-γ, conditioned medium (Mock) or HCV virus (HCVcc, viral titer: 1.84×10^8 vge/ml by qRT-PCR) as described in Fig. 53. The culture supernatants from each of these treatments were collected 24 hr after the treatment and added onto SH-SY5Y cells (+PHA). SH-SY5Y cells were cultured for 72 hr and then subjected to the MTT assay. Results were expressed as the percentage of PHA culture medium control (A). Meanwhile, SH-SY5Y cells were directly exposed to each of these four treatments (-PHA) and cultured for 72 hr, followed by the MTT assay (B). (C) Dose-dependent HCVcc neurotoxicity. Two-fold serial dilutions of HCVcc (viral titer: 1.88×10^8 vge/ml by qRT-PCR) were added onto SH-SY5Y cells as described. MTT assay was performed 72 hr post HCV exposure. Conditioned medium (Mock) was included as a control, and the results were expressed as the percentage of that of the Mock control.

DISCUSSION

Summary of the results

In CHAPTER 1, we characterized CCCM HCV infection of hepatocytes. We first demonstrated that a HCV infection in cell culture leads to the formation of clustered infected cells; the infectious foci, evident under low MOI and high cell density, are highly suggestive of cell-cell contact-mediated HCV transmission (**Fig. 6**). Replating of HCV-infected cells at different densities leads to density-dependent HCV spread, with foci formation observed at only high cell densities, indicating that HCV foci formation results from CCCM HCV transmission, not the proliferation of infected cells (**Fig. 7, 8**). We then established a co-culture assay and directly demonstrated CCCM HCV transmission in hepatocytes, including primary human hepatocytes (**Fig. 10, 11**). To understand the relative contributions of CCCM and cell-free virus infection in the 20 hr co-culture assay, we compared the kinetics of HCV infection in the co-culture assay to that of cell-free virus infection only in a transwell assay. The results show that CCCM HCV infection occurs at as early as 3 hr in the co-culture assay while cell-free virus infection only in the transwell assay is not detected until beyond 20 hr (**Fig. 12 A-C**). These results reveal the rapid kinetics of the CCCM HCV transmission and confirm that the observed newly infected cells in the 20 hr co-culture assay result from solely CCCM, not cell-free virus infection. In addition, we also characterized the roles of the four known HCV receptors (CD81, SR-B1, CLDN1, and OCLN), and the actin and the microtubule cytoskeletons in CCCM HCV transmission based on the co-culture assay. Knock-down of each of the HCV receptors individually by siRNAs all greatly inhibit the CCCM HCV infection, indicating an important role of each of these receptors in this process (**Fig. 14**). Importantly, concomitant knock-down of all four receptors almost completely abolishes the CCCM infection, suggesting that these receptors may work in a coordinated manner

(**Fig. 15**). Attempts to introduce susceptibility to CCCM HCV infection into cells missing or expressing a low level of one or more HCV receptor(s) (293T cells, HepG2, NKNT3, and CYNK10 hepatoma cells) by ectopic expression of the missing/ minimally-expressed HCV receptors in these cells all fail (**Fig. 18-21**), likely due to the lack of unknown facilitating factors or the presence of unknown inhibitory factors in these cells. Treatment of the co-cultures with the actin depolymerizing agent cytochalasin D inhibits the CCCM infection in a dose-dependent manner, while treatment with the microtubule depolymerizing agent nocodazole does not affect it (**Fig. 22**), indicating that the actin cytoskeleton, not the microtubule, plays an essential role in CCCM HCV infection. Furthermore, we adapted the tetracysteine-biarsenical dye labeling strategy in combination with 3-dimensional live cell fluorescence microscopic imaging and dissected the spatial and temporal details of the CCCM HCV transfer process. Sequential HCV transfer from one donor to multiple targets and concurrent transfer between one donor and multiple targets were observed (**Fig. 27**). Lamellipodium/ lamellipodium-like structures at the contact sites for each of the observed transfer events in Fig. 27 were found with a close examination of those sites by 3D reconstruction, indicating that lamellipodium may play a role in the CCCM HCV transfer process (**Fig. 28**). The transfer of one single μm -sized HCV core punctum into target cells in real time was also confirmed and the four steps in CCCM HCV transfer are illustrated: donor cell-target cell contact, formation of viral punctum-target cell conjugation, transfer of the viral punctum, and post-transfer (**Fig. 29**). Lastly, using three different strategies including extended co-culturing time in the presence of nAbs, FACS sorting of target cells and G418 selective killing of donor cells, we demonstrated that the CCCM HCV transfer in the co-culture assay leads to productive infection in the target cells (**Fig. 31-33**). Taken together, CCCM HCV transfer is rapid, HCV receptors- and actin cytoskeleton-

dependent and productive in nature, and it constitutes an important and effective route for HCV infection and dissemination in hepatocytes.

In CHAPTER 2, we characterized the relationship between exosomes and the infectious HCV virions. We first demonstrated that HCV infection does not affect exosome secretion or size distribution on an iodixanol density gradient (**Fig. 34, 35**). But interestingly, we next showed that cell culture-produced exosomes and a subpopulation (about 1-10%) of HCV from HCV-infected hepatocytes were co-fractionated on the iodixanol gradient – the “exosome-associated HCV” (**Fig. 37**). The co-fractionation was also confirmed using different methods for concentrating virus and exosome (PEG precipitation and ultracentrifugation), as well as different rotors for the density gradient fractionation (SW55Ti and NVT65) (**Fig. 38, 39**). Importantly, the HCV-exosome co-fractionation was also observed in HCV-positive patient plasma and the amount of HCV RNA that was detected in exosome-containing fractions were much higher than that in exosome-free fractions (**Fig. 40**). Furthermore, the exosome-associated form of HCV contained both viral RNA and viral capsid (core) and envelope (E2) proteins; it also retained its infectivity to hepatocytes, albeit less effective than the exosome-free form of HCV (**Fig 41**). Taken together, the results here suggest that exosome-associated HCV constitutes an alternative route for HCV infection and spread.

In CHAPTER 3, we characterized the interaction between HCV and astrocytes, one of the abundant CNS cells and one of the putative HCV target cells in the brain. First, using the HCVcc system, we showed that primary human astrocytes were not productively infected either by cell-free or CCCM HCV infection (**Fig. 43 & 44**). We then examined different steps of HCV life cycle in astrocytes and determined possible restriction steps in these cells. Using the HCVpp system and spinoculation, we showed

that there was no HCV envelop-mediated entry into PHA, although all the four known HCV receptors were expressed in PHA (**Fig. 45-47**). Using the bicistronic HCV-Rluc subgenomic replicon, we showed that HCV RNA translation was supported in PHA and further enhanced by the expression of a liver-specific microRNA, the miR122 (**Fig. 49**). However, albeit an overall positive effect of miR122 on HCV translation, RNA stability, and replication on astrocytes (**Fig. 50**), introduction of miR122 expression was not able to rescue the abortive HCV-Rluc RNA replication in PHA (**Fig. 51**). Next, we attempted to prime PHA with cytokines/chemokines/LPS for higher HCV replication, but it was found that pre-treatment of astrocytes with proinflammatory cytokines such as IL-1 β , TNF- α and IFN- γ inhibited HCV RNA expression in PHA (**Fig. 52**). Furthermore, our examination of the expression of various proinflammatory cytokines in PHA following HCV challenge showed that HCV specifically stimulated IL-18 expression in PHA (**Fig. 53**), suggesting potential roles of IL-18 and astrocytes in HCV-related CNS abnormalities. Lastly, we demonstrated that HCV itself was sufficient to cause neurotoxicity in a dose-dependent manner (**Fig. 54**). Taken together, the results here suggest that astrocytes are not productively infected by HCV and they support HCV translation but not entry and replication. However, HCV-induced IL-18 expression in astrocytes and HCV direct neurotoxicity may contribute to HCV-related CNS abnormalities.

CCCM HCV infection in vivo

Despite significant advances since the establishment of the JFH1-Huh7 HCV cell culture system in 2005 (70-72), the process of HCV transmission and spread in the liver following infection remains poorly understood. Liver is one of the organs with extremely high cell density [2-3.0 x 10⁵ hepatocytes/cm² (99)], which provides HCV with numerous cell-cell contact sites. In chronically HCV-infected liver, viral replication and intrahepatic

HCV RNA level are very low (7-64 genomic equivalent *per cell*) (97, 251) and nAbs and other immunological responses are often present (100). However, even with the presence of those nAbs that are capable of neutralizing cell-free virus infectivity *in vitro* (203), prevalence of infected hepatocytes in the liver of chronic patients is normally high (96, 251). In this study, we showed that HCV infection in cell culture led to foci formation (**Fig. 6**) and that cell-cell contact facilitated HCV spread among hepatocytes (**Fig. 7, 8 & 10**) including primary human hepatocytes (**Fig. 11**). We further showed that CCCM HCV infection is a rapid process compared to cell-free HCV infection (**Fig. 12**). Previous studies show similar infectious foci in patient liver biopsies and a gradient dispersion of viral genome around the center of the focus (95-97); CCCM HCV infection is found relatively less sensitive to nAbs and neutralizing patient sera than cell-free HCV infection [**Fig. 30, 31** and (98)]. Taken together, it is highly conceivable that CCCM HCV occurs *in vivo*, and it could even be more favorable than cell-free HCV infection given the compact nature of the liver. Thus, CCCM HCV transmission should be considered when designing any future anti-HCV vaccines and therapeutics.

Roles of HCV receptors in the CCCM HCV infection

CD81, the first discovered HCV receptor identified by screening for HCV E2-binding activity (25), is believed to mediate cell-free HCV virus entry in both an early E2-binding step and a late post-binding step in association with CLDN1 (30, 33, 34). SR-B1, another E2-binding HCV receptor, also mediates cell-free HCV virus attachment and entry in an early step in this multi-step entry process (252-255). The other two HCV receptors, CLDN1 and OCLN, are both tight junction proteins recently identified by screening for cellular determinants able to confer HCVpp entry into non-susceptible cells (28, 29). To determine the roles of each of these four HCV receptors in CCCM HCV

infection, we first used a siRNA strategy to knockdown the expression of each of them individually in Huh7.5.1 target cells and found between 46% to 72% decreases in CCCM HCV infection, suggesting a fundamental role of each of them in this process (**Fig. 14**). Furthermore, simultaneous knockdown of all of them almost completely abolishes CCCM HCV infection, suggesting that they may mediate CCCM HCV infection in a combinatorial mechanism (**Fig. 15**). To further understand the roles of the four receptors in CCCM infection, we performed the co-culture assay using CD81-negative HepG2, low CLDN1-expressing NKNT3 and CYNK10, and low SR-B1, no CLDN1-expressing 293T (**Table 1 and Fig. 16**). All these cell lines are refractory to both cell-free and CCCM HCV infection (**Fig. 17**). However, ectopic expression of the missing/ low-expressing receptor(s) does not render these cells susceptible to CCCM HCV infection (**Fig. 18-21**). These results together suggest that all four HCV receptors are essential but not sufficient for CCCM HCV infection. Consistent with our findings, previous studies show that SR-B1 antagonists, an anti-CLDN1 serum, and OCLN knockdown by shRNA all inhibit CCCM HCV infection (256), suggesting that all three of them are required for this process. However, the role of CD81 in the CCCM HCV infection appears to be controversial in the literature. One study shows that CD81 is dispensable for CCCM infection using a mutant JFH1 carrying CD81 binding-deficient E2 glycoprotein (257). Interestingly, this study does not show convincingly that the mutant JFH1 absolutely cannot infect hepatocytes by cell-free virus infection; their co-culture assay does not include any nAb and the time of co-culturing is not indicated, but very likely longer than 24 hr. Under those conditions, the “CD81-dispensable CCCM transmission” observed in their co-culture assay could be a result of leaking cell-free virus infection, as we showed that cell-free HCV infection can be detected in the co-culture after 24 hr if performed without nAbs (**Fig. 31**). On the other hand, consistent with our findings, another group demonstrates the absolute requirement for CD81 in CCCM infection using the

combination of a Huh7-derived low CD81-expressing Lunet cell and an anti-CD81 antibody to ensure that no CD81-mediated cell-free virus infection occurs in their co-culture assay (256). Taken together, results from our study in CHAPTER 1 and the second study mentioned above suggest that CD81 is required for the CCCM HCV infection.

Difficulties of CCCM HCV infection of cells other than Huh7.5.1 cells and primary hepatocytes

In this study, we show successful CCCM HCV transmission from infected Huh7.5.1 to Huh7.5.1 itself and primary human hepatocytes (**Fig. 10, 11**); we also show no CCCM HCV transmission from infected Huh7.5.1 to 293T cells, HepG2, NKNT3, CYNK10 hepatoma cells, or primary astrocytes, even when the missed and/or low-expressing receptor(s) are introduced into these cells (**Fig. 17-21, 44**). There are several possible reasons for this apparent inconsistency. First, though it is not clear about NKNT3 and CYNK10 cells, 293T, HepG2 or PHA do not support HCV replication due to the lack of miR122 expression for all and also other unknown reasons for PHA (**Fig. 51**). Even if CCCM HCV transmission may still occur without HCV replication in the target cell, it is very likely that efficient viral replication in the target cells following CCCM transfer can facilitate the detection of the transfer. Therefore, the lack of support for HCV replication in these cells may contribute to difficulties in the detection of CCCM HCV transmission in them. Second, even though cell-free virus entry into 293T and HepG2 cells are efficient when all the four receptors are expressed (258, 259), it is not guaranteed that these four are also sufficient for the CCCM HCV transfer since the mechanisms underlying it (discussed in details later) are still not completely clear. It is possible that other factors besides the four known receptors, facilitating or inhibitory, are missing or present in

those cells that fail to be transferred. Alternatively, it is also possible that the specific type of contact or structure (refer to the discussion of mechanism) that is required for the CCCM HCV transfer cannot form well or efficiently between the donor Huh7.5.1 and those target cells.

The role of actin cytoskeleton in CCCM HCV infection

CCCM infection has been shown in many different animal viruses, and its role in immune evasion and rapid viral dissemination has recently gained more attention (74). CCCM viral transmission in animal cells can occur in a variety of ways. Among the known are through virological synapses (HIV-1 and HTLV-1), nanotubes (HIV-1), viral transfer across tight junctions (HSV), and viral induction of actin tails (VV) (74). Interestingly, all the above CCCM routes involve actin and/or microtubule cytoskeletons. In addition, CCCM spread have also been found very common in plant virus infection and usually involves targeting of virus-encoded movement protein(s) (MP) to plant-specific organelles plasmodesmata (PD), which are narrow tunnels in the cell wall for intercellular communication (75). Movement strategies for CCCM viral spread differ upon viruses and MPs. In tobacco mosaic virus (TMV) infection, MP binds and chaperones genomic RNA in the virus replication complexes (VRC) and targets the whole VRC to PD for CCCM viral spread (260). In the grapevine fanleaf virus (GFLV) infection, MP recruits the PD receptor plasmodesmata located protein (PDLP) to PD to mediate the formation of tubules through which the assembled virions traverse PD (so-called “tubule-forming virus”) (261). Interestingly again, in virtually all CCCM plant virus infections, movement of MP, VRC, virions, or other essential cellular co-factors to and/or through PD all require an intact cytoskeleton, particularly the actomyosin moter system (260-263). Thus, we further determined the roles of actin and/or microtubule

cytoskeletons in CCCM HCV infection. Actin cytoskeleton has been shown to be involved in interaction with multiple steps of cell-free HCV infection including virus entry (228, 264) and replication (265, 266). In agreement with these findings, our results show that an intact actin network is required for CCCM HCV transfer, as treatment with actin polymerization inhibitor cytochalasin D in the co-culture assay prevents CCCM HCV transfer (**Fig. 22 A, C**). Based on the known function of cytochalasin D and our finding that HCV secretion from infected cells is not affected by the treatment (**Fig. 22 F**), cytochalasin D likely inhibits the transfer process at the donor cell-target cell contact sites or during the uptake of viral puncta by the target cells. On the other hand, treatment of the co-culture with the microtubule depolymerizing agent, nocodazole, at a concentration sufficient to disassemble microtubules [**Fig. 22B** and (230)], has little effect on CCCM HCV transfer (**Fig. 22D**). In contrast to our studies, other studies find that nocodazole treatment inhibits microtubule-dependent transport of the HCV replication complex and initiation of productive HCV infection and, as a result, HCV RNA replication (265, 267, 268). Moreover, two recent reports show that post-assembly vesicular HCV core puncta traffics via microtubules, which is inhibited by nocodazole treatment (66, 208). It is interesting to point out that the above-mentioned studies all use much higher concentrations of nocodazole, mostly 10 - 40 times higher than what are used in our studies. These extremely high concentrations of nocodazole used in those studies could be the main reason for the discrepancies.

Temporal and spatial details of CCCM HCV transmission by 3D live imaging

It is believed that HCV virus is released from infected cells through the secretory pathway (269). After translation and processing on the ER membrane, the mature HCV core is relocated to the surface of lipid droplets (270). When the RNA genome produced

from the replication complex on the membranous web and envelope proteins (E1/E2) on the ER are ready, viral budding towards the ER lumen takes place on the ER outer membrane in close proximity to the lipid droplets (another proposed mechanism believes budding occurs on LD) (66). These intracellular viruses become infectious upon envelopment; they are thought to be loaded into secretory vesicles that egress via the ER-*trans* Golgi secretory pathway and released to the extracellular space upon fusion of the vesicles with the plasma membrane (208). However, the actual “fusion” or “release” process has never been captured with fluorescence or electron microscopy. Our live cell imaging studies show that during CCCM HCV transmission, large amounts of mobile viral puncta move to the contacted surfaces between the donor and target cells, form conjugates with the target cell, and then transfer into the target cell (**Fig. 27-29**). These core puncta are μm -sized and are unlikely single viral particles, but more likely vesicles loaded with virus particles (100-1000 virions/ punctum based on size) (66, 208). The transfer of a single core punctum takes 18 min (**Fig. 29A**); the transfer process lasts for 171 min on average (**Fig. 29B**). Moreover, the transfer events can occur at multiple donor-target cell contact sites (**Fig. 27A ii**) or concurrently between one donor and multiple targets (**Fig.27 B**). Therefore, during the entire CCCM transfer process, a great number of viral puncta, which correspond to an even greater number of viral particles, can be delivered into the target cell, contrasting the cell-free virus infection, in which one virion enters one target cell at a time. It is not guaranteed that each of the viral particles in each of the transferred puncta proceeds through the downstream viral life cycle in the target cell, yet the high input of CCCM viral transfer certainly leads to productive infection of the target cell (**Fig. 31-33**).

Potential mechanism(s) of CCCM HCV infection – the possible involvement of lamellipodium

As discussed above, CCCM viral transmission can occur in a variety of ways. According to our live cell imaging data, no cell protrusions resembling actin tails in poxvirus-infected cells are observed, so CCCM HCV infection does not appear to take place by inducing actin tail formation. Similarly, no cell fusion or syncytium formation is noticed: CCCM HCV infection unlikely occurs through plasma membrane fusion of infected and uninfected cells. Cell-free HCV virus infection requires two receptors belonging to tight junction (TJ) proteins, CLDN1 and OCLN. However, recent studies demonstrated that HCV entry into hepatocytes does not occur at the site of functional TJs, but basolateral CLDN1 pools outside of TJ (264, 271, 272). Functional TJs are one of the important characteristics of hepatocyte polarization; interestingly, HCV infection depolarizes primary hepatocytes and HepG2 hepatoma cells (273) and in turn, polarization in HepG2 hepatoma cells restricts HCV infection (272). Thus, the requirement of both CLDN1 and OCLN for CCCM HCV transmission (**Fig. 14D**) does not necessarily indicate that HCV adopts the strategy of “transfer across TJ” like HSV for its CCCM infection; direct evidence is needed to address the possibilities in the future. Our results show that CCCM HCV infection relies on cell density (**Fig. 7, 8**) and mainly occurs between adjacent cells (**Fig. 27-29**), not cells apart from each other and connected by nanotubes or filopodia. Therefore the transfer is unlikely to occur in a way similar to HIV-1's traveling on nanotubes or MLV's traveling on filopodia.

Lamellipodium is broad, sheet-like protrusion of the cell, which contains a branched network of actin filaments (274). In the live images of CCCM HCV transfer, lamellipodium filled with viral puncta in donor cells is frequently observed. This phenomenon is sometimes very obvious (**Fig. 27A iii, iv**) and sometimes less apparent

(**Fig. 27A i, ii, C and D**). But after close examination with higher magnification and 3D re-construction in the latter cases, lamellipodium-like protrusions in the frontier of donor-target contact surface are also observed (**Fig. 28**). In addition, it is interesting to point out that in one recorded transfer event, after the donor cell pulls back its lamellipodium and the CCCM transfer is complete (**Fig. 27A iv**), the target cell (T3) extends out a lamellipodium towards the donor cell (**Fig. 27A v**). These observations suggest that lamellipodium or lamellipodium-like cell protrusions may be the specific form of cell-cell contact involved in the CCCM HCV transmission, though further experiments with lamellipodium-specific markers, such as GFP-tagged actin (275) or the Rac small GTPase (276), are needed to prove or disprove this hypothesis. This model is also consistent with the requirement of the actin cytoskeleton for CCCM HCV transfer (**Fig. 22**), as actin is integral in lamellipodium dynamics and function (274). Nevertheless, in some of the transfer events, especially those with single viral punctum (**Fig. 29 A**), no apparent lamellipodium is observed on the donor-target contact surface, suggesting that other yet to be identified mechanism(s) could also be involved in CCCM HCV infection.

Although the above model about the central role of lamellipodium in CCCM HCV transfer merits further investigation, it is evident that the mechanisms of CCCM HCV transmission are different from most of those discovered for other viruses. It is not only because no actin tail, nanotubes, or uninfected cell-derived filopodia are observed during the live imaging of CCCM HCV transmission, but also due to the lack of some prerequisites for those forms of CCCM transmission. On one hand, many of the viruses that transmit via CCCM route, e.g., VV, HIV-1 and MLV, bud at the plasma membrane; some of the budded viruses adhere to the plasma membrane and then can either be projected to uninfected cells by actin tail (VV), or travel along a nanotube (HIV-1) or filopodium (MLV) to reach and infect uninfected cells (74). On the other hand, viral

envelope proteins of many of those viruses are expressed on the plasma membrane, where they have an opportunity to bind to receptors on an uninfected cell; importantly, the binding of the viral envelope to receptor(s) is required for the anchoring of uninfected cell-derived filopodia by infected cells (MLV) and the formation of VS (HIV-1), and thereby CCCM viral transmission (74). However, neither of these two is true for HCV. First, HCV does not bud from or attach to the plasma membrane after release; it buds into ER and transits through the secretory pathway to reach the plasma membrane for release (66, 270, 277). Our live imaging data demonstrate both the intracellular trafficking and the CCCM transfer of HCV virus in the form of viral puncta containing more than one viral particle (**Fig. 27-29**), suggesting that HCV CCCM transfer is not a single viral particle-based event like those in HIV-1, MLV and VV CCCM transmission. Nevertheless, how are HCV particles bundled and transferred in the form of puncta which do not collapse during the transfer is to be answered in future studies. Second, HCV envelope proteins are expressed on ER (278, 279) and in MVB (144) but not the plasma membrane, which disallows the interaction between viral envelopes on infected cells and receptors on uninfected cells. Therefore the HCV CCCM transmission is very likely a result from exploratory protrusions in the absence of directional stimulation, in contrast to HIV-1 transmission across VS and MLV CCCM transmission along filopodia, both of which are guided by the binding of viral envelope proteins on infected cells to receptors on uninfected cells.

Taken together, the mechanisms of CCCM HCV transmission appear to be different from most of the other CCCM viral transmissions; exploratory lamellipodium and other undetermined mechanism(s) may be involved.

“Trojan exosomes” for HCV

Our results in CHAPTER 2 show that a subpopulation of HCV virions from both cell culture and patient plasma can be co-fractionated with exosomes (**Fig. 37-40**) and that these exosome-associated HCV remain infectious to hepatocytes (**Fig. 41**). Even though it cannot be completely excluded that the observed co-fractionation is due to the same density of some HCV virions and exosomes, a recent study demonstrates by cryo-electron microscopy that 5.6% of cell culture-produced HCV particles are surrounded by an additional layer of “envelope” and that each of these “envelope” contains one or more HCV virions (146). The biological nature of this extra “envelope” was not further investigated in the study but it was described as “exosome-like”. Results from the above-mentioned report and our present study are consistent and suggest a potential role of “Trojan exosomes” in delivering HCV virions to uninfected cells and thereby mediating HCV infection.

During the fractionation of cell culture-produced exosomes and HCV, about 1-10% HCV RNA and HCV core protein were detected in exosome fractions (fraction 2-4) (**Fig. 37-39**). But about 50% of HCV E2 protein was detected in exosome fractions and it appeared to be 20 KD larger on the immunoblot than that detected in HCV alone fractions (fraction 7-10) (**Fig. 37-39**). There are several possibilities for the size difference of E2 protein and the non-proportional distribution of HCV E2 protein and HCV RNA/core protein in the exosome fractions and virus-alone fractions. Different post-translational modifications may occur for the exosome form of E2, which may lead to a larger molecular weight. HCV E1 E2 envelope proteins have been shown to be secreted in exosomes when expressed alone in mammalian cells without HCV infection (143); it is possible that with HCV infection, some E2 protein is also expressed on the exosome membrane, leading to relatively more E2 detection in exosome fractions than

HCV core protein and RNA. Interestingly, different from cell-culture produced HCVcc, HCV-positive patient plasma were found to contain more HCV RNA in exosome fractions than exosome-free fractions (**Fig.40**), potentially suggesting an important role of exosome-associated HCV and its infection *in vivo*.

Exosome biogenesis occurs through at least three pathways: ESCRT-dependent, ceramide-dependent and tetraspanin-dependent pathways (101, 107). The latter two pathways are still at an early stage of investigation and it is currently unclear whether they are involved in HCV secretion. Interestingly, components in ESCRT complexes like Hrs, TSG101, Alix, VPS4B, and CHMP4b have all been demonstrated to be essential for HCV production (144, 280, 281), suggesting that an ESCRT-dependent pathway is also involved in HCV secretion. HCV envelopment is believed to occur on ER and intracellular HCV virus becomes infectious upon the envelopment (233, 270); previous studies with immunofluorescence staining and live cell imaging have demonstrated the egress of intracellular HCV core puncta (presumably infectious HCV particles) via the cellular secretory pathway including various endocytic compartments (e.g., early, late, and recycling endosomes, which are also the origin of exosomes) (208, 282). In addition, HCV core and E2 proteins, as well as the intracellular HCV particles have been found to localize in MVB by electron microscopy (144, 282, 283). Therefore, the secretion of HCV in exosome is very likely due to their similar biogenesis pathways. Nevertheless, it warrants further investigation whether HCV usurps the ESCRT-dependent exosome biogenesis pathway for its own secretion or it is merely a coincidence during their trafficking towards the plasma membrane.

Our results demonstrated that the exosome-associated HCV remained infectious to hepatocytes (**Fig. 41**) but the specific infectivity of the exosome-HCV was about 10-fold

lower compared to that of HCV alone (**Fig. 41**); there could be a few possibilities. HCV E2 – the HCV envelope protein that is believed to be responsible for receptor binding during HCV entry – is about 20 KD larger in the exosome-HCV than HCV alone; if post-translational modifications are underlying the molecular weight change of E2, they may also mark the binding sites on E2 for cellular receptors and thereby hindering the uptake of exosome-HCV by target cells. A recent study has demonstrated that HCV-infected hepatocytes produce exosomes containing HCV RNA (145). Therefore, the exosome-associated HCV fractions may have a lower efficiency per viral genome to establish a productive infection than HCV alone fractions. Moreover, the specific infectivity is also dependent on the average number of HCV virions per exosome and the binding affinity of the exosome-associated HCV to its target cells. Taken together, the molecular mechanism of exosome-associated HCV cell entry merits further investigation.

As a new route of HCV infection and transmission, exosome-associated HCV infection will unsurprisingly add another layer of complexity and flexibility to HCV transmission and pathogenesis. A recent study has shown that hepatitis A virus, a non-enveloped RNA virus causing acute enterically transmitted hepatitis, hijacks the exosome pathway to acquire for itself a host-derived cellular membrane, which protects the virus from neutralizing antibodies in the circulation (284). During our present study, a report was published demonstrating that exosome-mediated HCV infection is more resistant to three out of eight patient-derived neutralizing sera than cell-free HCV infection (285), suggesting a role of exosome-mediated transmission in HCV immune evasion. Nevertheless, it is not clear in that report how cell-free HCV virions and exosome-HCV were separated in their experiments because the strategy used by them – serial centrifugation without density gradient purification – is incapable to achieve the separation as we showed (**Fig. 37-39**).

Cell-free, CCCM and exosome-mediated HCV infection

Throughout this study, three different routes of HCV infection and transmission were examined: cell-free virus infection, CCCM infection and the exosome-mediated infection. All the three routes very likely share similar requirements for HCV replication once inside the target cells but they have their own characteristics during cell entry and exit. Cell-free virus entry is well-characterized and is basically receptor-mediated endocytosis (**Fig. 2**). Cell entry of CCCM HCV transmission is featured by receptors- and actin-dependency (**Fig. 14, 15, 22**), a time course similar to endocytosis (18 min, **Fig. 29**), and transfer in the form of puncta instead of single virion (**Fig. 27-29**). The mechanism of exosome-mediated HCV cell entry and whether this process is HCV receptors-dependent are currently unclear, though theoretically the expression of HCV glycoproteins on exosome is possible. For HCV release/cell exit, convergence of cell-free HCV and exosomes-associated HCV can occur at or immediately after assembly and/or during HCV egress in the secretory pathway, especially in MVB. Intracellular trafficking of assembled HCV particles in the form of viral puncta (could be MVB filled with HCV particles) has been observed in both cell-free HCV secretion (66, 208) and CCCM HCV transmission (**Fig. 27-29**). Therefore it seems that the difference between cell-free HCV release and CCCM HCV transmission emerges during the “exit” step itself: depending on whether the site for release is facing body fluids/culture supernatant or a neighboring cell, cell-free virus release or CCCM transmission takes place. Interestingly, it is currently unclear whether there is a mechanism for the HCV-infected donor cell to distinguish between uninfected and infected neighboring cells.

Albeit different in their mechanisms of action, the three HCV transmission routes all contribute to HCV infection and spread in their own ways. Cell-free virus infection is usually responsible for host-to-host transmission (the possible role of CCCM HCV

transmission cannot be excluded if infected blood cells are also involved) and initial infection of target cells/tissue (presumably liver because no data is available about how early immune cells and the CNS are infected). CCCM HCV transmission and exosome-mediated HCV transmission are then responsible for viral spread and dissemination in the host in the presence of immune effectors, especially nAbs; HCV spread within the high-cell-density likely mainly relies on CCCM transmission, while long-distance spread of HCV to a different tissue/organ is possible through exosome-mediated transmission. Based on whether exosome-mediated HCV infection is dependent on HCV receptors for cell entry, this transmission route may also have the advantage of bypassing HCV entry receptors and the ability to infect cells unsusceptible to cell-free HCV infection. CD5, which is not among the four known HCV receptors required for hepatocyte infection, has been identified as the receptor for HCV infection of T lymphocytes (179); exosome-HCV and its possible different membrane composition/cell entry mechanism may be underlying the extra-hepatic HCV tropism and different receptor-dependency. Moreover, recent studies also demonstrate the ability of exosomes to cross various biological barriers including the blood-brain barrier (286, 287); it cannot be excluded that HCV may enter the CNS in the “Trojan exosomes”.

HCV entry into the CNS – the infection of BBB, Trojan PBMC, or Trojan exosomes?

CNS abnormalities are observed in more than 50% HCV patients, regardless of the severity of liver diseases. How does HCV cross the blood-brain barrier and enter the CNS is one of the central questions in understanding HCV brain infection. A few recent studies demonstrate successful infection of neuroepithelioma and neuroendothelial cell lines with cell culture-produced HCVpp and HCVcc and propose that HCV may cross the BBB and enter the CNS by infecting endothelial cells in BBB and releasing HCV virions into the CNS (288-290). However, this hypothesis awaits further *in vivo* evidence such

as immunostaining for viral proteins and HCV RNA detection in the BBB endothelial cells of patient samples. On the other hand, the “Trojan PBMC” hypothesis is proposed based on the detection of productive HCV infection in patient PBMC, sequence similarities between PBMC- and brain- isolated HCV, and the known ability of PBMC to cross the BBB (170, 172, 183, 185). However, this hypothesis also awaits further evidence for the actual process of infected PBMC to cross the BBB; the newly developed humanized mouse model (291, 292) for HCV infection may provide direct evidence for it in the future. Last but not least, based on our findings that HCV can transmit in the form of exosome (Results section, CHAPTER 2) and recent discoveries of exosome’s ability to cross the BBB (286), it is possible that HCV enters the CNS in the form of “Trojan exosomes”. However, this hypothesis is beyond the scope of the current study and future experiments are needed to test it. Taken together, all of the three proposed entry paths for HCV infection of the CNS are possible, yet each of them and their relative contributions require further examination.

HCV and astrocytes

Previous studies with patient autopsy brain samples have identified astrocytes as one of the main HCV target cells in the brain by showing the presence of both HCV (+)-strand RNA and viral proteins in astrocytes (186, 187), whereas our results show that neither of the two most used HCV laboratory models, the HCVcc or HCVpp, were able to productively infect astrocytes (**Fig. 43, 44, 46, 47**). Our step-wise examination of HCV life cycle in astrocytes provided a better understanding of HCV’s interaction with/ non-productive infection of astrocytes. At the cell entry step, even though all the four known HCV receptors are expressed in PHA, their expression levels were much lower compared to Huh7.5.1 and their subcellular localizations were not always on the plasma membrane (**Fig. 45**), which may likely account for the functional defects of these

receptors. These findings were further verified by single-round HCVpp assay showing no HCV envelop-mediated pseudotyped virus entry into PHA (**Fig. 46A**). But interestingly, the luciferase activities in both Env^{pp}- and HCVpp- infected PHA were more than 5 fold higher than mock-infected PHA, which was not observed in Huh7.5.1 (**Fig. 46A**), suggesting non-specific endocytosis of Env^{pp} and HCVpp by PHA. Consistent with this finding, we also found that about 0.01% of HCVcc RNA is detected in PHA immediately following infection (**Fig. 43A**, 2 hr), which is likely a result of binding of HCVcc to PHA and subsequent uptake of HCVcc by PHA. The binding/uptake could be non-specific, as it's very inefficient compared to Huh7.5.1 (5-fold less RNA at 2 hr, **Fig. 43A**), which is known to take up HCV by receptor-mediated endocytosis. Astrocytes are well-known for their active endocytosis activity (293); HIV-1 is shown to enter astrocytes by endocytosis and very few of the endocytosed virions are able to escape from endosomal degradation to establish latent infection in astrocytes (294, 295). Therefore, it is possible that HCV can non-specifically and thus inefficiently bind to astrocytes and then be endocytosed.

At the RNA translation and replication step, our results show that (+)-strand HCV genomic RNA can be detected in astrocytes 72 hr after virus removal (**Fig. 43A**) and that astrocytes support HCV IRES-dependent translation (**Fig. 49B**) but not HCV RNA replication (**Fig. 51B & C**). These results are consistent with previous findings from patient brain samples that HCV (+)-strand RNA and viral proteins (evidence for translation) are present in astrocytes but no (-)-strand HCV RNA (evidence for replication) can be detected (186, 187). Importantly, HCV (+)-strand RNA were only detected in astrocytes from HIV-1/HCV co-infected patients but not from HCV mono-infected patients, even though HCV viral proteins are detected in both patient groups (186, 187). Therefore, HCV infection of astrocytes *in vivo* seems to be inefficient, at

least when without co-factors such as HIV-1 co-infection. This may also help explain why no HCV structural proteins core or E2 can be detected in our three day infection experiment (**Fig. 43B**): a result from the combination of low infection efficiency (no active replication), no continuous virus input and relatively low sensitivity of HCV core/ E2 immunostaining. In addition, we found that miR122, the essential microRNA for HCV RNA stability and replication (37, 46, 47), is expressed at extremely low level in PHA (**Fig. 49C**). We also showed that miR122 ectopic expression can enhance HCV RNA translation and overall HCV RNA stability and replication in PHA (**Fig. 49 & 50**). However, its expression alone was insufficient to enable astrocytes to support HCV replication (**Fig. 51B & C**), raising the possibility that astrocytes lack facilitating factors besides miR122 or have inhibitory factors for HCV replication. Furthermore, even if HCV free-virus infection and CCCM transmission both fail to infect astrocytes, it cannot be excluded that exosome-associated HCV may do so; it is also likely that there is potential compartmentalized HCV evolution in the CNS (183, 185, 296), while the HCV strains used in the current study are not neurotropic and do not afford the astrocyte infection (refer to the Perspective section for details).

Even though HCV infection of astrocytes is non-productive, its interaction with astrocytes including binding to and maybe endocytosis by astrocytes can still lead to changes in astrocytes. Our data demonstrated that PHA challenge with HCV for 2 hr stimulated IL-18 expression in PHA (**Fig. 53A**). Interestingly, a very recent report has also shown that HCV stimulates IL-1 β and IL-18 expression in macrophage and HCV p7 protein is identified to be responsible for the induction of IL-1 β (297). HCV HCV RNA is shown to be present in the form of exosomes (102) and trigger INF- α secretion in plasmacytoid dendritic cells (145). Human astrocytes express a panel of Toll-like receptors, with TLR3 expressed at a particularly high level (200). Activation of TLR3 by endosomal double-

strand RNA, which is commonly seen during RNA virus infection including HCV, usually leads to the production of proinflammatory cytokines in astrocytes, including IL-18 (200, 298). Nonetheless, further experiments are needed to understand how HCV-induced IL-18 production in astrocytes is triggered and which component(s) of the HCV virus is responsible for the induction. Besides astrocytes, microglia could also play important roles in HCV-related CNS abnormalities. Microglia from HCV-infected subjects are found to be positive for both (+)- and (-)-strand HCV RNA and viral proteins, indicating active viral replication and productive HCV infection in microglia (186, 187). In addition, microglia in HCV-infected brain are found to be highly activated and produce proinflammatory cytokines such as TNF- α , IL-1 β and IL-8 (188); *in vitro* infection of primary macrophage with HCV patient plasma also induces TNF- α and IL-8 production (178). Thus, HCV interactions with both astrocytes and microglia could contribute to HCV-associated CNS abnormalities.

Our finding that HCV exposure induced IL-18 expression in astrocytes should be considered highly significant in HCV interaction with astrocytes. IL-18 is a proinflammatory cytokine that belongs to the IL-1 family (e.g. IL-1 β) (299). It is mainly produced by macrophage in the peripheral and its expression is upregulated in a number of virus infections including influenza A virus, adenovirus and murine cytomegalovirus (300-302). IL-18 induces strong IFN- γ production via NF- κ B activation in a toll-like receptor (TLR) signal-dependent manner (303, 304); IFN- γ , in return, also induces more IL-18 expression, thus forming a positive feedback and eliciting an proinflammatory and anti-viral response (300, 302, 305). Recently, IL-18 polymorphisms are shown to be associated with the outcomes of HCV infection and treatment (306-308). In HCV patients, elevated sera and intrahepatic IL-18 levels and IL-18 receptor expression in liver are correlated with increased chronicity of the infection, higher levels of liver

inflammation, higher frequency of fibrosis, cirrhosis, and hepatocellular carcinoma, and worse disease outcome (309-311). These previous studies suggest that IL-18, as an integral part of HCV-induced immune response, contributes to HCV's disease progression in the liver. In the brain, IL-18 and its receptor are found expressed on astrocyte, microglia and neurons; they have been shown to be key players in neuroinflammation and neurodegeneration (250, 312). During Japanese Encephalitis virus infection, microglia and astrocytes both produce IL-18 and IL-1 β , which induces the release of more proinflammatory cytokines and impairment of neuronal survival (313). It is clear that the roles of IL-18 in HCV-associated CNS abnormalities merit further investigation.

IL-18 was shown to be induced in HCV-stimulated PHA (**Fig. 53**). We naturally followed up to determine that whether conditioned media from these astrocytes (presumably containing IL-18 and possibly other yet to be identified neurotoxic factors) were neurotoxic; they were not (**Fig. 54A**). But it is important to point out that the IFN- γ -stimulated PHA conditioned media didn't exhibit neurotoxicity, either (**Fig.54A**). The negative results could be simply explained by the low level of IL-18 in the culture supernatant or IFN- γ used. Nevertheless, undetectable neuron viability change does not necessarily indicate that increased IL-18 level is not able to affect neuron functions in more subtle ways, considering its critical role in neuroninflammation (250). However, it was very surprising that HCV itself was sufficient to cause neurotoxicity at the viral titer of 4.7×10^7 vge/ml (**Fig. 54B & C**). Whether this viral titer required for neurotoxicity is physiologically relevant or not is unknown at present; to our knowledge there is no literature about the amount of viral RNA in brain samples of HCV-infected subjects. Recombinant HCV core protein (subtype 1b) has been recently shown to cause

neurotoxicity in both cell culture and mice (314), suggesting that HCV core protein contributes to HCV neurotoxicity. But it does not exclude the possibility that other components of the virus such as the envelope proteins and viral RNA may also contribute to HCV neurotoxicity; further experiments are needed to address this question. In addition, recent studies find that neurons also express TLRs including TLR-3 and they are able to mount anti-viral IFN response upon various virus infection/stimulation (315), suggesting a potential mechanism of how virus components may lead to neuronal cell death.

Conclusions

In summary of this study, we characterized the CCCM HCV transmission by demonstrating its dependency on HCV receptors and actin cytoskeleton, its rapid and productive nature, and its spatial and temporal details under live cell imaging. We also showed evidence that a subpopulation of HCV virions in both infected-cell culture-supernatants and patient plasma co-fractionated with exosomes and these exosomes-associated HCV were infectious to hepatocytes, suggesting a new route of HCV transmission: exosomes-associated HCV infection. These findings about alternative routes for HCV transmission provide new insights into HCV infection and shall aid in the development of new and effective strategies for preventing and treating HCV infection. Furthermore, with available HCV cell culture model systems, we characterized the interaction between HCV and astrocytes, one of the putative HCV target cells in the brain. We demonstrated that astrocytes support HCV translation but not entry and replication. We also showed that HCV exposure stimulated IL-18 expression in astrocytes and that HCV itself exhibited direct neurotoxicity. These findings shall add to our understanding of HCV infection of the CNS and possible contributions to HCV-induced CNS abnormalities. All in all, the current study shall aid in the future

development of new therapies for preventing HCV infection and treating HCV infection in the periphery and the CNS.

PERSPECTIVE

Future directions

Base on the current study, future studies can be conducted to further understand the different transmission routes of HCV, HCV-related CNS abnormalities, and how our findings can benefit the prevention and treatment of HCV infection and related diseases. Even though our results suggest a potential role of lamellipodium (**Fig. 27-29**), the underlying mechanisms of CCCM HCV transmission remain largely unclear. The same live cell imaging experiment as in Fig. 27-29 but with donor cells also labeled with lamellipodium-specific markers, such as GFP-tagged actin (275) or the Rac small GTPase (276), can be performed (the target cells can be labeled with cell-tracking dyes of other colors) to test the possible involvement of lamellipodium. In addition, similar live imaging with GFP-tagged actin or HCV receptors in the presence of cytochalasin D may clarify the specific roles of actin in CCCM transfer; live imaging with MVB markers may reveal the true identity of the viral puncta; live imaging with the tagged TJ marker zonula occludens-1 (ZO-1) together with tagged CLDN1 or OCLN may reveal whether the CCCM HCV transfer is mediated by CLDN1 and OCLN inside functional TJs and thereby whether HCV adopts the “transfer across TJ” strategy for its CCCM transfer.

In addition, further experiments are needed to confirm the association/ inclusion of HCV virions in exosomes and to characterize this alternative route of HCV transmission. For instance, experiments can be performed to inhibit exosome production and determine its effect on HCV production, to immunocapture exosomes and determine whether HCV is co-captured, and to test whether cell entry of exosome-HCV is dependent on HCV receptors. The contribution of this new route of HCV transmission to viral spread and systemic infection can also be examined. For instance, it can be determined whether

exosome-associated HCV can bypass the HCV receptors and contribute to extra-hepatic HCV infection, and whether “Trojan exosome” can cross the BBB and bring HCV into the CNS.

Moreover, based on our finding that HCV exposure leads to direct neurotoxicity (**Fig. 54**), future studies can be performed to understand the underlying mechanisms. Neither HCV RNA nor viral proteins were found in neurons from post-mortem HCV patient brain samples, suggesting that HCV does not infect neurons (186, 187). Therefore, HCV’s direct neurotoxicity must be caused by one or more of its structural components, which include HCV RNA, core protein, envelope proteins E1, E2 and maybe the viroporin p7. All of HCV core, E1, E2, and p7 proteins have been suggested to induce apoptosis when expressed alone or in the context of HCV infection in hepatocytes and immune cells [reviewed in (316)], but not much is known when they are exposed to cells without intracellular expression or productive infection. The only exception is a recent study showing that exposure to recombinant HCV core protein led to neurotoxicity (314), but the underlying mechanisms are not clear. Therefore, to understand HCV direct neurotoxicity, the first step is to determine which structural component(s) of HCV are responsible for it; recombinant HCV proteins E1, E2, p7, and *in vitro* synthesized HCV RNA can be tested. Follow-up experiments can be performed to determine the cellular signaling pathways underlying the observed neurotoxicity: TLR pathways, Fas-/TNF-/tumor-necrosis-related apoptosis-inducing ligand (TRAIL)-mediated apoptosis, autophagy-induced cell death, or some other pathways. Injection of the neurotoxic HCV component(s) directly into mouse brain can also be performed to determine whether neurotoxicity and/or behavior changes are observed.

Furthermore, our study showed that HCV exposure leads to IL-18 production in PHA (**Fig. 53**); future studies can be conducted to characterize this process and explore its potential impact on neuron functions. Our results showed HCV-induced IL-18 expression at the transcriptional level, but IL-18 is also well-known to be regulated at post-translational level by caspase-1 (303). Therefore, it can be first determined whether HCV also induces pro-IL18 cleavage to increase the level of bioactive IL-18. The time course of HCV-induced IL-18 production can then be determined by, e.g., collecting PHA at 6, 12, 24, 48 hr post HCV exposure. To confirm HCV-stimulated IL-18 production in astrocytes *in vivo*, IL-18 expression at both mRNA and protein level may be examined by astrocytes isolation with LCM from post-mortem HCV patient brain samples followed by qRT-PCR or enzyme-linked immunosorbent assay (ELISA). HCV component(s) responsible for IL-18 induction can be determined next. Since our results showed that IL-18 was induced within 24 hr post-exposure, HCV structural component(s) are very likely responsible for it; recombinant core, E1, E2, p7 and *in vitro* synthesized HCV RNA may be tested. Cellular signaling molecules/pathways involved in this process can also be determined: TLRs, caspases, NF- κ B signaling, or maybe something else. After characterization of HCV-induced IL-18 production in PHA, its potential role in neuron function can be explored next. Even though HCV-stimulated PHA conditioned medium didn't cause direct neurotoxicity (**Fig. 53**), it may still lead to neuron dysfunction by affecting, e.g., action potential firing, synapse formation, or dendritic spine formation. Thus, the role of HCV-stimulated PHA conditioned medium in neuron function should be examined more comprehensively and nAb against IL-18 may be used in combination to understand the potential role of IL-18 during this process. Besides possible direct effect on neuron functions, HCV-stimulated astrocytes may also exert its impact on neurons through interactions with microglia, another important player in neuroinflammation. Therefore, it is also interesting to expose microglia to HCV-stimulated PHA conditioned

medium and then examine changes in proinflammatory cytokines production in treated microglia and whether conditioned medium from these microglia may lead to any demise on neuron functions or not.

Lastly, future studies can also focus on the interaction between HCV and microglia, the other putative HCV target cells in the brain, and the possible impact of this interaction on neurons. Besides cell-culture produced HCV model systems, patient sera and a lymphotropic HCV strain, the SB strain (refer to “Extra-hepatic HCV tropism” below for details), may also be tested.

Towards a “cure” for chronic hepatitis C

HCV drug development has greatly advanced since the establishment of HCVcc system in 2005; the first two direct-antiviral agents (DAA), the NS3/4A protease inhibitors telaprevir and boceprevir, were approved in May 2011 and more DAAs targeting different viral proteins and cellular co-factors in different steps of HCV life cycle are currently under clinical trials (317). It is expected that a combinatory therapy composed of different DAAs, similar to the HIV-1 HARRT therapy, will eventually become the new SOC of HCV treatment in the near future. Such a combinatory therapy is expected to meet at least the following two requirements. First, it must be free of interferon α , which leads to very severe adverse effects and high discontinuation rates. Secondly, it must have as high as possible cure rates, which is a benefit from the combinatory design of the therapy that minimal viral resistance exists when DAAs targeting different viral life cycle steps are administrated simultaneously. The cure rate of a therapy is indicated by the percentage of patients achieving sustained virological response (SVR): SVR12 indicates undetectable HCV RNA level in 12 weeks post-treatment. At the American Association for the Study of Liver Diseases (AASLD) meeting in November 2012, cure

rates of up to 100% from a multitude of interferon-free HCV clinical trials were presented. The AVIATOR trial from Abbott Laboratories, the AI444-040 trial from Bristol-Myers Squibb/Gilead Sciences, and the ELECTRON trial from Gilead Sciences, all of which are phase II trials, are the most promising. They show SVR12 in between 84-100% in the treatment-naïve group with HCV subtype 1 and the AVIATOR trial also shows 89-93% SVR12 in the treatment-experienced group with HCV subtype 1 (318-320). Among HCV subtype 2 and 3 patients, the AI444-040 trial shows the highest cure rates: 88-100% SVR24 in the treatment-naïve group (319). Further clinical trials with the above promising candidates are moving forward; early stages of interferon-free clinical trials for other HCV subtypes are also ongoing. However, the above clinical trials mainly focus on patients with no or mild liver damages; HCV treatment in patients with severe liver diseases such as compensated cirrhosis is more complicated due to poor tolerability and high discontinuation rates (321, 322). Treatment of HCV in HIV-1-co-infected patients and post-liver transplant patients are also more difficult because of the potential drug-drug interactions between HCV drugs and HIV-1 drugs or immunosuppressant. Nevertheless, researches and clinical trials for both situations are ongoing and the results are promising (323-327). Since the discovery of HCV in 1989, we had never been closer to a cure for HCV than we are now; the results from the ongoing clinical trials grant us reasons to believe that chronic hepatitis C, a disease that claims more than 350,000 lives annually, may be cured with three months of oral antiviral drugs in the near future.

HCV mouse models

Despite intense research efforts on small animal models for HCV in last two decades, chimpanzees are still the only complete animal model for HCV infection, which recapitulates the full viral life cycle and host immune response. They remain the best

model for studying HCV-related innate and adaptive host immune responses and testing HCV vaccines, though it is not considered a good model for the study of chronic liver diseases and HCC (291). Great advances have been made in the development of HCV mouse models in recent years. Generally, two strategies for humanized mouse models are adopted: to genetically humanize cellular factors required for a complete HCV life cycle in mouse hepatocytes, or to replace mouse liver and/or immune cells with human hepatocytes and/ or leukocytes engraftment. For the first strategy, a recent report shows that with blunted innate immunity, abundant miR-122, and expression of HCV receptors, mouse liver-derived cell lines can be infected with HCV and produce infectious virus (328). But there is still a distance from a cell-culture model to a mouse model. For the second strategy, the uPa-SCID mice (urokinase-type plasminogen activator-severe combined immunodeficiency) and the FRG mice [Fah (femeral acetoacetate hydrolase)^{-/-}Rag2^{-/-}IL2rg^{-/-}] are developed based on the combination of immunodeficient mice, genetic modifications to degrade mouse hepatocytes, and transplantation of primary human hepatocytes (329-331). These two models demonstrate high levels of HCV infection in the liver and high titers of viremia; they are thereby used to test antivirals before chimpanzee study and clinical trial (329, 332-334). However, due to their immunodeficiency background, both of these two models lack adaptive immune response against HCV. Therefore a new mouse model was developed recently to overcome this issue: the AFC8 (albumin promoter)-hu HSC/hep mice (292). Cell death of mouse hepatocytes is induced in the mice and co-transplantation of human hematopoietic stem cells (HSC) and hepatocyte progenitors is performed, resulting in liver repopulation with human hepatocytes and immune reconstitution with human leukocytes. Therefore, this model features HCV-specific cellular immune response, hepatitis and liver fibrosis. It constitutes the first small animal model of HCV infection suitable for studying adaptive immunity and pathogenesis. Though limitations of the

current model are present that no HCV viremia can be detected in the infected mice, likely due to the low level of human hepatocytes engraftment (~15%), it is possible that the problem can be solved by future optimization of the model. More importantly, as the only available small animal HCV model with both human hepatocytes and human immune system, this model may be utilized to study HCV infection of the immune cells, and to test the “Trojan PBMC” and the “Trojan exosome” hypotheses for HCV entry into the CNS.

HCV infection of PBMC and its contribution to the pathogenesis of HCV-related diseases

The association of HCV infection with immune dysfunction and LPD has been established for a long time (164-168). Active replication of HCV in PBMC, after decades of debates, is also accepted now based on two lines of evidence. On one hand, HCV (-)-strand RNA, the replication intermediate, is successfully detected in PBMC with improved methodology (156, 157, 335). On the other hand, viral RNA persists in mononuclear blood cells inoculated into SCID mice for up to two months and a second *in vivo* passage of HCV-RNA-positive cells to other mice is successful (336). The contribution of HCV infection of PBMC to the pathogenesis of HCV-related diseases include its impact on immune system functions, its involvement in LPDs, and its role in the persistence of HCV infection and HCV recurrence.

First, immune responses in chronic hepatitis C patients have been well-studied, though seldom do studies explore the role of HCV infection of PBMC in immune system function, likely due to the small percentage of infected cells and relatively low viral replication in PBMC (16). The few available studies show some interesting results. One of them suggests that endogenous presentation of HCV antigens by infected B-cells and

monocytes may contribute to immune tolerance of HCV and viral persistence (177). The other two studies from one group demonstrate that HCV infection and replication in T cells leads to impaired IFN- γ signaling, reduced proliferation and enhanced Fas-mediated apoptosis. These results suggest that HCV replication in T cells may play a role in both the disturbance of Th1 commitment/ Th1 hyporesponsiveness and the regulation of T cell proliferation and apoptosis (337, 338). Future studies are needed to further understand the impact of HCV infection of PBMC on immune system functions.

Second, even though the association of HCV with LPDs is established, the underlying mechanisms are not completely understood. But it is believed that the activation of the oncogene bcl-2 plays a critical role. The frequency of bcl-2 rearrangement is significantly higher in chronic HCV infection, especially in cases evolved to MC and LPD (339, 340). Bcl-2 recombination [translocation (14;18)] leads to the activation of the bcl-2 oncogene and the inhibition of B-cell apoptosis, resulting in progressive accumulation of lymphocytic cells and eventually LPD (341, 342).

Lastly, as one of the extra-hepatic reservoirs harboring viral replication, it is suggested that HCV infection of PBMC contribute to persistent HCV infection and HCV recurrence in spontaneously or therapeutically cleared patients and patients with liver transplantation (156, 157, 172).

Extra-hepatic HCV tropism

In spite of detection of viral RNA and proteins in patient PBMC and successful infection of PBMC with HCV patient plasma, entry, infection and replication of cell-culture produced HCV in PBMC and lymphocytic cell lines have been unsuccessful [(181, 182) and our unpublished data]. Similarly, infection of and replication in primary human

astrocytes are not detected with HCVpp/ HCVcc/ HCV-Rluc, though RNA translation is supported in PHA (Results section, CHAPTER 3). Interestingly, sequence analysis of HCV RNA isolated from different patient tissues shows that RNA sequence from the CNS is closer to that from PBMC, but not serum or liver (183, 185), indicating compartmentalization of viral quasispecies. The four known HCV receptors are expressed on PHA (**Fig. 45**) and subsets of, if not all, PBMC (181), though at varying levels. But HCVpp entry into PBMC or PHA does not occur [**Fig. 46, 47** and (181)]. In addition, CD5 is recently identified as the receptor mediating entry of patient plasma-derived HCV into T lymphocytes (179, 180): it seems that different HCV receptors are mediating HCV entry into different cells. Comparison of HCV RNA isolated from different tissues show sequence differences between liver and lymphoid/ brain isolates in both the hypervariable region (HVR) of the glycoprotein E2 and the 5'UTR, which are critical regions for receptor binding/ cell entry and RNA replication, respectively (185, 296). Collectively, the above information is suggestive of a model of extra-hepatic (PBMC and CNS) HCV infection, that intrinsic sequence differences between current cell-culture produced HCV and patient-derived HCV define the different tissue tropisms: liver or lymphoid/ brain. Most of the cell-culture produced HCV strains are selected and widely used based on their high infectivity of hepatocytes, which may explain their inability to infect extra-hepatic cells. Interestingly, a lymphotropic strain of HCV, the SB strain, was established ten years ago; it is cultured in a B-cell line (SB cells) derived from an HCV-infected non-Hodgkin's B-cell lymphoma (343). The SB strain belongs to HCV subtype 2b and it can productively infect B-cells and to a less extent, T cells (337, 338, 343, 344). Nevertheless, the genome of the SB strain is not sequenced; its infection of other PBMC subsets or hepatocytes is not yet tested. With more characterization in the future, the SB strain may become a good cell culture model system for studying extra-hepatic HCV infections/ manifestations. It may also provide a powerful tool for testing

antivirals for the treatment of extra-hepatic infections and contribute to further understanding of HCV infection of PBMC/ brain and HCV-related extra-hepatic diseases.

Treatment of HCV in PBMC and the CNS

HCV recurrence is sometimes observed in patients receiving liver transplantation and patients spontaneously or therapeutically cleared of HCV (156, 157, 165, 171). Sequence analysis of HCV RNA before and after recurrence/ transplantation suggests that the relapse can be from undetectable HCV in the liver (“occult” infection) or viral reservoir in PBMC (156, 345, 346). It is expected that new HCV treatment regimens with combinations of DAAs can achieve SVR in up to 100% patients. Unfortunately, SVR does not necessarily always lead to a true cure. It remains unknown whether the upcoming new “cocktail therapy” can completely eradicate occult HCV and HCV reservoirs at extra-hepatic sites, such as PBMC and the brain. Two major concerns exist. On one hand, all the DAAs are screened in HCV-infected hepatocytes due to the lack of a widely accepted lymphotropic HCV strain and a corresponding HCV-PBMC cell culture model. Considering the potential differences between hepatic and extra-hepatic HCV strains, it cannot be guaranteed that these DAAs will be as effective treating HCV infection of PBMC/ brain cells as they are for hepatocytes. On the other hand, even though the new regimen is able to clear HCV in the periphery, HCV reservoir in the privileged brain remains a risk factor for relapse. Therefore the problem of HCV reemergence after the achievement of peripheral SVR may still exist. Future studies on HCV infection of brain cells such as microglia and its impact on neuron functions are needed to further understand the mechanisms of HCV infection of the CNS and how it can be treated to accomplish a true systemic cure for HCV in the new “cocktail therapy” era. Last but not least, with “Trojan exosomes” as a potential route for HCV entry into

the CNS, in turn, “Trojan exosomes” loaded with anti-HCV drugs may be used as a method to cross the BBB and deliver the antivirals into the brain.

REFERENCES

1. Mohd Hanafiah K, Groeger J, Flaxman AD, Wiersma ST. 2013. Global epidemiology of hepatitis C virus infection: new estimates of age-specific antibody to HCV seroprevalence. *Hepatology* 57: 1333-42
2. Armstrong GL, Wasley A, Simard EP, McQuillan GM, Kuhnert WL, Alter MJ. 2006. The prevalence of hepatitis C virus infection in the United States, 1999 through 2002. *Ann Intern Med* 144: 705-14
3. Mallet V, Vallet-Pichard A, Pol S. 2010. New trends in hepatitis C management. *La Presse Médicale* 39: 446-51
4. Poynard T, Bedossa P, Opolon P. 1997. Natural history of liver fibrosis progression in patients with chronic hepatitis C. The OBSVIRC, METAVIR, CLINIVIR, and DOSVIRC groups. *Lancet* 349: 825-32
5. Brown RS. 2005. Hepatitis C and liver transplantation. *Nature* 436: 973-8
6. Ip PP, Nijman HW, Wilschut J, Daemen T. 2012. Therapeutic vaccination against chronic hepatitis C virus infection. *Antiviral Res* 96: 36-50
7. Feinstone SM, Hu DJ, Major ME. 2012. Prospects for prophylactic and therapeutic vaccines against hepatitis C virus. *Clin Infect Dis* 55 Suppl 1: S25-32
8. Sarrazin C, Zeuzem S. 2010. Resistance to Direct Antiviral Agents in Patients With Hepatitis C Virus Infection. *Gastroenterology* 138: 447-62
9. Schinazi RF, Bassit L, Gavegnano C. 2010. HCV drug discovery aimed at viral eradication. *Journal of Viral Hepatitis* 17: 77-90
10. Irshad M, Khushboo I, Singh S. 2008. Hepatitis C virus (HCV): a review of immunological aspects. *Int Rev Immunol* 27: 497-517
11. Mallet V, Vallet-Pichard A, Pol S. 2010. New trends in hepatitis C management. *Presse Med* 39: 446-51
12. Tellinghuisen TL, Evans MJ, von Hahn T, You S, Rice CM. 2007. Studying Hepatitis C Virus: Making the Best of a Bad Virus. *Journal of Virology* 81: 8853-67
13. Koike K. 2009. Steatosis, liver injury, and hepatocarcinogenesis in hepatitis C viral infection. *Journal of Gastroenterology* 44: 82-8
14. Chung RT, Gale M, Jr., Polyak SJ, Lemon SM, Liang TJ, Hoofnagle JH. 2008. Mechanisms of action of interferon and ribavirin in chronic hepatitis C: Summary of a workshop. *Hepatology* 47: 306-20
15. Tang H, Grisé H. 2009. Cellular and molecular biology of HCV infection and hepatitis. *Clinical Science* 117: 49-65
16. Dustin LB, Rice CM. 2007. Flying Under the Radar: The Immunobiology of Hepatitis C. *Annual Review of Immunology* 25: 71-99
17. Neuman MG, Sha K, Esguerra R, Zakhari S, Winkler RE, Hilzenrat N, Wyse J, Cooper CL, Seth D, Gorrell MD, Haber PS, McCaughan GW, Leo MA, Lieber CS, Voiculescu M, Buzatu E, Ionescu C, Dudas J, Saile B, Ramadori G. 2007. Inflammation and Repair in Viral Hepatitis C. *Digestive Diseases and Sciences* 53: 1468-87
18. Thimme R, Neumann-Haefelin C, Boettler T, Blum HE. 2008. Highlight: 3rd Semmering Conference 2007. *Biological Chemistry* 389: 457-67
19. Castello G, Scala S, Palmieri G, Curley SA, Izzo F. 2010. HCV-related hepatocellular carcinoma: From chronic inflammation to cancer. *Clinical Immunology* 134: 237-50
20. Pawlotsky JM. 2003. Hepatitis C virus genetic variability: pathogenic and clinical implications. *Clin Liver Dis* 7: 45-66

21. Budkowska A. 2009. Mechanism of cell infection with hepatitis C virus (HCV) – a new paradigm in virus-cell interaction. *Pol J Microbiol* 58: 93-8
22. Barth H, Schafer C, Adah MI, Zhang F, Linhardt RJ, Toyoda H, Kinoshita-Toyoda A, Toida T, Van Kuppevelt TH, Depla E, Von Weizsacker F, Blum HE, Baumert TF. 2003. Cellular binding of hepatitis C virus envelope glycoprotein E2 requires cell surface heparan sulfate. *J Biol Chem* 278: 41003-12
23. Seipp S, Mueller HM, Pfaff E, Stremmel W, Theilmann L, Goeser T. 1997. Establishment of persistent hepatitis C virus infection and replication in vitro. *J Gen Virol* 78 (Pt 10): 2467-76
24. Monazahian M, Bohme I, Bonk S, Koch A, Scholz C, Grethe S, Thomssen R. 1999. Low density lipoprotein receptor as a candidate receptor for hepatitis C virus. *J Med Virol* 57: 223-9
25. Pileri P, Uematsu Y, Campagnoli S, Galli G, Falugi F, Petracca R, Weiner AJ, Houghton M, Rosa D, Grandi G, Abrignani S. 1998. Binding of hepatitis C virus to CD81. *Science* 282: 938-41
26. Catanese MT, Ansuini H, Graziani R, Huby T, Moreau M, Ball JK, Paonessa G, Rice CM, Cortese R, Vitelli A, Nicosia A. 2009. Role of Scavenger Receptor Class B Type I in Hepatitis C Virus Entry: Kinetics and Molecular Determinants. *Journal of Virology* 84: 34-43
27. Scarselli E, Ansuini H, Cerino R, Roccasecca RM, Acali S, Filocamo G, Traboni C, Nicosia A, Cortese R, Vitelli A. 2002. The human scavenger receptor class B type I is a novel candidate receptor for the hepatitis C virus. *EMBO J* 21: 5017-25
28. Evans MJ, von Hahn T, Tscherne DM, Syder AJ, Panis M, Wolk B, Hatzioannou T, McKeating JA, Bieniasz PD, Rice CM. 2007. Claudin-1 is a hepatitis C virus co-receptor required for a late step in entry. *Nature* 446: 801-5
29. Ploss A, Evans MJ, Gaysinskaya VA, Panis M, You H, de Jong YP, Rice CM. 2009. Human occludin is a hepatitis C virus entry factor required for infection of mouse cells. *Nature* 457: 882-6
30. Brazzoli M, Bianchi A, Filippini S, Weiner A, Zhu Q, Pizza M, Crotta S. 2008. CD81 is a central regulator of cellular events required for hepatitis C virus infection of human hepatocytes. *J Virol* 82: 8316-29
31. Zeisel MB, Koutsoudakis G, Schnober EK, Haberstroh A, Blum HE, Cosset Fo-Lc, Wakita T, Jaeck D, Doffoel M, Royer C, Soulier E, Schvoerer E, Schuster C, Stoll-Keller Fo, Bartenschlager R, Pietschmann T, Barth H, Baumert TF. 2007. Scavenger receptor class B type I is a key host factor for hepatitis C virus infection required for an entry step closely linked to CD81. *Hepatology* 46: 1722-31
32. Benedicto I, Molina-Jimenez F, Bartosch B, Cosset FL, Lavillette D, Prieto J, Moreno-Otero R, Valenzuela-Fernandez A, Aldabe R, Lopez-Cabrera M, Majano PL. 2009. The tight junction-associated protein occludin is required for a postbinding step in hepatitis C virus entry and infection. *J Virol* 83: 8012-20
33. Harris HJ, Davis C, Mullins JG, Hu K, Goodall M, Farquhar MJ, Mee CJ, McCaffrey K, Young S, Drummer H, Balfe P, McKeating JA. 2010. Claudin association with CD81 defines hepatitis C virus entry. *J Biol Chem* 285: 21092-102
34. Harris HJ, Farquhar MJ, Mee CJ, Davis C, Reynolds GM, Jennings A, Hu K, Yuan F, Deng H, Hubscher SG, Han JH, Balfe P, McKeating JA. 2008. CD81 and claudin 1 coreceptor association: role in hepatitis C virus entry. *J Virol* 82: 5007-20
35. Hsu M, Zhang J, Flint M, Logvinoff C, Cheng-Mayer C, Rice CM, McKeating JA. 2003. Hepatitis C virus glycoproteins mediate pH-dependent cell entry of pseudotyped retroviral particles. *Proc Natl Acad Sci U S A* 100: 7271-6

36. Tscherne DM, Jones CT, Evans MJ, Lindenbach BD, McKeating JA, Rice CM. 2006. Time- and temperature-dependent activation of hepatitis C virus for low-pH-triggered entry. *J Virol* 80: 1734-41
37. Jopling CL, Yi M, Lancaster AM, Lemon SM, Sarnow P. 2005. Modulation of hepatitis C virus RNA abundance by a liver-specific MicroRNA. *Science* 309: 1577-81
38. Gosert R, Egger D, Lohmann V, Bartenschlager R, Blum HE, Bienz K, Moradpour D. 2003. Identification of the hepatitis C virus RNA replication complex in Huh-7 cells harboring subgenomic replicons. *J Virol* 77: 5487-92
39. Komurian-Pradel F, Perret M, Deiman B, Sodoyer M, Lotteau V, Paranhos-Baccala G, Andre P. 2004. Strand specific quantitative real-time PCR to study replication of hepatitis C virus genome. *J Virol Methods* 116: 103-6
40. Quadri R, Rubbia-Brandt L, Abid K, Negro F. 2001. Detection of the negative-strand hepatitis C virus RNA in tissues: implications for pathogenesis. *Antiviral Res* 52: 161-71
41. Sherker AH, Twu JS, Reyes GR, Robinson WS. 1993. Presence of viral replicative intermediates in the liver and serum of patients infected with hepatitis C virus. *J Med Virol* 39: 91-6
42. Goergen D, Niepmann M. 2012. Stimulation of Hepatitis C Virus RNA translation by microRNA-122 occurs under different conditions in vivo and in vitro. *Virus Res* 167: 343-52
43. Fehr C, Conrad KD, Niepmann M. 2012. Differential stimulation of hepatitis C virus RNA translation by microRNA-122 in different cell cycle phases. *Cell Cycle* 11: 277-85
44. Henke JI, Goergen D, Zheng J, Song Y, Schuttler CG, Fehr C, Junemann C, Niepmann M. 2008. microRNA-122 stimulates translation of hepatitis C virus RNA. *EMBO J* 27: 3300-10
45. Conrad KD, Giering F, Erfurth C, Neumann A, Fehr C, Meister G, Niepmann M. 2013. MicroRNA-122 dependent binding of Ago2 protein to hepatitis C virus RNA is associated with enhanced RNA stability and translation stimulation. *PLoS One* 8: e56272
46. Li Y, Masaki T, Yamane D, McGivern DR, Lemon SM. 2013. Competing and noncompeting activities of miR-122 and the 5' exonuclease Xrn1 in regulation of hepatitis C virus replication. *Proc Natl Acad Sci U S A* 110: 1881-6
47. Shimakami T, Yamane D, Jangra RK, Kempf BJ, Spaniel C, Barton DJ, Lemon SM. 2012. Stabilization of hepatitis C virus RNA by an Ago2-miR-122 complex. *Proc Natl Acad Sci U S A* 109: 941-6
48. Jangra RK, Yi M, Lemon SM. 2010. Regulation of hepatitis C virus translation and infectious virus production by the microRNA miR-122. *J Virol* 84: 6615-25
49. Fukuhara T, Kambara H, Shiokawa M, Ono C, Katoh H, Morita E, Okuzaki D, Maehara Y, Koike K, Matsuura Y. 2012. Expression of microRNA miR-122 facilitates an efficient replication in nonhepatic cells upon infection with hepatitis C virus. *J Virol* 86: 7918-33
50. Kambara H, Fukuhara T, Shiokawa M, Ono C, Ohara Y, Kamitani W, Matsuura Y. 2012. Establishment of a novel permissive cell line for the propagation of hepatitis C virus by expression of microRNA miR122. *J Virol* 86: 1382-93
51. Su TH, Liu CH, Liu CJ, Chen CL, Ting TT, Tseng TC, Chen PJ, Kao JH, Chen DS. 2013. Serum microRNA-122 level correlates with virologic responses to pegylated interferon therapy in chronic hepatitis C. *Proc Natl Acad Sci U S A* 110: 7844-9
52. Janssen HL, Reesink HW, Lawitz EJ, Zeuzem S, Rodriguez-Torres M, Patel K, van der Meer AJ, Patick AK, Chen A, Zhou Y, Persson R, King BD, Kauppinen S, Levin

- AA, Hodges MR. 2013. Treatment of HCV infection by targeting microRNA. *N Engl J Med* 368: 1685-94
53. McLauchlan J. 2009. Hepatitis C virus: viral proteins on the move. *Biochem Soc Trans* 37: 986-90
54. Barba G, Harper F, Harada T, Kohara M, Goulinet S, Matsuura Y, Eder G, Schaff Z, Chapman MJ, Miyamura T, Brechot C. 1997. Hepatitis C virus core protein shows a cytoplasmic localization and associates to cellular lipid storage droplets. *Proc Natl Acad Sci U S A* 94: 1200-5
55. Boulant S, Targett-Adams P, McLauchlan J. 2007. Disrupting the association of hepatitis C virus core protein with lipid droplets correlates with a loss in production of infectious virus. *J Gen Virol* 88: 2204-13
56. Miyanari Y, Atsuzawa K, Usuda N, Watashi K, Hishiki T, Zayas M, Bartenschlager R, Wakita T, Hijikata M, Shimotohno K. 2007. The lipid droplet is an important organelle for hepatitis C virus production. *Nat Cell Biol* 9: 1089-97
57. Shi ST, Polyak SJ, Tu H, Taylor DR, Gretch DR, Lai MM. 2002. Hepatitis C virus NS5A colocalizes with the core protein on lipid droplets and interacts with apolipoproteins. *Virology* 292: 198-210
58. Boulant S, Douglas MW, Moody L, Budkowska A, Targett-Adams P, McLauchlan J. 2008. Hepatitis C virus core protein induces lipid droplet redistribution in a microtubule- and dynein-dependent manner. *Traffic* 9: 1268-82
59. Jirasko V, Montserret R, Appel N, Janvier A, Eustachi L, Brohm C, Steinmann E, Pietschmann T, Penin F, Bartenschlager R. 2008. Structural and functional characterization of nonstructural protein 2 for its role in hepatitis C virus assembly. *J Biol Chem* 283: 28546-62
60. Jones CT, Murray CL, Eastman DK, Tassello J, Rice CM. 2007. Hepatitis C virus p7 and NS2 proteins are essential for production of infectious virus. *J Virol* 81: 8374-83
61. Lohmann V, Korner F, Koch J, Herian U, Theilmann L, Bartenschlager R. 1999. Replication of subgenomic hepatitis C virus RNAs in a hepatoma cell line. *Science* 285: 110-3
62. Pietschmann T, Kaul A, Koutsoudakis G, Shavinskaya A, Kallis S, Steinmann E, Abid K, Negro F, Dreux M, Cosset FL, Bartenschlager R. 2006. Construction and characterization of infectious intragenotypic and intergenotypic hepatitis C virus chimeras. *Proc Natl Acad Sci U S A* 103: 7408-13
63. Steinmann E, Penin F, Kallis S, Patel AH, Bartenschlager R, Pietschmann T. 2007. Hepatitis C virus p7 protein is crucial for assembly and release of infectious virions. *PLoS Pathog* 3: e103
64. Benga WJ, Krieger SE, Dimitrova M, Zeisel MB, Parnot M, Lupberger J, Hildt E, Luo G, McLauchlan J, Baumert TF, Schuster C. 2010. Apolipoprotein E interacts with hepatitis C virus nonstructural protein 5A and determines assembly of infectious particles. *Hepatology* 51: 43-53
65. Long G, Hiet MS, Windisch MP, Lee JY, Lohmann V, Bartenschlager R. 2011. Mouse hepatic cells support assembly of infectious hepatitis C virus particles. *Gastroenterology* 141: 1057-66
66. Counihan NA, Rawlinson SM, Lindenbach BD. 2011. Trafficking of hepatitis C virus core protein during virus particle assembly. *PLoS Pathog* 7: e1002302
67. Bartosch B, Dubuisson J, Cosset FL. 2003. Infectious Hepatitis C Virus Pseudo-particles Containing Functional E1-E2 Envelope Protein Complexes. *Journal of Experimental Medicine* 197: 633-42
68. Krieger SE, Zeisel MB, Davis C, Thumann C, Harris HJ, Schnober EK, Mee C, Soulier E, Royer C, Lambotin M, Grunert F, Dao Thi VL, Dreux M, Cosset FL, McKeating JA, Schuster C, Baumert TF. 2010. Inhibition of hepatitis C virus infection by anti-

- claudin-1 antibodies is mediated by neutralization of E2-CD81-claudin-1 associations. *Hepatology* 51: 1144-57
69. Mee CJ, Grove J, Harris HJ, Hu K, Balfe P, McKeating JA. 2007. Effect of Cell Polarization on Hepatitis C Virus Entry. *Journal of Virology* 82: 461-70
70. Zhong J, Gastaminza P, Cheng G, Kapadia S, Kato T, Burton DR, Wieland SF, Uprichard SL, Wakita T, Chisari FV. 2005. Robust hepatitis C virus infection in vitro. *Proc Natl Acad Sci U S A* 102: 9294-9
71. Lindenbach BD, Evans MJ, Syder AJ, Wolk B, Tellinghuisen TL, Liu CC, Maruyama T, Hynes RO, Burton DR, McKeating JA, Rice CM. 2005. Complete replication of hepatitis C virus in cell culture. *Science* 309: 623-6
72. Wakita T, Pietschmann T, Kato T, Date T, Miyamoto M, Zhao Z, Murthy K, Habermann A, Krausslich HG, Mizokami M, Bartenschlager R, Liang TJ. 2005. Production of infectious hepatitis C virus in tissue culture from a cloned viral genome. *Nat Med* 11: 791-6
73. Blight KJ, McKeating JA, Rice CM. 2002. Highly permissive cell lines for subgenomic and genomic hepatitis C virus RNA replication. *J Virol* 76: 13001-14
74. Sattentau Q. 2008. Avoiding the void: cell-to-cell spread of human viruses. *Nat Rev Microbiol* 6: 815-26
75. Ritzenthaler C. 2011. Parallels and distinctions in the direct cell-to-cell spread of the plant and animal viruses. *Curr Opin Virol* 1: 403-9
76. Sattentau QJ. 2011. The direct passage of animal viruses between cells. *Curr Opin Virol* 1: 396-402
77. Duprex WP, McQuaid S, Hangartner L, Billeter MA, Rima BK. 1999. Observation of measles virus cell-to-cell spread in astrocytoma cells by using a green fluorescent protein-expressing recombinant virus. *J Virol* 73: 9568-75
78. Cole NL, Grose C. 2003. Membrane fusion mediated by herpesvirus glycoproteins: the paradigm of varicella-zoster virus. *Rev Med Virol* 13: 207-22
79. Frankel SS, Wenig BM, Burke AP, Mannan P, Thompson LD, Abbondanzo SL, Nelson AM, Pope M, Steinman RM. 1996. Replication of HIV-1 in dendritic cell-derived syncytia at the mucosal surface of the adenoid. *Science* 272: 115-7
80. Dingwell KS, Brunetti CR, Hendricks RL, Tang Q, Tang M, Rainbow AJ, Johnson DC. 1994. Herpes simplex virus glycoproteins E and I facilitate cell-to-cell spread in vivo and across junctions of cultured cells. *J Virol* 68: 834-45
81. Iwasaki Y, Clark HF. 1975. Cell to cell transmission of virus in the central nervous system. II. Experimental rabies in mouse. *Lab Invest* 33: 391-9
82. Mettenleiter TC. 2003. Pathogenesis of neurotropic herpesviruses: role of viral glycoproteins in neuroinvasion and transneuronal spread. *Virus Res* 92: 197-206
83. Lawrence DM, Patterson CE, Gales TL, D'Orazio JL, Vaughn MM, Rall GF. 2000. Measles virus spread between neurons requires cell contact but not CD46 expression, syncytium formation, or extracellular virus production. *J Virol* 74: 1908-18
84. Doceul V, Hollinshead M, van der Linden L, Smith GL. 2010. Repulsion of superinfecting virions: a mechanism for rapid virus spread. *Science* 327: 873-6
85. Sherer NM, Lehmann MJ, Jimenez-Soto LF, Horensavitz C, Pypaert M, Mothes W. 2007. Retroviruses can establish filopodial bridges for efficient cell-to-cell transmission. *Nat Cell Biol* 9: 310-5
86. Kadiu I, Gendelman HE. 2011. Human immunodeficiency virus type 1 endocytic trafficking through macrophage bridging conduits facilitates spread of infection. *J Neuroimmune Pharmacol* 6: 658-75
87. Sowinski S, Jolly C, Berninghausen O, Purbhoo MA, Chauveau A, Kohler K, Oddos S, Eissmann P, Brodsky FM, Hopkins C, Onfelt B, Sattentau Q, Davis DM. 2008.

Membrane nanotubes physically connect T cells over long distances presenting a novel route for HIV-1 transmission. *Nat Cell Biol* 10: 211-9

88. Hubner W, McNerney GP, Chen P, Dale BM, Gordon RE, Chuang FY, Li XD, Asmuth DM, Huser T, Chen BK. 2009. Quantitative 3D video microscopy of HIV transfer across T cell virological synapses. *Science* 323: 1743-7

89. Igakura T, Stinchcombe JC, Goon PK, Taylor GP, Weber JN, Griffiths GM, Tanaka Y, Osame M, Bangham CR. 2003. Spread of HTLV-I between lymphocytes by virus-induced polarization of the cytoskeleton. *Science* 299: 1713-6

90. Jolly C, Kashefi K, Hollinshead M, Sattentau QJ. 2004. HIV-1 cell to cell transfer across an Env-induced, actin-dependent synapse. *J Exp Med* 199: 283-93

91. Jolly C, Sattentau QJ. 2004. Retroviral spread by induction of virological synapses. *Traffic* 5: 643-50

92. Lairmore MD, Haines R, Anupam R. 2012. Mechanisms of human T-lymphotropic virus type 1 transmission and disease. *Curr Opin Virol* 2: 474-81

93. Chen P, Hubner W, Spinelli MA, Chen BK. 2007. Predominant mode of human immunodeficiency virus transfer between T cells is mediated by sustained Env-dependent neutralization-resistant virological synapses. *J Virol* 81: 12582-95

94. Jolly C, Mitar I, Sattentau QJ. 2007. Requirement for an Intact T-Cell Actin and Tubulin Cytoskeleton for Efficient Assembly and Spread of Human Immunodeficiency Virus Type 1. *Journal of Virology* 81: 5547-60

95. Loo YM, Owen DM, Li K, Erickson AK, Johnson CL, Fish PM, Carney DS, Wang T, Ishida H, Yoneyama M, Fujita T, Saito T, Lee WM, Hagedorn CH, Lau DT, Weinman SA, Lemon SM, Gale M, Jr. 2006. Viral and therapeutic control of IFN-beta promoter stimulator 1 during hepatitis C virus infection. *Proc Natl Acad Sci U S A* 103: 6001-6

96. Pal S, Shuhart MC, Thomassen L, Emerson SS, Su T, Feuerborn N, Kae J, Gretch DR. 2006. Intrahepatic hepatitis C virus replication correlates with chronic hepatitis C disease severity in vivo. *J Virol* 80: 2280-90

97. Chang M, Williams O, Mittler J, Quintanilla A, Carithers RL, Jr., Perkins J, Corey L, Gretch DR. 2003. Dynamics of hepatitis C virus replication in human liver. *Am J Pathol* 163: 433-44

98. Timpe JM, Stamataki Z, Jennings A, Hu K, Farquhar MJ, Harris HJ, Schwarz A, Desombere I, Roels GL, Balfe P, McKeating JA. 2008. Hepatitis C virus cell-cell transmission in hepatoma cells in the presence of neutralizing antibodies. *Hepatology* 47: 17-24

99. Nakamura T, Nakayama Y, Teramoto H, Nawa K, Ichihara A. 1984. Loss of reciprocal modulations of growth and liver function of hepatoma cells in culture by contact with cells or cell membranes. *Proc Natl Acad Sci U S A* 81: 6398-402

100. Logvinoff C, Major ME, Oldach D, Heyward S, Talal A, Balfe P, Feinstone SM, Alter H, Rice CM, McKeating JA. 2004. Neutralizing antibody response during acute and chronic hepatitis C virus infection. *Proc Natl Acad Sci U S A* 101: 10149-54

101. Raposo G, Stoorvogel W. 2013. Extracellular vesicles: exosomes, microvesicles, and friends. *J Cell Biol* 200: 373-83

102. Vlassov AV, Magdaleno S, Setterquist R, Conrad R. 2012. Exosomes: current knowledge of their composition, biological functions, and diagnostic and therapeutic potentials. *Biochim Biophys Acta* 1820: 940-8

103. Mathivanan S, Lim JW, Tauro BJ, Ji H, Moritz RL, Simpson RJ. 2010. Proteomics analysis of A33 immunoaffinity-purified exosomes released from the human colon tumor cell line LIM1215 reveals a tissue-specific protein signature. *Mol Cell Proteomics* 9: 197-208

104. Keller S, Konig AK, Marme F, Runz S, Wolterink S, Koensgen D, Mustea A, Sehoul J, Altevogt P. 2009. Systemic presence and tumor-growth promoting effect of ovarian carcinoma released exosomes. *Cancer Lett* 278: 73-81
105. Bang C, Thum T. 2012. Exosomes: new players in cell-cell communication. *Int J Biochem Cell Biol* 44: 2060-4
106. Rieu S, Geminard C, Rabesandratana H, Sainte-Marie J, Vidal M. 2000. Exosomes released during reticulocyte maturation bind to fibronectin via integrin alpha4beta1. *Eur J Biochem* 267: 583-90
107. Tamai K, Tanaka N, Nakano T, Kakazu E, Kondo Y, Inoue J, Shiina M, Fukushima K, Hoshino T, Sano K, Ueno Y, Shimosegawa T, Sugamura K. 2010. Exosome secretion of dendritic cells is regulated by Hrs, an ESCRT-0 protein. *Biochem Biophys Res Commun* 399: 384-90
108. Buschow SI, Nolte-'t Hoen EN, van Niel G, Pols MS, ten Broeke T, Lauwen M, Ossendorp F, Melief CJ, Raposo G, Wubbolts R, Wauben MH, Stoorvogel W. 2009. MHC II in dendritic cells is targeted to lysosomes or T cell-induced exosomes via distinct multivesicular body pathways. *Traffic* 10: 1528-42
109. Stuffers S, Sem Wegner C, Stenmark H, Brech A. 2009. Multivesicular endosome biogenesis in the absence of ESCRTs. *Traffic* 10: 925-37
110. Trajkovic K, Hsu C, Chiantia S, Rajendran L, Wenzel D, Wieland F, Schwille P, Brugger B, Simons M. 2008. Ceramide triggers budding of exosome vesicles into multivesicular endosomes. *Science* 319: 1244-7
111. van Niel G, Charrin S, Simoes S, Romao M, Rochin L, Saftig P, Marks MS, Rubinstein E, Raposo G. 2011. The tetraspanin CD63 regulates ESCRT-independent and -dependent endosomal sorting during melanogenesis. *Dev Cell* 21: 708-21
112. Camussi G, Deregibus MC, Bruno S, Cantaluppi V, Biancone L. 2010. Exosomes/microvesicles as a mechanism of cell-to-cell communication. *Kidney Int* 78: 838-48
113. Janowska-Wieczorek A, Majka M, Kijowski J, Baj-Krzyworzeka M, Reza R, Turner AR, Ratajczak J, Emerson SG, Kowalska MA, Ratajczak MZ. 2001. Platelet-derived microparticles bind to hematopoietic stem/progenitor cells and enhance their engraftment. *Blood* 98: 3143-9
114. Denzer K, van Eijk M, Kleijmeer MJ, Jakobson E, de Groot C, Geuze HJ. 2000. Follicular dendritic cells carry MHC class II-expressing microvesicles at their surface. *J Immunol* 165: 1259-65
115. Mallegol J, Van Niel G, Lebreton C, Lepelletier Y, Candalh C, Dugave C, Heath JK, Raposo G, Cerf-Bensussan N, Heyman M. 2007. T84-intestinal epithelial exosomes bear MHC class II/peptide complexes potentiating antigen presentation by dendritic cells. *Gastroenterology* 132: 1866-76
116. Nolte-'t Hoen EN, Buschow SI, Anderton SM, Stoorvogel W, Wauben MH. 2009. Activated T cells recruit exosomes secreted by dendritic cells via LFA-1. *Blood* 113: 1977-81
117. Rana S, Yue S, Stadel D, Zoller M. 2012. Toward tailored exosomes: the exosomal tetraspanin web contributes to target cell selection. *Int J Biochem Cell Biol* 44: 1574-84
118. Hemler ME. 2003. Tetraspanin proteins mediate cellular penetration, invasion, and fusion events and define a novel type of membrane microdomain. *Annu Rev Cell Dev Biol* 19: 397-422
119. Montecalvo A, Larregina AT, Shufesky WJ, Stolz DB, Sullivan ML, Karlsson JM, Baty CJ, Gibson GA, Erdos G, Wang Z, Milosevic J, Tkacheva OA, Divito SJ, Jordan R, Lyons-Weiler J, Watkins SC, Morelli AE. 2012. Mechanism of transfer of functional microRNAs between mouse dendritic cells via exosomes. *Blood* 119: 756-66

120. Morelli AE. 2006. The immune regulatory effect of apoptotic cells and exosomes on dendritic cells: its impact on transplantation. *Am J Transplant* 6: 254-61
121. Barres C, Blanc L, Bette-Bobillo P, Andre S, Mamoun R, Gabius HJ, Vidal M. 2010. Galectin-5 is bound onto the surface of rat reticulocyte exosomes and modulates vesicle uptake by macrophages. *Blood* 115: 696-705
122. Tian T, Wang Y, Wang H, Zhu Z, Xiao Z. 2010. Visualizing of the cellular uptake and intracellular trafficking of exosomes by live-cell microscopy. *J Cell Biochem* 111: 488-96
123. Bobrie A, Colombo M, Raposo G, Thery C. 2011. Exosome secretion: molecular mechanisms and roles in immune responses. *Traffic* 12: 1659-68
124. Rak J. 2010. Microparticles in cancer. *Semin Thromb Hemost* 36: 888-906
125. Hood JL, San RS, Wickline SA. 2011. Exosomes released by melanoma cells prepare sentinel lymph nodes for tumor metastasis. *Cancer Res* 71: 3792-801
126. Faure J, Lachenal G, Court M, Hirrlinger J, Chatellard-Causse C, Blot B, Grange J, Schoehn G, Goldberg Y, Boyer V, Kirchhoff F, Raposo G, Garin J, Sadoul R. 2006. Exosomes are released by cultured cortical neurones. *Mol Cell Neurosci* 31: 642-8
127. Kramer-Albers EM, Bretz N, Tenzer S, Winterstein C, Mobius W, Berger H, Nave KA, Schild H, Trotter J. 2007. Oligodendrocytes secrete exosomes containing major myelin and stress-protective proteins: Trophic support for axons? *Proteomics Clin Appl* 1: 1446-61
128. Lachenal G, Pernet-Gallay K, Chivet M, Hemming FJ, Belly A, Bodon G, Blot B, Haase G, Goldberg Y, Sadoul R. 2011. Release of exosomes from differentiated neurons and its regulation by synaptic glutamatergic activity. *Mol Cell Neurosci* 46: 409-18
129. Fevrier B, Vilette D, Archer F, Loew D, Faigle W, Vidal M, Laude H, Raposo G. 2004. Cells release prions in association with exosomes. *Proc Natl Acad Sci U S A* 101: 9683-8
130. Emmanouilidou E, Melachroinou K, Roumeliotis T, Garbis SD, Ntzouni M, Margaritis LH, Stefanis L, Vekrellis K. 2010. Cell-produced alpha-synuclein is secreted in a calcium-dependent manner by exosomes and impacts neuronal survival. *J Neurosci* 30: 6838-51
131. Alvarez-Llamas G, de la Cuesta F, Barderas ME, Darde V, Padial LR, Vivanco F. 2008. Recent advances in atherosclerosis-based proteomics: new biomarkers and a future perspective. *Expert Rev Proteomics* 5: 679-91
132. Al-Nedawi K, Meehan B, Rak J. 2009. Microvesicles: messengers and mediators of tumor progression. *Cell Cycle* 8: 2014-8
133. Simpson RJ, Lim JW, Moritz RL, Mathivanan S. 2009. Exosomes: proteomic insights and diagnostic potential. *Expert Rev Proteomics* 6: 267-83
134. Chaput N, Thery C. 2011. Exosomes: immune properties and potential clinical implementations. *Semin Immunopathol* 33: 419-40
135. Szilagy JF, Cunningham C. 1991. Identification and characterization of a novel non-infectious herpes simplex virus-related particle. *J Gen Virol* 72 (Pt 3): 661-8
136. Kelly BJ, Fraefel C, Cunningham AL, Diefenbach RJ. 2009. Functional roles of the tegument proteins of herpes simplex virus type 1. *Virus Res* 145: 173-86
137. Gourzones C, Gelin A, Bombik I, Klibi J, Verillaud B, Guigay J, Lang P, Temam S, Schneider V, Amiel C, Baconnais S, Jimenez AS, Busson P. 2010. Extra-cellular release and blood diffusion of BART viral micro-RNAs produced by EBV-infected nasopharyngeal carcinoma cells. *Virology* 7: 271
138. Wiley RD, Gummuluru, S. 2006. Immature dendritic cell-derived exosomes can mediate HIV-1 trans infection. *Proceedings of the National Academy of Sciences* 103: 738-43

139. Meckes DG, Jr., Raab-Traub N. 2011. Microvesicles and viral infection. *J Virol* 85: 12844-54
140. Gould SJ, Booth, A. M., Hildreth, J. E. 2003. The Trojan exosome hypothesis. *Proceedings of the National Academy of Sciences* 100: 10592-7
141. Izquierdo-Useros N, Naranjo-Gomez M, Erkizia I, Puertas MC, Borrás FE, Blanco J, Martínez-Picado J. 2010. HIV and mature dendritic cells: Trojan exosomes riding the Trojan horse? *PLoS Pathog* 6: e1000740
142. Nguyen DG, Booth, A., Gould, S.J., Hildreth, J.E. 2003. Evidence That HIV Budding in Primary Macrophages Occurs through the Exosome Release Pathway. *Journal of Biological Chemistry* 278: 52347-54
143. Masciopinto F, Giovani C, Campagnoli S, Galli-Stampino L, Colombatto P, Brunetto M, Yen TSB, Houghton M, Pileri P, Abrignani S. 2004. Association of hepatitis C virus envelope proteins with exosomes. *European Journal of Immunology* 34: 2834-42
144. Tamai K, Shiina M, Tanaka N, Nakano T, Yamamoto A, Kondo Y, Kakazu E, Inoue J, Fukushima K, Sano K, Ueno Y, Shimosegawa T, Sugamura K. 2012. Regulation of hepatitis C virus secretion by the Hrs-dependent exosomal pathway. *Virology* 422: 377-85
145. Dreux M, Garaigorta U, Boyd B, Decembre E, Chung J, Whitten-Bauer C, Wieland S, Chisari FV. 2012. Short-range exosomal transfer of viral RNA from infected cells to plasmacytoid dendritic cells triggers innate immunity. *Cell Host Microbe* 12: 558-70
146. Gastaminza P, Dryden KA, Boyd B, Wood MR, Law M, Yeager M, Chisari FV. 2010. Ultrastructural and biophysical characterization of hepatitis C virus particles produced in cell culture. *J Virol* 84: 10999-1009
147. Johnstone RM, Adam M, Hammond JR, Orr L, Turbide C. 1987. Vesicle formation during reticulocyte maturation. Association of plasma membrane activities with released vesicles (exosomes). *J Biol Chem* 262: 9412-20
148. BRAKKE MK. 1951. Density Gradient Centrifugation: A New Separation Technique. *Journal of the American Chemical Society* 73: 1847-8
149. Van Veldhoven PP, Baumgart E, Mannaerts GP. 1996. Iodixanol (Optiprep), an improved density gradient medium for the iso-osmotic isolation of rat liver peroxisomes. *Anal Biochem* 237: 17-23
150. Caby MP, D. Lankar, C. Vincendeau-Scherrer, G. Raposo, and C. Bonnerot. 2005. Exosomal-like vesicles are present in human blood plasma. *International Immunology* 17: 879-87
151. Hilsabeck RC, Perry W, Hassanein TI. 2002. Neuropsychological impairment in patients with chronic hepatitis C. *Hepatology* 35: 440-6
152. Laskus T, Radkowski M, Adair DM, Wilkinson J, Scheck AC, Rakela J. 2005. Emerging evidence of hepatitis C virus neuroinvasion. *AIDS* 19 Suppl 3: S140-4
153. Tillmann HL. 2004. Hepatitis C virus infection and the brain. *Metab Brain Dis* 19: 351-6
154. Kramer L, Bauer E, Funk G, Hofer H, Jessner W, Steindl-Munda P, Wrba F, Madl C, Gangl A, Ferenci P. 2002. Subclinical impairment of brain function in chronic hepatitis C infection. *J Hepatol* 37: 349-54
155. Forton DM, Allsop JM, Cox IJ, Hamilton G, Wesnes K, Thomas HC, Taylor-Robinson SD. 2005. A review of cognitive impairment and cerebral metabolite abnormalities in patients with hepatitis C infection. *AIDS* 19 Suppl 3: S53-63
156. Pham TNQ, MacParland SA, Mulrooney PM, Cooksley H, Naoumov NV, Michalak TI. 2004. Hepatitis C Virus Persistence after Spontaneous or Treatment-Induced Resolution of Hepatitis C. *Journal of Virology* 78: 5867-74

157. Radkowski M, Gallegos-Orozco JF, Jablonska J, Colby TV, Walewska-Zielecka B, Kubicka J, Wilkinson J, Adair D, Rakela J, Laskus T. 2005. Persistence of hepatitis C virus in patients successfully treated for chronic hepatitis C. *Hepatology* 41: 106-14
158. Goh J, Coughlan B, Quinn J, O'Keane JC, Crowe J. 1999. Fatigue does not correlate with the degree of hepatitis or the presence of autoimmune disorders in chronic hepatitis C infection. *Eur J Gastroenterol Hepatol* 11: 833-8
159. Foster GR, Goldin RD, Thomas HC. 1998. Chronic hepatitis C virus infection causes a significant reduction in quality of life in the absence of cirrhosis. *Hepatology* 27: 209-12
160. Forton DM, Thomas HC, Murphy CA, Allsop JM, Foster GR, Main J, Wesnes KA, Taylor-Robinson SD. 2002. Hepatitis C and cognitive impairment in a cohort of patients with mild liver disease. *Hepatology* 35: 433-9
161. Forton DM, Allsop JM, Main J, Foster GR, Thomas HC, Taylor-Robinson SD. 2001. Evidence for a cerebral effect of the hepatitis C virus. *Lancet* 358: 38-9
162. Weissenborn K, Krause J, Bokemeyer M, Hecker H, Schuler A, Ennen JC, Ahl B, Manns MP, Boker KW. 2004. Hepatitis C virus infection affects the brain-evidence from psychometric studies and magnetic resonance spectroscopy. *J Hepatol* 41: 845-51
163. Choo QL, Kuo G, Weiner AJ, Overby LR, Bradley DW, Houghton M. 1989. Isolation of a cDNA clone derived from a blood-borne non-A, non-B viral hepatitis genome. *Science* 244: 359-62
164. Zignego AL, Giannini C, Gragnani L. 2012. HCV and lymphoproliferation. *Clin Dev Immunol* 2012: 980942
165. Bare P. 2009. Hepatitis C virus and peripheral blood mononuclear cell reservoirs Patricia Bare. *World J Hepatol* 1: 67-71
166. Giannini C, Petrarca A, Monti M, Arena U, Caini P, Solazzo V, Gragnani L, Milani S, Laffi G, Zignego AL. 2008. Association between persistent lymphatic infection by hepatitis C virus after antiviral treatment and mixed cryoglobulinemia. *Blood* 111: 2943-5
167. Arcaini L, Merli M, Volpetti S, Rattotti S, Gotti M, Zaja F. 2012. Indolent B-cell lymphomas associated with HCV infection: clinical and virological features and role of antiviral therapy. *Clin Dev Immunol* 2012: 638185
168. Libra M, Polesel J, Russo AE, De Re V, Cina D, Serraino D, Nicoletti F, Spandidos DA, Stivala F, Talamini R. 2010. Extrahepatic disorders of HCV infection: a distinct entity of B-cell neoplasia? *Int J Oncol* 36: 1331-40
169. Gisbert JP, Garcia-Buey L, Pajares JM, Moreno-Otero R. 2003. Prevalence of hepatitis C virus infection in B-cell non-Hodgkin's lymphoma: systematic review and meta-analysis. *Gastroenterology* 125: 1723-32
170. Zignego AL, Giannini C, Monti M, Gragnani L. 2007. Hepatitis C virus lymphotropism: lessons from a decade of studies. *Dig Liver Dis* 39 Suppl 1: S38-45
171. Radkowski M, Horban A, Gallegos-Orozco JF, Pawelczyk A, Jablonska J, Wilkinson J, Adair D, Laskus T. 2005. Evidence for viral persistence in patients who test positive for anti-hepatitis C virus antibodies and have normal alanine aminotransferase levels. *J Infect Dis* 191: 1730-3
172. Blackard JT, Kemmer N, Sherman KE. 2006. Extrahepatic replication of HCV: insights into clinical manifestations and biological consequences. *Hepatology* 44: 15-22
173. Valli MB, Crema A, Lanzilli G, Serafino A, Bertolini L, Ravagnan G, Ponzetto A, Menzo S, Clementi M, Carloni G. 2007. Molecular and cellular determinants of cell-to-cell transmission of HCV in vitro. *J Med Virol* 79: 1491-9
174. Valli MB, Serafino A, Crema A, Bertolini L, Manzin A, Lanzilli G, Bosman C, Iacovacci S, Giunta S, Ponzetto A, Clementi M, Carloni G. 2006. Transmission in vitro of hepatitis C virus from persistently infected human B-cells to hepatoma cells by cell-to-cell contact. *J Med Virol* 78: 192-201

175. Lerat H, Berby F, Trabaud MA, Vidalin O, Major M, Trepo C, Inchauspe G. 1996. Specific detection of hepatitis C virus minus strand RNA in hematopoietic cells. *J Clin Invest* 97: 845-51
176. MacParland SA, Pham TN, Gujar SA, Michalak TI. 2006. De novo infection and propagation of wild-type Hepatitis C virus in human T lymphocytes in vitro. *J Gen Virol* 87: 3577-86
177. Pham TN, King D, Macparland SA, McGrath JS, Reddy SB, Bursey FR, Michalak TI. 2008. Hepatitis C virus replicates in the same immune cell subsets in chronic hepatitis C and occult infection. *Gastroenterology* 134: 812-22
178. Radkowski M, Bednarska A, Horban A, Stanczak J, Wilkinson J, Adair DM, Nowicki M, Rakela J, Laskus T. 2004. Infection of primary human macrophages with hepatitis C virus in vitro: induction of tumour necrosis factor-alpha and interleukin 8. *J Gen Virol* 85: 47-59
179. Sarhan MA, Pham TN, Chen AY, Michalak TI. 2012. Hepatitis C virus infection of human T lymphocytes is mediated by CD5. *J Virol* 86: 3723-35
180. Sarhan MA, Chen AY, Russell RS, Michalak TI. 2012. Patient-derived hepatitis C virus and JFH-1 clones differ in their ability to infect human hepatoma cells and lymphocytes. *J Gen Virol* 93: 2399-407
181. Marukian S, Jones CT, Andrus L, Evans MJ, Ritola KD, Charles ED, Rice CM, Dustin LB. 2008. Cell culture-produced hepatitis C virus does not infect peripheral blood mononuclear cells. *Hepatology* 48: 1843-50
182. Murakami K, Kimura T, Osaki M, Ishii K, Miyamura T, Suzuki T, Wakita T, Shoji I. 2008. Virological characterization of the hepatitis C virus JFH-1 strain in lymphocytic cell lines. *J Gen Virol* 89: 1587-92
183. Laskus T, Radkowski M, Bednarska A, Wilkinson J, Adair D, Nowicki M, Nikolopoulou GB, Vargas H, Rakela J. 2002. Detection and Analysis of Hepatitis C Virus Sequences in Cerebrospinal Fluid. *Journal of Virology* 76: 10064-8
184. Vargas HE, Laskus T, Radkowski M, Wilkinson J, Balan V, Douglas DD, Harrison ME, Mulligan DC, Olden K, Adair D, Rakela J. 2002. Detection of hepatitis C virus sequences in brain tissue obtained in recurrent hepatitis C after liver transplantation. *Liver Transpl* 8: 1014-9
185. Radkowski M, Wilkinson J, Nowicki M, Adair D, Vargas H, Ingui C, Rakela J, Laskus T. 2002. Search for hepatitis C virus negative-strand RNA sequences and analysis of viral sequences in the central nervous system: evidence of replication. *J Virol* 76: 600-8
186. Wilkinson J, Radkowski M, Laskus T. 2008. Hepatitis C Virus Neuroinvasion: Identification of Infected Cells. *Journal of Virology* 83: 1312-9
187. Letendre S, Paulino Amy D, Rockenstein E, Adame A, Crews L, Cherner M, Heaton R, Ellis R, Everall Ian P, Grant I, Masliah E. 2007. Pathogenesis of Hepatitis C Virus Coinfection in the Brains of Patients Infected with HIV. *The Journal of Infectious Diseases* 196: 361-70
188. Wilkinson J, Radkowski M, Eschbacher JM, Laskus T. 2010. Activation of brain macrophages/microglia cells in hepatitis C infection. *Gut*
189. Verucchi G, Calza L, Manfredi R, Chiodo F. 2004. Human immunodeficiency virus and hepatitis C virus coinfection: epidemiology, natural history, therapeutic options and clinical management. *Infection* 32: 33-46
190. Sulkowski MS. 2012. Hepatitis C virus-human immunodeficiency virus coinfection. *Liver Int* 32 Suppl 1: 129-34
191. Cherner M, Letendre S, Heaton RK, Durelle J, Marquie-Beck J, Gragg B, Grant I. 2005. Hepatitis C augments cognitive deficits associated with HIV infection and methamphetamine. *Neurology* 64: 1343-7

192. van Gorp WG, Hinkin CH. 2005. Triple trouble: cognitive deficits from hepatitis C, HIV, and methamphetamine. *Neurology* 64: 1328-9
193. Murray J, Fishman SL, Ryan E, Eng FJ, Walewski JL, Branch AD, Morgello S. 2008. Clinicopathologic correlates of hepatitis C virus in brain: A pilot study. *Journal of Neurovirology* 14: 17-27
194. Bouzier-Sore AK, Merle M, Magistretti PJ, Pellerin L. 2002. Feeding active neurons: (re)emergence of a nursing role for astrocytes. *J Physiol Paris* 96: 273-82
195. Chen Y, Swanson RA. 2003. Astrocytes and brain injury. *J Cereb Blood Flow Metab* 23: 137-49
196. Farina C, Aloisi F, Meinl E. 2007. Astrocytes are active players in cerebral innate immunity. *Trends Immunol* 28: 138-45
197. Bsibsi M, Persoon-Deen C, Verwer RW, Meeuwssen S, Ravid R, Van Noort JM. 2006. Toll-like receptor 3 on adult human astrocytes triggers production of neuroprotective mediators. *Glia* 53: 688-95
198. Bsibsi M, Ravid R, Gveric D, van Noort JM. 2002. Broad expression of Toll-like receptors in the human central nervous system. *J Neuropathol Exp Neurol* 61: 1013-21
199. Jack CS, Arbour N, Manusow J, Montgrain V, Blain M, McCrea E, Shapiro A, Antel JP. 2005. TLR signaling tailors innate immune responses in human microglia and astrocytes. *J Immunol* 175: 4320-30
200. Carpentier PA, Duncan DS, Miller SD. 2008. Glial toll-like receptor signaling in central nervous system infection and autoimmunity. *Brain Behav Immun* 22: 140-7
201. Ransohoff RM, Brown MA. 2012. Innate immunity in the central nervous system. *J Clin Invest* 122: 1164-71
202. Sharma SD. 2010. Hepatitis C virus: molecular biology & current therapeutic options. *Indian J Med Res* 131: 17-34
203. Zeisel MB, Fafi-Kremer S, Fofana I, Barth H, Stoll-Keller F, Doffoel M, Baumert TF. 2007. Neutralizing antibodies in hepatitis C virus infection. *World J Gastroenterol* 13: 4824-30
204. Petrovic D, Dempsey E, Doherty DG, Kelleher D, Long A. 2012. Hepatitis C virus – T-cell responses and viral escape mutations. *Eur J Immunol* 42: 17-26
205. Helle F, Duverlie G, Dubuisson J. 2011. The hepatitis C virus glycan shield and evasion of the humoral immune response. *Viruses* 3: 1909-32
206. Park IW, Ndjomou J, Fan Y, Henao-Mejia J, He JJ. 2009. Hepatitis C virus is restricted at both entry and replication in mouse hepatocytes. *Biochem Biophys Res Commun* 387: 489-93
207. Martin BR, Giepmans BN, Adams SR, Tsien RY. 2005. Mammalian cell-based optimization of the biarsenical-binding tetracysteine motif for improved fluorescence and affinity. *Nat Biotechnol* 23: 1308-14
208. Collier KE, Heaton NS, Berger KL, Cooper JD, Saunders JL, Randall G. 2012. Molecular determinants and dynamics of hepatitis C virus secretion. *PLoS Pathog* 8: e1002466
209. He J, Chen Y, Farzan M, Choe H, Ohagen A, Gartner S, Busciglio J, Yang X, Hofmann W, Newman W, Mackay CR, Sodroski J, Gabuzda D. 1997. CCR3 and CCR5 are co-receptors for HIV-1 infection of microglia. *Nature* 385: 645-9
210. Fan Y, Zou W, Green LA, Kim BO, He JJ. 2011. Activation of Egr-1 expression in astrocytes by HIV-1 Tat: new insights into astrocyte-mediated Tat neurotoxicity. *J Neuroimmune Pharmacol* 6: 121-9
211. Liu Z, He JJ. 2013. Cell-cell contact-mediated hepatitis C virus (HCV) transfer, productive infection, and replication and their requirement for HCV receptors. *J Virol* 87: 8545-58

212. Takeuchi T, Katsume A, Tanaka T, Abe A, Inoue K, Tsukiyama-Kohara K, Kawaguchi R, Tanaka S, Kohara M. 1999. Real-time detection system for quantification of hepatitis C virus genome. *Gastroenterology* 116: 636-42
213. Friedman A, Perrimon N. 2006. A functional RNAi screen for regulators of receptor tyrosine kinase and ERK signalling. *Nature* 444: 230-4
214. Boeuf P, Vigan-Womas I, Jublot D, Loizon S, Barale JC, Akanmori BD, Mercereau-Puijalon O, Behr C. 2005. CyProQuant-PCR: a real time RT-PCR technique for profiling human cytokines, based on external RNA standards, readily automatable for clinical use. *BMC Immunol* 6: 5
215. Giulietti A, Overbergh L, Valckx D, Decallonne B, Bouillon R, Mathieu C. 2001. An overview of real-time quantitative PCR: applications to quantify cytokine gene expression. *Methods* 25: 386-401
216. LaPensee CR, Hugo ER, Ben-Jonathan N. 2008. Insulin stimulates interleukin-6 expression and release in LS14 human adipocytes through multiple signaling pathways. *Endocrinology* 149: 5415-22
217. Kruger S, Brandt E, Klinger M, Kreft B. 2000. Interleukin-8 secretion of cortical tubular epithelial cells is directed to the basolateral environment and is not enhanced by apical exposure to Escherichia coli. *Infect Immun* 68: 328-34
218. Cantin R, Diou J, Bélanger D, Tremblay AM, Gilbert C. 2008. Discrimination between exosomes and HIV-1: Purification of both vesicles from cell-free supernatants☆. *Journal of Immunological Methods* 338: 21-30
219. Mothes W, Sherer NM, Jin J, Zhong P. 2010. Virus cell-to-cell transmission. *J Virol* 84: 8360-8
220. Lopez-Balderas N, Huerta L, Villarreal C, Rivera-Toledo E, Sandoval G, Larralde C, Lamoyi E. 2007. In vitro cell fusion between CD4(+) and HIV-1 Env(+) T cells generates a diversity of syncytia varying in total number, size and cellular content. *Virus Res* 123: 138-46
221. Polcicova K, Goldsmith K, Rainish BL, Wisner TW, Johnson DC. 2005. The extracellular domain of herpes simplex virus gE is indispensable for efficient cell-to-cell spread: evidence for gE/gI receptors. *J Virol* 79: 11990-2001
222. Roper RL, Wolffe EJ, Weisberg A, Moss B. 1998. The envelope protein encoded by the A33R gene is required for formation of actin-containing microvilli and efficient cell-to-cell spread of vaccinia virus. *J Virol* 72: 4192-204
223. Bartosch B, Vitelli A, Granier C, Goujon C, Dubuisson J, Pascale S, Scarselli E, Cortese R, Nicosia A, Cosset FL. 2003. Cell entry of hepatitis C virus requires a set of co-receptors that include the CD81 tetraspanin and the SR-B1 scavenger receptor. *J Biol Chem* 278: 41624-30
224. Flint M, von Hahn T, Zhang J, Farquhar M, Jones CT, Balfe P, Rice CM, McKeating JA. 2006. Diverse CD81 proteins support hepatitis C virus infection. *J Virol* 80: 11331-42
225. Zhang J, Randall G, Higginbottom A, Monk P, Rice CM, McKeating JA. 2004. CD81 is required for hepatitis C virus glycoprotein-mediated viral infection. *J Virol* 78: 1448-55
226. Meertens L, Bertaux C, Cukierman L, Cormier E, Lavillette D, Cosset FL, Dragic T. 2008. The tight junction proteins claudin-1, -6, and -9 are entry cofactors for hepatitis C virus. *J Virol* 82: 3555-60
227. Bertaux C, Dragic T. 2006. Different domains of CD81 mediate distinct stages of hepatitis C virus pseudoparticle entry. *J Virol* 80: 4940-8
228. Codran A, Royer C, Jaeck D, Bastien-Valle M, Baumert TF, Kieny MP, Pereira CA, Martin JP. 2006. Entry of hepatitis C virus pseudotypes into primary human hepatocytes by clathrin-dependent endocytosis. *J Gen Virol* 87: 2583-93

229. Ito K, Yamaoka Y, Ota H, El-Zimaity H, Graham DY. 2008. Adherence, internalization, and persistence of *Helicobacter pylori* in hepatocytes. *Dig Dis Sci* 53: 2541-9
230. Ang F, Wong AP, Ng MM, Chu JJ. 2010. Small interference RNA profiling reveals the essential role of human membrane trafficking genes in mediating the infectious entry of dengue virus. *Virology* 7: 24
231. Kolesnikova L, Bohil AB, Cheney RE, Becker S. 2007. Budding of Marburgvirus is associated with filopodia. *Cell Microbiol* 9: 939-51
232. Zieve GW, Turnbull D, Mullins JM, McIntosh JR. 1980. Production of large numbers of mitotic mammalian cells by use of the reversible microtubule inhibitor nocodazole. Nocodazole accumulated mitotic cells. *Exp Cell Res* 126: 397-405
233. Kopp M, Murray CL, Jones CT, Rice CM. 2010. Genetic analysis of the carboxy-terminal region of the hepatitis C virus core protein. *J Virol* 84: 1666-73
234. Whitt MA, Mire CE. 2011. Utilization of fluorescently-labeled tetracysteine-tagged proteins to study virus entry by live cell microscopy. *Methods* 55: 127-36
235. Owsianka AM, Tarr AW, Keck ZY, Li TK, Witteveldt J, Adair R, Fong SK, Ball JK, Patel AH. 2008. Broadly neutralizing human monoclonal antibodies to the hepatitis C virus E2 glycoprotein. *J Gen Virol* 89: 653-9
236. Keck ZY, Xia J, Cai Z, Li TK, Owsianka AM, Patel AH, Luo G, Fong SK. 2007. Immunogenic and functional organization of hepatitis C virus (HCV) glycoprotein E2 on infectious HCV virions. *J Virol* 81: 1043-7
237. Lee SC, Hatch WC, Liu W, Kress Y, Lyman WD, Dickson DW. 1993. Productive infection of human fetal microglia by HIV-1. *Am J Pathol* 143: 1032-9
238. Lee SC, Liu W, Brosnan CF, Dickson DW. 1992. Characterization of primary human fetal dissociated central nervous system cultures with an emphasis on microglia. *Lab Invest* 67: 465-76
239. Peterson PK, Gekker G, Hu S, Lokensgard J, Portoghese PS, Chao CC. 1999. Endomorphin-1 potentiates HIV-1 expression in human brain cell cultures: implication of an atypical mu-opioid receptor. *Neuropharmacology* 38: 273-8
240. Ye L, Wang X, Wang S, Luo G, Wang Y, Liang H, Ho W. 2008. Centrifugal enhancement of hepatitis C virus infection of human hepatocytes. *J Virol Methods* 148: 161-5
241. Li R, Qin Y, He Y, Tao W, Zhang N, Tsai C, Zhou P, Zhong J. 2011. Production of hepatitis C virus lacking the envelope-encoding genes for single-cycle infection by providing homologous envelope proteins or vesicular stomatitis virus glycoproteins in trans. *J Virol* 85: 2138-47
242. Narbus CM, B. Israelow, M. Sourisseau, M. L. Michta, S. E. Hopcraft, G. M. Zeiner and M. J. Evans. 2011. HepG2 cells expressing microRNA miR-122 support the entire hepatitis C virus life cycle. *J Virol* 85: 12087-93
243. Ousman SS, Kubes P. 2012. Immune surveillance in the central nervous system. *Nat Neurosci* 15: 1096-101
244. Janabi N, Di Stefano M, Wallon C, Hery C, Chiodi F, Tardieu M. 1998. Induction of human immunodeficiency virus type 1 replication in human glial cells after proinflammatory cytokines stimulation: effect of IFN γ , IL1 β , and TNF α on differentiation and chemokine production in glial cells. *Glia* 23: 304-15
245. Li W, Henderson LJ, Major EO, Al-Harhi L. 2011. IFN- γ mediates enhancement of HIV replication in astrocytes by inducing an antagonist of the beta-catenin pathway (DKK1) in a STAT 3-dependent manner. *J Immunol* 186: 6771-8
246. Carroll-Anzinger D, Kumar A, Adarichev V, Kashanchi F, Al-Harhi L. 2007. Human immunodeficiency virus-restricted replication in astrocytes and the ability of

- gamma interferon to modulate this restriction are regulated by a downstream effector of the Wnt signaling pathway. *J Virol* 81: 5864-71
247. Carroll-Anzinger D, Al-Harhi L. 2006. Gamma interferon primes productive human immunodeficiency virus infection in astrocytes. *J Virol* 80: 541-4
248. Suk K, Yeou Kim S, Kim H. 2001. Regulation of IL-18 production by IFN gamma and PGE2 in mouse microglial cells: involvement of NF-kB pathway in the regulatory processes. *Immunol Lett* 77: 79-85
249. Alboni S, Cervia D, Sugama S, Conti B. 2010. Interleukin 18 in the CNS. *J Neuroinflammation* 7: 9
250. Felderhoff-Mueser U, Schmidt OI, Oberholzer A, Buhner C, Stahel PF. 2005. IL-18: a key player in neuroinflammation and neurodegeneration? *Trends Neurosci* 28: 487-93
251. Agnello V, Abel G, Knight GB, Muchmore E. 1998. Detection of widespread hepatocyte infection in chronic hepatitis C. *Hepatology* 28: 573-84
252. Catanese MT, Graziani R, von Hahn T, Moreau M, Huby T, Paonessa G, Santini C, Luzzago A, Rice CM, Cortese R, Vitelli A, Nicosia A. 2007. High-Avidity Monoclonal Antibodies against the Human Scavenger Class B Type I Receptor Efficiently Block Hepatitis C Virus Infection in the Presence of High-Density Lipoprotein. *Journal of Virology* 81: 8063-71
253. Dreux M, Dao Thi VL, Fresquet J, Guérin M, Julia Z, Verney G, Durantel D, Zoulim F, Lavillette D, Cosset F-L, Bartosch B, Evans MJ. 2009. Receptor Complementation and Mutagenesis Reveal SR-BI as an Essential HCV Entry Factor and Functionally Imply Its Intra- and Extra-Cellular Domains. *PLoS Pathogens* 5: e1000310
254. Koutsoudakis G, Kaul A, Steinmann E, Kallis S, Lohmann V, Pietschmann T, Bartenschlager R. 2006. Characterization of the early steps of hepatitis C virus infection by using luciferase reporter viruses. *J Virol* 80: 5308-20
255. Voisset C, Callens N, Blanchard E, Op De Beeck A, Dubuisson J, Vu-Dac N. 2005. High density lipoproteins facilitate hepatitis C virus entry through the scavenger receptor class B type I. *J Biol Chem* 280: 7793-9
256. Brimacombe CL, Grove J, Meredith LW, Hu K, Syder AJ, Flores MV, Timpe JM, Krieger SE, Baumert TF, Tellinghuisen TL, Wong-Staal F, Balfe P, McKeating JA. 2011. Neutralizing antibody-resistant hepatitis C virus cell-to-cell transmission. *J Virol* 85: 596-605
257. Witteveldt J, Evans MJ, Bitzegeio J, Koutsoudakis G, Owsianka AM, Angus AG, Keck ZY, Fong SK, Pietschmann T, Rice CM, Patel AH. 2009. CD81 is dispensable for hepatitis C virus cell-to-cell transmission in hepatoma cells. *J Gen Virol* 90: 48-58
258. Da Costa D, Turek M, Felmler DJ, Girardi E, Pfeffer S, Long G, Bartenschlager R, Zeisel MB, Baumert TF. 2012. Reconstitution of the entire hepatitis C virus life cycle in nonhepatic cells. *J Virol* 86: 11919-25
259. Narbus CM, Israelow B, Sourisseau M, Michta ML, Hopcraft SE, Zeiner GM, Evans MJ. 2011. HepG2 cells expressing microRNA miR-122 support the entire hepatitis C virus life cycle. *J Virol* 85: 12087-92
260. Kawakami S, Watanabe Y, Beachy RN. 2004. Tobacco mosaic virus infection spreads cell to cell as intact replication complexes. *Proc Natl Acad Sci U S A* 101: 6291-6
261. Amari K, Lerich A, Schmitt-Keichinger C, Dolja VV, Ritzenthaler C. 2011. Tubule-guided cell-to-cell movement of a plant virus requires class XI myosin motors. *PLoS Pathog* 7: e1002327
262. Harries PA, Schoelz JE, Nelson RS. 2010. Intracellular transport of viruses and their components: utilizing the cytoskeleton and membrane highways. *Mol Plant Microbe Interact* 23: 1381-93

263. Avisar D, Prokhnevsky AI, Dolja VV. 2008. Class VIII myosins are required for plasmodesmatal localization of a closterovirus Hsp70 homolog. *J Virol* 82: 2836-43
264. Collier KE, Berger KL, Heaton NS, Cooper JD, Yoon R, Randall G. 2009. RNA interference and single particle tracking analysis of hepatitis C virus endocytosis. *PLoS Pathog* 5: e1000702
265. Bost AG, Venable D, Liu L, Heinz BA. 2003. Cytoskeletal requirements for hepatitis C virus (HCV) RNA synthesis in the HCV replicon cell culture system. *J Virol* 77: 4401-8
266. Berger KL, Cooper JD, Heaton NS, Yoon R, Oakland TE, Jordan TX, Mateu G, Grakoui A, Randall G. 2009. Roles for endocytic trafficking and phosphatidylinositol 4-kinase III alpha in hepatitis C virus replication. *Proc Natl Acad Sci U S A* 106: 7577-82
267. Roohvand F, Maillard P, Lavergne JP, Boulant S, Walic M, Andreo U, Goueslain L, Helle F, Mallet A, McLauchlan J, Budkowska A. 2009. Initiation of hepatitis C virus infection requires the dynamic microtubule network: role of the viral nucleocapsid protein. *J Biol Chem* 284: 13778-91
268. Wolk B, Buchele B, Moradpour D, Rice CM. 2008. A dynamic view of hepatitis C virus replication complexes. *J Virol* 82: 10519-31
269. Shulla A, Randall G. 2012. Hepatitis C virus-host interactions, replication, and viral assembly. *Curr Opin Virol*
270. Popescu CI, Rouille Y, Dubuisson J. 2011. Hepatitis C virus assembly imaging. *Viruses* 3: 2238-54
271. Reynolds GM, Harris HJ, Jennings A, Hu K, Grove J, Lalor PF, Adams DH, Balfe P, Hubscher SG, McKeating JA. 2008. Hepatitis C virus receptor expression in normal and diseased liver tissue. *Hepatology* 47: 418-27
272. Mee CJ, Harris HJ, Farquhar MJ, Wilson G, Reynolds G, Davis C, van ISC, Balfe P, McKeating JA. 2009. Polarization restricts hepatitis C virus entry into HepG2 hepatoma cells. *J Virol* 83: 6211-21
273. Mee CJ, Farquhar MJ, Harris HJ, Hu K, Ramma W, Ahmed A, Maurel P, Bicknell R, Balfe P, McKeating JA. 2010. Hepatitis C virus infection reduces hepatocellular polarity in a vascular endothelial growth factor-dependent manner. *Gastroenterology* 138: 1134-42
274. Svitkina TM, Borisy GG. 1999. Arp2/3 complex and actin depolymerizing factor/cofilin in dendritic organization and treadmilling of actin filament array in lamellipodia. *J Cell Biol* 145: 1009-26
275. Haudenschild DR, Chen J, Steklov N, Lotz MK, D'Lima DD. 2009. Characterization of the chondrocyte actin cytoskeleton in living three-dimensional culture: response to anabolic and catabolic stimuli. *Mol Cell Biomech* 6: 135-44
276. Schlunck G, Damke H, Kiosses WB, Rusk N, Symons MH, Waterman-Storer CM, Schmid SL, Schwartz MA. 2004. Modulation of Rac localization and function by dynamin. *Mol Biol Cell* 15: 256-67
277. Roingard P, Hourieux C, Blanchard E, Prensier G. 2008. Hepatitis C virus budding at lipid droplet-associated ER membrane visualized by 3D electron microscopy. *Histochem Cell Biol* 130: 561-6
278. Cocquerel L, Meunier JC, Pillez A, Wychowski C, Dubuisson J. 1998. A retention signal necessary and sufficient for endoplasmic reticulum localization maps to the transmembrane domain of hepatitis C virus glycoprotein E2. *J Virol* 72: 2183-91
279. Cocquerel L, Duvet S, Meunier JC, Pillez A, Cacan R, Wychowski C, Dubuisson J. 1999. The transmembrane domain of hepatitis C virus glycoprotein E1 is a signal for static retention in the endoplasmic reticulum. *J Virol* 73: 2641-9
280. Ariumi Y, Kuroki M, Maki M, Ikeda M, Dansako H, Wakita T, Kato N. 2011. The ESCRT system is required for hepatitis C virus production. *PLoS One* 6: e14517

281. Corless L, Crump CM, Griffin SD, Harris M. 2010. Vps4 and the ESCRT-III complex are required for the release of infectious hepatitis C virus particles. *J Gen Virol* 91: 362-72
282. Lai CK, Jeng KS, Machida K, Lai MM. 2010. Hepatitis C virus egress and release depend on endosomal trafficking of core protein. *J Virol* 84: 11590-8
283. Shimizu YK, Feinstone SM, Kohara M, Purcell RH, Yoshikura H. 1996. Hepatitis C virus: detection of intracellular virus particles by electron microscopy. *Hepatology* 23: 205-9
284. Feng Z, Hensley L, McKnight KL, Hu F, Madden V, Ping L, Jeong SH, Walker C, Lanford RE, Lemon SM. 2013. A pathogenic picornavirus acquires an envelope by hijacking cellular membranes. *Nature* 496: 367-71
285. Ramakrishnaiah V, Thumann C, Fofana I, Habersetzer F, Pan Q, de Ruiter PE, Willemsen R, Demmers JA, Stalin Raj V, Jenster G, Kwekkeboom J, Tilanus HW, Haagmans BL, Baumert TF, van der Laan LJ. 2013. Exosome-mediated transmission of hepatitis C virus between human hepatoma Huh7.5 cells. *Proc Natl Acad Sci U S A* 110: 13109-13
286. Grapp M, Wrede A, Schweizer M, Huwel S, Galla HJ, Snaidero N, Simons M, Buckers J, Low PS, Urlaub H, Gartner J, Steinfeld R. 2013. Choroid plexus transcytosis and exosome shuttling deliver folate into brain parenchyma. *Nat Commun* 4: 2123
287. O'Loughlin AJ, Woffindale CA, Wood MJ. 2012. Exosomes and the emerging field of exosome-based gene therapy. *Curr Gene Ther* 12: 262-74
288. Fletcher NF, Yang JP, Farquhar MJ, Hu K, Davis C, He Q, Dowd K, Ray SC, Krieger SE, Neyts J, Baumert TF, Balfe P, McKeating JA, Wong-Staal F. 2010. Hepatitis C virus infection of neuroepithelioma cell lines. *Gastroenterology* 139: 1365-74
289. Fletcher NF, Wilson GK, Murray J, Hu K, Lewis A, Reynolds GM, Stamataki Z, Meredith LW, Rowe IA, Luo G, Lopez-Ramirez MA, Baumert TF, Weksler B, Couraud PO, Kim KS, Romero IA, Jopling C, Morgello S, Balfe P, McKeating JA. 2012. Hepatitis C virus infects the endothelial cells of the blood-brain barrier. *Gastroenterology* 142: 634-43 e6
290. Burgel B, Friesland M, Koch A, Manns MP, Wedemeyer H, Weissenborn K, Schulz-Schaeffer WJ, Pietschmann T, Steinmann E, Ciesek S. 2011. Hepatitis C virus enters human peripheral neuroblastoma cells - evidence for extra-hepatic cells sustaining hepatitis C virus penetration. *J Viral Hepat* 18: 562-70
291. Bukh J. 2012. Animal models for the study of hepatitis C virus infection and related liver disease. *Gastroenterology* 142: 1279-87 e3
292. Washburn ML, Bility MT, Zhang L, Kovalev GI, Buntzman A, Frelinger JA, Barry W, Ploss A, Rice CM, Su L. 2011. A humanized mouse model to study hepatitis C virus infection, immune response, and liver disease. *Gastroenterology* 140: 1334-44
293. Megias L, Guerri C, Fornas E, Azorin I, Bendala E, Sancho-Tello M, Duran JM, Tomas M, Gomez-Lechon MJ, Renau-Piqueras J. 2000. Endocytosis and transcytosis in growing astrocytes in primary culture. Possible implications in neural development. *Int J Dev Biol* 44: 209-21
294. Gorry PR, Ong C, Thorpe J, Bannwarth S, Thompson KA, Gatignol A, Vesselingh SL, Purcell DF. 2003. Astrocyte infection by HIV-1: mechanisms of restricted virus replication, and role in the pathogenesis of HIV-1-associated dementia. *Curr HIV Res* 1: 463-73
295. Liu Y, Liu H, Kim BO, Gattone VH, Li J, Nath A, Blum J, He JJ. 2004. CD4-independent infection of astrocytes by human immunodeficiency virus type 1: requirement for the human mannose receptor. *J Virol* 78: 4120-33
296. Forton DM, Karayiannis P, Mahmud N, Taylor-Robinson SD, Thomas HC. 2004. Identification of unique hepatitis C virus quasispecies in the central nervous system and

- comparative analysis of internal translational efficiency of brain, liver, and serum variants. *J Virol* 78: 5170-83
297. Shrivastava S, Mukherjee A, Ray R, Ray RB. 2013. Hepatitis C Virus Induces Interleukin-1beta (IL-1beta)/IL-18 in Circulatory and Resident Liver Macrophages. *J Virol* 87: 12284-90
298. Hudson CA, Christophi GP, Gruber RC, Wilmore JR, Lawrence DA, Massa PT. 2008. Induction of IL-33 expression and activity in central nervous system glia. *J Leukoc Biol* 84: 631-43
299. Akira S. 2000. The role of IL-18 in innate immunity. *Curr Opin Immunol* 12: 59-63
300. Sareneva T, Matikainen S, Kurimoto M, Julkunen I. 1998. Influenza A virus-induced IFN-alpha/beta and IL-18 synergistically enhance IFN-gamma gene expression in human T cells. *J Immunol* 160: 6032-8
301. Xing Z, Zganiacz A, Wang J, Divangahi M, Nawaz F. 2000. IL-12-independent Th1-type immune responses to respiratory viral infection: requirement of IL-18 for IFN-gamma release in the lung but not for the differentiation of viral-reactive Th1-type lymphocytes. *J Immunol* 164: 2575-84
302. Pien GC, Satoskar AR, Takeda K, Akira S, Biron CA. 2000. Cutting edge: selective IL-18 requirements for induction of compartmental IFN-gamma responses during viral infection. *J Immunol* 165: 4787-91
303. van de Veerdonk FL, Netea MG, Dinarello CA, Joosten LA. 2011. Inflammasome activation and IL-1beta and IL-18 processing during infection. *Trends Immunol* 32: 110-6
304. Dinarello CA. 1999. IL-18: A TH1-inducing, proinflammatory cytokine and new member of the IL-1 family. *J Allergy Clin Immunol* 103: 11-24
305. Pirhonen J. 2001. Regulation of IL-18 expression in virus infection. *Scand J Immunol* 53: 533-9
306. An P, Thio CL, Kirk GD, Donfield S, Goedert JJ, Winkler CA. 2008. Regulatory polymorphisms in the interleukin-18 promoter are associated with hepatitis C virus clearance. *J Infect Dis* 198: 1159-65
307. Manohar K, Suneetha PV, Sukriti, Pati NT, Gupta AC, Hissar S, Sakhuja P, Sarin SK. 2009. Association of IL-18 promoter polymorphism with liver disease severity in HCV-infected patients. *Hepatol Int* 3: 371-7
308. Haas SL, Weiss C, Bugert P, Gundt J, Witt H, Singer MV, Berg T, Bocker U. 2009. Interleukin 18 promoter variants (-137G>C and -607C>A) in patients with chronic hepatitis C: association with treatment response. *J Clin Immunol* 29: 620-8
309. Sharma A, Chakraborti A, Das A, Dhiman RK, Chawla Y. 2009. Elevation of interleukin-18 in chronic hepatitis C: implications for hepatitis C virus pathogenesis. *Immunology* 128: e514-22
310. Mohran ZY, Ali-Eldin FA, Abdel Aal HA. 2011. Serum interleukin-18: does it have a role in the diagnosis of hepatitis C virus related hepatocellular carcinoma? *Arab J Gastroenterol* 12: 29-33
311. Asakawa M, Kono H, Amemiya H, Matsuda M, Suzuki T, Maki A, Fujii H. 2006. Role of interleukin-18 and its receptor in hepatocellular carcinoma associated with hepatitis C virus infection. *Int J Cancer* 118: 564-70
312. Conti B, Park LC, Calingasan NY, Kim Y, Kim H, Bae Y, Gibson GE, Joh TH. 1999. Cultures of astrocytes and microglia express interleukin 18. *Brain Res Mol Brain Res* 67: 46-52
313. Das S, Mishra MK, Ghosh J, Basu A. 2008. Japanese Encephalitis Virus infection induces IL-18 and IL-1beta in microglia and astrocytes: correlation with in vitro cytokine responsiveness of glial cells and subsequent neuronal death. *J Neuroimmunol* 195: 60-72

314. Vivithanaporn P, Maingat F, Lin LT, Na H, Richardson CD, Agrawal B, Cohen EA, Jhamandas JH, Power C. 2010. Hepatitis C virus core protein induces neuroimmune activation and potentiates Human Immunodeficiency Virus-1 neurotoxicity. *PLoS One* 5: e12856
315. Chakraborty S, Nazmi A, Dutta K, Basu A. 2010. Neurons under viral attack: victims or warriors? *Neurochem Int* 56: 727-35
316. Aweya JJ, Tan YJ. 2011. Modulation of programmed cell death pathways by the hepatitis C virus. *Front Biosci (Landmark Ed)* 16: 608-18
317. Buhler S, Bartenschlager R. 2012. New targets for antiviral therapy of chronic hepatitis C. *Liver Int* 32 Suppl 1: 9-16
318. Gane EJ SC, Hyland RH, et al. . 2012. Once daily sofosbuvir (GS-7977) regimens in HCV genotype 1–3: The ELECTRON trial (Abstract 229). In *63rd Annual Meeting of the American Association for the Study of Liver Diseases (AASLD)*. Boston, MA
319. Sulkowski MS GD, Rodriguez-Torres M, et al.; A1444040 Study Group. . 2012. High rate of sustained virologic response with the all-oral combination of daclatasvir (NS5a inhibitor) plus sofosbuvir (nucleotide NS5b inhibitor) with or without ribavirin, in treatment-naïve patients chronically infected with HCV GT 1, 2, or 3 (Abstract LB-2). . In *63rd Annual Meeting of the American Association for the Study of Liver Diseases (AASLD)*. Boston, MA.
320. Kowdley KV LE, Poordad F, et al. . 2012. A 12-week interferon-free treatment regimen with ABT-450/r, ABT 267, ABT-333, and ribavirin achieves SVR12 rates (observed data) of 99% in treatment-naïve patients and 93% in prior null responders with HCV genotype 1 infection (Abstract LB-1). In *63rd Annual Meeting of the American Association for the Study of Liver Diseases (AASLD)*. Boston, MA.
321. Hézode C DC, Zoulim F, et al. 2012. Safety and efficacy of telaprevir or boceprevir in combination with peginterferon alfa/ribavirin, in 455 cirrhotic non responders. Week 16 analysis of the French early access program (ANRS CO20-CUPIC) in real-life setting (Abstract 51). In *63rd Annual Meeting of the American Association for the Study of Liver Diseases (AASLD)*. Boston, MA.
322. Gallegos-Orozco JF CA, Carey EJ, et al. 2012. Liver transplant center focused experience with peginterferon alfa-2a, ribavirin and telaprevir therapy in patients with genotype 1 hepatitis C cirrhosis (Abstract 53). In *Paper presented at: 63rd Annual Meeting of the American Association for the Study of Liver Diseases (AASLD)*. Boston, MA.
323. Sulkowski MS SK, Soriano V, et al.; Study 110 Team. 2012. Telaprevir in combination with peginterferon alfa-2a/ribavirin in HIV/HCV co-infected patients: SVR24 final study results (Abstract 54). In *63rd Annual Meeting of the American Association for the Study of Liver Diseases (AASLD)*. Boston, MA.
324. Kirby B MA, Rossi S, et al. 2012. No clinically significant pharmacokinetic drug interactions between sofosbuvir (GS-7977) and HIV antiretrovirals atripla®, rilpivirine, darunavir/ritonavir, or raltegravir in healthy volunteers (Abstract 1877). In *63rd Annual Meeting of the American Association for the Study of Liver Diseases (AASLD)*. Boston, MA.
325. Burton JR OLJ, Verna EC, et al. 2012. A multicenter study of protease inhibitor-triple therapy in HCV-infected liver transplant recipients: report from the CRUSH-C group (Abstract 211). In *63rd Annual Meeting of the American Association for the Study of Liver Diseases (AASLD)*. Boston, MA.
326. Mathias A CM, Clemons D, et al. 2012. No clinically significant pharmacokinetic drug-drug interactions between sofosbuvir (GS-7977) and the immunosuppressants, cyclosporine A or tacrolimus in healthy volunteers (Abstract 1869). In *63rd Annual*

Meeting of the American Association for the Study of Liver Diseases (AASLD). Boston, MA.

327. Ouwerkerk-Mahadevan S SA, Mortier S, et al. 2012. No clinically significant interaction between the investigational HCV protease inhibitor TMC435 and the immunosuppressives cyclosporine and tacrolimus (Abstract 80). In *63rd Annual Meeting of the American Association for the Study of Liver Diseases (AASLD)*. Boston, MA.

328. Frentzen A, Kusuma A, Guerlevik E, Hueging K, Knocke S, Ginkel C, Brown RJ, Heim M, Dill MT, Kroger A, Kalinke U, Kaderali L, Kuehnel F, Pietschmann T. 2013. Cell entry, efficient RNA replication, and production of infectious hepatitis C virus progeny in mouse liver-derived cells. *Hepatology*

329. Mercer DF, Schiller DE, Elliott JF, Douglas DN, Hao C, Rinfret A, Addison WR, Fischer KP, Churchill TA, Lakey JR, Tyrrell DL, Kneteman NM. 2001. Hepatitis C virus replication in mice with chimeric human livers. *Nat Med* 7: 927-33

330. Azuma H, Paulk N, Ranade A, Dorrell C, Al-Dhalimy M, Ellis E, Strom S, Kay MA, Finegold M, Grompe M. 2007. Robust expansion of human hepatocytes in Fah^{-/-}/Rag2^{-/-}/Il2rg^{-/-} mice. *Nat Biotechnol* 25: 903-10

331. Bissig KD, Le TT, Woods NB, Verma IM. 2007. Repopulation of adult and neonatal mice with human hepatocytes: a chimeric animal model. *Proc Natl Acad Sci U S A* 104: 20507-11

332. Bissig KD, Wieland SF, Tran P, Isogawa M, Le TT, Chisari FV, Verma IM. 2010. Human liver chimeric mice provide a model for hepatitis B and C virus infection and treatment. *J Clin Invest* 120: 924-30

333. Hiraga N, Imamura M, Abe H, Hayes CN, Kono T, Onishi M, Tsuge M, Takahashi S, Ochi H, Iwao E, Kamiya N, Yamada I, Tateno C, Yoshizato K, Matsui H, Kanai A, Inaba T, Tanaka S, Chayama K. 2011. Rapid emergence of telaprevir resistant hepatitis C virus strain from wildtype clone in vivo. *Hepatology* 54: 781-8

334. Ohara E, Hiraga N, Imamura M, Iwao E, Kamiya N, Yamada I, Kono T, Onishi M, Hirata D, Mitsui F, Kawaoka T, Tsuge M, Takahashi S, Abe H, Hayes CN, Ochi H, Tateno C, Yoshizato K, Tanaka S, Chayama K. 2011. Elimination of hepatitis C virus by short term NS3-4A and NS5B inhibitor combination therapy in human hepatocyte chimeric mice. *J Hepatol* 54: 872-8

335. Pal S, Sullivan DG, Kim S, Lai KK, Kae J, Cotler SJ, Carithers RL, Jr., Wood BL, Perkins JD, Gretch DR. 2006. Productive replication of hepatitis C virus in perihepatic lymph nodes in vivo: implications of HCV lymphotropism. *Gastroenterology* 130: 1107-16

336. Bronowicki JP, Lorient MA, Thiers V, Grignon Y, Zignego AL, Brechot C. 1998. Hepatitis C virus persistence in human hematopoietic cells injected into SCID mice. *Hepatology* 28: 211-8

337. Kondo Y, Machida K, Liu HM, Ueno Y, Kobayashi K, Wakita T, Shimosegawa T, Lai MM. 2009. Hepatitis C virus infection of T cells inhibits proliferation and enhances fas-mediated apoptosis by down-regulating the expression of CD44 splicing variant 6. *J Infect Dis* 199: 726-36

338. Kondo Y, Sung VM, Machida K, Liu M, Lai MM. 2007. Hepatitis C virus infects T cells and affects interferon-gamma signaling in T cell lines. *Virology* 361: 161-73

339. Zignego AL, Giannelli F, Marrocchi ME, Giannini C, Gentilini P, Innocenti F, Ferri C. 1997. Frequency of bcl-2 rearrangement in patients with mixed cryoglobulinemia and HCV-positive liver diseases. *Clin Exp Rheumatol* 15: 711-2

340. Zignego AL, Ferri C, Giannelli F, Giannini C, Caini P, Monti M, Marrocchi ME, Di Pietro E, La Villa G, Laffi G, Gentilini P. 2002. Prevalence of bcl-2 rearrangement in patients with hepatitis C virus-related mixed cryoglobulinemia with or without B-cell lymphomas. *Ann Intern Med* 137: 571-80

341. Jaeger U, Karth GD, Knapp S, Friedl J, Laczika K, Kusec R. 1994. Molecular mechanism of the t(14;18) – a model for lymphoid-specific chromosomal translocations. *Leuk Lymphoma* 14: 197-202
342. Giannini C, Giannelli F, Zignego AL. 2006. Association between mixed cryoglobulinemia, translocation (14;18), and persistence of occult HCV lymphoid infection after treatment. *Hepatology* 43: 1166-7; author reply 7-8
343. Sung VM, Shimodaira S, Doughty AL, Picchio GR, Can H, Yen TS, Lindsay KL, Levine AM, Lai MM. 2003. Establishment of B-cell lymphoma cell lines persistently infected with hepatitis C virus in vivo and in vitro: the apoptotic effects of virus infection. *J Virol* 77: 2134-46
344. Kondo Y, Ueno Y, Kakazu E, Kobayashi K, Shiina M, Tamai K, Machida K, Inoue J, Wakui Y, Fukushima K, Obara N, Kimura O, Shimosegawa T. 2011. Lymphotropic HCV strain can infect human primary naive CD4+ cells and affect their proliferation and IFN-gamma secretion activity. *J Gastroenterol* 46: 232-41
345. Laskus T, Radkowski M, Wilkinson J, Vargas H, Rakela J. 2002. The origin of hepatitis C virus reinfesting transplanted livers: serum-derived versus peripheral blood mononuclear cell-derived virus. *J Infect Dis* 185: 417-21
346. Lee WM, Polson JE, Carney DS, Sahin B, Gale M, Jr. 2005. Reemergence of hepatitis C virus after 8.5 years in a patient with hypogammaglobulinemia: evidence for an occult viral reservoir. *J Infect Dis* 192: 1088-92

CURRICULUM VITAE

Ziqing Liu

Education

- 2008-2014:** *Indiana University, Indianapolis, IN*
Degree: Ph. D. in Microbiology and Immunology
Advisor: Professor Andy Yu, Professor Johnny He
- 2004-2008:** *University of Science and Technology of China*
Degree: B.S. in Life Science

Honors, Awards, Fellowships

- 2013** Health Point 1st Place Translational Research Award
UNTHSC Annual Research Appreciation Day
- 2012** Student Travel Grant
The 31st Annual American Society for Virology Meeting
- 2007** Finalist & Best Foundational Technology Prize
2007 International Genetically Engineered Machine Competition
- 2006, 2007** Morning Light Scholarship
Morning Light Foundation, China

Research Experience

- 2008-2013** Graduate Student
Professor Johnny He's Laboratory
Indiana University School of Medicine
Field of Study: Hepatitis C Virus
- Nov 2007-
Jul 2008** Undergraduate Student
Professor Changlin Tian's Laboratory
University of Science and Technology of China
Field of Study: Structural Biology with NMR
- Jan 2007-
Oct 2007** Undergraduate Student
Professor Haiyan Liu's Laboratory
University of Science and Technology of China
Field of Study: Synthetic Biology

Teaching Experience

- 2007** Teaching Assistant in Microbiology J210
Indiana University School of Medicine

Publications

Peer-Reviewed Publications:

Liu Z, He JJ (2013). Cell-cell contact-mediated hepatitis C virus (HCV) transfer, productive infection and replication and its requirement for HCV receptors. Journal of Virology, 87(15):8545-58.

Liu Z, He JJ. Hepatitis C virus (HCV) interaction with astrocytes: non-productive infection and induction of IL-18 (*Submitted*)

Liu Z, He JJ. Exosome-associated hepatitis C virus and its infectivity. (*Submitted*)

Park IW, Ndjomou J, Wen Y, **Liu Z**, Ridgway ND, Kao CC, He JJ (2013). Inhibition of HCV Replication by Oxysterol-Binding Protein-Related Protein 4 (ORP4) through Interaction with HCV NS5B and Alteration of Lipid Droplet Formation. Plos One, 8(9):e75648.

Zhao F, **Liu Z**, Vaughan R, Kao CC, Ho WZ, Hefferon K, Li G, He JJ. A single amino acid change from leucine to proline at position 491 of hepatitis C virus non-structural protein 3 (HCV NS3) impairs its helicase/NTPase activities and abrogates HCV replication. (*To be submitted*)

Zhao F, **Liu Z**, Ranjith-Kumar CT, Kao CC, Park IW, Li G, He JJ. Two lethal mutations in the hepatitis C virus NS5B protein are critical for RNA-dependent RNA polymerase activity. (*To be submitted*)

Amet T, Ghabril M, Chalasani N, Byrd D, Hu N, Grantham A, **Liu Z**, Qin X, He JJ, Yu Q (2012). CD59 incorporation protects hepatitis C virus against complement-mediated destruction. Hepatology, 55(2):354-63.

Zhan J, Ding B, Ma R, Ma X, Su X, Zhao Y, **Liu Z**, Wu J, Liu H (2010). Develop reusable and combinable designs for transcriptional logic gates. Molecular Systems Biology, 6:388.

Abstracts:

Liu Z, He JJ. Cell-cell contact-mediated hepatitis C virus infection and its requirement for HCV receptors. The 31st Annual American Society for Virology Meeting, Madison, 7/21-7/25, 2012.

Zhan J, Ding B, Ma R, Ma X, Su X, Zhao Y, **Liu Z**, Wu J, Liu H. Extensible Logic Circuits in Bacteria. The 4th International Genetically Engineered Machine Competition, Boston, Nov, 2007.